INFORMATION TO USERS

This manuscript has been reproduced from the microfilm master. UMI films the text directly from the original or copy submitted. Thus, some thesis and dissertation copies are in typewriter face, while others may be from any type of computer printer.

The quality of this reproduction is dependent upon the quality of the copy submitted. Broken or indistinct print, colored or poor quality illustrations and photographs, print bleedthrough, substandard margins, and improper alignment can adversely affect reproduction.

In the unlikely event that the author did not send UMI a complete manuscript and there are missing pages, these will be noted. Also, if unauthorized copyright material had to be removed, a note will indicate the deletion.

Oversize materials (e.g., maps, drawings, charts) are reproduced by sectioning the original, beginning at the upper left-hand corner and continuing from left to right in equal sections with small overlaps.

Photographs included in the original manuscript have been reproduced xerographically in this copy. Higher quality 6" x 9" black and white photographic prints are available for any photographs or illustrations appearing in this copy for an additional charge. Contact UMI directly to order.

ProQuest Information and Learning
300 North Zeeb Road, Ann Arbor, MI 48106-1346 USA
800-521-0600

Physiology and Pharmacology of Excitation-Contraction Coupling in Normal and Diseased Cardiac Cells

by

Wei Xiong, MD

Submitted to the Faculty of Graduate Studies in partial fulfillment of the requirement for the degree of Doctor of Philosophy

at

Dalhousie University
Halifax, Nova Scotia

July 2001

DALHOUSIE UNIVERSITY

FACULTY OF GRADUATE STUDIES

The undersigned hereby certify that they have read and recommend to the Faculty of Graduate Studies for acceptance a thesis entitled "Physiology and Pharmacology of Excitation-Contraction Coupling in Normal and Diseased Cardiac Cells" by Wei Xiong in partial fulfillment of the requirements for the degree of Doctor of Philosophy.

Dated: July 20, 2001

External Examiner:

Research Supervisor:

Examining Committee:

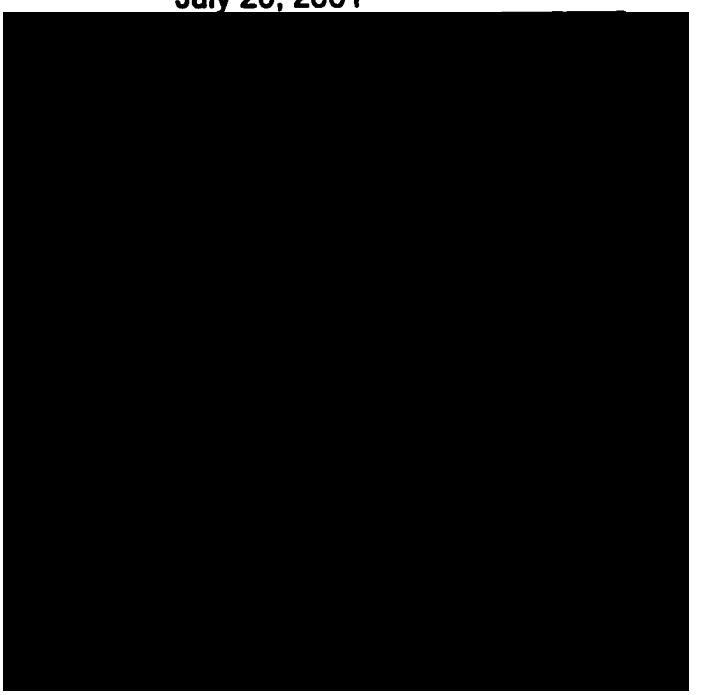

DALHOUSIE UNIVERSITY

Date: July 20, 2001

AUTHOR: Wei Xiong, MD

TITLE: Physiology and Pharmacology of Excitation-Contraction Coupling in Normal and Diseased Cardiac Cells

DEPARTMENT OR SCHOOL: Department of Pharmacology

DEGREE: PhD CONVOCATION: October YEAR: 2001

Permission is herewith granted to Dalhousie University to circulate and to have copied for non-commercial purposes, at its discretion, the above title upon the request of individuals or institutions.

Signature of Author

The author reserves other publication rights, and neither the thesis nor extensive extracts from it may be printed or otherwise reproduced without the author's written permission.

The author attests that permission has been obtained for the use of any copyrighted material appearing in this thesis (other than brief excerpts requiring only proper acknowledgment in scholarly writing), and that all such use is clearly acknowledged.

This thesis is dedicated in loving memory to my dearest Mom Wan-Qing, who passed away when I was here in my PhD training, for her infinite love and unconditional support along my life's journey. I don't know how much I owe you, but I know that I can never pay it off. I miss and love you every day more than you'll ever know….

This thesis also is dedicated to the loving memory of my Dad and Grandma for their thoughtful care for me in my childhood. I tucked my head under your wing and basked in your love. Your precious love touched my heart and let me face my unique life without a heart totally broken apart….

TABLE OF CONTENTS

LIST OF FIGURES

LIST OF TABLES

ABSTRACT

Cardiac excitation-contraction (E-C) coupling includes two mechanisms: 1) calcium-induced calcium release (CICR); 2) the voltage-sensitive release mechanism (VSRM). Cell shortening and currents were measured in voltage clamped guinea pig or hamster ventricular myocytes at 37 °C. Na^+ current was inhibited. Transient outward current also was inhibited in hamster cells. In cardiomyopathic (CM) hamster myocytes, VSRM but not CICR contractions were significantly reduced in magnitude. Sarcoplasmic reticulum (SR) Ca^{2+} content, assessed with 10 mM caffeine, was unaltered in CM cells. Fractional SR Ca^{2+} release was estimated by normalizing VSRM and CICR contractions to caffeine-induced contractures. Fractional SR Ca^{2+} release by the VSRM, but not CICR was significantly reduced in CM cells. In guinea pig myocytes, the nonspecific phosphodiesterase (PDE) inhibitor IBMX increased both VSRM and CICR contractions and also stimulated L-type Ca^{2+} current ($I_{Ca\text{-}L}$). In contrast, the specific PDE III inhibitor amrinone enhanced VSRM contractions without stimulation of $I_{Ca\text{-}L}$ or CICR. Both IBMX and amrinone increased SR Ca^{2+} content. However, both drugs increased fractional SR Ca^{2+} release by the VSRM, but not CICR. In normal hamster myocytes, amrinone selectively enhanced the VSRM without an effect on CICR. In contrast, amrinone had no effect on contractions in CM cells. In addition, amrinone decreased $I_{Ca\text{-}L}$ in normal and CM cells. Amrinone also caused a small increase in SR Ca^{2+} content and selectively increased VSRM fractional release in normal cells, but this action was absent in CM cells. Together, these results suggest that impaired contractility in CM cells is attributable to depression of the VSRM, which is related to defective fractional release of SR Ca^{2+} by the VSRM. Amrinone selectively potentiates the VSRM in normal cells, but cannot restore depressed VSRM contractions in CM cells. This may be related to an inability of amrinone to increase fractional release by the VSRM in CM myocytes.

LIST OF ABBREVIATIONS

AC	adenylate cyclase
A.D.	Anno Domini
Ag/AgCl	silver/silver-chloride
AKAPs	A-kinase anchoring proteins
AP	action potential
B.C.	Before Christ
8-bromo-cAMP	8-bromo-cyclic-adenosine monophosphate
cAMP	cyclic-adenosine monophosphate
cGMP	cyclic-guanylyl monophosphate
Ca^{2+}	calcium
$[Ca^{2+}]i$	intracellular calcium concentration
CaMK	Ca^{2+}-calmodulin dependent protein kinase
Cd^{2+}	cadmium
CHF	Canadian Hybrid Farms
CICR	calcium-induced calcium release
DHPR	dihydropyridine receptor
DMSO	dimethyl sulphoxide
EGTA	ethylene glycol-bis(β-aminoethyl ether) N,N,N'N'-tetraacetic acid
E-C coupling	excitation-contraction coupling
FKBP	FK-506 binding proteins
G protein	guanine nucleotide binding protein
G_i	inhibitory G-protein

G_s	stimulatory G-protein
H^+	hydrogen
$I_{Ca\text{-}L}$	L-type calcium current
$I_{Ca\text{-}T}$	T-type calcium current
I_{Na}	sodium current
IBMX	3-isobutyl-1-methylxanthine
K^+	potassium
M	molar
mg	milligram
Mg^{2+}	magnesium
ml	milliliter
mM	millimolar
mV	millivolts
nA	nanoampere
Na^+	sodium
$I_{Na^+\text{-}Ca^{2+}}$	sodium-calcium exchange current
Ni^{2+}	nickel
PDE	phosphodiesterase
PKA	protein kinase A
PKC	protein kinase C
PKG	cGMP-dependent protein kinase
RyR(s)	ryanodine receptor(s)
SR	sarcoplasmic reticulum

TnC	troponin C
TnI	troponin I
TnT	troponin T
T-tubule	transverse-tubule
TTX	tetrodotoxin
V_{PC}	post-conditioning potential
VSRM	voltage-sensitive release mechanism
β-AR	β-adrenoceptor
δ-SG	δ-sarcoglycan
μM	micomolar
μm	micrometer
4-AP	4-aminopyridine

ACKNOWLEDGEMENTS

First and foremost, I would to thank my supervisor Dr. Susan Howlett for providing me with a valuable opportunity to work in this great laboratory that focused on the front-end area in cardiac excitation-contraction (E-C) coupling. I am especially indebted to her for her excellent hypotheses that made my research progress much smoother, more fruitfully and consequently my hard work more fun and enjoyable. I also thank her for her great patience and guidance when I, a newcomer from a country with mysterious Oriental heritage of 7000 years, encountered culture and value shock in the new Western environment. In addition, I owe many thanks to her for her tremendous spare time she devoted and invaluable comments she contributed to my thesis editing. I also am much grateful to Dr. Greg Ferrier, a co-founder of the VSRM, who has offered invaluable advice and encouragement in my research project. With his "Nova Scotia lighthouse", I can see the light (VSRM) at the end of the "E-C coupling" tunnel, which is localized in the tiny *"fuzzy"* space between the Ca^{2+} channel and SR ryanodine receptor. While some people had some reservations or even biased comments about the VSRM, my research work makes me a strong believer in it. The VSRM attracted me, an international cardiologist with strong curiosity in heart failure, to come from the other end of the world to work in this lab. Honestly, I had a bit of suspicion in the VSRM when I came to the lab. I was not totally convinced until I got my results first-hand. I am a practical person and I would have ended up with a Master's degree if I had not had enough confidence in the VSRM. Many thanks to Susan and Greg for letting me work on this topic for almost five years, with meaningful contributions to my belief.

I would also like to thank Peter Nicholl and Cindy Mapplebeck for providing excellent technical assistance in isolating hamster ventricular myocytes, which tend to be very twitchy cells. Their hard work made my experiments much smooth. A noteworthy mention is that I benefit tremendously from Peter's gift in computer software, which is an obvious and rare asset to this lab. In addition, I gratefully received help from other technicians, both present and past---- Claire, Isabel, Zhu, Joan and Steve.

My thanks also are extended to numerous students with an interesting variety of personalities in these combined labs. Bill Louch is a friendly and easy-going buddy both

in the lab and in pubs down in the Southern city of New Orleans. Marc Richard is a fun guy with a good sense of humor and exceptional honesty. Heidi Moore is a diligent beaver and respectful vegetarian, who has some strict rules and likes a veggie pizza without topping (cheese). Adrian Au was a diligent worker from Hong Kong, but had a crush on Japanese sushi more than Chinese spring rolls. He also had multiple interests in different disciplines such as pharmacology, basic cardiovascular research and clinical medicine, but eventually pursued a career as a dentist. Dentists like sushi! Like me, Corey Felix also is a parent student. However, that's not news anymore. Heidi is the headline news and she is expecting a baby very soon. While students get many results in scientific experiments, all the students in this department who have their babies are associated with our combined labs, making our labs more fruitful in different aspects. I would also like to thank other students, Moira Myszak, Cindy Mason, Jennifer Martin, Jennifer Ryan, Edie Baxter, Diane Bird, Anna-Maria Szczesniak, Xuejun Liu, Yushan Wang, Scott Grandy and Robin Smith for their true friendship. The whole bunch of students makes the working environment atmosphere more relaxed and enjoyable.

I owe many thanks to Dr. Jean Gray, who deserves honorable mention for strongly encouraging me to prepare a manuscript of a review article. Because of her outstanding guidance and great patience, I have a 21-page review paper added to my publication list. I also benefit tremendously from her clinical pharmacology course. My heartfelt gratitude also is extended to Dr. Melanie Kelly whose strong encouragement led to the birth of my beautiful baby daughter Barbara, which was not an initial plan. Dr. Kelly also is a faculty member who knows most about my research outside of our labs. I benefited a lot from her class (and grant proposal writing). She was on the committee of my PhD comprehensive examination and currently is on my PhD thesis examining committee. I am especially indebted to you and Dr. Gray for giving me infinite amounts of support and encouragement of my career goal.

I would like to thank our graduate studies coordinator Dr. Tom White, my advisory committee chairwoman Dr. Theresa Peterson, and the office staff, Janet, Luisa, Karen and Sandi for their sincere support and help during my graduate studies. My thanks also are extended to the rest of faculty, staff and students for our friendly environment and my unforgettable experience.

Thanks to the prestigious Killam Trust for awarding me a Killam Scholar in my PhD studies.

Lastly but not the least, I would like to sincerely thank Chanjuan for her true friendship and support during my PhD studies, and baby Barbara for making me happier during my life-altering tough times. My heartfelt thanks also go to my brother for his strong support and great understanding during the critical stage of my Mom's illness. It is impossible that I could continue my studies in Canada without much interruption if he, or Chanjuan who was on the maternity leave, did not extend me a helping hand.

PUBLICATIONS

The following papers and abstracts (presentation) in my PhD studies have been published, or are in press or in preparation:

Xiong W, Ferrier GR and Howlett SE. Reduced inotropic response to amrinone in cardiomyopathic (CM) hamsters is related to defective Ca^{2+} release by the voltage-sensitive release mechanism (VSRM). (In preparation)

Xiong W, Moore HM, Howlett SE and Ferrier GR (2001) In contrast to forskolin and IBMX, amrinone stimulates the cardiac voltage-sensitive release mechanism without increasing calcium-induced calcium release. *Journal of Pharmacology and Experimental Therapeutics* (In press)

Xiong W, Ferrier GR, Howlett SE (2001) Reduced inotropic response to amrinone in cardiomyopathic (CM) hamsters is related to defective Ca release by the voltage-sensitive release mechanism (VSRM). *Biophysical Journal* 80:596A.

Ferrier GR, Moore HM, Xiong W and Howlett SE (2001) In contrast to forskolin and IBMX, amrinone stimulates the cardiac voltage-sensitive release mechanism (VSRM) without increasing calcium current. *Biophysical Journa*l 80: 597A-598A.

Howlett SE, Moore HM, Xiong W, Ferrier GR (2000) In contrast to forskolin, amrinone stimulates cardiac contractions initiated by a voltage-sensitive release mechanism without increasing calcium current. Gordon Conference, Connecticut College, New London, CT July 22-27, 2000.

Xiong W, Ferrier GR and Howlett SE (2000). Depression of the voltage-sensitive release mechanism in cardiomyopathic hamster ventricular myocytes is not reversed by exposure to the phosphodiesterase III inhibitor amrinone. *Biophysical Journal* 78:372A.

Howlett SE, Xiong W, Mapplebeck C and Ferrier GR (1999) Role of voltage-sensitive release mechanism in depression of cardiac contraction in myopathic hamsters. *American Journal of Physiology* 277:H1690-H1700.

Xiong W and Gray J (1999) The roles of receptor abnormalities in the pathogenesis and chronic complications of type 2 diabetes mellitus. *Journal of Clinical and Investigative Medicine* 22:85-105.

Xiong W, Ferrier GR and Howlett SE (1998) Amrinone potentiates contractions initiated by a voltage sensitive mechanism in ventricular myocytes from normal but not cardiomyopathic hamsters. *Biophysical Journal* 74:A54.

INTRODUCTION

1. OVERVIEW

The heart and circulatory system

The heart was first described by Aristotle (384-322 B.C.), who thought that the heart was the seat of the soul and the center of man. However, the contractile function of the heart was not recognized until Galen (130-201 A.D.) found that the heart was responsible for the circulation of blood. Nevertheless, it was not until William Harvey (1578-1657) that the anatomy and physiology of the heart and circulation was scientically established, a milestone in the history of cardiovascular research. Harvey proved the blood was circulated through the body and predicted the existence of capillary circulation (Willius and Keys, 1941; Roththschuh, 1973; Opie, 1984).

Today we know that the heart continuously pumps oxygenated blood to the peripheral circulatory system and transports and distributes oxygen and other essential substances to tissues of the body. The right side of the heart receives venous blood from vena cava and ejects it to the lungs via the pulmonary artery, where carbon dioxide is exchanged for oxygen. The oxygenated blood from pulmonary veins and the left atrium enters the left ventricle, which pumps blood into the aorta. The aorta branches into arteries, arterioles, and eventually capillaries that not only deliver oxygen and nutrients to tissues but also remove waste products from tissues. The blood then returns to the heart through the venous system (reviewed by Miles et al., 1997).

The electrical conduction system

The ability of the heart to pump blood is triggered by an electrical impulse. Under normal conditions, the cardiac electrical impulse originates at the sinus node that is

located near the junction of the superior vena cava and the right atrium. The electrical impulse travels down to the atrioventricular node, which functions as a delay in conduction to allow enough ventricular filling of blood before ventricular contraction. The impulse then conducts through the His bundle which branches into the ventricles, where the impulse eventually descends along the Purkinje fibers to ventricular muscle (reviewed by Miles et al., 1997).

Cardiac muscle

The fundamental contractile unit of a cardiac myocyte is the sarcomere, of which the resting length is about 2.2 μm (reviewed by Bern and Levy, 1997). The sarcomere consists of thick filaments (myosin) and thin filaments (actin, troponin, tropomyosin). The myosin has long tails, which form the main axis of myosin, and heads that contain ATP hydrolysis sites and interact with actin. Contraction is activated by an increase in intracellular Ca^{2+} in the micromolar range. Ca^{2+} binds to the Ca^{2+} binding subunit of troponin, which causes a series of conformational alterations in the troponin-tropomyosin complex and removes inhibition of the interaction of myosin and actin (Roos, 1997). The sarcomere runs from Z line to Z line. The thin filaments anchored to the Z line project towards the center of the sarcomere to overlap and interact with the thick filaments. During contraction, the thin filaments slide along the thick filaments and pull the Z lines together, thereby leading to cell shortening (reviewed by Bern and Levy, 1997).

The heart is a myogenic organ. The intrinsically generated impulse passes from one myocyte to neighboring myocytes by gap junctions. The gap junctions are localized at intercalated disks, where myocardial cells meet each other longitudinally. The gap junctions are composed of six polypeptides with a central pore to produce a low-

resistance path between cells, allowing rapid spread of the cardiac impulse from one cell to another. Therefore, the heart may behave as an electrical syncytium (reviewed by Bern and Levy, 1997).

2. MAJOR CELLULAR STRUCTURES RELATED TO CARDIAC EXCITATION-CONTRACTION COUPLING

The process by which excitation of the cardiac cell membrane leads to contraction is known as cardiac excitation-contraction (E-C) coupling. Many structures in cardiac myocytes are involved in E-C coupling. The most important of these will be reviewed below.

Sarcolemma/transverse tubules

In cardiac muscle, invaginations of the sarcolemma (or cell membrane) known as transverse tubules (T-tubules) at the Z line are in close proximity to the sarcoplasmic reticulum (SR), forming a diad. The T-tubules are continuous with the surface sarcolemma. The action potential spreads from the cell membrane into the T-tubules, where the SR and sarcolemma appose each other in a tiny *fuzzy* space (~15 nm) (Figure A) (Lederer et al., 1990). The trigger for SR Ca^{2+} release in cardiac ventricular myocytes is the subject of intense investigation as discussed in detail later. However, the diadic cleft containing SR Ca^{2+} release channels and sarcolemmal ion channels is a very important functional unit for coupling excitation to cardiac contraction.

Figure A. Schematic model of the *fuzzy* space. SR Ca^{2+} release channels are localized in close proximity to L-type Ca^{2+} channels and the putative voltage sensor on the T-tubules. The Na^{+}-Ca^{2+} exchanger also is located in the *fuzzy* space (~15 nm). The "foot" process of SR Ca^{2+} release channel is approximately 12 nm in length.

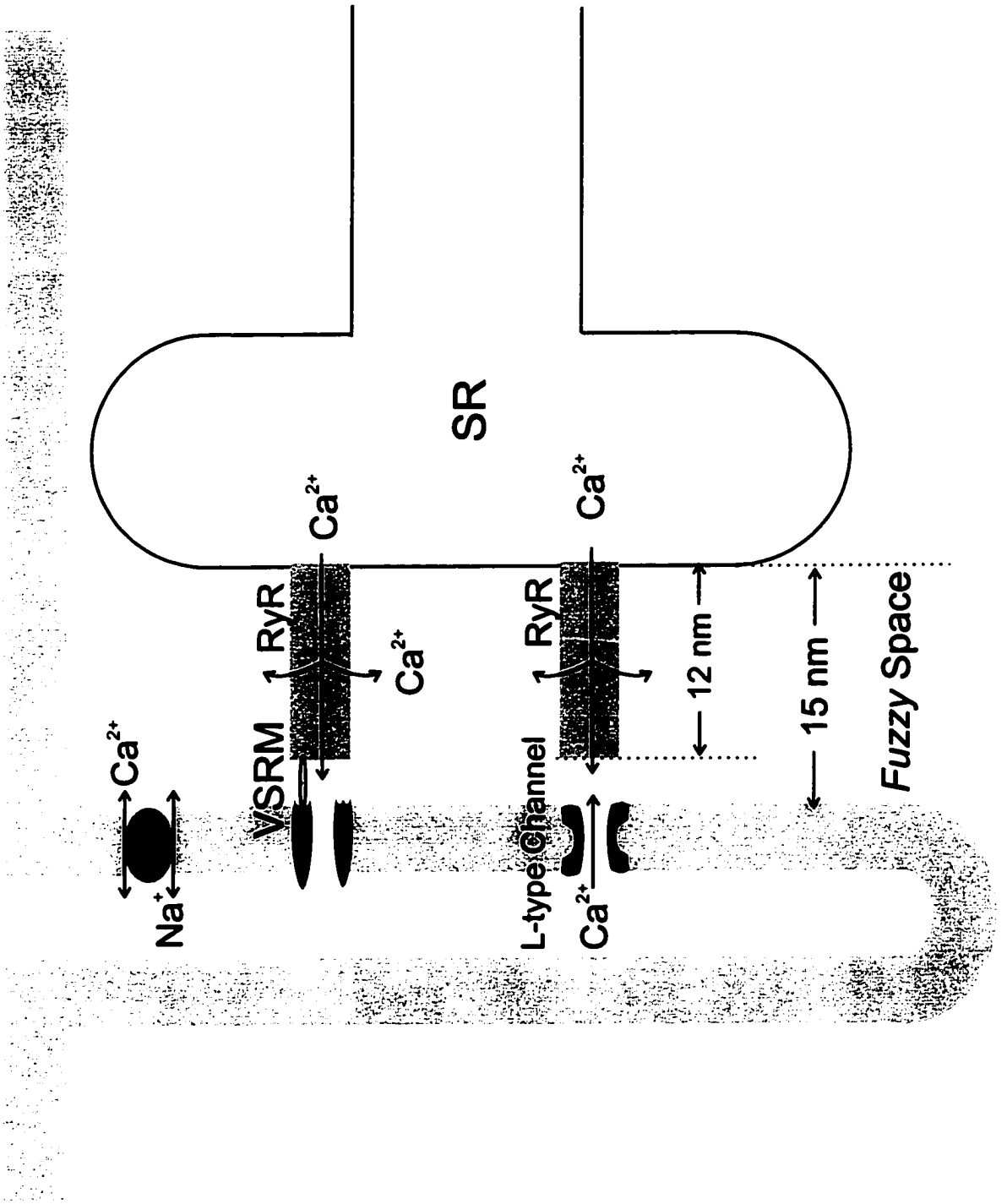
SR
Ca2+
Ca2+
RyR
RyR
Ca2+
Ca2+
VSRM
L-type Channel
12 nm
15 nm
Fuzzy Space
Ca2+
Na+
Ca2+

Figure A

Transport across the cell membrane

Excitation of the cardiac myocyte occurs as a result of the movement of ions across the sarcolemma. There are many proteins responsible for influx and efflux of ions across the sarcolemma. Some are ion channels, such as Na^+ channels, L-type Ca^{2+} channels and T-type Ca^{2+} channels. They do not need energy and thus are passive. The direction of rapid diffusion of ions depends on the electrochemical gradient. However, certain specific amino acids in channel proteins forming the ion-conducting pore determine the selectivity of a channel for a specific ion over others. Moreover, some cell membrane proteins act as primary active transport to carry ions against an electrochemical gradient at the expense of ATP. The primary active transporter proteins in the myocardial cell membrane include the Na^+-K^+ ATPase and the Ca^{2+}-ATPase (Ca^{2+} pump). The Na^+-K^+ ATPase expels 3 Na^+ out of the cell in exchange for 2 K^+ into the cell. Furthermore, other transporters couple two or more ions. With the transport of one ion "downhill" providing the energy, other ions can be transported "uphill". In cardiac muscle, the important transport proteins include Na^+-Ca^{2+} exchanger and Na^+–H^+ exchanger. The Na^+-Ca^{2+} exchanger removes about 20-30% of Ca^{2+} from the cytoplasm during cardiac relaxation (Bers, 1991; Bers, 2000). The Na^+ –H^+ exchanger may lead to Na^+ influx into the cell by removing H^+ from the cell (Philipson, 1997).

The various kinds of ion channels, exchangers and pumps make a significant contribution to E-C coupling and Ca^{2+} homeostasis. At the steady state, any Ca^{2+} influx must be balanced by the same amount of Ca^{2+} efflux to maintain Ca^{2+} homeostasis. In cardiac myocytes, Ca^{2+} mainly enters the cell via L-type Ca^{2+} channels (Bers, 2000). During relaxation, Ca^{2+} is expelled out of the cell by the Na^+-Ca^{2+} exchanger, and to a

much lesser degree by the sarcolemmal Ca^{2+} pump (Bers, 2000). Mitochondria can take up Ca^{2+}, but only contribute to about 1% of the removal of Ca^{2+} from the cytoplasm. The minor contribution to Ca^{2+} homeostasis and relatively slow kinetics indicate that mitochondria do not play an important role in sequestration of Ca^{2+} in normal beat-to-beat contraction. However, mitochondria can take up a large amount of Ca^{2+} to prevent intracellular Ca^{2+} overload if intracellular Ca^{2+} concentration reaches a very high level (Moreno-Sanchez and Hansford, 1988; McCormack et al., 1989).

L-type Ca^{2+} channels

The voltage-dependent L-type Ca^{2+} channel (L for long lasting or large conductance) is distributed throughout the heart. The cardiac L-type Ca^{2+} channel is a multisubunit protein, including α_1, α_2-δ and β subunits (Nargeot et al., 1997). The cardiac α_1 subunit (α_{1C} subunit) of the L-type Ca^{2+} channel is a pore-forming subunit (Mikami et al., 1989; Bers and Perez-Reyes, 1999). The α_{1C} subunit can conduct weak Ca^{2+} current (Richard et al., 1998). However, co-expression of cardiac β subunits can markedly increase the L-type Ca^{2+} current ($I_{Ca\text{-}L}$). The α_{1C} subunit also bears pharmacological binding sites for Ca^{2+} channel blockers (Bers and Perez-Reyes, 1999). It has been shown that the α_{1C} subunit is associated with the cytoplasmic β subunit and a transmembrane α_2-δ subunit. Coexpression of α_2-δ with α_{1C} can increase dihydropyridine binding sites and $I_{Ca\text{-}L}$ (Bers and Perez-Reyes, 1999).

The cardiac L-type Ca^{2+} channel can be phosphorylated by protein kinase A (PKA), protein kinase C (PKC), cGMP-dependent protein kinase (PKG) and Ca^{2+}/calmodulin kinase (CaMK) II (McDonald et al., 1994). β-adrenergic agonists can cause a significant

increase in $I_{Ca\text{-}L}$ in cardiac ventricular myocytes as well as shifts of the voltage-dependence of activation and inactivation to more negative potentials (Tsien et al., 1986; Hartzell, 1988; McDonald et al., 1994). Single-channel studies have shown that phosphorylation by PKA increases the open probability of L-type Ca^{2+} channels (McDonald et al., 1994). Both α and β subunits bear phosphorylation sites for PKA. However, the precise mechanism underlying phosphorylation of L-type Ca^{2+} channels by PKA remains unclear. A study of Gao et al. has suggested that the PKA-mediated regulation of L-type Ca^{2+} channels is critically dependent on a functional A-kinase (PKA) anchoring protein (AKAP) known as AKAP79 and phosphorylation at Ser 1928 in the C-terminus of the α_{1C} subunit (Gao et al., 1997).

T-type Ca^{2+} channels

Ca^{2+} also can enter the myocardial cell via the T-type Ca^{2+} channel (T for transient or tiny conductance) at more negative membrane potentials than the L-type Ca^{2+} channel (Bean, 1985; Nilius et al., 1985; Mitra and Morad, 1986; Hirano et al., 1989; Tseng and Boyden, 1989; Zhou and Lipsius, 1994). $I_{Ca\text{-}L}$ is activated by depolarization to near –30 mV, whereas the T-type Ca^{2+} current ($I_{Ca\text{-}T}$) is activated at much more negative potentials (about –60 mV). $I_{Ca\text{-}T}$ is smaller and inactivates more rapidly when compared with $I_{Ca\text{-}L}$ in ventricular myocytes (Bean, 1985; Mitra and Morad, 1986; Hirano et al., 1989). Therefore, the T-type Ca^{2+} channel and L-type Ca^{2+} channel have different electrophysiological properties.

The physiological role of the T-type Ca^{2+} channel in hearts is not very clear. Unlike L-type Ca^{2+} channels, T-type Ca^{2+} channels have a restricted distribution in the heart. The

density of T-type Ca^{2+} channels is higher in sino-atrial nodal, atrial and Purkinje cells than in ventricular cells (Hagiwara et al., 1988, Hirano et al., 1989; Tseng and Boyden, 1989; Zhou and Lipsius, 1994). It appears that T-type Ca^{2+} channels may play a role in pacemaker activity (Nilius et al., 1985; Nilius, 1986; Zhou and Lipsius, 1994). It has been shown that the diastolic depolarization in sino-atrial node cells is closely correlated to the activation of $I_{Ca\text{-}T}$ (Nilius, 1986). Moreover, an abundance of $I_{Ca\text{-}T}$ has been found in neonatal rat ventricular and chick embryonic ventricular myocytes (Kawano et al., 1989; Lemaire et al., 1998). However, loss of $I_{Ca\text{-}T}$ may result from normal maturation (Richard et al., 1998). Furthermore, $I_{Ca\text{-}T}$ density is increased in hypertrophied ventricles (Nuss and Houser, 1992; Sen and Smith, 1994). Thus, T-type Ca^{2+} channels appear to be related to ventricular postnatal growth and hypertrophy (Richard et al., 1998).

The L- and T-type Ca^{2+} channels also have distinct pharmacological properties. The L-type Ca^{2+} channel can be blocked by organic compounds such as dihydropyridines (DHP) (e.g. nifedipine), phenylalkylamines (e.g. verapamil), and benzothiazepines (e.g. diltiazem) and inorganic compounds such as cadmium. The T-type Ca^{2+} channel is relatively insensitive to both organic and inorganic blockers of the L-type Ca^{2+} channel but is blocked by mibefradil, Ni^{+}, and amiloride (Mitra and Morad, 1986; Hagiwara et al., 1988; McDonald et al., 1994; Vassort and Alvarez, 1994). Unlike $I_{Ca\text{-}L}$, $I_{Ca\text{-}T}$ is not stimulated by PKA. However, it can be enhanced by growth hormones, angiotensin II, and endothelin-1 (Richard et al., 1998).

Sarcoplasmic reticulum

The SR plays a key role in cardiac Ca^{2+} homeostasis and regulation of beat-to-beat contraction in the heart. During relaxation, the SR takes up Ca^{2+} via a Ca^{2+} pump for storage, making it available for release via Ca^{2+} release channels in the subsequent heart beat cycle. The SR contains many important proteins that are involved in the maintenance of Ca^{2+} homeostasis. These proteins include the Ca^{2+} release channel, Ca^{2+}-ATPase, phospholamban, and Ca^{2+}-binding proteins such as calsequestrin (reviewed by Rapundalo, 1998).

The SR consists of three regions: 1) the junctional SR, on which the ryanodine-sensitive Ca^{2+} release channels are located within close proximity to the sarcolemma and T-tubules; 2) the longitudinal or network SR, which forms a mesh-like network around the myofilaments of myocytes and contains Ca^{2+}-ATPase/phospholamban complexes that take up Ca^{2+} into the SR; and 3) the cobular SR, which appears to be extended junctional SR, not in the vicinity of the sarcolemma (Frank and Garfinkel, 1997).

Ryanodine-sensitive Ca^{2+} release channels

The SR Ca^{2+} release channel plays an important role in cardiac Ca^{2+} signaling by mediating Ca^{2+} release from the SR. A key component of cardiac EC coupling is a dyadic cleft (~15 nm), with the junctional SR and sarcolemma on each side bridged by a 12 nm projection or "foot" process, which is a part of the SR Ca^{2+} release channel (Frank and Garfinkel, 1997). This tiny but critical space, called *fuzzy* space (Figure A), contains the SR Ca^{2+} release channels, L-type Ca^{2+} channels and Na^{+}-Ca^{2+} exchanger (Lederer et al., 1990). With the help of double labeling immunofluorescence, laser scanning confocal

microscopy and electron microscopy, SR Ca^{2+} release channels have been demonstrated to be localized in close proximity to L-type Ca^{2+} channels on the T-tubules (Carl et al., 1995).

Since the neutral plant alkaloid ryanodine can bind to the SR Ca^{2+} release channel with high affinity, it is also known as the ryanodine receptor (RyR) (Hajdu and Leonard, 1961; Jenden and Fairhurst, 1969). At low concentrations (1 nM ~ 1 μM), ryanodine locks the SR Ca^{2+} release channels in an open subconductance state and causes Ca^{2+} to leak out from the SR. At very high concentrations (>100 μM) of ryanodine, the SR Ca^{2+} release channel seems to be locked in a closed state (Bers, 1991).

The RyR is encoded by three different genes, namely the skeletal muscle gene (RyR1), cardiac muscle gene (RyR2), and brain gene (RyR3) (Fleischer and Inui, 1989; Meissner, 1994; Coronado, 1994; Sutko and Airey, 1996; Xu et al., 1998). RyR1 and RyR2 appear to be homotetramers. They contain four large subunits and four small subunits. The small subunits are FK-506 binding proteins (FKBP), which are thought to play an important role in stabilizing the tetramer array and providing the mechanical coupling between adjacent tetramers (Xu et al., 1998; Marx et al., 1998; Bers and Perez-Reyes, 1999). The RyR have two major structural regions. The C-terminal region forms a central pore and the N-terminal region appears to be the foot structure spanning the gap between the SR and T-tubules (Rapundalo, 1998). These "feet" are tetrads with a central channel opening in the SR and with side channels facing the cleft space (Langer, 1997).

The cardiac RyR can be regulated by many agents. RyR2 can be activated by 1-100 μM Ca or millimolar concentrations of ATP, and inhibited by millimolar Mg or micromolar ruthenium red (Bers, 1991; Bers and Perez-Reyes, 1999). RyR2 has been

shown to be phosphorylated by cAMP-dependent protein kinase A (PKA) (Takasago et al., 1989; Yoshida et al., 1992; Strand et al., 1993). RyR2 can also be phosphorylated by CaMK at serine 2809 (Witcher et al., 1991; Strand et al., 1993).

SR Ca^{2+} pump

The amount of Ca^{2+} entering the cytosol from the SR and through Ca^{2+} channels on the sarcolemma must be removed each cardiac cycle to reach equilibrium. The sequestration of Ca^{2+} into the SR by the SR Ca^{2+} pump facilitates the rate of dissociation of Ca^{2+} from the myofilaments and thus favors relaxation. The SR Ca^{2+} pump is located in the longitudinal part of the SR (Frank and Garfinkel, 1997). At the expense of one ATP, two Ca^{2+} ions are taken up into the SR. Since the Ca^{2+} pumped into the lumen of the SR is available for release during the next stimulation, the SR Ca^{2+} pump not only has influence on relaxation but also on contraction.

The SR Ca^{2+} pump in heart is encoded by the gene known as SERCA2 (Burk et al., 1989). The activity of the Ca^{2+} pump can be regulated by phosphorylation. However, it is phospholamban, a protein associated with SR Ca^{2+}-ATPase, rather than Ca^{2+} ATPase per se, that is phosphorylated. Under basal, unphosphorylated states, phospholamban inhibits the activity of the Ca^{2+}-ATPase (Koss and Kranias, 1996). In contrast, phosphorylation of phospholamban removes the inhibition, thereby enhancing the reuptake of Ca^{2+} into the lumen of the SR (Kranias, 1985). Studies have demonstrated that the increased sequestration of Ca^{2+} in the SR is due to an increase in Ca^{2+} ATPase affinity for Ca^{2+}, rather than an increase in the maximal velocity of the enzyme (Kranias, 1985; Kadambi et al., 1996).

Phospholamban is phosphorylated at serine 16 by PKA (Kirchberger et al., 1974; Tada et al., 1974; Simmerman et al., 1986; Wegener et al., 1989). Phospholamban can also be phosphorylated at threonine 17 by CaMK (Le Peuch et al., 1979; Simmerman et al., 1986; Wegener et al., 1989). In addition to enhancement of $I_{Ca\text{-}L}$, one of the main mechanisms underlying the positive inotropic effects of β-adrenergic agonists seems to be enhancement of SR Ca^{2+} uptake (Bers, 1991). Wegener et al. have shown phosphorylation at serine-16 precedes that at threonine-17 during β-adrenergic stimulation (Wegener et al., 1989). Dephosphorylation at threonine-17 also follows that at serine-16 (Talosi et al., 1993). The incremental phosphorylation of phospholamban by PKA may reflect a graded regulation of cardiac relaxation by phospholamban (Simmerman and Jones, 1998).

Myofilaments and contractile proteins

The contractile unit of the myocardial cell is the sarcomere, which contains thick and thin filaments. The thick filaments are mainly made of myosin while thin filaments are composed of actin, tropomyosin and the troponin complex. The troponin complex consists of troponin C (TnC, or the Ca^{2+} binding subunit), troponin I (TnI, or the inhibitory subunit that inhibits the interaction between actin and myosin), and troponin T (TnT, or the tropomyosin binding subunit) (Roos, 1997). The myofilaments are the downstream end effectors of cardiac E-C coupling. Binding of Ca^{2+} to TnC enhances the interaction between TnC and TnI and as such weakens the interaction between TnI and actin. The resulting conformational change in the troponin-tropomyosin complex removes inhibition of the interaction of actin and myosin (Zot and Potter, 1987;

Chalovich, 1992; Tobacman, 1996). The globular heads of myosin have actin-binding sites and ATPase activity. At the expense of ATP, the thin filaments slide past the adjacent thick filaments, thereby causing cell shortening in cardiac myocytes. The relaxation is largely mediated by Ca^{2+} pumped into the SR, which rapidly reduces intracellular Ca^{2+} concentration and facilitates the dissociation of Ca^{2+} from TnC.

3. MECHANISMS OF CARDIAC E-C COUPLING

The wave of excitation spreads into the T-tubules to depolarize the cell and activate voltage-dependent ion channels, thereby initiating an action potential. During an action potential, a large quantity of Ca^{2+} is released from the SR. The released Ca^{2+} binds to myofilaments and causes cell shortening. The trigger for SR Ca^{2+} release following depolarization of the cell membrane is the subject of intense investigation. It will be discussed in the next section.

Ca^{2+}-induced Ca^{2+} release

An important trigger for SR Ca^{2+} release in the heart is a process known as Ca^{2+}-induced Ca^{2+} release (CICR). Fabiato demonstrated the role of Ca^{2+} in triggering SR Ca^{2+} release by rapid application of Ca^{2+} to mechanically "skinned" (sarcolemma-removed) cardiac myocytes (Fabiato, 1985a, b, c). It was also shown that other ions including Na^{+}, Mg^{2+}, K^{+} and H^{+} did not directly trigger SR Ca^{2+} release (Fabiato, 1985a). Subsequent studies showed that a small increase in intracellular Ca^{2+} concentration induced by photolysis of photolabile chelated Ca^{2+} caused cardiac contraction in intact cells (Valdeolmillos et al, 1989; Nabauer and Morad, 1990). Furthermore, the presence of Ca^{2+}

rather than Ba^{2+} in the extracellular solution is a mandatory requirement for initiation of Ca^{2+} release and contraction (Nabauer et al., 1989).

$I_{Ca\text{-}L}$-induced Ca^{2+} release

Numerous studies have demonstrated that the voltage-dependence of Ca^{2+} transients and cell shortening is similar to the voltage-dependence of $I_{Ca\text{-}L}$ (London and Krueger, 1986; Cannell et al., 1987; Beuckelmann and Wier, 1988; Arreola et al., 1991; Cleemann and Morad, 1991). In addition, the magnitude of Ca^{2+} transients and contractions is proportional to the magnitude of $I_{Ca\text{-}L}$. Moreover, a large inward current triggered by repolarization from potentials beyond the reversal potential for $I_{Ca\text{-}L}$ (tail current) also initiates a Ca^{2+} transient and cell shortening (Barcenas-Ruiz and Wier, 1987). These studies strongly suggest that Ca^{2+} influx via the L-type Ca^{2+} channel can trigger Ca^{2+} release from the SR in cardiac myocytes.

With the help of laser-scanning confocal microscopy, more direct evidence has been accumulated for CICR. First, Cheng et al. showed small, spontaneous, nonpropagating SR Ca^{2+} release, namely "Ca^{2+} sparks" (Cheng et al., 1993). They proposed that a Ca^{2+} spark from the opening of a single RyR is the elementary event of SR Ca^{2+} release. Second, other studies have demonstrated that the opening of a single L-type Ca^{2+} channel is sufficient to trigger a Ca^{2+} spark (Lopez-Lopez et al., 1995; Santana et al., 1996; Cannell and Soeller, 1999; Collier et al., 1999). However, whether the Ca^{2+} spark is the fundamental release event of SR Ca^{2+} release has been challenged. Lipp and Niggli showed that, in the absence of Ca^{2+} sparks, flash photolysis of caged Ca^{2+} evoked spatially homogeneous Ca^{2+} transients, indicating that the elementary event of Ca^{2+}

signalling may be smaller in size or amplitude than a Ca^{2+} spark (Lipp and Niggli, 1996). A subsequent study using low photolytic power to generate photolytic Ca^{2+} signals with much lower amplitude or size, observed Ca^{2+} release fluxes 20-40 times smaller than a typical Ca^{2+} spark, suggesting that an even smaller "Ca^{2+} quark" may be the fundamental event of SR Ca^{2+} release (Lipp and Niggli, 1998). A Ca^{2+} quark could result from the opening of a single RyR while a Ca^{2+} spark may be caused by the opening of a cluster of RyRs (Lipp and Niggli, 1998). These studies have led to the formation of concept called local control theory, in which SR Ca^{2+} release is controlled by Ca^{2+} influx via immediately adjacent Ca^{2+} channels, rather than an increase in global Ca^{2+} concentration (Cannell et al., 1994; Lopez-Lopez et al., 1995; Santana et al., 1996). Ca^{2+} influx via a single L-type Ca^{2+} channel is thought to lead to an increase in intracellular Ca^{2+} concentration in a limited space and thus local SR Ca^{2+} release (Ca^{2+} sparks) through SR Ca^{2+} release channels. The temporal and spatial summation of Ca^{2+} sparks leads to whole cell Ca^{2+} transients (Cannell et al., 1995; Lopez-Lopez et al., 1995; Santana et al., 1996; Katoh et al., 2000). Therefore, the local theory argues against regenerative activation of SR Ca^{2+} release channels, in which Ca^{2+} release from the SR presumably, in turn, recruits nearby SR Ca^{2+} release channels and thus may cause global recruitment of SR Ca^{2+} release channels.

$I_{Ca\text{-}T}$-induced Ca^{2+} release

Several studies have suggested that Ca^{2+} entering via T-type Ca^{2+} channels also may trigger CICR in ventricular and Purkinje cells. $I_{Ca\text{-}T}$-induced Ca^{2+} release is thought to have a delayed onset and slower kinetics compared with $I_{Ca\text{-}L}$ (Sipido et al., 1998; Zhou

and January, 1998). In addition, $I_{Ca\text{-}T}$ is thought to be a less efficient trigger than $I_{Ca\text{-}L}$ in initiating SR Ca^{2+} release (Sipido et al., 1998; Zhou and January, 1998). The reason for that remains unclear. It was speculated that in comparison with L type Ca^{2+} channels, T-type Ca^{2+} channels may be located at a greater or more variable distance from SR Ca^{2+} release channels (Zhou and January, 1998). Therefore, these studies indicate that $I_{Ca\text{-}T}$ is likely to play only a minor role in triggering CICR.

Ca^{2+} influx via reverse mode Na^+-Ca^{2+} exchange

The key role of the Na^+-Ca^{2+} exchanger is to extrude Ca^{2+} from cardiac myocytes. However, studies have suggested that Ca^{2+} can enter the cell via reverse mode Na^+-Ca^{2+} exchange under conditions when the cell membrane is depolarized, especially with voltage steps to very positive potentials (Levi et al., 1994; Wasserstrom and Vites, 1996; Baartscheer et al., 1996; Litwin et al., 1998) or when intracellular Na^+ is high (Barcenas-Ruiz et al., 1987; Bers et al., 1988; Beuckelmann and Wier, 1989). Moreover, Na^+ entry into the cell through the Na^+ channel may increase local Na^+ concentrations and promote reverse mode Na^+-Ca^{2+} exchange (Leblanc and Hume, 1990; Sham et al., 1992; Levesque et al., 1994; Lipp and Niggli, 1994; Vites and Wasserstrom, 1996).

It has been shown that Na^+-Ca^{2+} exchange may promote Ca^{2+} entry into cardiac cells and initiate SR Ca^{2+} release (Terrar and White, 1989; Leblanc and Hume, 1990; Levi et al., 1994; Wasserstrom and Vites, 1996). On the other hand, other studies have suggested that Ca^{2+} entry via the Na^+-Ca^{2+} exchanger may directly bind to myofilaments and initiate cardiac contraction. These studies showed that slow ramp-like contractions and slow Ca^{2+} transients are insensitive to ryanodine (Barcenas-Ruiz and Wier, 1987; Schuttler et al.,

1991). However, the physiological significance of CICR triggered by Na^+-Ca^{2+} exchange remains unclear. The efficiency of reverse Na^+-Ca^{2+} exchange to trigger SR Ca^{2+} release is low compared with that of $I_{Ca\text{-}L}$ (Sipido et al., 1997). In addition, it is not clear whether RyRs and Na^+-Ca^{2+} exchangers are co-localized in junctional SR (Bers, 2000). Furthermore, it was estimated that a very small percentage of Ca^{2+} entry relates to Na^+-Ca^{2+} exchange during a normal action potential (Bers, 2000). Therefore, the role of reverse mode Na^+-Ca^{2+} exchange in CICR under physiological conditions appears to be limited.

Ca^{2+} influx via Na^+ channels

The α-subunit of the cardiac Na^+ channel is composed of four homologous domains, each of which consists of six transmembrane segments. The amino acid loop between segments 4 and 5 constitutes a P-loop that relates to unique permeation of ions. A lysine in the P-loop in domain III is critical to the selection of Na^+ over other ions (Heinemann et al., 1992; Perez-Garcia et al., 1997). However, it has been shown that Ca^{2+} can enter the cardiac cell via tetrodotoxin-sensitive Na^+ channels in the absence of extracelluar Na^+ (Lemaire et al., 1995; Aggarwal et al., 1997). When the β-adrenergic receptor or PKA is activated, Ca^{2+} entry via the Na^+ channel is thought to trigger Ca^{2+} release from the SR (Santana et al., 1998). This phenomenon, called slip-mode Ca^{2+} conductance of the Na^+ channel, was also shown to exist in the presence of cardiotonic steroids (Santana et al., 1998). However, the physiological significance of slip-mode conductance in triggering CICR under physiological conditions remains undetermined.

Voltage-sensitive release mechanism (VSRM)

Recent studies have suggested the existence of a distinct mechanism for cardiac excitation-contraction coupling that can activate SR Ca^{2+} release independently of Ca^{2+} entry into myocytes. Studies have indicated that this mechanism may play an important role in initiation of contraction in ventricular myocytes (Ferrier & Howlett, 1995; Hobai et al., 1997; Howlett & Ferrier GR, 1997; Ferrier et al., 1998; Howlett et al. 1998; Ferrier et al., 2000a, Mackiewicz et al., 2000; Zhu and Ferrier, 2000; Ferrier and Howlett, 2001). This distinct mechanism is called the voltage-sensitive release mechanism (VSRM) because these studies indicate that the magnitude of SR Ca^{2+} transients and contraction can be graded by membrane potential, rather than the magnitude of $I_{Ca\text{-}L}$. The VSRM has many properties that may serve to distinguish it from CICR (Ferrier & Howlett, 1995; Howlett & Ferrier GR, 1997; Ferrier et al., 1998; Howlett et al. 1998; Ferrier et al., 2000a; Zhu and Ferrier, 2000). These properties of the VSRM are discussed below.

First, the magnitude of Ca^{2+} transients and contractions triggered by the VSRM is not proportional to the magnitude of $I_{Ca\text{-}L}$. In CICR the magnitude of contractions and $I_{Ca\text{-}L}$ reach a peak around 0 mV and decline to zero at voltage steps to about +60 mV (Ferrier and Howlett, 1995; Howlett and Ferrier, 1997; Howlett et al., 1998; Ferrier et al, 1998; Zhu and Ferrier, 2000a). This bell-shaped contraction-voltage relationship, which mirrors the bell-shaped current-voltage relationship (Barcenas-Ruiz and Wier, 1987; Beuckelmann and Wier, 1988; duBell and Houser; 1989; Cleemann and Morad, 1991), is one of strongest pieces of evidence for CICR. In contrast, the voltage dependence of Ca^{2+} transients and contractions initiated by the VSRM is sigmoidal, which suggests that the VSRM is a distinct mechanism (Ferrier and Howlett, 1995; Howlett and Ferrier, 1997;

Howlett et al., 1998; Ferrier et al, 1998; Zhu and Ferrier, 2000). Ca^{2+} transients and contractions triggered by the VRSM are activated near –65 mV, reach a plateau near –20 mV and remain large at membrane potentials as positive as +80 mV where inward currents decline to zero. Therefore, these observations suggest that the VSRM and CICR are distinct mechanisms for cardiac E-C coupling.

Second, the VSRM can trigger SR Ca^{2+} release and contraction independently of $I_{Ca\text{-}L}$, Na^+ current and Na^+-Ca^{2+} exchange. The VSRM and CICR can be separated by sequential voltage test steps in the same cardiac myocyte (Ferrier & Howlett, 1995; Howlett & Ferrier GR, 1997; Howlett et al. 1998). It has been demonstrated that SR Ca^{2+} transients and contractions can be triggered by the VSRM when $I_{Ca\text{-}L}$, Na^+ current and/or Na^+-Ca^{2+} exchange are inhibited (Ferrier & Howlett, 1995; Hobai et al., 1997; Ferrier et al., 1998; Howlett et al. 1998; Ferrier et al., 2000a; Mackiewicz et al., 2000; Zhu and Ferrier, 2000). When $I_{Ca\text{-}L}$ is blocked by 100 μM cadmium or 2.5 μM nifedipine, VSRM contractions are intact but CICR contractions are virtually abolished (Howlett and Ferrier, 1997; Howlett et al., 1998; Zhu and Ferrier, 2000). In addition, the VSRM is not inhibited by 2-5 mM Ni^{2+} (Hobai et al., 1997; Ferrier et al., 2000a; Mackiewicz et al., 2000), which can block $I_{Ca\text{-}T}$ (Tytgat et al., 1990; McDonald et al., 1994). These results suggest that $I_{Ca\text{-}T}$ does not initiate the VSRM. Under some conditions Na^+ or Ca^{2+} may enter through the Na^+ channel and trigger CICR (Leblanc and Hume, 1990; Santana et al., 1998). However, the VSRM is unaffected by the Na^+ channel blockers tetrodotoxin, or lidocaine or both together (Ferrier & Howlett, 1995; Howlett et al., 1999; Zhu and Ferrier, 2000). This indicates that Ca^{2+} influx through Na^+ channels does not activate the VSRM to elicit SR Ca^{2+} release and contractions (Ferrier & Howlett, 1995; Howlett et al., 1998; Zhu and

Ferrier, 2000). CICR also may be initiated by Ca^{2+} influx via reverse mode Na^{+}-Ca^{2+} exchange (Barcenas-Ruiz L et al., 1987; Bers et al., 1988, Beuckelmann and Wier, 1989; Bers et al., 1990). Studies have shown that SR Ca^{2+} release and contractions triggered by reverse mode Na^{+}-Ca^{2+} exchange are inhibited in the presence of 2 mM Ni^{+} and/or in the absence of intracellular Na^{+} (Kimura, et al., 1987; Sham et al., 1992; Nuss and Houser, 1992; Levi et al., 1996). However, the SR Ca^{2+} release initiated by the VSRM is unaffected by 2-5 mM Ni^{+} and/or by the absence of intracellular Na^{+} (Hobai et al., 1997; Ferrier et al., 2000a). These findings suggest that activation of the VSRM does not require Ca^{2+} influx via ion channels or the Na^{+}-Ca^{2+} exchanger.

Third, the VSRM exhibits voltage-dependent inactivation, which allows it to be distinguished from CICR. Inactivation is an important characteristic of voltage-sensitive membrane proteins. Along with activation, inactivation can determine the membrane potential at which transitions among open, inactivated and closed states of channels occur. These properties provide useful tools with which various channels can be identified or differentiated (Hille, 1992). Studies have shown that VSRM contractions exhibit steady-state inactivation properties (Howlett and Ferrier, 1997; Howlett et al, 1998; Howlett et al., 1999; Ferrier et al., 2000a; Zhu and Ferrier, 2000). Steady-state inactivation of the VSRM can be shown by eliciting contractions with voltage test steps following depolarization to different membrane potentials (Howlett and Ferrier, 1997; Howlett et al, 1998). These studies show that VSRM contractions are fully available with preceding depolarization steps to about –65 mV. Steady-state inactivation of the VSRM occurs as the preceding depolarization step is made to more positive potentials. Complete inactivation is observed near -35 mV. The sigmoidal steady-state inactivation curve of

the VSRM is well fit by a Boltzman function with a half-inactivation potential about –47 mV (Howlett and Ferrier, 1997; Howlett et al, 1998; Howlett et al., 1999; Ferrier et al., 2000a; Zhu and Ferrier, 2000). In contrast, the half-inactivation voltage for $I_{Ca\text{-}L}$ is approximately –25 mV (McDonald et al., 1994; Howlett et al., 1998). In addition, it has been demonstrated that CICR initiated by reverse mode Na^+-Ca^{2+} exchange has no inactivation characteristics (Nuss and Houser, 1992; Levi et al., 1996; Wasserstrom and Vites, 1996; Litwin et al., 1998). Thus, CICR contractions triggered by reverse mode Na^+-Ca^{2+} exchange persist in the presence of preceding depolarization steps that inactivate the VSRM. Therefore, these inactivation properties of the VSRM allow it to be distinguished from CICR either coupled to $I_{Ca\text{-}L}$ or reverse mode Na^+-Ca^{2+} exchange.

Fourth, the VSRM also is distinguished from CICR by its association with cardiac relaxation. A recent study has demonstrated that, unlike CICR, the VSRM exhibits both a phasic and a sustained component of cardiac contraction (Ferrier et al., 2000a). The sustained component of the VSRM exhibits many of the same properties as the phasic component of the VSRM. The sustained component exhibits sigmoidal voltage dependence of Ca^{2+} transients and contractions. Blockade of $I_{Ca\text{-}L}$ by cadmium does not affect the sustained component of contractions, suggesting that CICR coupled to $I_{Ca\text{-}L}$ does not make a contribution to sustained contractions or transients (Ferrier et al., 2000a). Moreover, the sustained component of contractions is not altered by changes in extracellular or intracellular Na^+ concentration, indicating that it is not related to CICR coupled to Na^+-Ca^{2+} exchange (Ferrier et al., 2000a). Unlike the phasic component of the VSRM, the sustained component is not inactivated by maintained depolarization but it

does deactivate when cells are repolarized. This suggests that the sustained component of the VSRM may contribute to cardiac relaxation.

Taken together, these studies indicate that Ca^{2+} transients and contractions triggered by the VSRM exhibit distinct properties. The VSRM can initiate cardiac contractions independently of $I_{Ca\text{-}L}$, $I_{Ca\text{-}T}$, inward currents carried by the Na^+ channel, or Na^+-Ca^{2+} exchange. Furthermore, the sustained component of the VSRM may link cardiac contraction to relaxation, indicating the VSRM plays an important role in dynamic regulation of both systole and diastole.

Modulation of the VSRM by phosphorylation

Initial experiments to characterize the VSRM were conducted with high resistance microelectrodes (Ferrier and Howlett, 1995). These electrodes have a relatively small tip diameter that minimizes dialysis of the cell interior with the electrode solution. Many eletrophysiological experiments are conducted with patch pipettes because patch pipettes with a larger diameter tip allow addition of chemical compounds to the intracellular environment. However, because patch pipettes have a larger diameter tip, dialysis of essential components of cytoplasm by the patch-pipette solution poses another problem that may not be ignored (Isenberg and Wendt-Gallitelli, 1989). Interestingly, in initial experiments with patch pipettes filled with standard K^+–based intracellular solution, the VSRM component of contractions and transients was absent (Hobai et al., 1997; Ferrier et al., 1998; Zhu and Ferrier, 2000). However, studies showed that addition of 50 μM 8-bromo-cAMP to patch-pipette solution restored the VSRM (Hobai et al., 1997; Ferrier et al., 1998). A subsequent study showed evidence that addition of calmodulin to patch-

pipette solution also could restore the VSRM component of contractions and Ca^{2+} transients (Zhu and Ferrier, 2000). These observations suggest that patch-pipette solutions may cause cellular dialysis and disrupt essential pathways involved in regulation of the VSRM.

Studies also demonstrated that activation of the VSRM contractions by cAMP was inhibited by 5 μM H-89 (Ferrier et al., 1998), which is a PKA inhibitor. In addition, activation of the VSRM contractions by calmodulin was inhibited by 5 μM KN-62 (Zhu and Ferrier, 2000), which is a CaMK inhibitor. These results indicate that both the adenylyl cyclase/PKA pathway and the CaM kinase pathway are involved in regulation of contractions triggered by the VSRM. Moreover, in experiments conducted with patch pipettes, KN-62 has no effect on restoration of the VSRM by cAMP (Zhu and Ferrier, 2000). In contrast, H-89 has no effect on restoration of the VSRM by calmodulin (Zhu and Ferrier, 2000). This suggests that these two pathways regulate the VSRM component of contractions independently. Furthermore, in experiments performed with high-resistance microelectrodes to minimize cellular dialysis with microelectrode solution, either H-89 or KN-62 reduced the magnitude of VSRM contractions to 50%. However, the combination of H-89 and KN-62 almost abolished contractions initiated by the VSRM (Zhu and Ferrier, 2000). Therefore, both the cAMP/PKA and CaMK pathways make significant contributions to the VSRM component of cardiac contraction.

Addition of cAMP to patch-pipette solutions also slightly increases both CICR contractions and $I_{Ca\text{-}L}$ (Ferrier et al., 1998). However, restoration of VSRM contractions by cAMP is not likely to be due to the small increase in Ca^{2+} current since blockade of $I_{Ca\text{-}L}$ by the Ca^{2+} channel blocker cadmium has no effect on the VSRM component of

contractions (Ferrier et al., 1998). Furthermore, calmodulin increases Ca^{2+} transients and contractions initiated by the VSRM but does not affect the magnitude of $I_{Ca\text{-}L}$ and its associated CICR contractions (Zhu and Ferrier, 2000). These findings suggest that restoration of the VSRM by phosphorylation is independent of $I_{Ca\text{-}L}$.

The role of phosphodiesterases in regulation of the VSRM

As discussed in the preceding sections, cAMP has been shown to play an important role in regulation of the VSRM in ventricular myocytes (Hobai et al., 1997; Zhu et al, 1997; Ferrier et al., 1998). Intracellular levels of cyclic nucleotides (cAMP and cGMP) are regulated through: 1) synthesis by adenylyl and guanylyl cyclases; and 2) hydrolysis by phosphodiesterases (PDEs). Since cAMP is subject to hydrolysis by PDEs, it is possible that PDEs play an important role in modulation of phosphorylation of the VSRM, although this has not been determined experimentally.

PDEs are members of a superfamily of enzymes that regulate intracellular levels of the second messengers cAMP and cGMP by catalyzing hydrolysis of these cyclic nucleotides. PDEs include at least eleven different gene families (Beavo, 1995; Soderling et al., 1998; Soderling et al., 1998; Fawcett et al., 2000). These families differ in molecular structure, affinities for substrates such as cAMP and cGMP, and sensitivities to specific inhibitors (Beavo 1995; Conti et al., 1995; Manganiello et al, 1995). PDEs in mammals have a common structure that consists of a conserved catalytic core of ~270 amino acids in the C-terminal (Charbonneau et al., 1986). However, different PDE families have widely divergent N-terminal regions, which determine gene-family-specific regulatory properties. These properties include N-terminal hydrophobic membrane-

association (PDE3), N-terminal membrane-targeting (PDE4) domains and PKA phosphorylation sites (PDEs 1, 3, 4) (Beavo 1995; Conti et al., 1995; Manganiello et al., 1995).

There are at least four different isoforms of PDEs present in the heart, namely PDEs I, II, III and IV, which are classified based on protein and cDNA sequences (reviewed by Beavo and Reifsnyder, 1990). However, PDEs I and II do not play an important role in positive inotropic effects in mammalian heart, whereas PDEs III and IV are closely associated with positive inotropy in cardiac tissue of mammals (Kajimoto et al., 1997). Therefore, the following introduction of PDEs is mainly focused on PDEs III and IV.

PDE I. Ca^{2+}-Calmodulin-dependent PDE (Ca^{2+}/CaM-PDE).

Ca^{2+}/CaM-PDE is activated by Ca^{2+}-calmodulin. Ca^{2+}/CaM-PDE hydrolyzes both cAMP and/or cGMP, depending on the animal species. It hydrolyzes both cAMP and cGMP in guinea pig heart with both a low affinity (K_m= 50 μM) and a high affinity (K_m= 1 μM) (Weishaar et al., 1986), whereas it seems to hydrolyze cGMP alone in rat heart (Thompson et al., 1979). PDE I is a soluble enzyme found in cytosol in guinea pig, rat and human ventricle myocytes (Reeves et al., 1987; Bode et al., 1988-89). Although inhibition of PDE I may be associated with stimulation of $I_{Ca\text{-}L}$, its potency is weakest among PDEs I-IV with respect to modulation of $I_{Ca\text{-}L}$. PDE I is selectively inhibited by M& B 22,498 (Weishaar et al., 1987).

PDE II. cGMP-stimulated PDE (cGs-PDE).

PDE II is activated by cGMP rather than calmodulin (Weishaar et al., 1987). PDE II hydrolyzes both cAMP and cGMP (Weishaar et al., 1987). The cAMP hydrolytic activity of PDE II can be stimulated by cGMP. In guinea pig heart, PDE II hydrolyzes both cAMP and cGMP with apparent equal affinity ($K_m \cong$ 20-30 μM). PDE II is found in the cytosol (Reeves et al., 1987; Weishaar et al., 1987; Bode et al., 1988-89). Inhibition of PDE II leads to stimulation of $I_{Ca\text{-}L}$ in human atrial cells (Rivet-Bastide et al., 1997). It has been suggested that, in comparison to amphibian ventricles, PDE II in mammalian ventricular cells plays a minor role in regulation of Ca^{2+} current (Fischmeister and Hartzell, 1990; Mery et al., 1991). Nonhydrolyzable 8-bromo-cGMP reduces $I_{Ca\text{-}L}$ by stimulation of cAMP breakdown in frog, but not in guinea pig and rat ventricular cells (Levi et al., 1989; Fischmeister and Hartzell, 1990; Mery et al., 1991). PDE II can be selectively inhibited by erythro-9-(2-hydroxyl-3-nonyl)adenine (EHNA) (Mery et al., 1995).

PDE III. cGMP-inhibited PDE (cGi-PDE).

PDE III is one of the major PDEs involved in positive inotropy in mammalian hearts (Kajimoto et al., 1997). PDE III hydrolyzes both cAMP and cGMP with a high affinity (K_m in the range of 0.1-0.8 μM) and the Vmax for cGMP hydrolysis is approximately one-tenth of the Vmax for cAMP (Beavo 1995; Conti et al., 1995; Manganiello et al, 1995). PDE III is inhibited by cGMP and by cardiotonic PDE III inhibitors including amrinone, milrinone, enoximone, imazodan, indolidan and cilostamide (Harrison et al., 1986; Beavo and Reifsnyder, 1990).

The PDE III family is composed of two members, PDE3A and PDE3B. Human PDE3A and 3B are encoded by different genes on chromosomes 12 and 11, respectively (Degerman et al, 1997). PDE3A is present in heart and platelets, whereas PDE3B is found in adipose tissue, brain and liver (Grant and Colman, 1984; Harrison et al., 1986; Pyne et al., 1987; Meacci et al., 1992; Taira et al., 1993). Both PDE3A and 3B can be detected in human vascular smooth muscle (Palmer and Maurice, 2000).

The PDE3 catalytic domain in the C-terminal is distinguished from those of other PDE families by a unique 44 amino acid insertion (Dergerman et al., 1997). PDE3A and PDE3B differ in the insertion, only sharing 39% amino acid identity. Although PDE3A and PDE3B are quite different in the N-terminal regions, both of them have hydrophobic membrane-associated domains. Two human PDE3A mRNA species of ~7.6 and ~4.4 kilobases encode predicted ~125- and 80-kDa proteins, respectively (Kasuya et al., 1995). The two transcripts from the same gene are transcribed from different start transcription sites, indicating that they have different N-terminal regions. Expression of the two PDE3A cDNAs has shown that the ~125- and 80-kDa proteins are predominantly present in particulate and cytosolic fractions, respectively (Kasuya et al., 1995). Another study has shown that truncated recombinant PDE3 lacking the hydrophobic domain in the N-terminus is predominantly cytosolic, whereas full-length PDE3 recombinant is predominantly particulate (Leroy et al., 1996). The hydrophobic domain in the N-terminus in the longer mRNA may be critical for membrane association (Kasuya et al., 1995; Leroy et al., 1996).

Major therapeutic actions of PDE III inhibitors include positive inotropic effects in heart, dilation of vascular smooth muscle and inhibition of platelet aggregation (Hidaka

et al., 1984; Weishaar et al., 1985; Alvarez et al., 1986; Morgan et al., 1986). PDE III activities have been found in both cytosolic and SR-enriched fractions of mammalian myocardium (Kithas et al., 1988; Artman et al., 1989; Smith et al., 1993). However, the positive inotropic response to PDE III inhibitors is associated with inhibition of membrane-bound PDE III (Weishaar et al., 1987). It has been shown that the effect of the specific PDE III inhibitor LY195115 (indolidan) is mainly attributed to inhibition of PDE III in the SR (Kauffman et al., 1986, Kauffman et al., 1989). These studies indicate that local increases in cAMP in intracellular compartments may be important for the positive inotropic responses to specific PDE III inhibitors (Weishaar et al., 1992). Moreover, in left ventricular myocardium from human, canine, rabbit and guinea pig hearts, it has been reported that SR-associated PDE III is a phosphoprotein that corresponds to the predicted ~125kDa protein, whereas cytosolic PDE III is a phosphoprotein with lower molecular weight (Smith et al., 1993). Furthermore, Lugnier et al. have shown that PDE III is primarily located in T-tubule junctional SR structures (Lugnier et al., 1993). Thus, SR-associated PDE III plays a major role in positive inotropic effects in heart.

PDE IV. cGMP-noninhibitable PDE or cAMP-specific PDE.

PDE IV specifically hydrolyzes cAMP with a K_m of approximately 1 μM. Although it hydrolyzes cGMP, the K_m for cGMP hydrolysis is more than 50 μM (Conti et al., 1992). Specific inhibitors of PDE IV include rolipram and RO201724. PDE IV is present in many tissues including cardiac muscle, liver, kidney, gonads, brain and tracheal smooth muscle (Burns et al., 1996). PDE IV activities are found in both the cytosol and/or the plasma membrane. The PDE IV gene family consists of PDE4A, PDE4B,

PDE4C, and PDE4D. It has been shown that the "long" isoforms of the human PDE4D (PDE4D3, PDE4D4 and PDE4D5) that contains distinct regions of N-terminal sequence is present in the particulate fraction, whereas the "short" isoforms of the human PDE4D (PDE4D1, PDE4D2) that lack the distinct regions are only found in cytosol (Bolger et al., 1997). Since the N-terminal of PDE IV has important functions including binding to membranes, the N-terminal regions are thought to be responsible for association with the plasma membrane (Shakur et al, 1993; Bolger et al., 1997; Torphy and Page, 2000). Furthermore, a study of the distribution of PDE activities in heart has suggested that PDE IV is mainly associated with the surface sarcolemmal membrane (Lugnier et al., 1993). Inhibition of PDE IV is involved in stimulation of $I_{Ca\text{-}L}$ and its potency regarding modulation of $I_{Ca\text{-}L}$ is strongest among PDEs I-IV (Verde et al., 1999).

PDE and the VSRM

PDEs may play an important role in regulation of the VSRM. Studies conducted with patch-pipettes have shown that inclusion of the PDE-resistant analogues, 8-bromo- and dibutyryl-cAMP to patch-pipette solutions restores the VSRM (Hobai et al., 1997; Zhu et al, 1997; Ferrier et al., 1998). However, the VSRM cannot be restored by unsubstituted cAMP (tris- or Na-salt) (Ferrier et al., 2000b), which is easily subject to hydrolysis by PDEs (Meyer and Miller, 1974). In addition, the non-selective PDE inhibitor isobutyl-methylxanthine (IBMX) can activate the VSRM in cells dialyzed with pipette solutions without inclusion of cAMP or calmodulin (Ferrier et al., 2000b). These results suggest that inhibition of PDE can activate the VSRM by prevention of breakdown of cAMP.

In this current study, we hypothesize that cardiac contractions triggered by the VSRM can be potentiated by non-specific PDE inhibitors such as IBMX and by specific PDE III inhibitors such as amrinone.

4. DEPRESSED CONTRACTILE FUNCTION AND ALTERATIONS IN CARDIAC E-C COUPLING IN CARDIOMYOPATHIC HAMSTERS

The VSRM has been demonstrated to be an important component of cardiac contractile function in normal heart. However, it is not yet known whether disruptions in the VSRM might contribute to depressed contractile function in heart disease. Therefore, it is important to understand whether the VSRM is depressed in diseased hearts that display decreased contractile performance.

The animal model of cardiomyopathy and heart failure

One animal model of heart disease that exhibits reduced cardiac contractile function is the golden Syrian cardiomyopathic (CM) hamster. Inbred strains of golden Syrian CM hamsters are well-characterized genetic models of cardiomyopathy and heart failure (Bajusz, 1969; Bajusz et al., 1969). Cardiomyopathy is a primary disorder of cardiac muscle that leads to abnormal myocardial performance (Mason, 1994). It is not the result of other diseases such as myocardial infarction, arterial hypertension, valvular stenosis or regurgitation (Mason, 1994). CM hamsters have both hereditary cardiomyopathy and muscular dystrophy (Hunter et al., 1984). It has been shown that there is a deficiency in the 50-kDa dystrophin-associated glycoprotein in the sarcolemma of both cardiac and skeletal muscles from the BIO 14.6 strain of Syrian CM hamsters (Roberds et al., 1993).

This dystrophin-associated glycoprotein provides a linkage between the subsarcolemmal cytoskeleton and the extracellular matrix (Roberds et al., 1993). The primary genetic defect in the BIO 14.6 CM hamster is a defect in the gene that codes for the δ-sarcoglycan (δ-SG) protein in heart and skeletal muscle (Sakamoto et al, 1997). Studies have demonstrated that a large genomic deletion includes a 30 kb interval 5' upstream of the second exon as well as the first exon of the δ-SG gene (Sakamoto et al, 1997; Sakamoto et al., 1999). A deficiency in δ-SG is thought to cause perturbation of the dystrophin-glycoprotein complex and impair sarcolemmal integrity (Straub et al., 1998). Thus, disruption of the dystrophin-glycoprotein complex may play a role in cardiac and skeletal muscle necrosis in CM hamsters (Roberds et al., 1993).

CHF 146 CM hamsters

Most studies on Syrian CM hamster models have used either Bio 14.6 or UM-X7.1 strains with hypertrophic cardiomyopathy. The Bio 14.6 strain was introduced by Bajusz et al. at the Bio-Research Institute (Cambridge, Massachusetts) (Bajusz et al., 1969). The UM-X7.1 strain was a derivative of the Bio 14.6 strain and was developed at the University of Montreal (Jasmin and Proschek, 1982). The CM hamsters used in this study were CHF 146 hamsters purchased from Canadian Hybrid Farms (Halls Harbour, Nova Scotia, Canada). The CHF 146 CM hamster is descended from the BIO 14.6 line (Hunter et al., 1984).

Alterations in cardiac muscle are noted as early as 30 days of age in CM hamsters. Dilatation of the right ventricle is observed at 30 days of age and necrosis begins at 40-50 days of age in these CM hamsters (Jasmin and Proschek, 1982). In CM hamsters at 5

weeks of age, echocardiography has shown a mildly enlarged diastolic dimension with reduced left ventricular percent fractional shortening (Ikeda et al., 2000). Left ventricular percent fractional shortening and diastolic dimension further is decreased by 9 weeks of age (Ikeda et al., 2000). By 45 days of age, CM hamsters show a decreased stroke volume, cardiac output and rate of rise of left ventricular developed pressure (dP/dt) with an increased left ventricular end diastolic pressure (Awad and Welty, 1990). By 60 days of age, extensive necrotic lesions with some calcium deposition are present in left ventricles (Hunter et al., 1984). At this age, CM hamsters show focal myolysis with loss of sarcoplasm and very mild fibrosis in the heart (Hunter et al., 1984). At 90 days of age, severe necrotic lesions with obvious Ca^{2+} deposition can be found in both left and right ventricles. Scarring and calcification are remarkable in CM heart when necrosis reaches its peak around 90 days of age (Hunter et al., 1984). Mild heart failure, characterized as measurable fluid accumulation and liver enlargement, is present by 90 days of age in CHF 146 hamsters (Hunter et al., 1984). At the same time, gross dilatation of the right auricle become obvious. By 120 days of age, extensive fibrotic and calcified lesions are found in the CM heart. Ventricular hypertrophy progresses from about 120 days of age in CM hamsters (Jasmin and Proschek, 1982; Hunter et al., 1984). In animals older than 120 days, patchy interstitial fibrosis is detected in CM hamster ventricles. The terminal stage of heart failure occurs at between 200-300 days of age in CM hamsters (Jasmin and Proschek, 1982). Thus, the CM hamster exhibits predictable and progressive cardiomyopathy with hypertrophy, dilatation and the terminal stage of heart failure.

Depressed contractility and abnormalities in cardiac Ca^{2+} homeostasis in cardiomyopathic hamsters

It is well established that contractile performance is reduced in CM hamster hearts. At the single myocyte level, decreased cell shortening is observed in myocytes from 8-month old hamsters (Sen et al., 1990b; Sen et al., 1990c). Reduced contractility of isolated muscle from CM hamster ventricles also is documented (Capasso et al., 1989; Rouleau et al., 1989; Strobeck et al., 1997). Furthermore, impaired contractile function has been reported at the organ level in CM hearts (Awad and Welty, 1990; Buser et al., 1995; Ikeda et al., 2000).

Abnormalities in cardiac E-C coupling are thought to play an important role in depressed contractile function in the CM hamster heart. Fundamental alterations in cardiac Ca^{2+} homeostasis are believed to contribute to the abnormalities in contractile performance (Tomaselli and Marban, 1999). A comprehensive discussion of cardiac Ca^{2+} homeostasis in diseased heart is beyond the scope of the current section. The following introduction of abnormalities in Ca^{2+} -handling proteins in heart dysfunction is limited to the CM hamster.

$I_{Ca\text{-}L}$ and $I_{Ca\text{-}T}$

Since previous studies have used conditions that can inactivate the VSRM, it is unclear whether depressed contraction in CM hearts is attributable to CICR, the VSRM or both mechanisms. $I_{Ca\text{-}L}$ is a major trigger for CICR. In young CM hamsters that are at the prehypertrophic stage of disease, most studies suggest that $I_{Ca\text{-}L}$ density is not altered. The maximum number of dihydropyridine receptor binding sites (Bmax) is not

significantly changed between 35 to 60 day old CM hamster hearts and age-matched controls, indicating that the number of Ca^{2+} channels is unchanged (Howlett et al., 1988; Bazan et al., 1991). In agreement with these findings, Tawada-Iwata reported that $I_{Ca\text{-}L}$ density is unchanged in 30- to 70-day-old CM hamsters (Tawada-Iwata et al., 1993). In hypertrophied CM hearts, the Bmax of nitrendipine receptors is increased (Finkel et al., 1987). In CM hamsters at the stage of overt heart failure, $I_{Ca\text{-}L}$ density has been reported to be either unchanged (Sen et al., 1990b; Sen and Smith, 1994) or decreased (Rossner, 1991; Hatem et al., 1994). Similarly, the Bmax of dihydropyridine receptors is unchanged (Finkel et al., 1987; Sen et al., 1990b). These findings are consistent with findings in other animal models of heart failure (Richard et al., 1998). Interestingly, $I_{Ca\text{-}T}$ density is increased in CM hearts at the stage of overt heart failure (Sen and Smith, 1994). In addition, $I_{Ca\text{-}T}$ is activated and inactivated at more negative potentials (Sen and Smith, 1994). Therefore, it appears that neither $I_{Ca\text{-}T}$ nor $I_{Ca\text{-}L}$ contributes to depressed contractility in young CM hamster hearts.

SR Ca^{2+} release channels / RyRs and Ca^{2+} content

There is evidence that SR Ca^{2+} release channels are altered in CM hearts. Lachnit et al. showed that crude homogenates exhibited a reduction in [^{3}H]ryanodine binding sites and mRNA levels in Bio 14.6 CM hamster hearts, at the prehypertrophic stage of disease (Lachnit et al., 1994). Another report showed that in hypertrophic CM hamster hearts, the Bmax of RyR was normal, but RyR protein levels were increased (Ueyama et al., 1998a). The increase in RyR protein level may be related to compensation for impaired contractile function (Ueyama et al., 1998a). In CM hamsters at the stage of overt heart

failure, both RyR protein levels and the Bmax of RyR are significantly decreased (Ueyama et al., 1998a; Ueyama et al., 1998b).

There also is evidence for changes in Ca^{2+} transients in CM hearts. It has been shown that peak Ca^{2+} transients are significantly reduced in CM hamsters (Kruger et al., 1994). Another study explored whether there were differences in SR Ca^{2+} load in CM hearts. Hatem et al found that there was no significant difference in Na^{+}-Ca^{2+} exchanger current, activated by rapid application of caffeine, in 220 to 300 day old normal and CM hamsters, indicating that SR Ca^{2+} load was unchanged in CM hearts (Hatem et al., 1994).

β-adrenoceptor-adenylyl cyclase-cAMP-PKA pathway

The activation of the sympathetic nervous system may lead to increased levels of circulating catecholamines. High plasma levels of catecholamines in heart failure are thought to result in a reduction in β-adrenergic receptor density and activity (de Tombe, 1998). A reduction in β_1-adrenoceptors has been found in CM hamster hearts (Kaura et al., 1996). Moreover, the cardiac norepinephrine concentration is significantly increased in CM hamsters at 90 days of age (Ikegaya et al., 1992). However, continuous exposure of myocytes to β-adrenergic agonists, such as elevated circulating catecholamines, results in desensitization of β_2-adrenergic receptors (Hammond, 1993). In CM hamsters at 90 days of age, functional uncoupling of the stimulatory guanine nucleotide-binding protein (G_s) to adenylyl cyclase was observed in CM hamster heart (Kessler et al., 1989). In addition, forskolin-stimulated adenylate cyclase activity also is significantly depressed in CM hamsters (Ikegaya et al., 1992; Kaura et al., 1996). Chronic stimulation by catecholamine infusion can cause increased inhibitory guanine nucleotide-binding protein

(G_i) expression (Eschenhagen et al., 1992a; Mende et al., 1992). Increased G_i content (Sen et al., 1990b; Sethi et al., 1994; Kaura et al., 1996) and functional activity (Sethi et al., 1994; Kaura et al., 1996) have been found in CM hearts. Taken together, a reduction in phosphorylation by the cAMP-PKA pathways is expected in CM hearts because of decreases in adenylyl cyclase, increases in G_i activity and functional uncoupling of G_s to adenylyl cyclase.

The VSRM in heart disease

The VSRM has never been examined in diseased heart. Earlier studies of cardiac E-C coupling in normal and diseased heart used conditions that can inhibit the VSRM (reviewed by Howlett and Ferrier, 1998). First, patch-clamp experiments were often conducted at room temperature (22-25 °C) in order to slow down the "run-down" of Ca^{2+} current. However, it has been shown that the VSRM is inhibited at room temperature (Ferrier and Redondo, 1996). Second, the VSRM cannot be observed if a holding potential of –40 mV is used to inactivate the Na^+ current to allow measurement of inward Ca^{2+} current. Since the VSRM exhibits steady-state inactivation and is fully inactivated by a holding potential of –35 mV, a holding potential of –40 mV almost abolishes the VSRM component of contractions (Howlett and Ferrier, 1997). As a result, only bell-shaped Ca^{2+} transient-voltage and contraction-voltage relationships are observed from a holding potential of –40 mV. Third, patch-pipette solutions typically have no exogenous cAMP or calmodulin. It has been demonstrated that patch-pipette solutions with cAMP (Zhu et al., 1997; Hobai et al., 1997; Ferrier et al., 1998) or calmodulin (Zhu and Ferrier, 2000) restore the VSRM, which is otherwise absent in experiments conducted with patch

clamp techniques due to cell dialysis. Therefore, since previous studies of cardiac E-C coupling utilized one or more conditions that could inhibit the VSRM, the contribution of this important trigger to contraction in diseased heart has not yet been examined.

The VSRM is an important component of cardiac contraction. Thus, exploration of the VSRM in CM hamster hearts will provide new insight into abnormalities of Ca^{2+} homeostasis that contribute to impaired contractile performance in heart disease. We hypothesize that contractions initiated by the VSRM are depressed in CM hamster heart. Furthermore, since the cAMP/PKA pathway is involved in modulation of the VSRM, we also hypothesize that agents that increase intracellular cAMP levels, such as the PDE III inhibitor amrinone, may restore the VSRM if it is depressed in CM heart.

5. HYPOTHESIS AND OBJECTIVES

Cardiac E-C coupling plays an essential role in contractile function in heart muscle. Abnormalities in cardiac E-C coupling are closely associated with impaired contractile performance in animal models of heart disease. Recent studies provide evidence that the VSRM plays an important role in cardiac E-C coupling in normal heart. Therefore, we hypothesize that abnormalities in the VSRM may contribute to depressed contractile performance in heart diseases. The specific objectives of the first part of the current study are: 1) to determine whether contraction of ventricular myocytes from 90-100 day old CM hamsters is decreased; and 2) to determine whether the impaired contractile performance is attributed to depressed contractions initiated by CICR, the VSRM or both mechanisms.

Studies have demonstrated that the cAMP-PKA pathway is involved in regulation of the VSRM. Amrinone is a specific PDE III inhibitor and can increase intracellular cAMP levels by prevention of degradation of cAMP. We hypothesize that amrinone will increase cardiac contractions triggered by the VSRM in ventricular myocytes from adult guinea pigs. The specific objectives of the second part of the current study are: 1) to determine whether amrinone can increase contraction in ventricular cells from guinea pig hearts; and 2) to determine whether the effects of amrinone are mediated by effects on contractions initiated by CICR, the VSRM or both mechanisms.

If our studies show that impaired cardiac contraction is attributed to depression of the VSRM in CM heart and if amrinone can increase cardiac contraction via potentiation of the VSRM component of contraction, we hypothesize that amrinone can improve impaired contraction by restoring VSRM contractions in CM hamster heart. The specific objectives of the third portion of my studies are: 1) to determine whether amrinone can improve impaired contractile performance in CM hamster heart; and 2) to determine whether depressed VSRM contractions can be restored by amrinone.

MATERIALS AND METHODS

1. ANIMALS

Experiments were conducted on cardiac ventricular myocytes isolated from either guinea pigs or hamsters. Albino guinea pigs, weighing 250-400 g, were purchased from Charles River Laboratories (St. Constant, Quebec, Canada). Approximately 90% of guinea pigs were male and the rest were female. Other experiments were conducted on ventricular myocytes from 90-100 day old golden Syrian cardiomyopathic (CM) hamsters (CHF 146) and age-matched normal golden Syrian hamsters (CHF 148). All the hamsters were male and were purchased from Canadian Hybrid Farms (Halls Harbour, Nova Scotia, Canada). All experiments were conducted in accordance with the guidelines published by the Canadian Council on Animal Care (Canadian Council on Animal Care, Volume 1, 1980; Volume 2, 1984, Ottawa, Ontario) and were approved by the Dalhousie University Committee on Animal Care. All the animals were kept in rooms with a 12-hour day/night cycle in the Dalhousie University Carleton Animal Care facility with free access to food and water.

2. VENTRICULAR MYOCYTE ISOLATION

Procedures for guinea pig cells

Two different procedures were employed for isolation of ventricular myocytes from guinea pigs in two different labs since the guinea pig cells were shared. Both methods gave rise to rod-shaped cells with clear striations. The viability of the cells was about 90% with each of the two methods. The two procedures for single cell isolation were employed at random and with a similar frequency.

Procedure 1

Guinea pigs were injected with heparin (3.3 IU/g) and anaesthetized with sodium pentobarbital (160 mg/kg) intraperitoneally 10 minutes prior to opening the chest. A parasternal incision was performed to open the thoracic cavity. The aorta was cannulated retrogradely via an incision of the ascending aorta and the heart was perfused with nominally Ca^{2+}-free solution (Table 1) bubbled with 100% O_2 (Union Carbide, Canada Limited). A peristaltic pump (Cole-Parmer Instruments Co., Chicago, IL) was employed to perfuse the heart at a rate of 7 ml/min. The temperature of the solution was maintained at 37 °C with a heated water bath (Model Haake D1-L, Fisher Scientific, Berlin, Germany).

Following the 7-minute perfusion with nominally Ca^{2+}-free solution, 25 mg collagenase A (Boehringer Mannheim) and 4.8 mg protease (Sigma type XIV) were then included in 50 ml of this solution. The heart was subjected to enzymatic dissociation for an additional 5 minutes. The perfusion pressure was recorded to monitor adequate enzymatic digestion. After enzymatic dissociation, the ventricles were cut from the heart and minced in a high-potassium substrate enriched solution (Table 2) (You et al., 1994).

Procedure 2

Guinea pigs were injected with heparin and sodium pentobarbital as described above. After 10 minutes, the thoracic cavity was quickly opened and the heart was excised and placed in nominally Ca^{2+}-free buffer solution (Table 3). The heart was then mounted on a Langendorff column and perfused retrogradely via the aorta with the same nominally

Table 1. Composition of the Nominally Ca^{2+}-Free Solution for Guinea Pig Myocyte Isolation in Procedure 1

Compound	*Concentration (mM)*
NaCl	120
KCl	4
$MgSO_4$	1.2
KH_2PO_4	1.2
HEPES	10
Glucose	12

pH 7.4 with NaOH

Table 2. Composition of High K^+ Solution

Compound	*Concentration (mM)*
KCl	30
KOH	85.5
KH_2PO_4	30
$MgSO_4$	3
Glutamic Acid	50
Taurine	20
HEPES	10
EGTA	0.5
Glucose	10

pH 7.4 with KOH

Table 3. Composition of the Nominally Ca^{2+}-Free Solution for Guinea Pig Myocyte Isolation in Procedure 2

Compound	*Concentration (mM)*
NaCl	120
KCl	3.8
$MgSO_4$	1
NaH_2PO_4	4
$NaHCO_3$	22
Glucose	5.5

pH 7.4 with NaOH

Ca^{2+}-free buffer solution for 7 minutes. The solution was maintained at 37 °C with a circulating water bath and gassed with 95% O_2/5% CO_2 (Union Carbide, Canada Limited). The fluid level in the Langendorff column was kept constant to maintain adequate perfusion pressure. The perfusate was then changed to 50 ml of nominally Ca^{2+}-free buffer solution supplemented with 50 mg collagenase (Worthington I) and 5 mg protease (Sigma type XIV). At the same time, the Ca^{2+} concentration was increased to 40 μM. The heart was subjected to enzymatic dissociation for 3-5 minutes. The ventricles were excised from the heart and minced in high-potassium substrate enriched solution described as above (Table 2).

In both procedures, chunks of tissue were rinsed with high-potassium solution several times to wash away residual enzyme. The tissue was stored in this solution up to eight hours. Before each transfer to the experimental chamber, the minced tissue was washed again. The freshly dissociated cells were then decanted and were ready for the experiment.

Procedures for hamster cells

Ten minutes prior to opening the chest, 90- to 100-day-old normal (CHF 148) and CM (CHF 146) hamsters were injected with heparin (3.3 IU/g) and anaesthetized with sodium pentobarbital (80 mg/kg) intraperitoneally. The thoracic cavity was opened with a parasternal incision. An incision of the ascending aorta was performed and then the aorta was cannulated retrogradely. The heart was perfused with the 100% oxygenated solution described above (Table 1) supplemented with 50 μM $CaCl_2$. A peristaltic pump (Cole-Parmer Instruments Co., Chicago, IL) was used to perfuse the heart at a rate of 10

ml/min. A heated water bath was employed to maintain the temperature of the solution at 37 °C. After the 6-minute perfusion with 50 μM Ca^{2+} solution, the hamster heart was perfused with nominally Ca^{2+}-free solution (Table 1) for an additional 6 minutes. Next, 20 mg collagenase A (Worthington), 15 mg protease (Boehringer Mannheim Corporation), 1.0 mg trypsin (Sigma) and 5 μl of 0.5 M $CaCl_2$ were then included in 50 ml of this solution (Table 1) (with final Ca^{2+} concentration of 50 μM). The hamster heart was subjected to enzymatic digestion for approximately 20 minutes. The perfusion pressure was recorded to ensure adequate enzymatic digestion. After enzymatic digestion, the ventricles were removed from the heart and minced in high-potassium substrate enriched solution (Table 2). This isolation procedure yielded about 60-70% rod-shaped, striated ventricular cells. No apparent difference in myocyte viability between normal and CM hamsters was noted.

Tissues were washed with high-potassium solution several times to remove residual enzyme. Myocardial tissue was stored in the same solution up to eight hours. Prior to each transfer to the experimental chamber, the minced tissue was rinsed again.

EXPERIMENTAL SETUP

The freshly isolated ventricular myocytes were placed in a perfusion chamber (24 x 12 x 6 mm) with an approximate volume of 1.7 ml. This rectangular shaped chamber was mounted on the stage of an inverted microscope (Model IMT-2, Olympus Optical Co., Ltd., Tokyo, Japan). The microscope, in turn, was mounted on an antivibration table that had four inflated rubber inner tubes under metal plates to minimize vibration. The perfusion chamber was fabricated from a piece of plexiglass with a plastic coverslip as its

bottom. The inlet and outlet of the perfusion chamber were at the opposite ends of the chamber. Ventricular cells were allowed to settle to the bottom of the chamber for 5 minutes prior to superfusion. In experiments where a rapid solution- switching device was employed (discussed in detail later), cells were allowed to adhere to the bottom of the bath for 15 minutes.

A pump (Model P20T, Dungey Inc., Agincourt, Ontario) was used to deliver the extracellular solution from a reservoir to the perfusion chamber at a rate of 3 ml/min. The solution turnover time from the reservoir to the chamber was approximately 90 seconds. The turnover time was determined experimentally by measuring the alteration in resting membrane potential in response to a 100% increase (from 2 mM to 4 mM) in potassium concentration of the extracellular solution. In the majority of experiments the extracellular solution contained 145 mM Na^+ solution (Table 4). In a few experiments a low sodium (45 mM) solution was used. This solution was supplemented with 100 mM choline to preserve osmolarity (Table 5). The temperature of the solution in the chamber was maintained at 36.5 ± 0.5 °C with a custom designed, circulating heated water system driven by an immersion circulating heater (Haake E2 model, Fisher Scientific, Berlin, Germany).

In all experiments, high-resistance microelectrodes (18-25 MΩ) were used to minimize cell dialysis. The high resistance microelectrodes were made of borosilicate capillary tubes with an outer diameter of 1.2 mm and inner diameter of 0.69 mm (Sutter Instruments Co., Novato, CA). These microelectrodes were made just prior to each experiment with a Flaming/Brown micropipette puller (Model P-87, Sutter Instruments Co., Novato, CA). Microelectrodes were filled with filtered 2.7 M KCl. The tip of a

Table 4. Composition of " Full Na^{+}" Solution

Compound	*Concentration (mM)*
NaCl	145
KCl	4
$MgCl_2$	1
$CaCl_2$	2
HEPES	10
Glucose	10
Lidocaine	0.2

pH 7.4 with NaOH

Table 5. Composition of "Low Na^{+}" Solution

Compound	*Concentration (mM)*
NaCl	45
Choline Cl	100
KCl	4
$MgCl_2$	1
$CaCl_2$	2
HEPES	10
Glucose	10
Lidocaine	0.2

pH 7.4 with NaOH

microelectrode was filled first with a drop of KCl. The KCl was injected from the back end of the pipette and it filled the tip by capillary action. Once the tip was filled, the remainder was back-filled carefully to ensure that no bubbles formed. The microelectrode was then inserted into a microelectrode holder (World Precision Instruments, Inc., Sarasota, FL) also filled with 2.7 M KCl. The microelectrode holder was, in turn, inserted into a pin jack on the headstage of a voltage clamp amplifier (Axoclamp 2A, Axon Instruments, Foster City, CA). A Ag/AgCl pellet at the bottom of the microelectrode holder provided an electrical interface between the electrolyte in the microelectrode and the amplifier. The headstage, which was connected to the main amplifier, was mounted on a high-quality precision mechanical micromanipulator (Leitz Inc, Wetzlar, Germany). The precision micromanipulator anchored to the antivibration table allowed impalement of single myocytes.

A silver wire connected to the headstage was utilized to ground the experimental chamber, which also completed the electric circuit. One end of the silver wire was chlorided with liquid household bleach (e.g., Javex), which contained sodium hypochlorite, to provide a Ag/AgCl coating before use. The Ag/AgCl wire was immersed in a small well filled with 2.7 M KCl. The small well and the experimental chamber were connected by an agar / KCl bridge. The U-shaped agar / KCl bridge was made from a length of glass tubing filled with 1% agar in 2.7 M KCl. The agar / KCl bridge limited the mobility of ions through the bridge and minimized junction potentials that might result from changes of the experimental solutions.

4. DATA RECORDING

Electrophysiological recording

The electrophysiological recording started with compensating for junctional potentials. When the tip of the microelectrode was immersed in the experimental solution, the junction potential was cancelled by zeroing the input voltage offset dial on the Axoclamp 2A amplifier. The junction potential results from various liquid and metal interfaces in the electrical circuit between the amplifier and ground. Next, the resistance of the microelectrode was measured and compensated before impalement of a cell. The resistance of the microelectrode was measured by passing 1 nA current. According to Ohm's law, the voltage drop is the product of current and resistance (E=IR, where E is voltage drop, I is current and R is resistance). When a 1 nA current was passed, the value of voltage in mV (e.g., 22 mV) shown on the LED meter on the amplifier indicated the value of resistance of the microelectrode in MΩ (e.g., 22 MΩ). The resistance of the microelectrode was then compensated by adjusting the voltage drop across the electrode to 0 mV. This was achieved by subtracting a signal proportional to the microelectrode voltage from amplifier output using "bridge balance" techniques within the Axoclamp 2A amplifier. Therefore, only the voltage drop across the cell membrane would be recorded during experiments. The capacitance of the microelectrode also was compensated before impalement, because capacitance could slow the rate of voltage changes. The capacitance compensation was made by adjusting the recording to follow the rectangular waveform as rapidly as possible without oscillation.

In order to impale the cell, the electrode was slowly lowered to approach, touch and press against the cell until the cell was impaled. Sometimes impalement of the myocyte

was performed with the aid of a "buzz" function, which was transient overcompensation of the capacitance with a very brief designated duration. The "buzz" helps the microelectrode to penetrate the myocyte. Sometimes a small negative current was applied to maintain the intracellular potential near the resting membrane potential immediately after impalement of the myocyte. In most cases, this negative current was removed gradually prior to voltage clamp experiments. The impalement was thought unsuccessful if the negative current injected initially was greater than 0.5 nA in order to maintain the intracellular membrane potential more negative than –80 mV.

In many experiments, voltage-clamp techniques were employed. Voltage clamp is achieved by measuring the potential across the membrane, comparing it with the desired potential and then injecting a current across the membrane sufficient to eliminate the difference between these two potentials. Within the Axoclamp 2A voltage clamp amplifier, one input to the differential amplifier is the measured membrane potential. This input is compared to the other input, which is a preset command potential determined by a specific voltage clamp protocol. A current from the output of the differential amplifier is injected into the cell to hold the membrane potential to the command potential, thereby "clamp" the voltage drop across the membrane. The magnitude of the current injected by the amplifier is the same as that of the membrane current of the cell in response to a change in membrane potential, but the polarity is opposite.

Since only one high-resistance microelectrode was used to impale a ventricular myocyte in the present study, this high-resistance microelectrode was utilized to both measure the membrane potential and inject the current. Thus, a discontinuous single-electrode voltage-clamp (dSEVC) mode with the Axoclamp 2A voltage clamp amplifier

was employed, in which measurement of the membrane potential and injection of the current occurred alternately (a sampling rate of 10-12 kHz). A sample-and-hold circuit samples the membrane potential and holds that for the rest of the cycle. The dSEVC is also known as switch clamp, since the amplifier switches between voltage recording and current injection during every cycle. After current injection, the amplifier switches back to voltage recording. The voltage recorded at this point largely includes the voltage drop across the high-resistance microelectrode, and therefore the microelectrode voltage must be allowed to have sufficient time to decay to zero before a new sample of the membrane potential can be taken. During dSEVC, the monitor output on the amplifier was continuously observed to ensure adequate time for the microelectrode voltage to completely decay before a new cycle began.

The voltage clamp protocols were generated with pCLAMP software (Axon Instruments, Inc, Foster City, CA). Digital oscilloscopes (Kikusui Model COR5541U, Kikusui Electronic Corp., Japan) were used to monitor voltage and current. The analog current and voltage signals from the amplifier were sent to a Labmaster analog-to-digital (A/D) interface at sample rates up to 50 kHz for digitizing. The digital signals were finally sent to a computer for display and storage. Acquisition and analysis of all data were also accomplished with pCLAMP software on a computer.

Cell shortening measurements

A closed-circuit television camera (Panasonic, Model 1-GP-CD60) was employed to acquire cell images. Cell images were displayed on a video monitor (Model OVM-12E12, Oriental Precision Co., Ltd., Sung Nam City, Korea). Unloaded cell shortening

was sampled at 120 Hz with a video edge detector (Model VED 103, Crescent Electronics, Sandy, UT). In some experiments (RESULTS Section I and II) the movement of one end of a cell was tracked. In others (RESULTS Section III), the movement of both ends of a cell was followed in order to measure cell length and percentage shortening. The output of the video edge detector was sent to a Labmaster (A/D) interface (TL1-125, Axon Instruments Inc.) and a digital oscilloscope (Kikusui Model COR5541U, Kikusui Electronic Corp., Japan). The digital signals of cell length and cell shortening were sent to a computer for display and storage. Acquisition and analysis of cell length and cell shortening were also accomplished with pCLAMP software on a computer.

Experimental protocols

All experiments were conducted at 37 °C. All extracellular buffer solutions included 200 μM lidocaine to inhibit Na^+ currents. In some experiments, 50 μM tetrodotoxin (TTX) was also employed to inhibit Na^+ currents. Specific details are indicated in the appropriate RESULTS section. In all experiments conducted on hamster myocytes, 2 mM 4-aminopyridine (4-AP) also was included in the extracellular buffer to inhibit the transient outward current because transient outward current would interfere with measurement of inward current. 4-AP was not employed on guinea pig myocytes because guinea pig ventricular myocytes lack transient outward current (Hoppe et al., 1999).

All voltage clamp protocols were performed with a holding potential of –80 mV. Ten conditioning pulses to 0 mV from the holding potential were given prior to test voltage steps to maintain consistent activation of the myocytes. Every conditioning pulse lasted

200 ms with the interpulse interval held at -80 mV for 150 ms between two conditioning pulses. Thus, the conditioning pulse train was delivered at a frequency of approximately 3 Hz. Following the last conditioning pulse, cells were repolarized and held at a post-conditioning potential (V_{PC}) of either -40 mV or -60 mV for 500 ms before test voltage steps unless otherwise specified in the appropriate RESULTS section.

3-isobutyl-1-methylxanthine (IBMX) (100 μM) and amrinone (100-1000 μM) were applied to myocytes by switching between different bath solutions that contained different concentrations of drugs. Cadmium (100 μM), TTX (50 μM) or caffeine (10 mM) was applied with a rapid solution switcher device for a brief period of time. Specific protocols will be described in the appropriate RESULTS section. The rapid solution switcher system had five barrels and was capable of delivering five different solutions (Levi et al., 1996). This device allowed the extracellular solution to be changed within approximately 300 ms. The rapid switcher was under the control of the voltage clamp protocol in pCLAMP software (version 6.0.3, Axon Instruments, Inc., Foster City, CA, USA) to ensure precise timing. The solution applied to the myocyte via the nozzle of the rapid solution switcher was maintained at 36.5 ± 0.5 °C by a heated circulating water system.

5. DRUGS AND CHEMICALS

Amrinone, lidocaine, caffeine and 4-AP were purchased from the Sigma Chemical Company (St. Louis, MO, USA). TTX (citrate-free) was purchased from Alomone Labs (Jerusalem, Israel), dimethyl sulfoxide (DMSO) from Molecular Probes (Eugene, OR, USA), choline chloride from Fisher Scientific (Fairlawn, NJ), IBMX and cadmium from

Calbiochem (La Jolla, CA, USA). The chemicals for buffer solutions were purchased from BDH Inc. (Toronto, Ontario, Canada), Fisher Scientific (Nepean, Ontario, Canada) or Sigma Chemical Co. (Oakville, Ontario, Canada).

A stock solution of amrinone (0.05 M) was prepared by dissolving the drug in 0.2 M HCl. The final buffer solution was adjusted to pH 7.40 with NaOH. IBMX was dissolved in 100% DMSO. The final concentration of DMSO in buffer solutions was 0.03%. Control solutions for IBMX experiments contained 0.03% DMSO to control for solvent effects. All other drugs were dissolved in deionized water or directly dissolved in buffer solutions.

6. DATA ANALYSES

Ionic currents, voltage and cell shortening were measured with pCLAMP software. The magnitude of peak inward current was measured as the difference between the peak downward deflection and a reference point at the end of the voltage step (Li et al., 1995). Cell capacitance was estimated by integrating the capacitive current with pCLAMP software. Cell capacitance is an index of cell surface area and the magnitude of currents is associated with cell area. Thus, cell capacitance can be utilized to normalize the magnitude of current and estimate current density. The amplitude of contraction was measured as the difference between maximum cell shortening and a reference point immediately before the onset of cell shortening. The amplitude of the second phasic contraction, triggered by a voltage clamp protocol with two sequential depolarizing steps, was measured with respect to a reference point immediately before the onset of the second phasic contraction. The amplitude of the caffeine-induced contracture was

measured as the difference between peak cell shortening and a reference point immediately before the onset of contracture. The integral of the caffeine-induced Na^+-Ca^{2+} exchange current (an index of SR releasable Ca^{2+} content) was calculated with pCLAMP software. When both ends of the cell were tracked by the video edge detector, both systolic and diastolic cell lengths were recorded and consequently fractional cell shortening could be calculated.

7. STATISTICS

All measured data are presented as means ± SEM (standard error of the mean). Differences between means from two experimental groups were analyzed with a Student's t-test. Differences between means from more than two experimental groups were analyzed by a one-way analysis of variance (ANOVA). Differences between current-voltage or contraction-voltage relationships were analyzed with a two-way repeated measures ANOVA. Post hoc comparisons were made with a Student-Newman-Keuls test. Differences were considered significant when $p < 0.05$. Statistical analyses were performed using Sigma Stat software (Jandel, version 2.03). The value of "n" represents the number of myocytes from which data were collected. No more than two replicates (myocytes) were collected from one heart.

RESULTS

1. CARDIAC EXCITATION-CONTRACTION COUPLING IN VENTRICULAR MYOCYTES FROM NORMAL AND CM HAMSTERS.

The VSRM makes a major contribution to cardiac E-C coupling in normal hearts. In this study, experiments were designed to test the hypothesis that the VSRM may contribute to depressed cardiac contraction in CM hamsters. However, it is possible that alterations in CICR may also contribute to poor contractile performance in CM hearts. Therefore, these studies examined the role of the VSRM and CICR in cardiac E-C coupling in this animal model of cardiomyopathy and heart failure.

(1) Evidence for a VSRM in normal hamster myocytes

The first series of experiments were designed to determine whether a VSRM exists in normal hamster ventricular myocytes. Previous studies in guinea pig ventricular myocytes have shown that activation of the VSRM persists when $I_{Ca\text{-}L}$ is blocked with Ca^{2+} channel blockers such as cadmium (Ferrier et al., 1998). Therefore, in the present study we determined whether VSRM contractions would be affected by the L-type Ca^{2+} channel blocker cadmium in normal hamster ventricular myocytes. These experiments were conducted in the presence of 50 μM TTX and 2 mM 4-AP. Figure 1-1 illustrates representative recordings of VSRM and CICR contractions and inward currents in the absence and presence of cadmium. The voltage clamp protocol shows that ten conditioning pulses from the holding potential of –80 mV to 0 mV were used to maintain continuous activation of cells prior to test steps. Cadmium (100 μM) was applied to the myocyte 3 s before and during the test step (Figure 1-1). The test step from –65 mV to

Figure 1-1. Activation of VSRM contractions was not dependent on Ca^{2+} entry via L-type Ca^{2+} channels in normal hamster myocytes. The voltage clamp protocol is shown at the top of the figure. 100 μM cadmium and 50 μM TTX were applied to the cell to inhibit L-type Ca^{2+} current and sodium current, respectively. Drugs were applied to 3s before test steps with a rapid solution switcher. A lower concentration of sodium (45 mM) with supplement of choline (100 mM) was used to increase contractions in this experiment. **Panel A:** Representative traces of contractions and currents activated by sequential steps to –40 and 0 mV. **Panel B:** Representative traces show that 100 μM Cd^{2+} substantially reduced the magnitude of L-type Ca^{2+} current and CICR contraction, but had little effect on the VSRM contraction in a normal hamster myocyte.

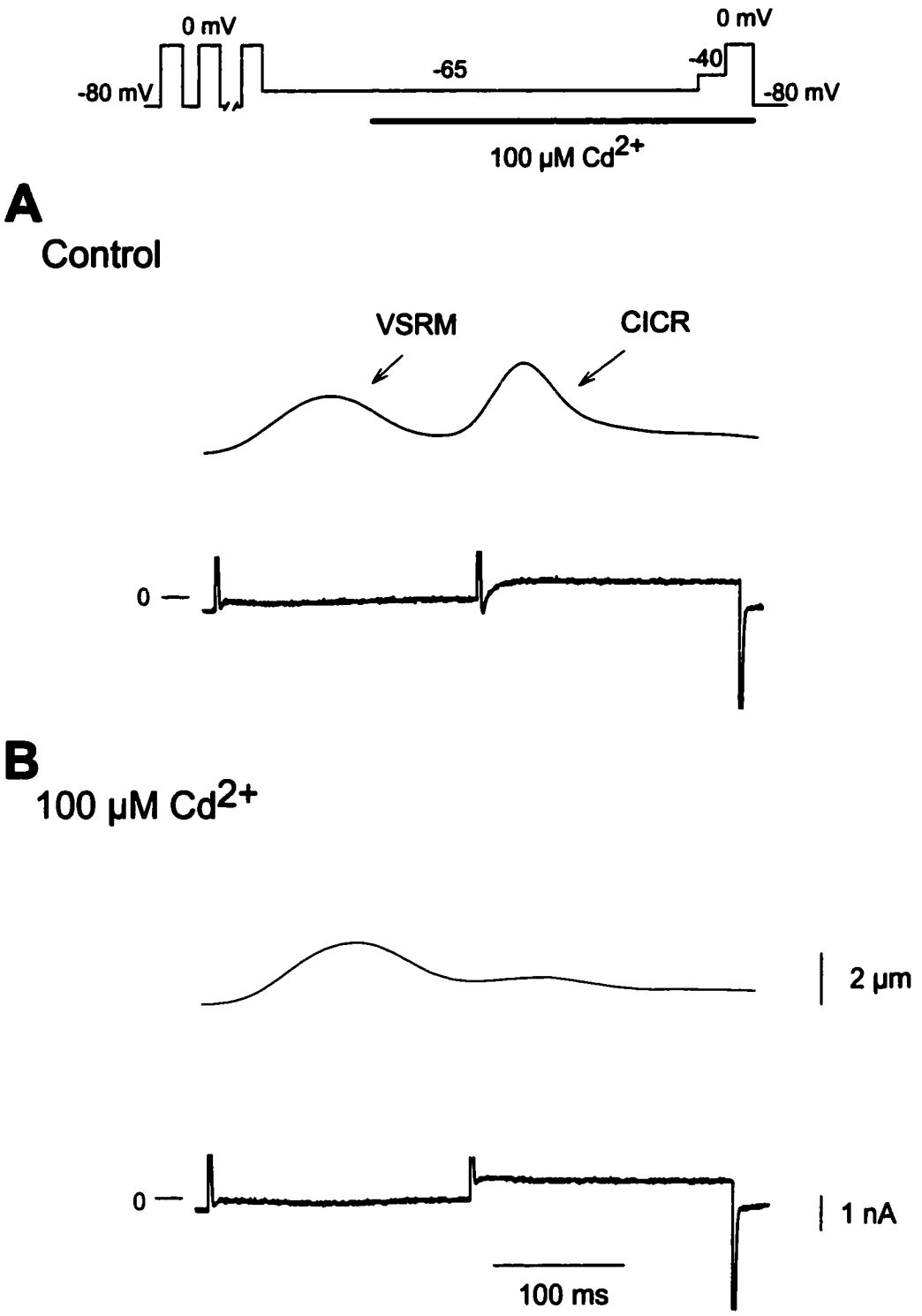
0 mV
0 mV
-80 mV
-65
-40
-80 mV
100 μM Cd2+
A
Control
VSRM
CICR
0
B
100 μM Cd2+
2 μm
0
1 nA
100 ms

Figure 1-1

–40 mV activated the VSRM, whereas the test step from –40 mV to 0 mV activated CICR only since the VSRM was inactivated (Ferrier and Howlett, 1995; Howlett and Ferrier, 1997; Howlett et al, 1998). Figure 1-1B demonstrates that $I_{Ca\text{-}L}$ and the CICR contraction were virtually abolished by 100 μM cadmium, but the VSRM contraction was not affected by rapid application of cadmium. Figure 1-2 shows mean data for experiments conducted as illustrated in Figure 1-1. VSRM contractions and currents activated by the test step to –40 mV were similar before and after exposure to cadmium (Figure 1-2A). However, the magnitudes of CICR contractions and $I_{Ca\text{-}L}$ were significantly decreased by cadmium ($P<0.05$). Thus, these results demonstrate that cadmium-resistant VSRM contractions are present in normal hamster myocytes.

(2) Contractile function in ventricular myocytes from normal and CM hamster hearts

The next series of experiments was designed to determine whether contractile performance was impaired in ventricular myocytes isolated from CM hamsters when compared to normal hamster myocytes. Figure 1-3A and B shows action potentials recorded from normal and CM myocytes. These studies were conducted in the absence of lidocaine, TTX and 4-AP to generate action potentials without currents blocked. The profile and duration of action potentials were similar between normal and CM cells. In both cell types, action potentials were characterized by a rapid upstroke and subsequent repolarization. However, the contractions activated by action potentials were markedly reduced in magnitude in CM myocytes compared to control (Figure 1-3C and D).

Figure 1-2. Mean data show that blockade of the L-type Ca^{2+} channel with cadmium virtually abolished L-type Ca^{2+} current and CICR contractions with little effect on the magnitude of VSRM contractions. Panel A: VSRM contractions initiated by a test step to –40 mV were not affected by 100 μM Cd^{2+}. Currents activated by this test step were not significantly changed before and after exposure to cadmium. **Panel B:** 100 μM Cd^{2+} significantly inhibited L-type Ca^{2+} current and CICR contractions. *Denotes significantly different from control ($p<0.05$), n= 6 myocytes.

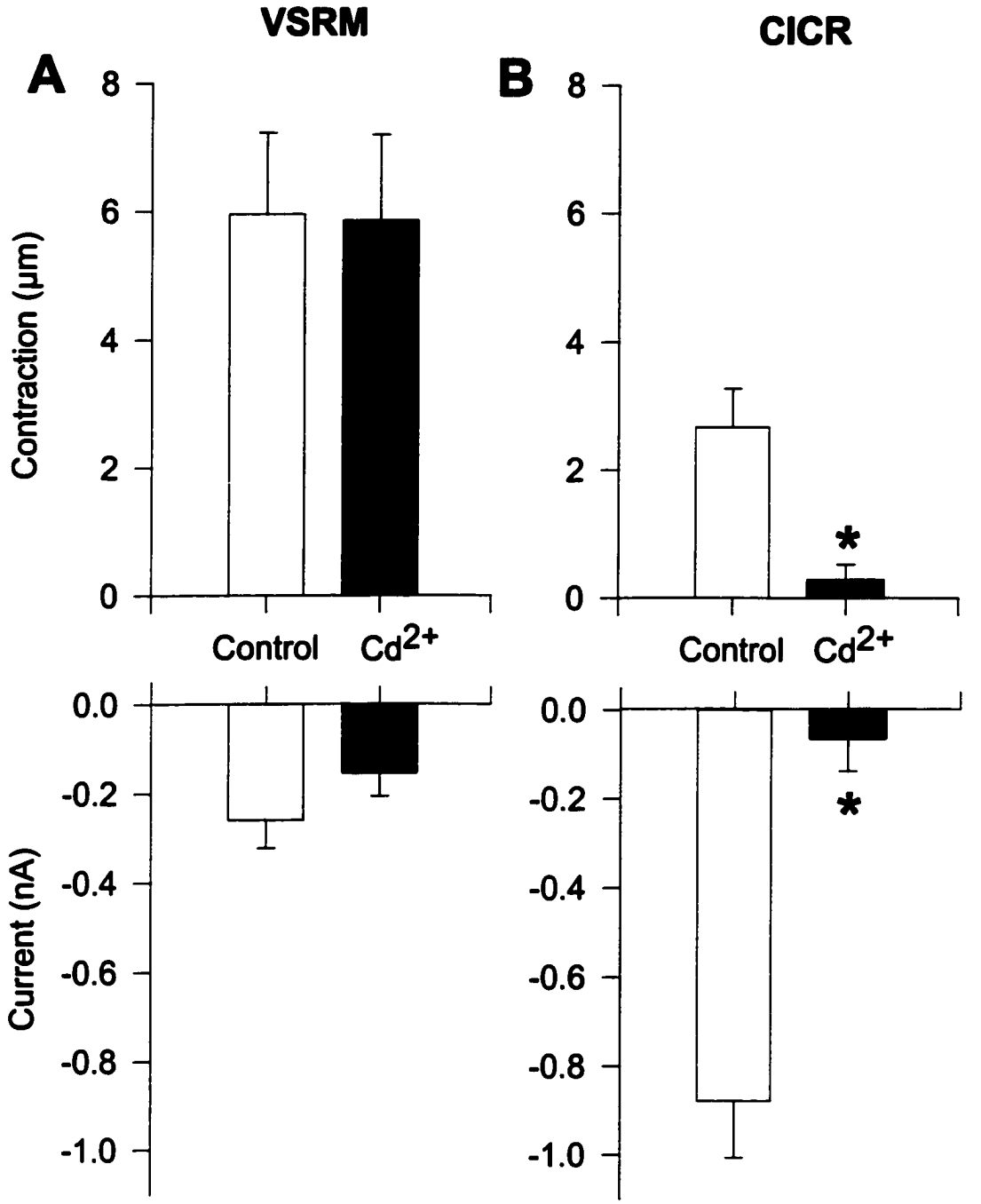
VSRM
CICR
A
B
Contraction (µm)
Current (nA)
8
6
4
2
0
0.0
-0.2
-0.4
-0.6
-0.8
-1.0
Control
Cd2+
*
*

Figure 1-2

Figure 1-3. Normal and CM ventricular myocytes displayed similar action potential profiles, but the magnitude of contraction activated by an action potential was reduced in CM cells. Panels A-B: Representative traces show that action potential profiles were similar in normal and CM myocytes. **Panels C and D:** Representative traces show that contractions triggered by the action potential were decreased in the CM cell.

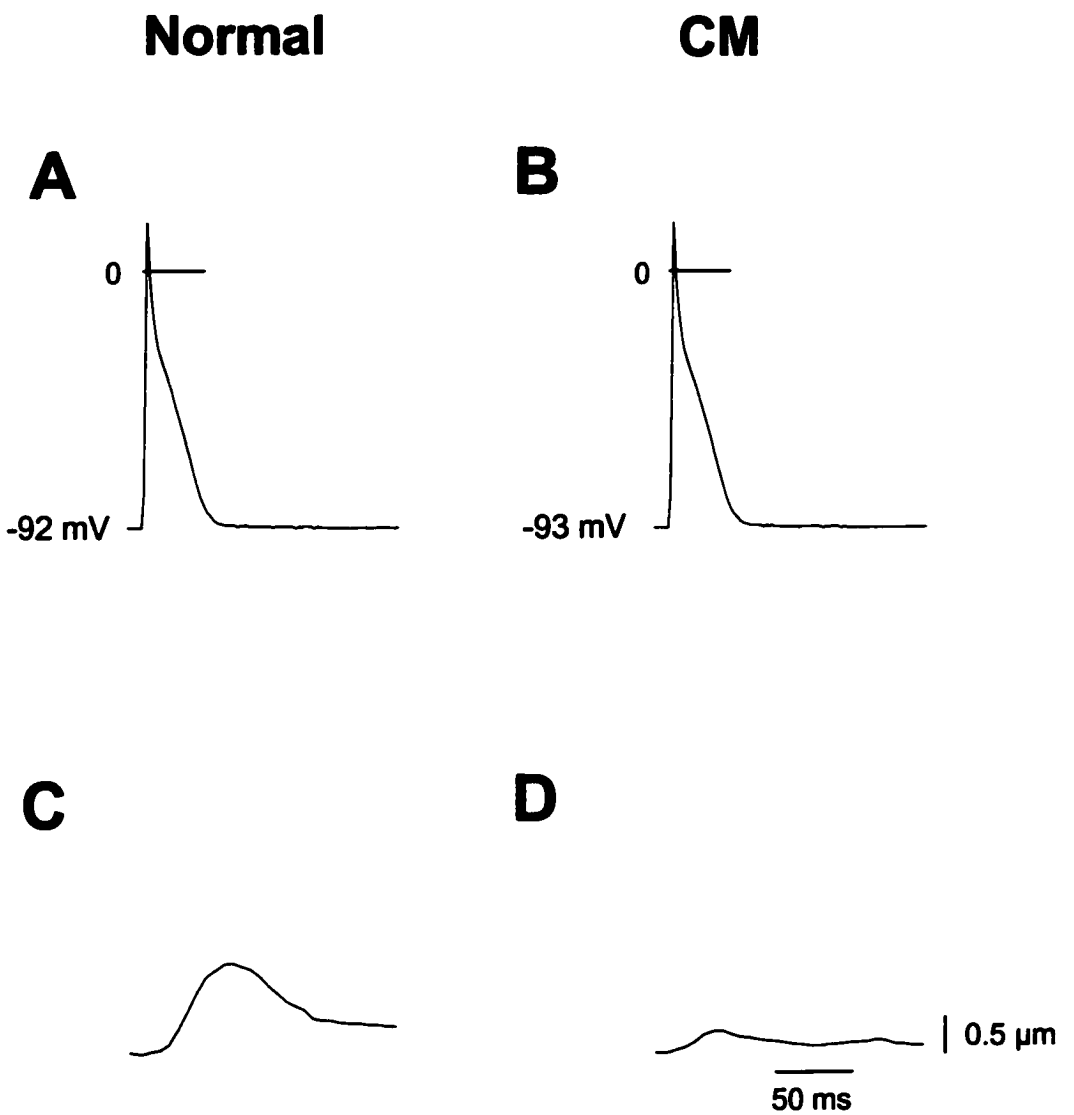

Figure 1-3

The mean data presented in Table 6 show that the resting membrane potentials were –88.6 ± 1.1 and –88.3 ± 1.3 mV in myocytes from normal and CM hearts, respectively. Thus, resting membrane potentials were not significantly altered in cells from diseased hearts. Action potential duration measured when cells were repolarized to –30 mV (APD_{30mV}) also was not significantly different between normal and CM cells. Similarly, there was no significant difference in action potential duration between normal and CM cells when myocytes were repolarized to –80 mV (APD_{80mV}). However, mean amplitudes of contractions initiated by action potentials were significantly decreased in CM myocytes when compared to normal ($p<0.05$). Other contractile characteristics were similar in normal and CM cells. Time to peak contraction and half-relaxation time also were similar (Table 6). Resting cell length was not significantly different between normal and CM hamsters.

Next, to rule out the possibility that small differences in action potential configuration could contribute to the reduction in contractility in CM cells, we examined contractions in voltage-clamped myocytes. Figure 1-4 shows representative traces of inward currents and contractions recorded under voltage clamp conditions in normal and CM cells. In these experiments, lidocaine was utilized to block sodium current and 2 mM 4-AP was employed to inhibit transient outward current. Under these conditions, the inward current initiated by a voltage step to 0 mV from a V_{PC} of –60 mV appeared similar between normal and CM myocytes (Figure 1-4A and B). In contrast, the amplitude of contractions was markedly reduced in CM myocytes compared to normal (Figure 1-4C and D). Table 6 shows that mean inward current density was not significantly different between normal and CM cells. However, the amplitude of

Table 6. Electrophysiological and Contractile Characteristics of Ventricular Myocytes from Normal and CM Hamsters

	Normal	**CM**
Resting cell length (μm)	151 ± 5	148 ± 4
Conventional recording (action potential and contractions)		
RMP (mV)	-88.6 ± 1.1	-88.3 ± 1.3
APD_{30mv} (ms)	37.1 ± 7.2	42.1 ± 11.6
APD_{80mV} (ms)	94.2 ± 13.3	99.4 ± 20.4
Contraction amplitude (μm)	2.4 ± 4.1	0.5 ± 0.1*
Time to peak contraction (ms)	39.8 ± 4.1	36.5 ± 2.2
Half-relaxation time (ms)	25.8 ± 2.4	27.8 ± 1.9
Voltage clamp recordings (inward current density and contractions)		
$I_{Ca\text{-}L}$ (pA/pF)	-7.92 ± 1.71	-5.86 ± 0.85
Contraction amplitude (μm)	2.7 ± 0.6	0.8 ± 0.2*
Time to peak contraction (ms)	39.3 ± 5.8	29.1 ± 2.8
Half-relaxation time (ms)	25.0 ± 2.2	24.4 ± 3.5

n=12 normal and 16 CM myocytes. RMP, resting membrane potential; APD_{30mV}, action potential duration at –30 mV; APD_{80mV}, action potential duration at –80 mV;
*Significantly different from normal, $p<0.05$

Figure 1-4. The magnitude of contraction initiated by a voltage step to 0 mV was reduced in ventricular myocytes from CM hamsters. The voltage clamp protocol is shown at the top of the figure. **Panels A and C:** Representative traces show that inward currents and contractions were activated by a voltage step to 0 mV from a V_{PC} of –60 mV in normal myocytes. **Panels B and D:** Representative traces show that contractions activated by the voltage step to 0 mV were decreased in a CM myocyte compared to normal, whereas inward currents appeared similar in normal and CM cells.

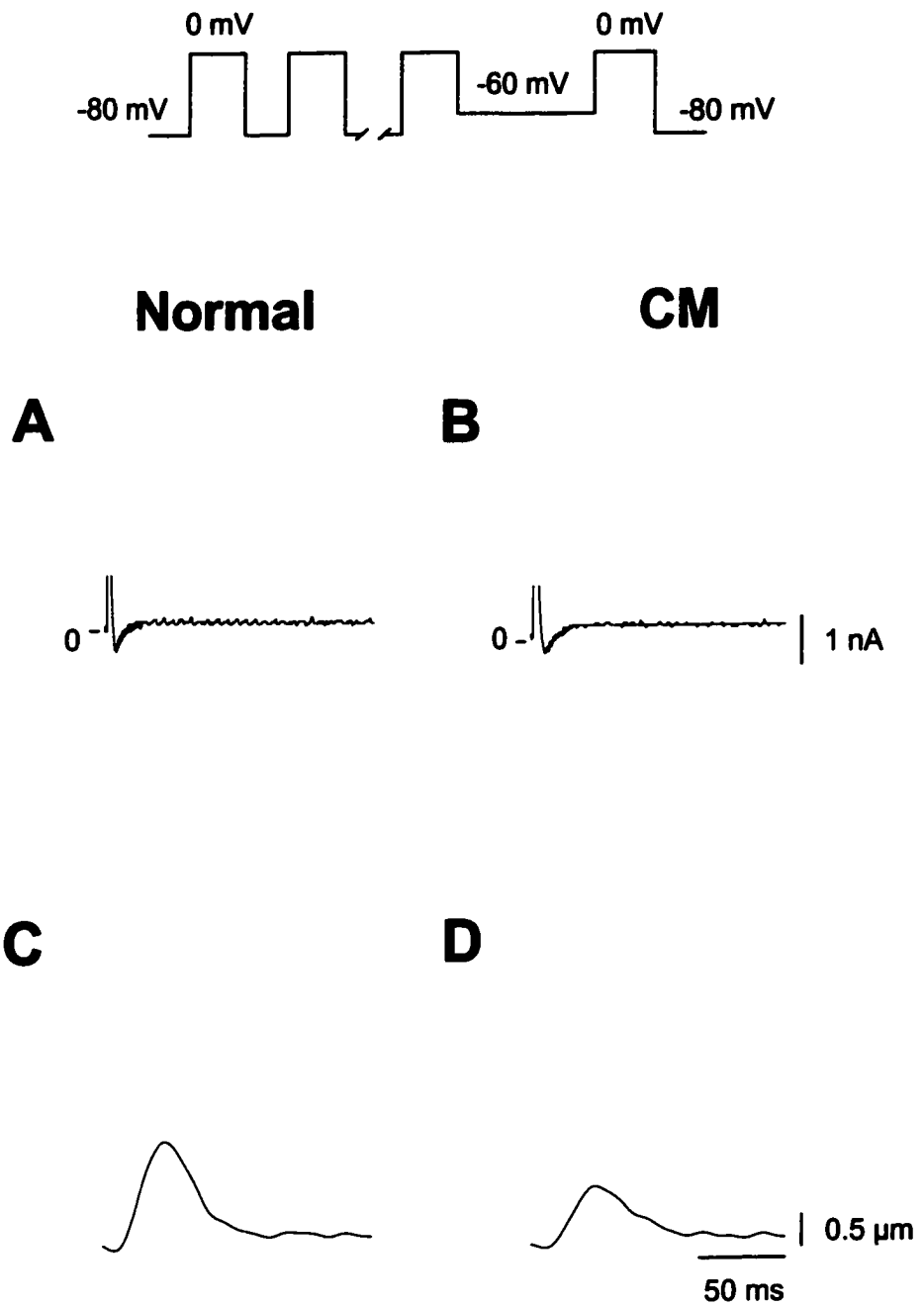

Figure 1-4

contraction was significantly reduced in CM cells ($p<0.05$). Additionally, normal and CM cells displayed similar time-to-peak contraction and half-relaxation time. These results suggest that: 1) depressed contractions in ventricular myocytes from CM hearts were due to alterations in cardiac E-C coupling; and 2) reduction in the magnitude of contractions in CM cells cannot be explained by changes in magnitude of inward currents.

(3) Contribution of the VSRM and CICR to contraction in normal and CM myocytes

Figures 1-3 and 1-4 demonstrated that the magnitude of cardiac contraction was reduced in myocytes from CM hearts. To determine whether this decrease in contractile amplitude was due to the VSRM, CICR or both mechanisms of E-C coupling, we separated the VSRM from CICR with a voltage clamp protocol. Sequential voltage steps to –40 and 0 mV were utilized to selectively activate VSRM and CICR contractions, respectively (Ferrier and Howlett, 1995; Howlett et al, 1998) (Figure 1-5). Figure 1-5A shows recordings of representative traces of contractions and currents activated by sequential voltage steps to –40 and 0 mV in a normal hamster myocyte. The test step to –40 mV activated a VSRM contraction and with very little inward current. The voltage step to 0 mV activated $I_{Ca\text{-}L}$ and a CICR contraction. Figure 1-5B shows that the VSRM contraction activated by the voltage step to –40 mV is virtually absent in the CM myocyte. However, the amplitude of the CICR contraction initiated by the voltage step to 0 mV appeared only slightly smaller in the CM cell. The magnitudes of $I_{Ca\text{-}L}$ appeared similar in normal and CM cells.

Figure 1-5. Contractions initiated by the VSRM were markedly reduced in the CM heart. The voltage clamp protocol is shown at the top of the figure. **Panel A:** Representative traces showed that the test step to -40 mV activated the VSRM and virtually no detectable inward current in a normal myocyte. The test step to 0 mV activated a CICR contraction and L-type Ca^{2+} current. **Panel B:** The VSRM contraction was virtually absent in the CM myocyte, although a small inward current was observed. The CICR contraction appeared to be slightly decreased in the CM myocyte, whereas the L-type Ca^{2+} current appeared similar in normal and CM cells.

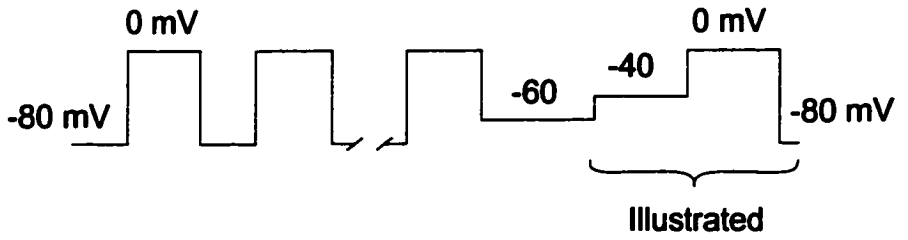
0 mV
0 mV
-40
-60
-80 mV
-80 mV
Illustrated

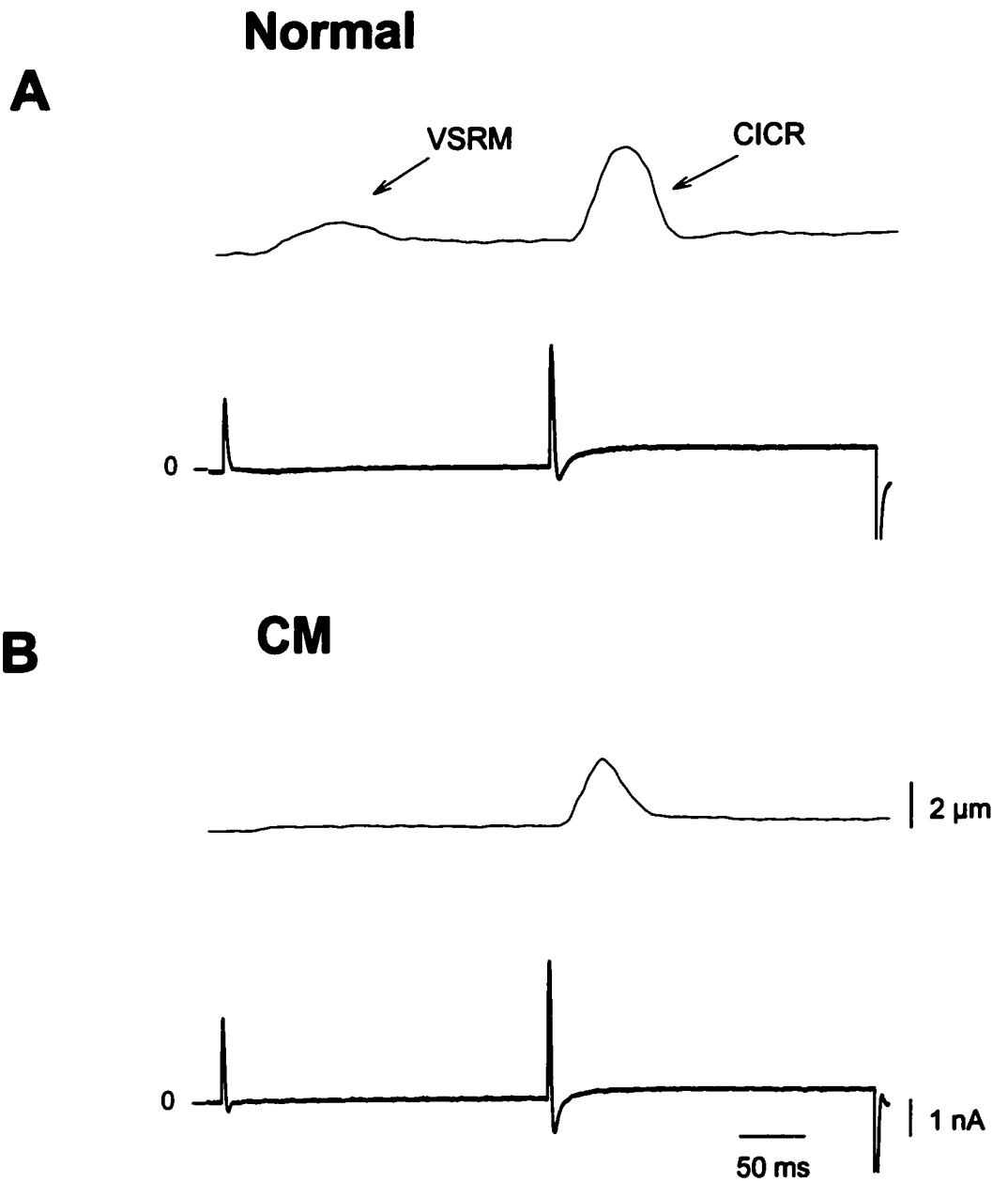
Normal
A
VSRM
CICR
0
B
CM
2 µm
0
1 nA
50 ms

Figure 1-5

Mean data for contractions and currents in normal and CM cells are shown in Figure 1-6. Figure 1-6A demonstrates that the mean amplitude of VSRM contractions was significantly reduced in myocytes from CM hearts when compared to normal ($p<0.05$). However, CICR contractions were not significantly decreased in CM cells (Figure 1-6C). Since it is possible that cell capacitance (an index of cell surface area) was different between normal and CM cells, inward current was normalized to cell capacitance, which was expressed as inward current density. Figures 1-6B and D demonstrate that the inward current density activated by voltage test steps to –40 and 0 mV was similar in normal and CM myocytes.

A reduction in amplitude of VSRM contractions in CM myocytes could be caused by changes in the voltage dependence of activation of the VSRM. To determine whether a shift in activation of the VSRM might affect the magnitude of contractions initiated by the VSRM, contraction-voltage relationships were determined from a V_{PC} of –60 mV to activate the VSRM (Figure 1-7A). The corresponding current-voltage relations are plotted in Figure 1-7B. The voltage clamp protocol is shown at the top of Figure 1-7. Following ten conditioning pulses, cells were depolarized from a V_{PC} of –60 mV to potentials up to +80 mV in 10 mV increments. In both normal and CM hamster myocytes, activation of the VSRM was first observed with a voltage step to –50 mV. The amplitude of contractions reached a peak near 0 mV and decreased slightly thereafter in normal and CM myocytes. Figure 1-7A demonstrates that, when the VSRM was available, contraction-voltage relations were significantly depressed in CM myocytes ($p<0.05$). However, inward current density was almost identical in normal and CM myocytes (Figure 1-7B). Figure 1-8 shows that when contraction-voltage relationships

Figure 1-6. Mean data show that VSRM contractions were significantly reduced in CM myocytes. Panels A and B: VSRM contractions were significantly decreased in magnitude in CM cells, but current density activated by the voltage step to –40 mV was unchanged. **Panels C and D:** The L-type Ca^{2+} current density was similar between normal and CM myocytes. CICR contractions were slightly reduced in CM myocytes, although this was not statistically significant. *Denotes significantly different from control ($p<0.05$), n= 13 normal and 14 CM myocytes.

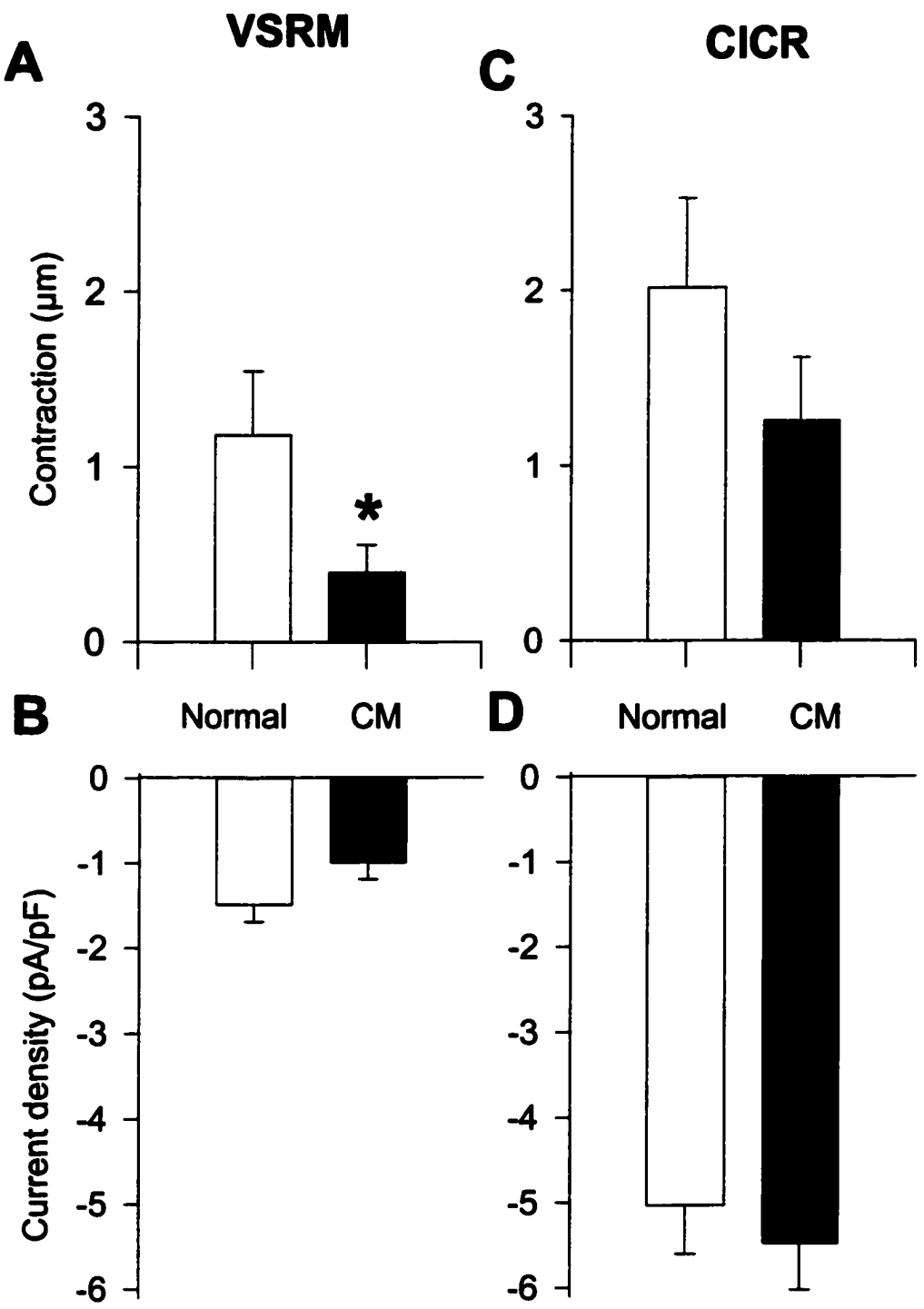
A
VSRM
C
CICR
Contraction (μm)
3
2
1
0
*
Normal
CM
B
D
Current density (pA/pF)
0
-1
-2
-3
-4
-5
-6

Figure 1-6

Figure 1-7. Mean data show that contraction-voltage relationships were significantly reduced in CM cells when the VSRM was available. Panel A: Contraction-voltage relationships obtained when cells were depolarized from –60 mV to activate the VSRM and CICR. The contraction-voltage relationship was significantly decreased in CM myocytes. **Panel B:** Current-voltage relationships determined with test steps from a V_{PC} of –60 mV were similar in normal and CM myocytes. *Denotes significantly different from control ($p<0.05$), n= 13 normal and 14 CM myocytes.

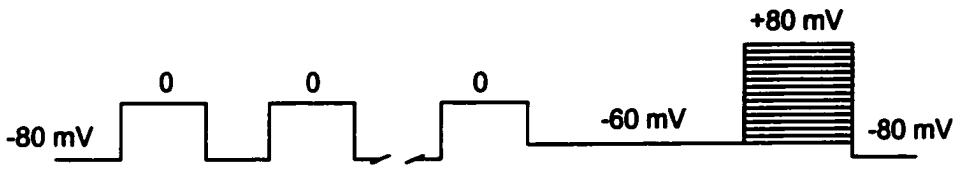
+80 mV
0
0
0
-80 mV
-60 mV
-80 mV

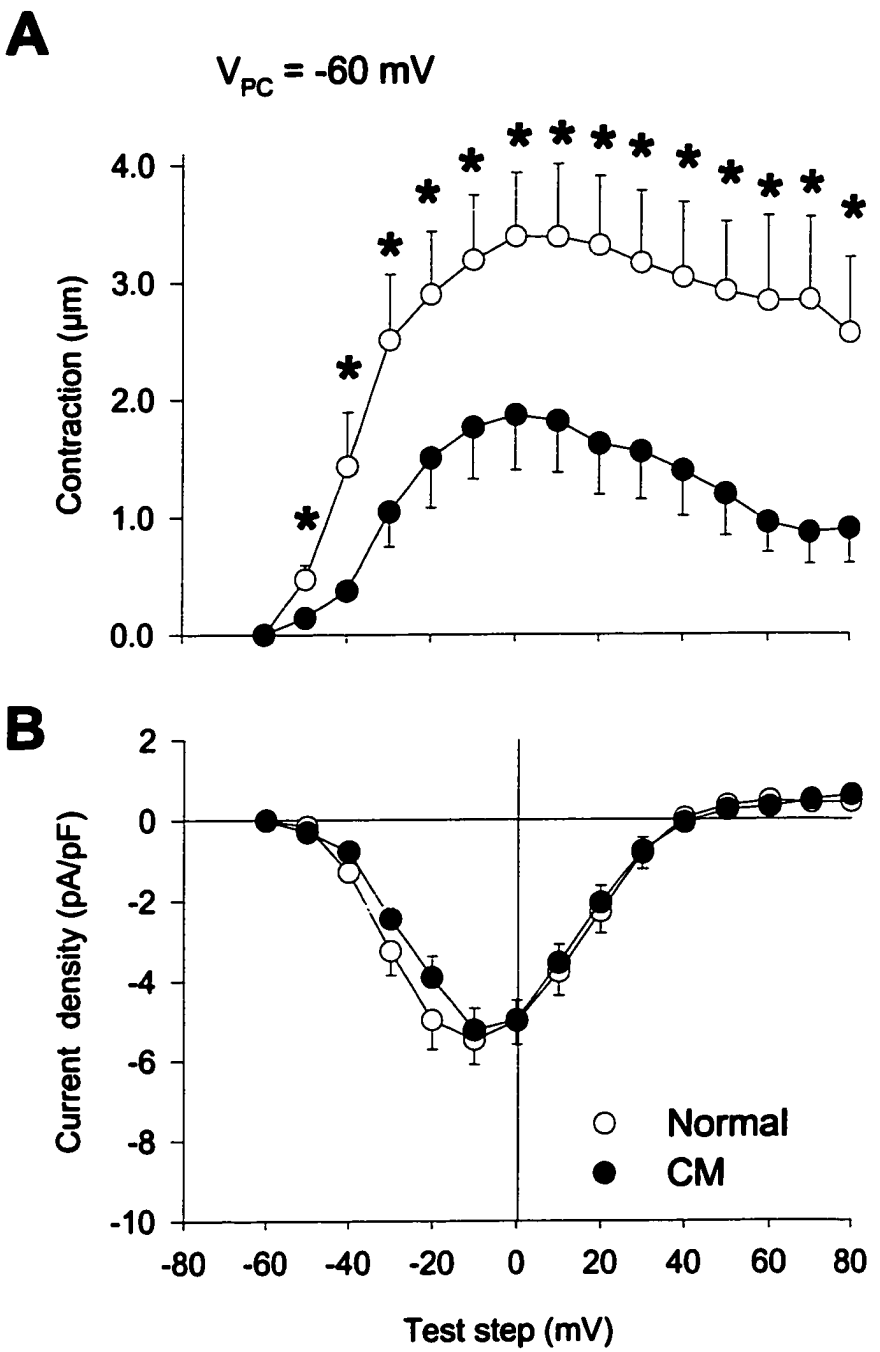
A
V_{PC} = -60 mV
Contraction (μm)
4.0
3.0
2.0
1.0
0.0
B
Current density (pA/pF)
2
0
-2
-4
-6
-8
-10
-80
-60
-40
-20
0
20
40
60
80
Test step (mV)
Normal
CM

Figure 1-7

Figure 1-8. Normalized contraction-voltage relationships determined from a V_{PC} of –60 mV were similar in normal and CM cells. When contractions were normalized to the amplitude of contractions at 0 mV, the normalized curves were virtually superimposable, in particular between –60 and +20 mV.

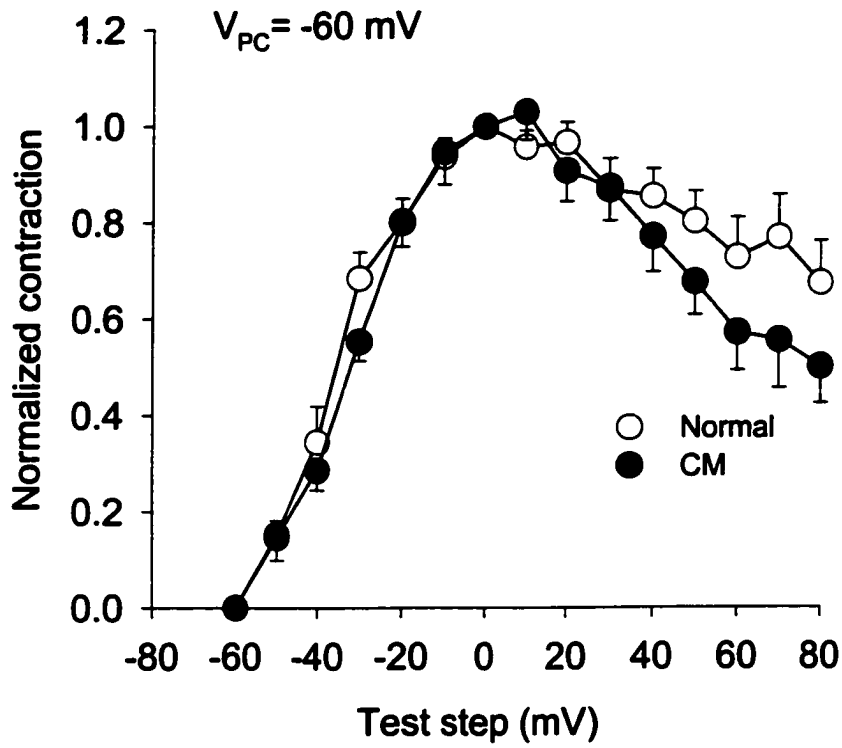
V_{PC}= -60 mV
Normalized contraction
1.2
1.0
0.8
0.6
0.4
0.2
0.0
-80
-60
-40
-20
0
20
40
60
80
Test step (mV)
Normal
CM

Figure 1-8

were normalized to the magnitude of contraction initiated by a voltage test step to 0 mV in each cell, the normalized curves were superimposable between –60 and +20 mV between normal and CM myocytes. Thus, a reduction in contractions cannot be ascribed to changes in voltage dependence of activation of the VSRM.

Next, we examined contraction-voltage and current-voltage relationships determined from a V_{PC} of –40 mV. Since depolarizing test steps from a V_{PC} of –40 mV inactivate the VSRM, this protocol would allow activation of phasic contractions by CICR only (Ferrier and Howlett, 1995; Howlett and Ferrier, 1997; Howlett et al., 1998). Figure 1-9A shows that the amplitude of CICR contractions over a wide range of membrane potentials was similar between normal and CM cells. Moreover, the magnitude of $I_{Ca\text{-}L}$ was identical in normal and CM myocytes. When contraction-voltage relations were normalized to the contraction initiated by a test step to 0 mV, the normalized curves for normal and CM cells were superimposable (Figure 1-10). These results suggest that CICR is similar in normal and CM cells. Thus, reduction in cardiac contractility in CM hamsters is attributable to depression of the VSRM component of cardiac E-C coupling.

(4) SR Ca^{2+} stores, assessed as caffeine-induced contractures and as the integral of the Na^{+}-Ca^{2+} exchange current, in normal and CM myocytes

To determine whether a change in SR releasable Ca^{2+} might contribute to the decrease in the VSRM in CM myocytes, we assessed the SR Ca^{2+} content in ventricular myocytes from normal and CM hearts. Rapid application of caffeine was used to assess SR releasable Ca^{2+} as used in previous studies (Bers, 1987; O'Neill et al., 1991). Cells were exposed to 10 mM caffeine for 4 s with a rapid solution-switcher device. Figure 1-

Figure 1-9. Mean data show that the contraction-voltage relations for CICR were similar in normal and CM cells. Panel A: Normal and CM myocytes displayed similar bell-shaped contraction-voltage relationships when cells were depolarized from a V_{PC} of –40 mV to inactivate the VSRM. **Panel B:** The current-voltage relationships determined with test steps from a V_{PC} of –40 mV were similar in normal and CM myocytes (n= 13 normal and 14 CM myocytes).

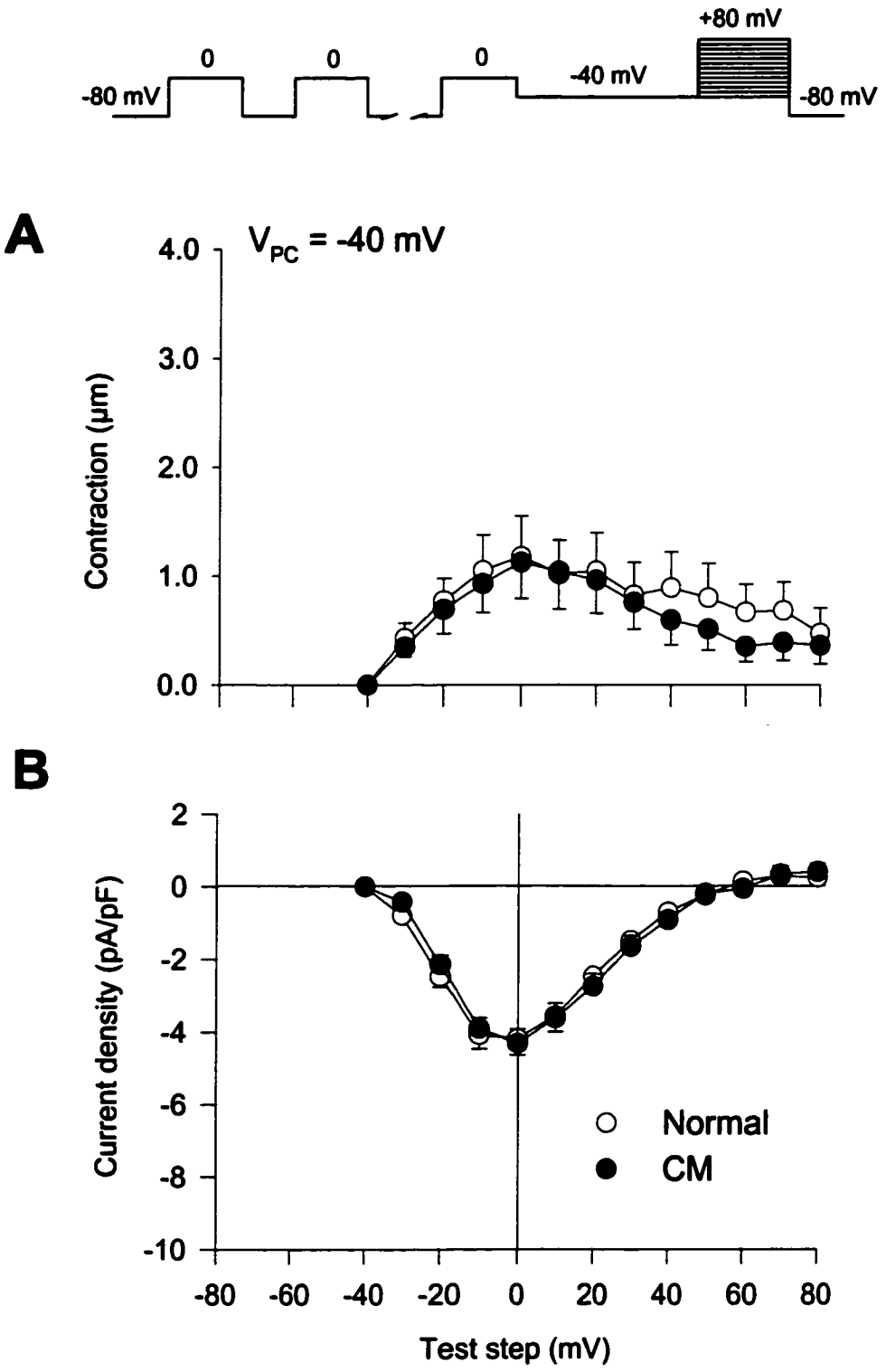
+80 mV
0
0
0
-40 mV
-80 mV
-80 mV
A
V_{PC} = -40 mV
Contraction (µm)
4.0
3.0
2.0
1.0
0.0
B
Current density (pA/pF)
2
0
-2
-4
-6
-8
-10
Normal
CM
-80
-60
-40
-20
0
20
40
60
80
Test step (mV)

Figure 1-9

Figure 1-10. Normalized contraction-voltage relationships determined from a V_{PC} of –40 mV were similar in normal and CM cells. When contractions were normalized to the amplitude of contractions at 0 mV, the normalized curves were similar in normal and CM myocytes.

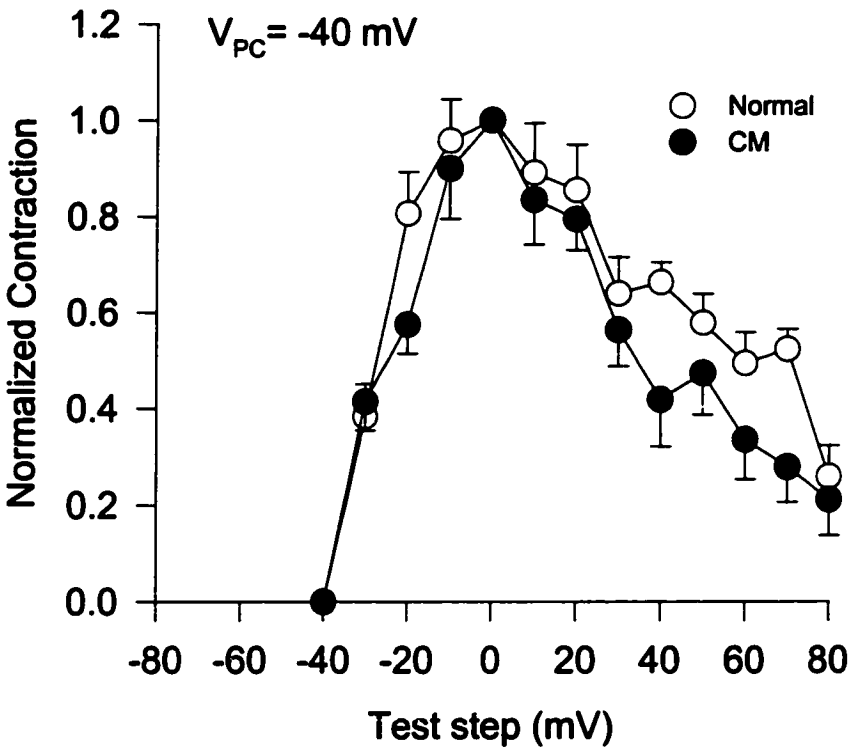
V_{PC}= -40 mV
Normal
CM
Normalized Contraction
1.2
1.0
0.8
0.6
0.4
0.2
0.0
-80
-60
-40
-20
0
20
40
60
80
Test step (mV)

Figure 1-10

11 shows representative recordings of caffeine-induced contractures and inward current. This inward current generated in response to caffeine application is believed to be due to Ca^{2+} extrusion via Na^{+}-Ca^{2+} exchanger as a result of SR Ca^{2+} release (Callewaert et al., 1989). The peak magnitudes of caffeine-induced contractures and inward currents were similar between normal (Figure 1-11A) and CM cells (Figure 1-11B).

Measurement of the integral of the Na^{+}-Ca^{2+} exchange current can be used to estimate the caffeine-releasable Ca^{2+} content of the SR (Negretti et al., 1995). Figure 1-12 illustrates mean data for the integral of the Na^{+}-Ca^{2+} exchange current and caffeine-induced contractures. We also normalized the integral of Na^{+}-Ca^{2+} exchange current to cell capacitance (an index of cell surface area) to rule out changes in cell surface area. Figure 1-12A shows that caffeine-induced contractures were not significantly different between normal and CM myocytes. In addition, the normalized integral of the Na^{+}-Ca^{2+} exchange current was similar between cells from normal and CM hearts. These results suggest that SR Ca^{2+} content was not significantly different between ventricular myocytes from normal and CM hamsters.

As SR Ca^{2+} stores appeared similar in normal and CM cells, an alternative possibility was that fractional release of SR Ca^{2+} by the VSRM was defective in CM hamsters. To examine this possibility, VSRM and CICR contractions activated by sequential steps to –40 and 0 mV(Figure 1-13A) were expressed as a fraction of caffeine-induced contractures (fractional release) in each cell (Figure 1-13B). Figure 1-13A shows the magnitudes of VSRM and CICR contractions in each cell exposed to caffeine. As described earlier, VSRM contractions were significantly decreased in CM myocytes ($p<0.05$). Mean data for fractional release of SR Ca^{2+} in normal and CM myocytes is

Figure 1-11. Caffeine-induced contractures and Na^+-Ca^{2+} exchange currents were similar in normal and CM cells. The voltage clamp protocol is shown at the top of the figure. Caffeine was rapidly applied for 4 s with a rapid solution-switcher. **Panel A:** Representative traces of the caffeine-induced contracture (top panel) and Na^+-Ca^{2+} exchange current (bottom panel) in a normal cell. **Panel B:** The caffeine-induced contracture (top panel) and Na^+-Ca^{2+} exchange current (bottom panel) recorded from a CM cell were similar to normal.

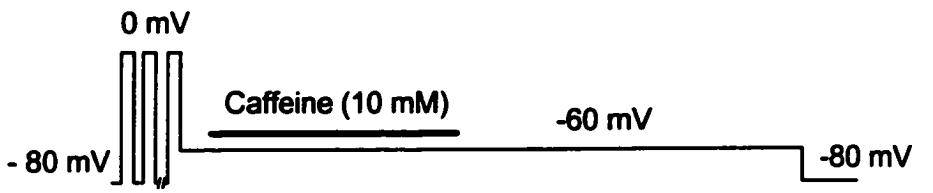

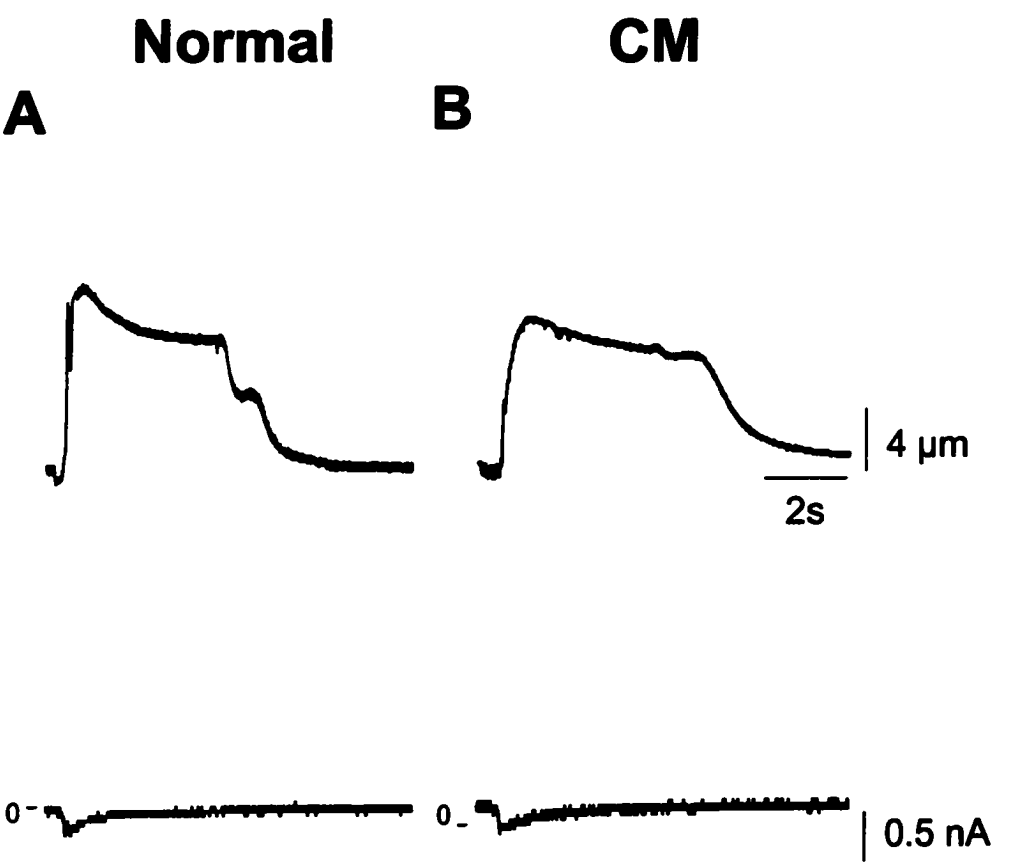

Figure 1-11

Figure 1-12. Mean data show that caffeine-induced contractures and the normalized integral of Na^+-Ca^{2+} exchange current were similar in cells from normal and CM hearts. Panel A: The peak amplitude of caffeine-induced contractures was similar in normal and CM myocytes. **Panel B:** Normalized integral of Na^+-Ca^{2+} exchange current was similar in normal and CM cells (n= 5 normal and 14 CM myocytes).

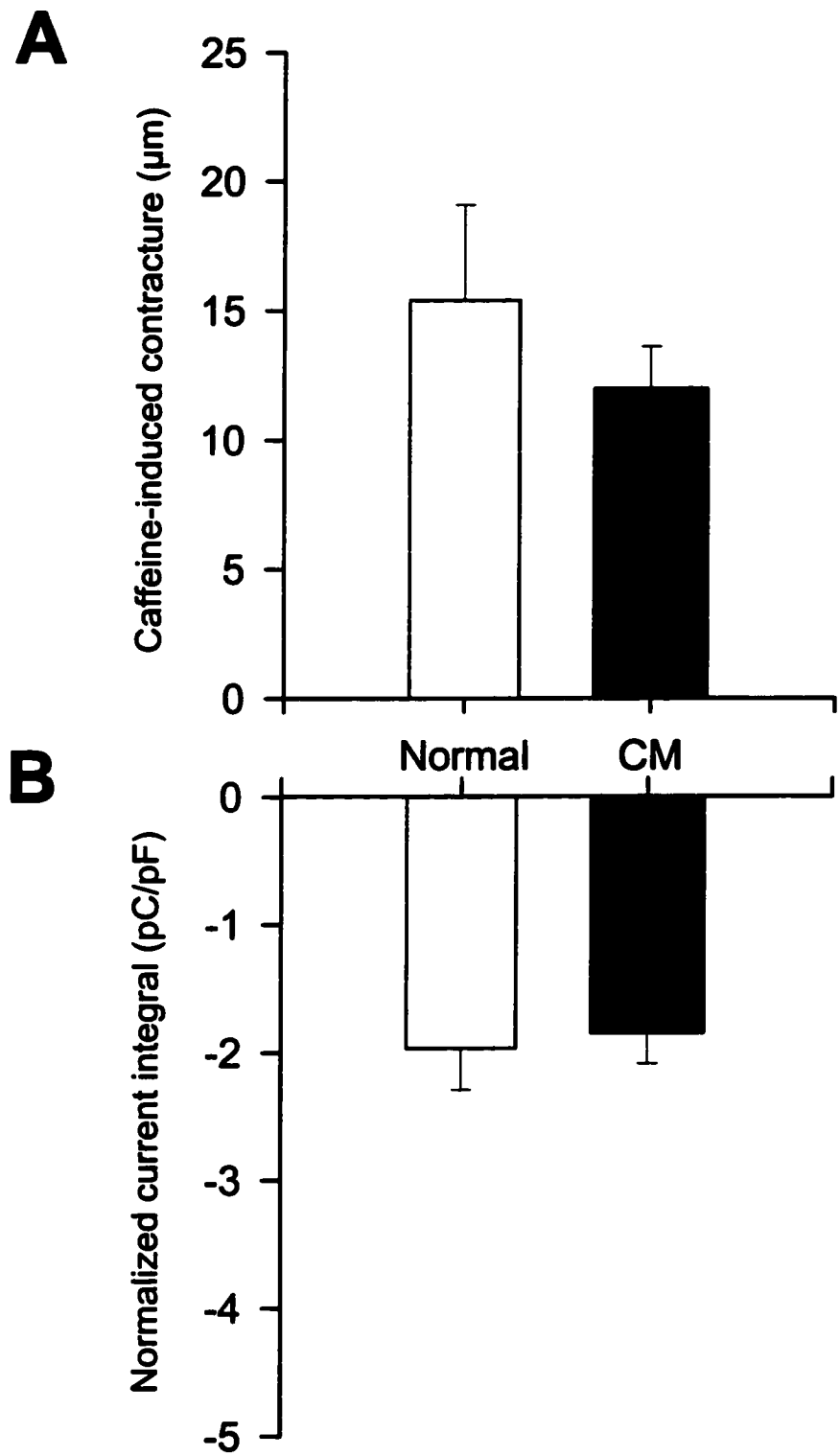
A
25
20
15
10
5
0
Caffeine-induced contracture (μm)
Normal
CM
B
0
-1
-2
-3
-4
-5
Normalized current integral (pC/pF)

Figure 1-12

Figure 1-13. Selective depression of the VSRM in CM myocytes is related to a selective reduction in fractional release of SR Ca^{2+} by the VSRM. The voltage clamp protocol is shown at the top of the figure. **Panel A:** Contractions initiated by the VSRM were significantly depressed in CM myocytes, but CICR contractions were similar in normal and CM cells. **Panel B:** Fractional release was estimated by normalizing VSRM and CICR contractions to the caffeine-induced contracture in each myocyte. Fractional release by the VSRM was significantly decreased in CM cells, although fractional release by CICR was not significantly different in normal and CM cells. *Denotes significantly different from control ($p<0.05$), n= 5 normal and 14 CM myocytes.

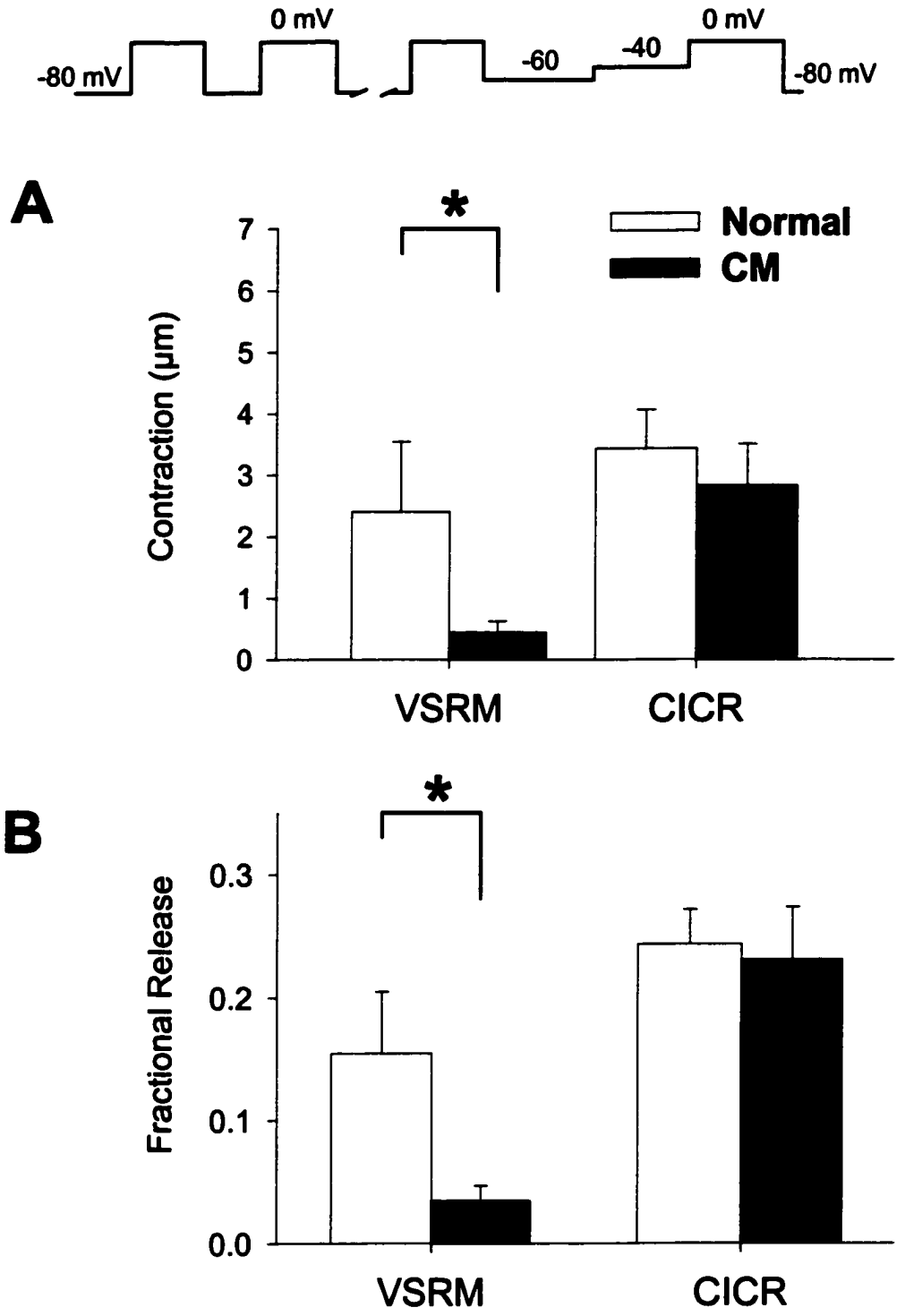
0 mV
0 mV
-80 mV
-60
-40
-80 mV
A
*
Normal
CM
Contraction (µm)
7
6
5
4
3
2
1
0
VSRM
CICR
B
*
Fractional Release
0.3
0.2
0.1
0.0
VSRM
CICR

Figure 1-13

shown in Figure 1-13B. Fractional SR Ca^{2+} release by the VSRM was significantly reduced in CM myocytes ($p<0.05$), whereas fractional release of SR Ca^{2+} by CICR was similar in normal and CM cells (Figure 1-13B).

In summary, the decrease in cardiac contractility in ventricular myocytes from CM hamster hearts can be attributed to depression of VSRM contractions, which cannot be explained by alterations in SR Ca^{2+} content. Our results suggest that the inability of the VSRM to release SR Ca^{2+} plays an important role in the depressed VSRM component of contraction.

2. INOTROPIC EFFECTS OF PDE INHIBITORS IN GUINEA PIG VENTRICULAR MYOCYTES

Modulation of the VSRM by the cAMP/PKA pathway has been suggested in recent studies (Hobai et al., 1997; Ferrier et al., 1998). Thus, changes in phosphorylation might contribute to depressed VSRM contractures in CM hamsters and agents that increase phosphorylation might augment VSRM contractions in CM heart. Intracellular cAMP levels are dependent on both synthesis of cAMP and hydrolysis by PDEs. In this study, we examined the effect of PDE inhibitors on VSRM contractions. In the first series of experiments, we examined PDE inhibitors in the well-characterized guinea pig ventricular myocyte model. We examined effects of both the non-specific PDE inhibitor, IBMX (Shahid and Nicholson, 1990) and specific PDE III inhibitor, amrinone (Harrison et al., 1986; Weishassr et al., 1986) on VSRM and CICR contractions.

(1) Positive inotropic effects of IBMX in guinea pig ventricular myocytes

The first series of experiments were designed to determine whether IBMX increased contraction in guinea pig ventricular myocytes. Figure 2-1 shows the effect of IBMX on cardiac contractions when the VSRM and CICR were available. The cell was depolarized to +10 mV from a V_{PC} of –60 mV to activate both VSRM and CICR contractions. Prior to the V_{PC}, ten conditioning pulses from the holding potential of –80 mV to 0 mV were used to maintain continuous activation of the cell prior to test steps. Representative traces of contractions and currents in the absence and presence of 100 μM IBMX are shown in Figure 2-1A. Results showed that the magnitude of contractions was markedly increased

Figure 2-1. The non-selective PDE inhibitor IBMX increased cardiac contraction and current in guinea pig ventricular myocytes. The voltage-clamp protocol is shown at the top of the figure. **Panels A and B:** Representative traces show that 100 μM IBMX increased the magnitude of contraction and current elicited by a test step from –60 mV to +10 mV, respectively. **Panel C:** Mean data show that IBMX significantly increased contractions. * Denotes significantly different from control ($p<0.05$); n =5.

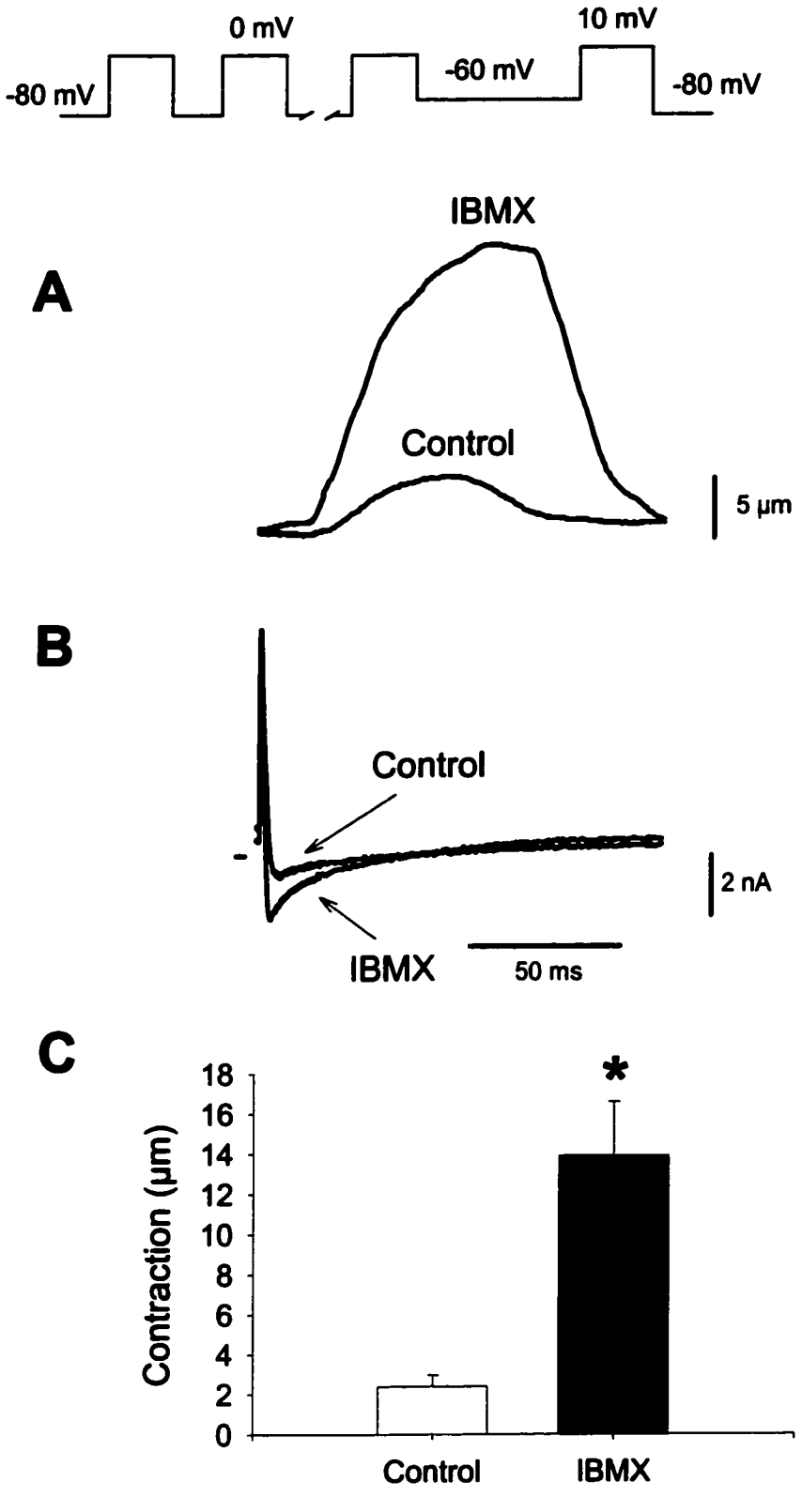
0 mV
10 mV
-80 mV
-60 mV
-80 mV
A
IBMX
Control
5 µm
B
Control
2 nA
IBMX
50 ms
C
Contraction (µm)
18
16
14
12
10
8
6
4
2
0
*
Control
IBMX

Figure 2-1

by IBMX. The effect of IBMX on inward currents is shown in Figure 2-1B. Inward current magnitude was markedly increased when the cell was exposed to IBMX. Figure 2-1C shows that the mean amplitude of contractions was significantly increased by IBMX ($p<0.05$).

The next set of experiments was designed to determine whether IBMX increased the magnitude of contraction by effects on the VSRM, CICR or both mechanisms. The voltage clamp protocol utilized to separate the VSRM contraction from CICR is shown at the top of Figure 2-2. Sequential voltage steps to –40 and 0 mV activated the VSRM and CICR contractions. Figure 2-2A shows that both VSRM and CICR contractions were activated by this protocol. The VSRM contraction was accompanied by little, if any, inward current in this example. The second contraction initiated by CICR was accompanied by $I_{Ca\text{-}L}$. Figure 2-2B shows the effects of IBMX on contractions elicited by voltage steps to –40 and 0 mV. Both contractions and inward currents activated by these voltage steps were increased in magnitude. Mean data for the effects of the non-specific PDE inhibitor IBMX are shown in Figure 2-3. IBMX dramatically increased magnitude of contractions elicited by test step to –40 mV, and caused a smaller increase in contractions triggered by CICR (Figure 1-3A). Figure 2-3B shows that IBMX significantly increased the magnitude of inward currents activated by test steps to both –40 and 0 mV.

We also determined the effect of IBMX on contraction-voltage and current-voltage relationships. The voltage clamp protocol is shown at the top of Figure 2-4. Following ten conditioning pulses, cells were depolarized from a V_{PC} of either –60 mV or –40 mV to potentials up to +80 mV in 10 mV increments. Figure 2-4A shows that IBMX enhanced

Figure 2-2. IBMX increased the magnitudes of contractions and currents elicited by steps from –60 to –40 and 0 mV. The voltage clamp protocol is shown at the top of the figure. **Panel A:** Representative traces show that sequential voltage steps from –60 to –40 and 0 mV were utilized to activate VSRM and CICR contractions (top) and currents (bottom). **Panel B:** IBMX increased the magnitudes of contraction and current initiated by the voltage step to –40 mV, and also increased contractions and inward current activated by the step to 0 mV.

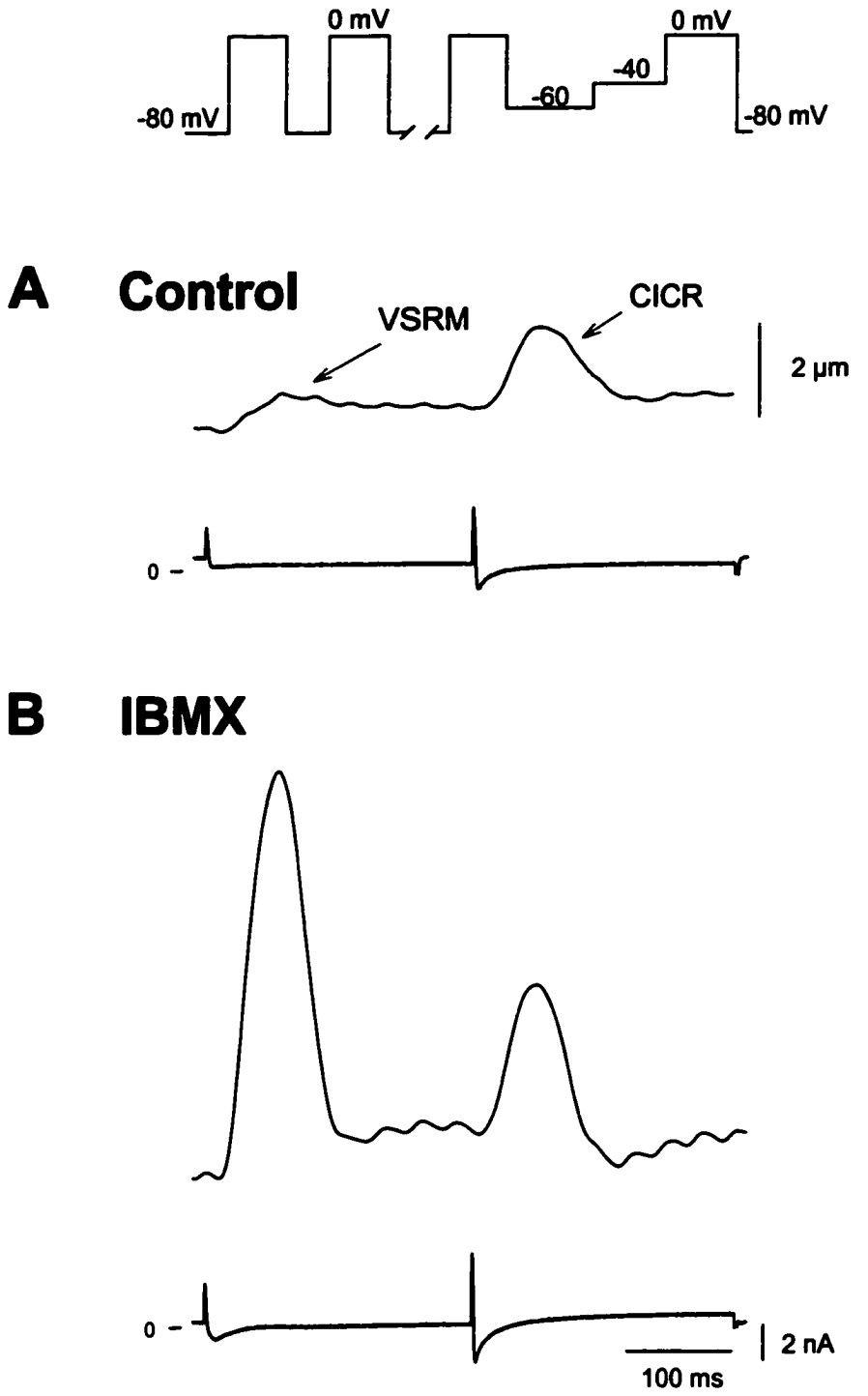
0 mV
0 mV
-40
-60
-80 mV
-80 mV
A Control
VSRM
CICR
2 µm
0
B IBMX
0
2 nA
100 ms

Figure 2-2

Figure 2-3. Mean data show that IBMX (100 μM) significantly increased contractions and inward currents elicited by test steps to –40 and 0 mV. Panel A: IBMX significantly increased contractions initiated by steps to –40 mV. IBMX also increased the magnitude of CICR contractions, although the difference was not statistically significant. **Panel B:** IBMX also significantly increased currents activated by test steps to –40 and 0 mV. *Denotes significantly different from control ($p<0.05$); n= 5.

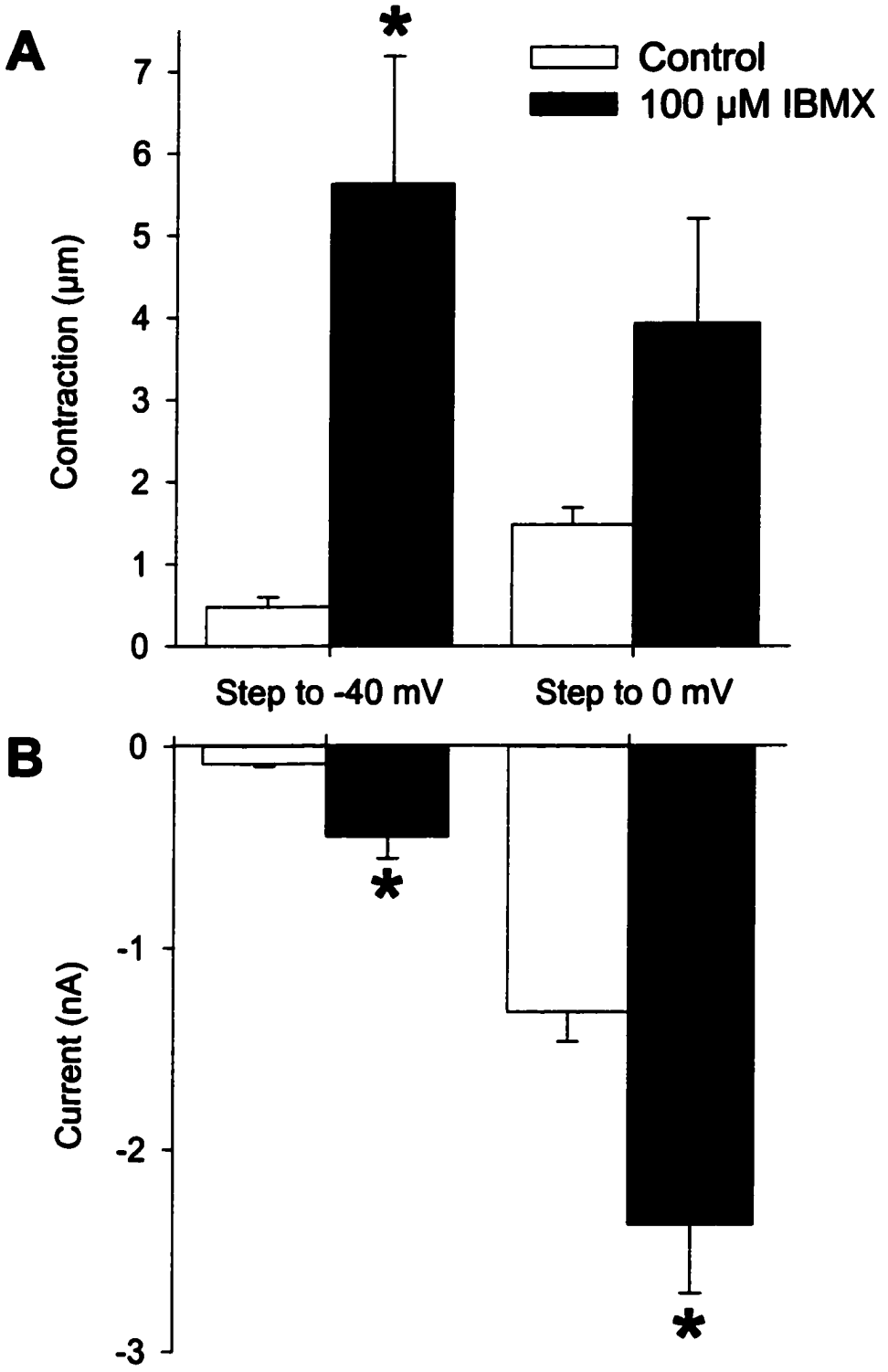
A
B
Control
100 µM IBMX
Contraction (µm)
Current (nA)
Step to -40 mV
Step to 0 mV
*
*
*
0
1
2
3
4
5
6
7
-1
-2
-3

Figure 2-3

Figure 2-4. IBMX increased the magnitudes of contraction-voltage and current-voltage relations initiated from V_{PC}s of both –60 and –40 mV. The voltage clamp protocol is shown at the top of the figure. **Panel A:** IBMX significantly increased the magnitude of sigmoidal contraction-voltage relations determined from a V_{PC} of –60 mV. The current also was increased. **Panel B:** The magnitude of bell-shaped contraction-voltage relations determined from a V_{PC} of –40 mV was increased after exposure to IBMX. Inward current also was increased. *Denotes significantly different from control ($p<0.05$); n= 5.

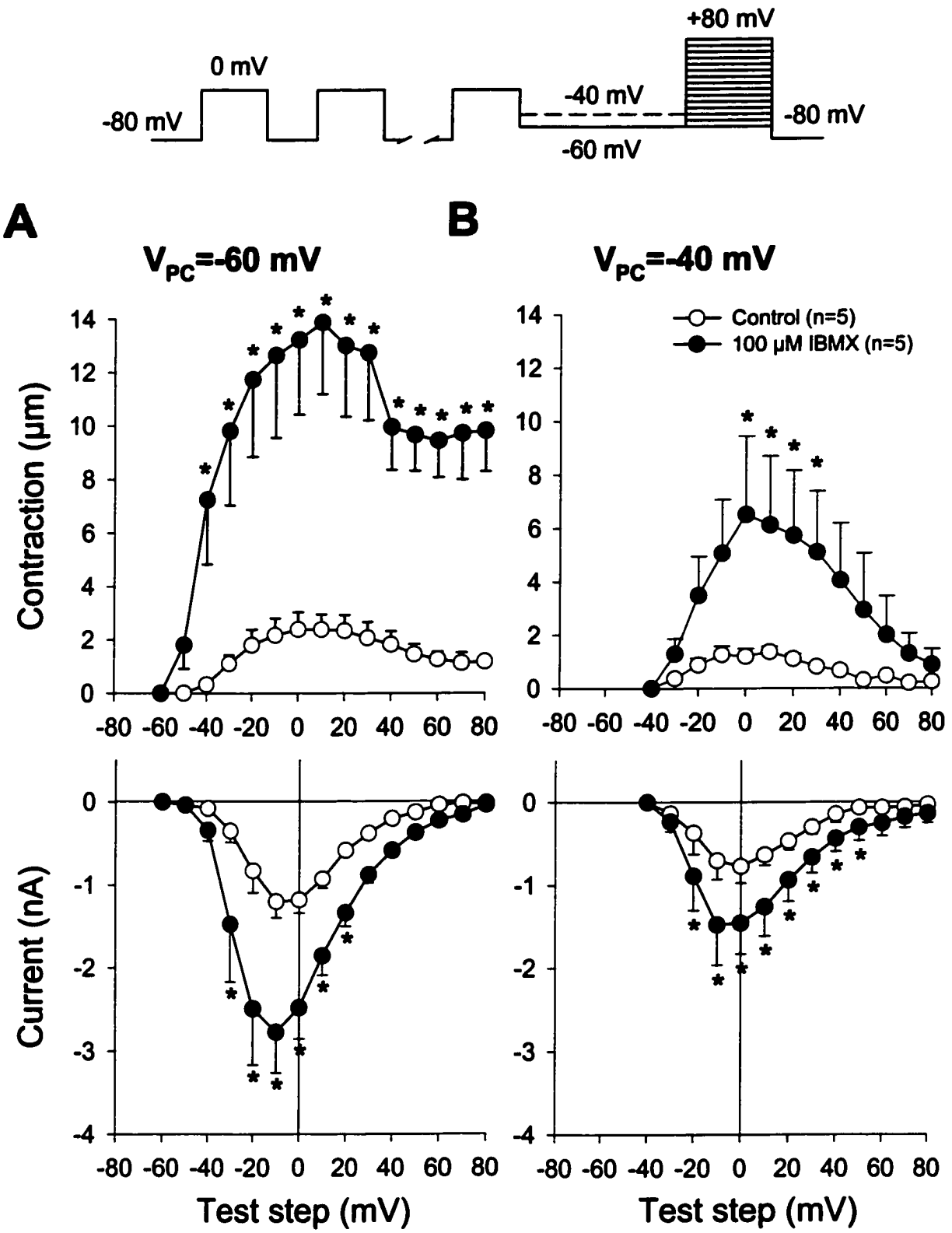
+80 mV
0 mV
-40 mV
-80 mV
-80 mV
-60 mV
A
B
V_{PC}=-60 mV
V_{PC}=-40 mV
Control (n=5)
100 μM IBMX (n=5)
Contraction (μm)
Current (nA)
Test step (mV)
Test step (mV)

Figure 2-4

the amplitude of contractions when myocytes were depolarized from a V_{PC} of –60 mV to allow activation of the VSRM. IBMX also increased the magnitude of inward currents ($p<0.05$). Figure 2-4B shows that IBMX also enhanced the peak of the bell-shaped contraction-voltage relationship when myocytes were depolarized from a V_{PC} of –40 mV to inactivate the VSRM ($p<0.05$). $I_{Ca\text{-}L}$ also was significantly increased in the presence of IBMX ($p<0.05$).

These results show that IBMX augmented contractions elicited by the test step to –40 mV, but also increased inward currents elicited by this step. In addition, IBMX caused an increase in magnitude of CICR contraction. Thus, it is unclear whether enhancement of contraction elicited by the test step to –40 mV represents potentiation of the VSRM, since inward current also was greatly increased and it is therefore not clear which mechanism(s) activated these contractions.

(2) Effects of amrinone on components of E-C coupling in guinea pig ventricular myocytes

The non-specific PDE inhibitor IBMX may cause a global increase in intracellular cAMP levels via inhibition of hydrolysis of cAMP by PDEs I through IV. However, inhibition of PDE III may regulate local cAMP levels (Kauuffman et al., 1986; Kauuffman et al., 1989; Lugnier et al., 1993). Therefore, in the next series of experiments we examined the effects of the specific PDE III inhibitor amrinone on VSRM and CICR contractions. Figure 2-5A shows sequential voltage steps utilized to elicit VSRM and CICR contractions in guinea pig ventricular myocytes. No detectable inward current was associated with the voltage step to activate VSRM contractions in this example.

Figure 2-5. Amrinone increased the magnitude of VSRM contractions. The voltage clamp protocol is shown at the top of the figure. **Panel A:** Representative traces show that contractions and currents were activated by sequential steps to –40 mV and 0 mV from a V_{PC} of –60 mV. **Panel B:** Amrinone (500 μM) caused a large increase in the VSRM contraction, but had little effect on CICR contractions and inward currents.

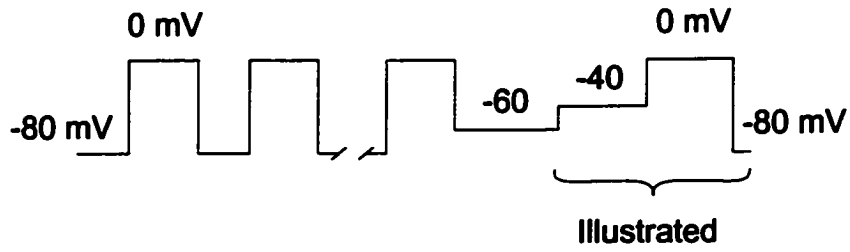

A Control

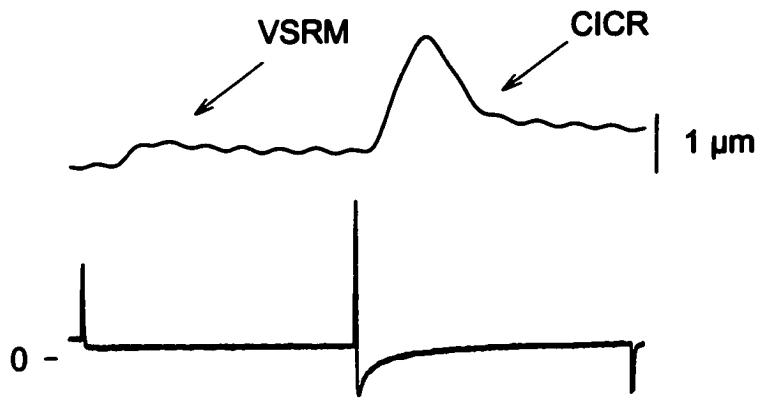

B Amrinone

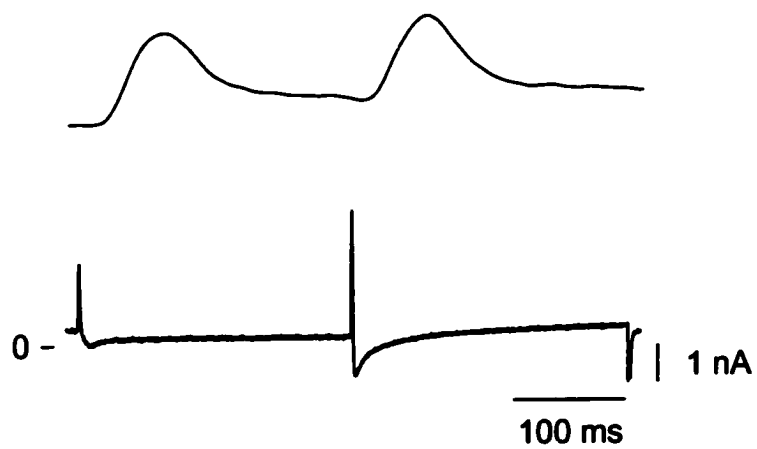

Figure 2-5

However, CICR contractions were associated with $I_{Ca\text{-}L}$. Representative recordings that illustrate the effect of amrinone on the VSRM are shown in Figure 2-5B. Amrinone (500 μM) markedly increased the magnitude of the VSRM contraction, but had no obvious effect on either contraction initiated by CICR or inward current activated by this test step. Figure 2-6 shows mean data for the effect of amrinone on contractions. Amrinone caused a significant increase in the amplitude of VSRM contractions with little effect on CICR contractions ($p<0.05$) (Figure 2-6A). Figure 2-6B shows that amrinone had no significant effect on magnitudes of inward currents activated by voltage steps to –40 and 0 mV. Thus, amrinone can selectively increase VSRM contractions without stimulation of CICR contractions.

Next, we examined contraction-voltage and current-voltage relations in the presence of amrinone at different concentrations. Following ten conditioning pulses, cells were depolarized from a V_{PC} of –40 mV to potentials up to +80 mV in 10 mV increments. Figures 2-7A and 7B show that 100 and 200 μM had no significant effect on either $I_{Ca\text{-}L}$ or contractions triggered by CICR. The magnitude of $I_{Ca\text{-}L}$ was slightly increased in the presence of 500 μM amrinone, but the magnitude of CICR contractions was not affected (Figure 7C). Thus, amrinone had little, if any, effect on CICR contractions.

Figure 2-8A through C show mean data for the effect of amrinone on contractions when the VSRM is available. Following ten conditioning pulses, cells were depolarized from a V_{PC} of –60 mV to potentials up to +80 mV in 10 mV increments. The amplitude of contractions was enhanced by amrinone in a concentration-dependent manner ($p<0.05$). Since 100 and 200 μM amrinone had no effect on CICR contractions (Figures 2-7A and B), this increased component of contractions likely was due to potentiation of

Figure 2-6. Mean data show that amrinone selectively increased VSRM contractions. Panel A: Amrinone (500 μM) significantly increased the magnitude of VSRM contractions, but had little effect on CICR contractions. **Panel B:** Amrinone had no effect on the magnitudes of inward currents elicited by voltage steps to either –40 or 0 mV. * Denotes significantly different from control ($p<0.05$); n= 5.

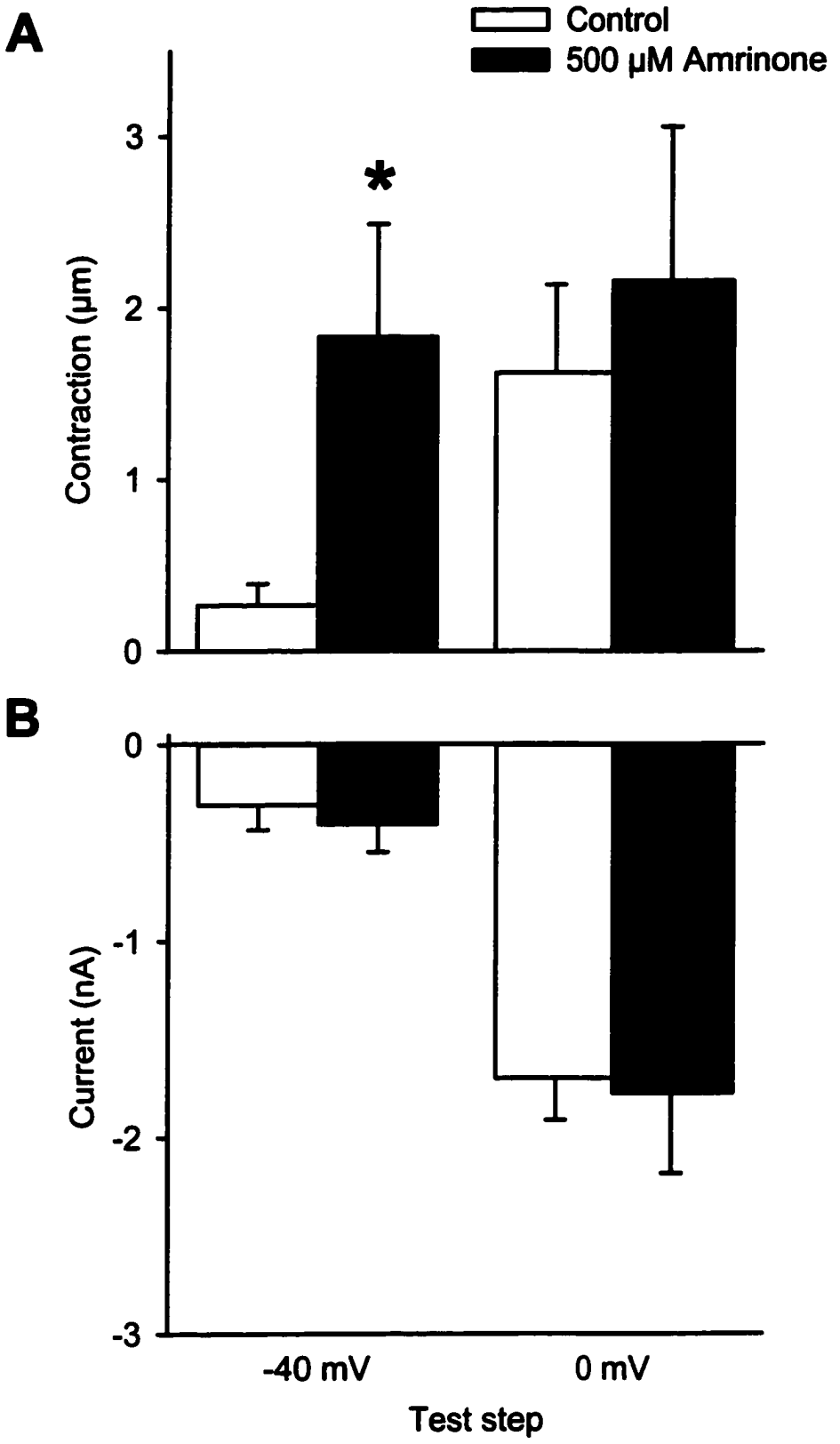
A
Control
500 µM Amrinone
*
Contraction (µm)
3
2
1
0
B
0
-1
-2
-3
Current (nA)
-40 mV
0 mV
Test step

Figure 2-6

Figure 2-7. Amrinone had no effect on cardiac contractions when the VSRM was inactivated. Panels A-C: When the VSRM was inactivated by V_{PC} of –40 mV and contractions were elicited by CICR alone, 100-500 μM amrinone had no effect on amplitudes of contraction-voltage relationships (top panels). Amrinone had little effect on the magnitude of inward current, except at the highest concentration (bottom panels). Open circles represent control data. Filled circles indicate data recorded in the presence of amrinone. * Denotes significantly different from control ($p<0.05$); n= 4-14.

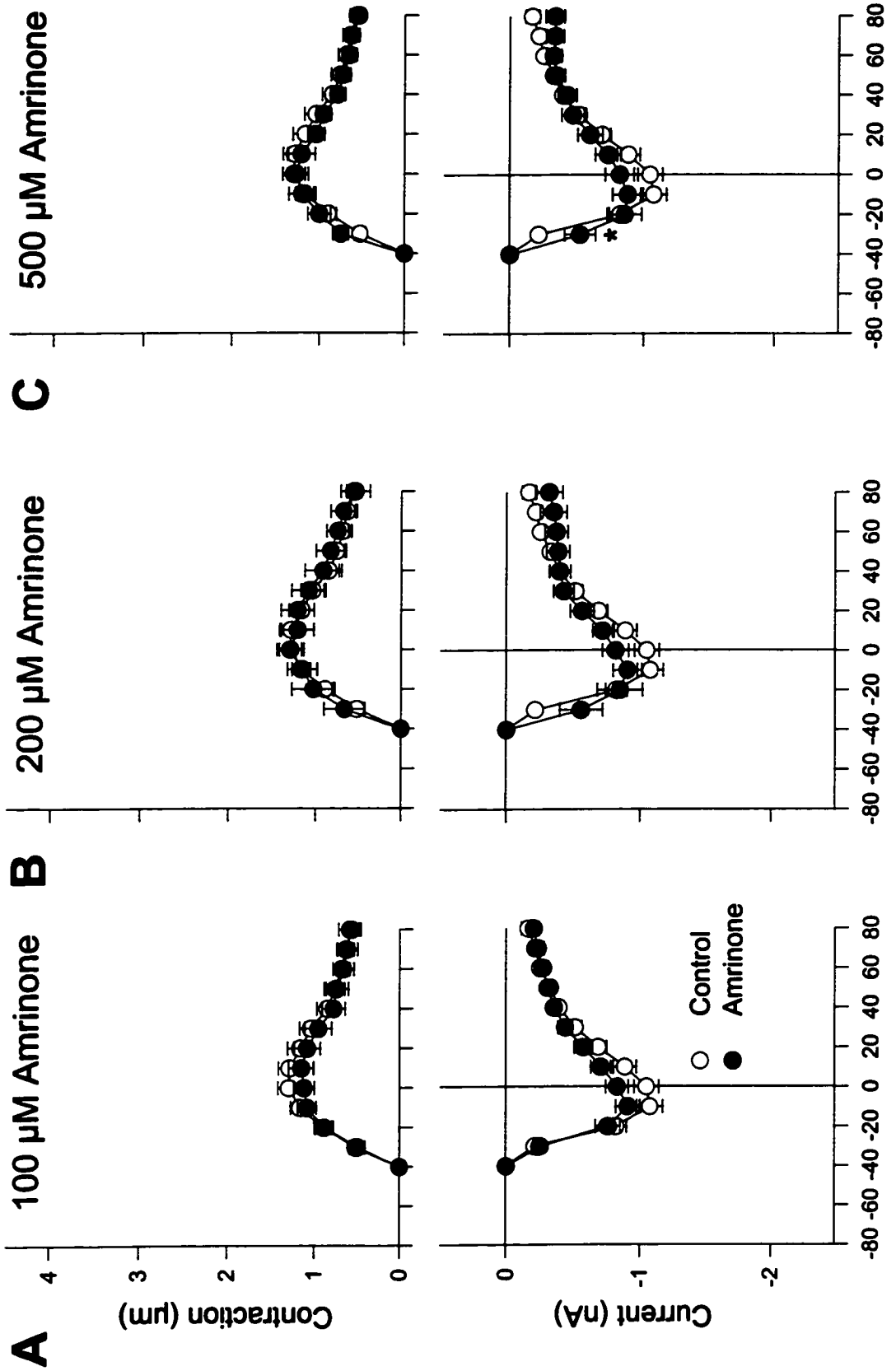
A
B
C
100 µM Amrinone
200 µM Amrinone
500 µM Amrinone
Contraction (µm)
Current (nA)
Test step (mV)
Control
Amrinone
*

Figure 2-7

Figure 2-8. Amrinone significantly increased cardiac contractions when the VSRM was available. Panels A-C: When test steps were made from a V_{PC} of –60 mV and the VSRM was available, amrinone significantly increased the amplitude of contraction-voltage relationships in a concentration-dependent manner (top panels). Amrinone had virtually no effect on the magnitude of the inward current at 100-200 μM, but 500 μM amrinone caused a small increase in current at negative potentials (bottom panels). Open circles represent control data. Filled circles indicate data recorded in the presence of amrinone. *Denotes significantly different from control ($p<0.05$); n= 4-14.

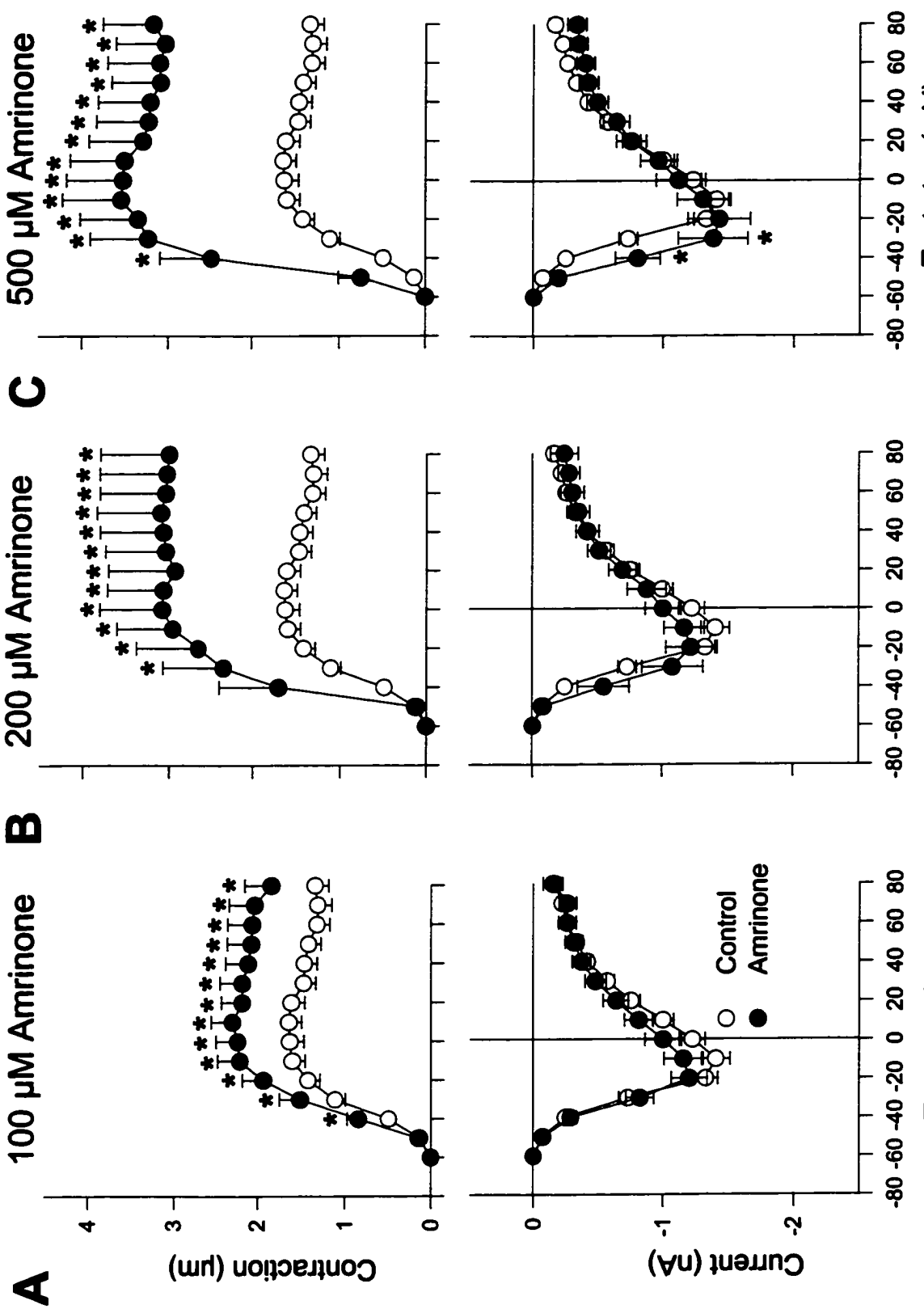
A
B
C
100 µM Amrinone
200 µM Amrinone
500 µM Amrinone
Contraction (µm)
Current (nA)
Test step (mV)
Control
Amrinone

Figure 2-8

the VSRM. Amrinone at concentrations of 100 and 200 μM had no significant effect on inward currents (Figures 2-8A and B). In the presence of 500 μM amrinone, the magnitude of inward currents was increased over a limited range of potentials (Figure 2-8C). Therefore, except at high concentrations, amrinone selectively enhanced cardiac contractions triggered by the VSRM, but had little effect on $I_{Ca\text{-}L}$.

(3) Effects of PDE inhibitors on SR Ca^{2+} release in guinea pig ventricular myocytes

In theory, PDE inhibitors might enhance contractions by increasing SR Ca^{2+} stores. Therefore, the effect of PDE inhibitors on SR Ca^{2+} content was assessed by a rapid caffeine application in guinea pig ventricular myocytes. Caffeine (10 mM) was applied to cells for 4 s as shown in the top panel of Figure 2-9. Figures 2-9A and 2-9B demonstrates representative recordings of caffeine-induced contractures and currents. 100 μM IBMX markedly increased the peak amplitude of caffeine-induced contractures and currents in the absence and presence of IBMX (Figures 2-9C and 2-9D). Mean data for caffeine-induced contractures before and during exposure to IBMX are shown in Figure 2-10. IBMX significantly increased the magnitudes of caffeine-induced contractures and currents, suggesting that IBMX increased SR Ca^{2+} content.

The effect of amrinone on SR Ca^{2+} content was also examined. Representative traces show that amrinone caused a small increase in peak amplitude of caffeine-induced contractures (Figure 2-11A and C). Similarly, amrinone slightly increased the magnitude of caffeine-induced current (Figure 2-11B and D). The mean data for the effect of amrinone on SR Ca^{2+} stores are shown in Figure 2-12. Amrinone caused a modest but

Figure 2-9. IBMX increased the peak amplitude of caffeine-induced contractures and Na^+-Ca^{2+} exchange current. The voltage clamp protocol is shown at the top of the figure. The rapid solution-switcher was used to apply caffeine (10 mM) for 4 seconds. **Panel A:** Representative trace of a caffeine-induced contracture. **Panel B:** Caffeine application caused inward Na^+-Ca^{2+} exchange current. **Panel C:** IBMX (100 μM) caused an increase in the peak and sustained amplitude of the caffeine-induced contracture. **Panel D:** The magnitude of inward current also was increased by IBMX.

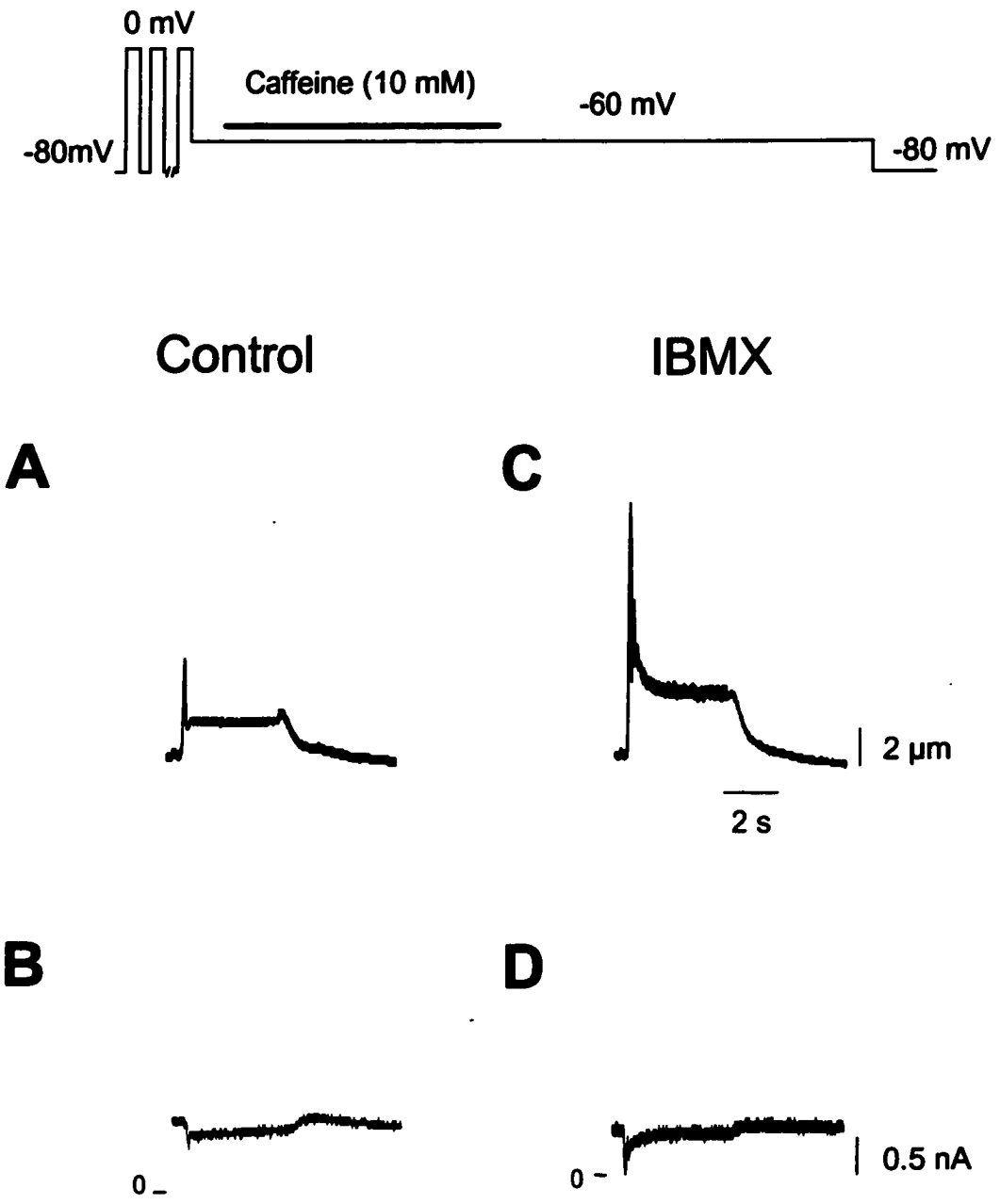
0 mV
Caffeine (10 mM)
-60 mV
-80mV
-80 mV
Control
IBMX
A
C
2 µm
2 s
B
D
0
0
0.5 nA

Figure 2-9

Figure 2-10. Mean data show that IBMX significantly increased the peak amplitudes of caffeine contractures and the integral of the Na^+-Ca^{2+} exchange current. Panel A: Mean data demonstrate that the amplitudes of caffeine contractures were significantly increased by 100 μM IBMX. **Panel B:** Mean data show that IBMX caused an increase in the integral of the Na^+-Ca^{2+} exchange current. *Denotes significantly different from control ($p<0.05$); n= 5.

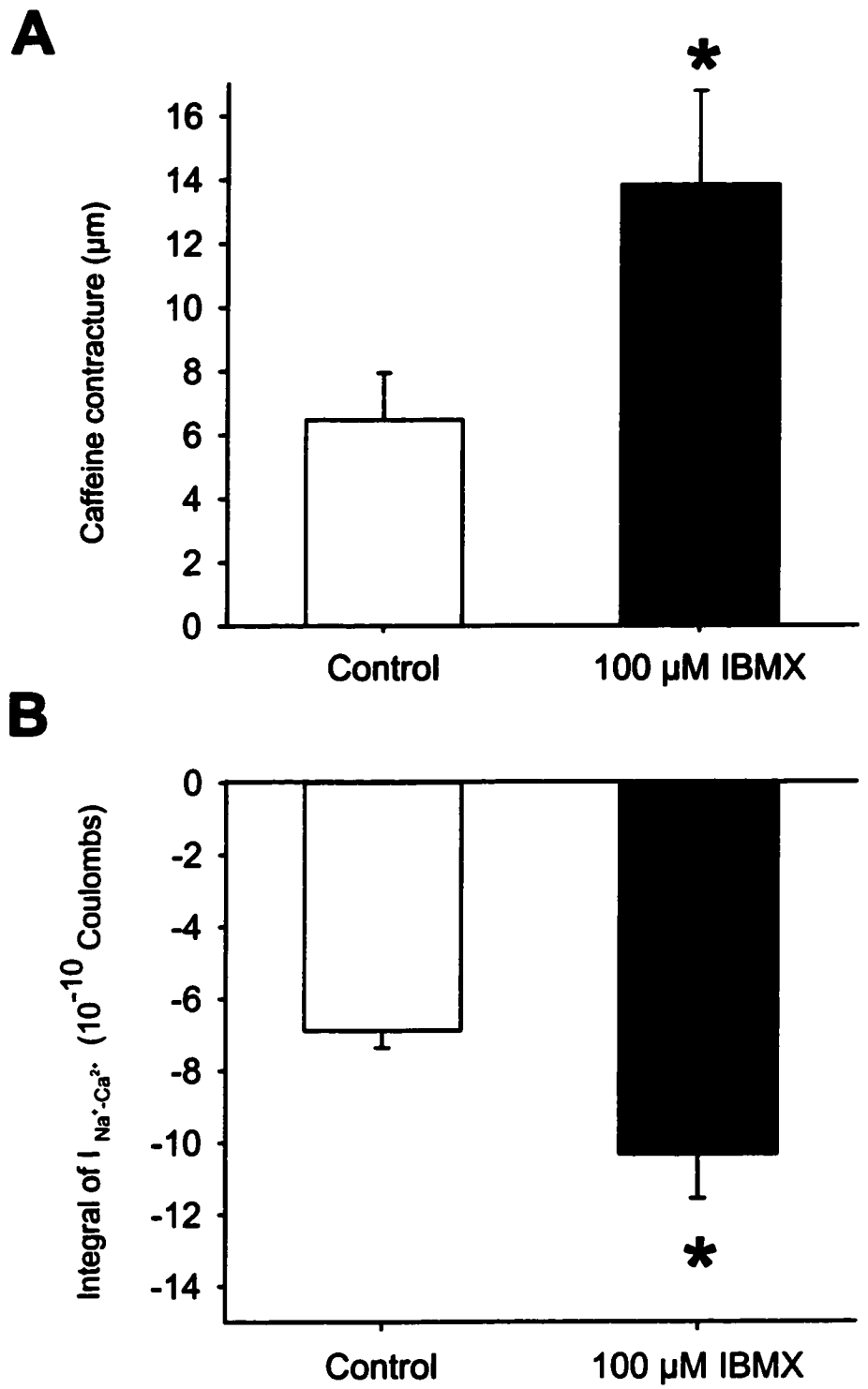
A
*
16
14
12
10
8
6
4
2
0
Caffeine contracture (µm)
Control
100 µM IBMX
B
0
-2
-4
-6
-8
-10
-12
-14
Integral of $I_{Na^+-Ca^{2+}}$ (10^{-10} Coulombs)
*
Control
100 µM IBMX

Figure 2-10

Figure 2-11. The PDE III inhibitor amrinone caused a modest increase in the peak amplitude of caffeine contracture and Na^+-Ca^{2+} exchange current. The voltage clamp protocol is shown at the top of the figure. **Panels A and B:** Representative traces of a caffeine-induced contracture and Na^+-Ca^{2+} exchange current. **Panels C and D:** Amrinone (500 μM) caused a modest increase in the peak amplitude of the caffeine contracture and the Na^+-Ca^{2+} exchange current.

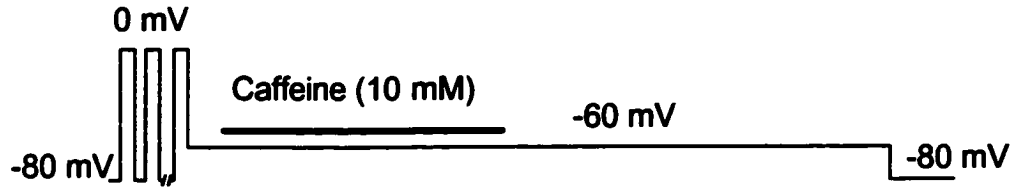
0 mV
Caffeine (10 mM)
-60 mV
-80 mV
-80 mV

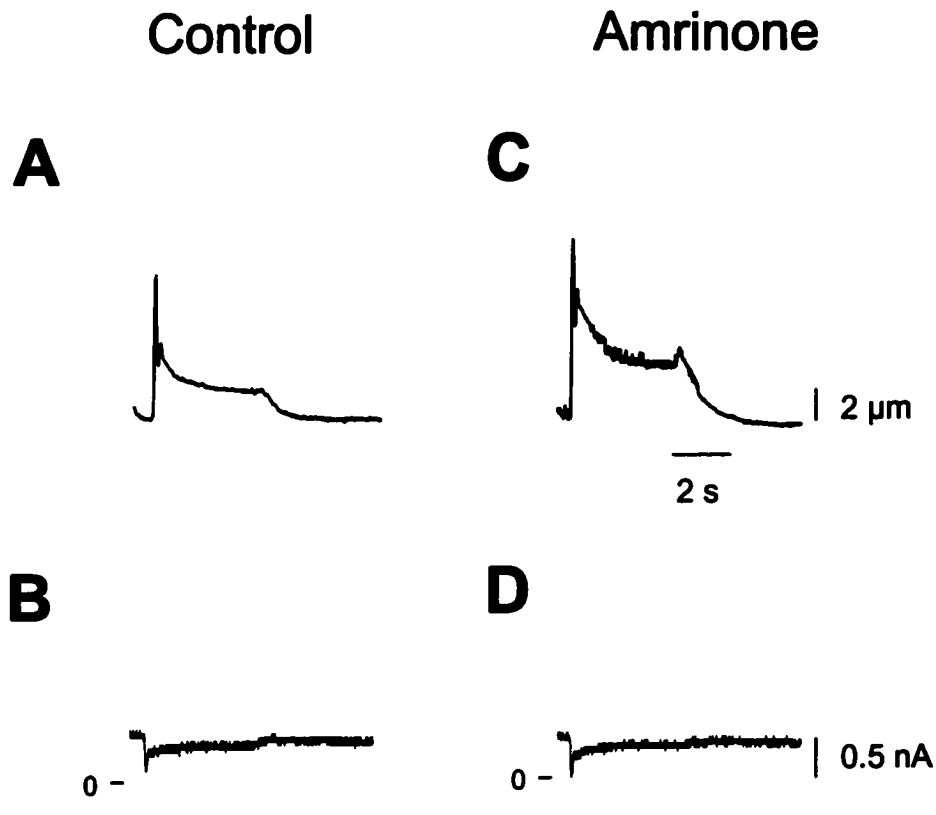
Control
Amrinone
A
C
2 µm
2 s
B
D
0 –
0 –
0.5 nA

Figure 2-11

Figure 2-12. Mean data show that amrinone significantly increased peak amplitudes of caffeine contractures and Na^+-Ca^{2+} exchange currents. Panel A: Mean amplitudes of caffeine contractures were increased significantly by 500 μM amrinone. **Panel B:** Mean data show that amrinone also increased the magnitude of the integral of the Na^+-Ca^{2+} exchange current. *Denotes significantly different from control ($p<0.05$); n= 5.

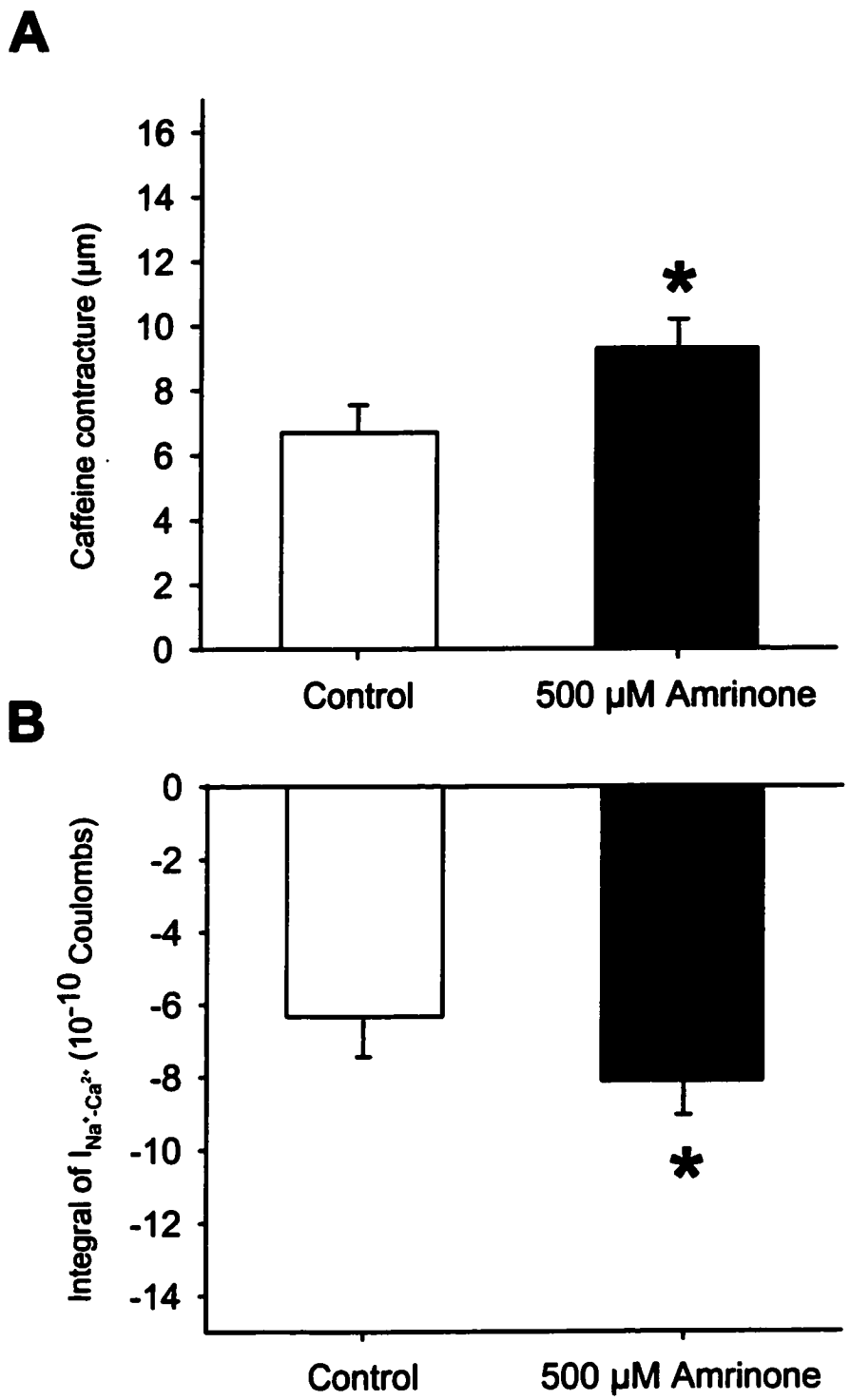
A
Caffeine contracture (µm)
16
14
12
10
8
6
4
2
0
*
Control
500 µM Amrinone
B
Integral of $I_{Na^+-Ca^{2+}}$ (10^{-10} Coulombs)
0
-2
-4
-6
-8
-10
-12
-14
*
Control
500 µM Amrinone

Figure 2-12

significant increase in the magnitudes of caffeine-induced contractures and caffeine-induced Na^{+}-Ca^{2+} exchange current. Therefore, these results suggest that amrinone causes a small increase in SR Ca^{2+} stores.

Next, we determined whether amrinone and IBMX increased fractional release by the VSRM, and CICR or both mechanisms. VSRM and CICR contractions were expressed as a fraction of caffeine-induced contractures to estimate fractional SR Ca^{2+} release by the VSRM and CICR. Contractions elicited by sequential voltage steps to –40 and 0 mV were normalized to caffeine-induced contractures in individual myocytes. Figure 2-13A shows that IBMX selectively increased fractional release of SR Ca^{2+} by the VSRM, but not by CICR ($p<0.05$). Amrinone also selectively increased fractional SR Ca^{2+} release by the VSRM, but had no effect on fractional release by CICR ($p<0.05$) (Figure 2-13B). Taken together, these results suggest that both the non-specific PDE inhibitor IBMX, and the selective PDE III inhibitor amrinone selectively enhance fractional release of SR Ca^{2+} by the VSRM.

Figure 2-13. IBMX and amrinone selectively increased fractional release of SR Ca^{2+} by the VSRM. Fractional release was estimated by normalizing VSRM and CICR contractions (IBMX, Figure 2-3 and amrinone, Figure 2-6) to the peak amplitude of caffeine-induced contractures (IBMX, Figure 2-10 and amrinone, Figure 2-12) in each myocyte. **Panel A:** IBMX significantly increased fractional release of SR Ca^{2+} by the VSRM with no effect on fractional release by CICR. **Panel B:** Amrinone caused a significant increase in fractional SR Ca^{2+} release by the VSRM without effect on fractional release by CICR. *Denotes significantly different from control ($p<0.05$); n= 5.

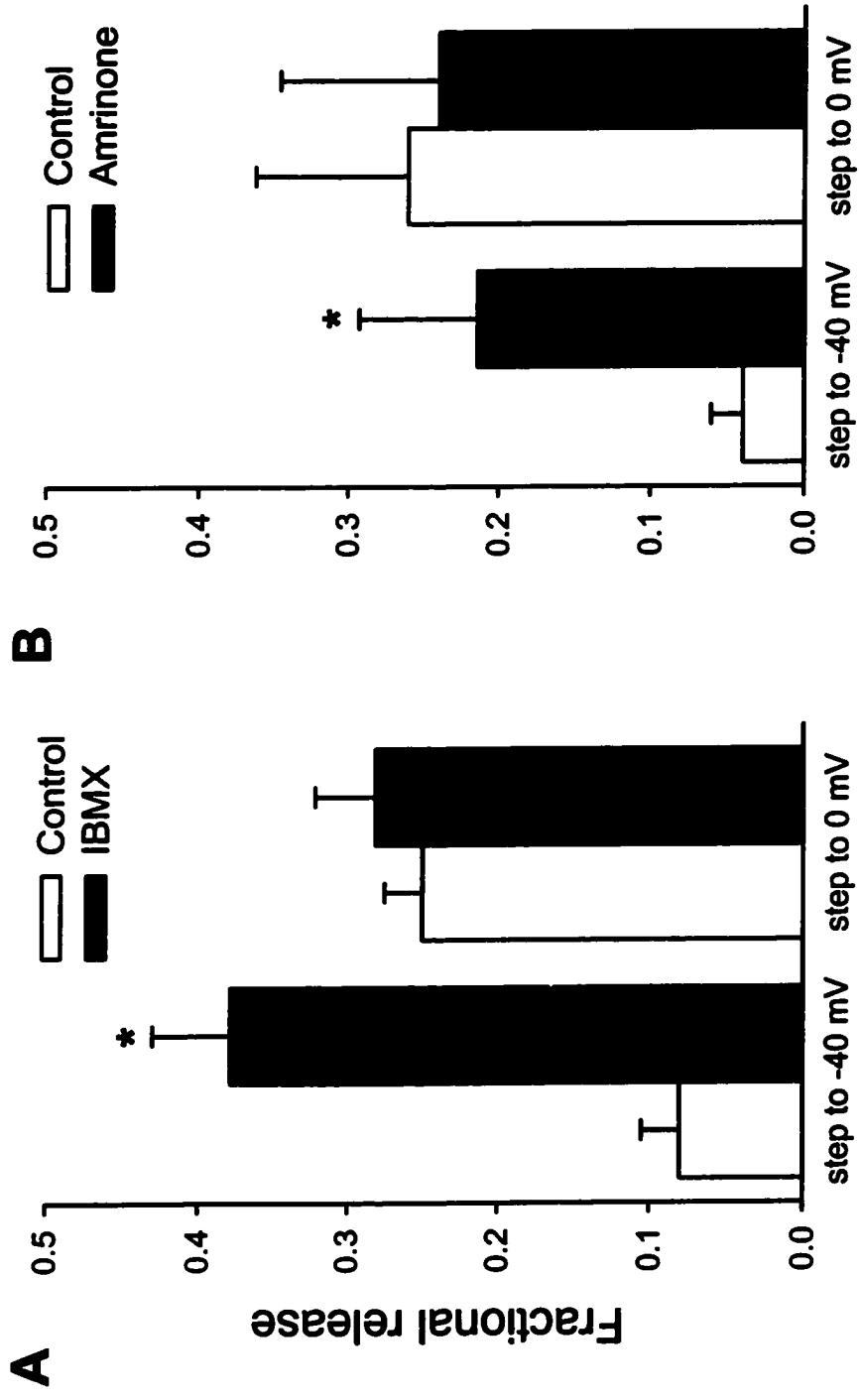
A
B
Fractional release
Control
IBMX
Control
Amrinone
0.5
0.4
0.3
0.2
0.1
0.0
*
*
step to -40 mV
step to 0 mV
step to -40 mV
step to 0 mV

Figure 2-13

3) AMRINONE CANNOT RESTORE DEPRESSED CONTRACTIONS TRIGGERED BY THE VSRM IN VENTRICULAR MYOCYTES FROM CM HAMSTERS.

Our studies have demonstrated that VSRM contractions are selectively decreased in myocytes from CM hamster hearts. Moreover, amrinone has been shown to selectively potentiate VSRM contractions in ventricular myocytes from guinea pigs. Hence, we hypothesize that amrinone may restore depressed VSRM contractions in CM myocytes.

(1) Inotropic effects of amrinone in ventricular myocytes from normal and CM hamsters

The first set of experiments determined the effects of amrinone on currents and contractions in normal hamster ventricular myocytes. Figure 3-1 shows recordings of representative traces of contractions and membrane currents in the absence and presence of amrinone in a normal myocyte. Cells were depolarized from a V_{PC} of –60 mV to activate the VSRM. Amrinone (300 μM) markedly increased the magnitude of contraction, although the inward current activated by this test step was slightly decreased in magnitude. Mean data for the effect of amrinone in normal cells is shown in Figure 3-2. Amrinone (300 μM) significantly increased the amplitude of contractions in normal cells ($p<0.05$). However, in contrast to observations in guinea pig ventricular myocytes, amrinone caused a significant reduction in inward current density in normal hamster myocytes ($p<0.05$).

The next series of experiments examined the effect of amrinone on current and contractions in CM cells. Representative traces of contractions and membrane currents

Figure 3-1. Amrinone increased cardiac contraction in normal hamster myocytes. The voltage clamp protocol is shown at the top of the figure. **Panel A:** Representative traces show that a voltage step to +20 mV from a V_{PC} of –60 mV activated contractions (top) and inward currents (bottom) in a normal cell. **Panel B:** In this cell, superfusion with 300 μM amrinone increased the amplitude of contraction (top), but inward current appeared slightly smaller (bottom).

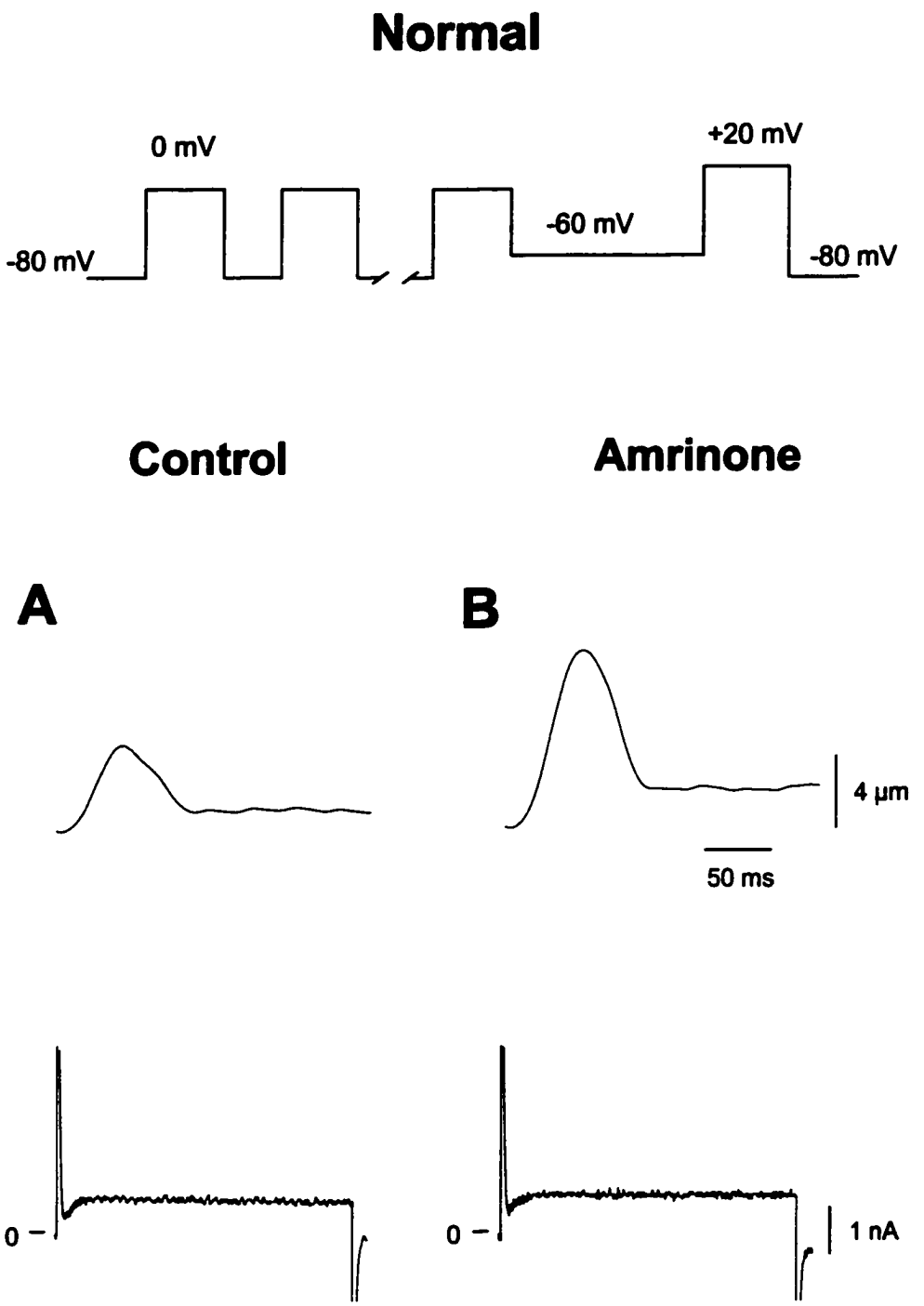
Normal
0 mV
+20 mV
-80 mV
-60 mV
-80 mV
Control
Amrinone
A
B
4 µm
50 ms
0
0
1 nA

Figure 3-1

Figure 3-2. Mean data show that amrinone significantly increased the magnitude of fractional shortening and inward currents in normal hamster cells. Cell shortening was normalized to resting cell length in each cell to represent fractional shortening. **Panel A:** Fractional shortening was significantly increased when cells were superfused with 300 μM amrinone. **Panel B:** Amrinone also significantly decreased the magnitude of inward currents in normal hamster cells. *Denotes significantly different from control ($p<0.05$), n= 9-11.

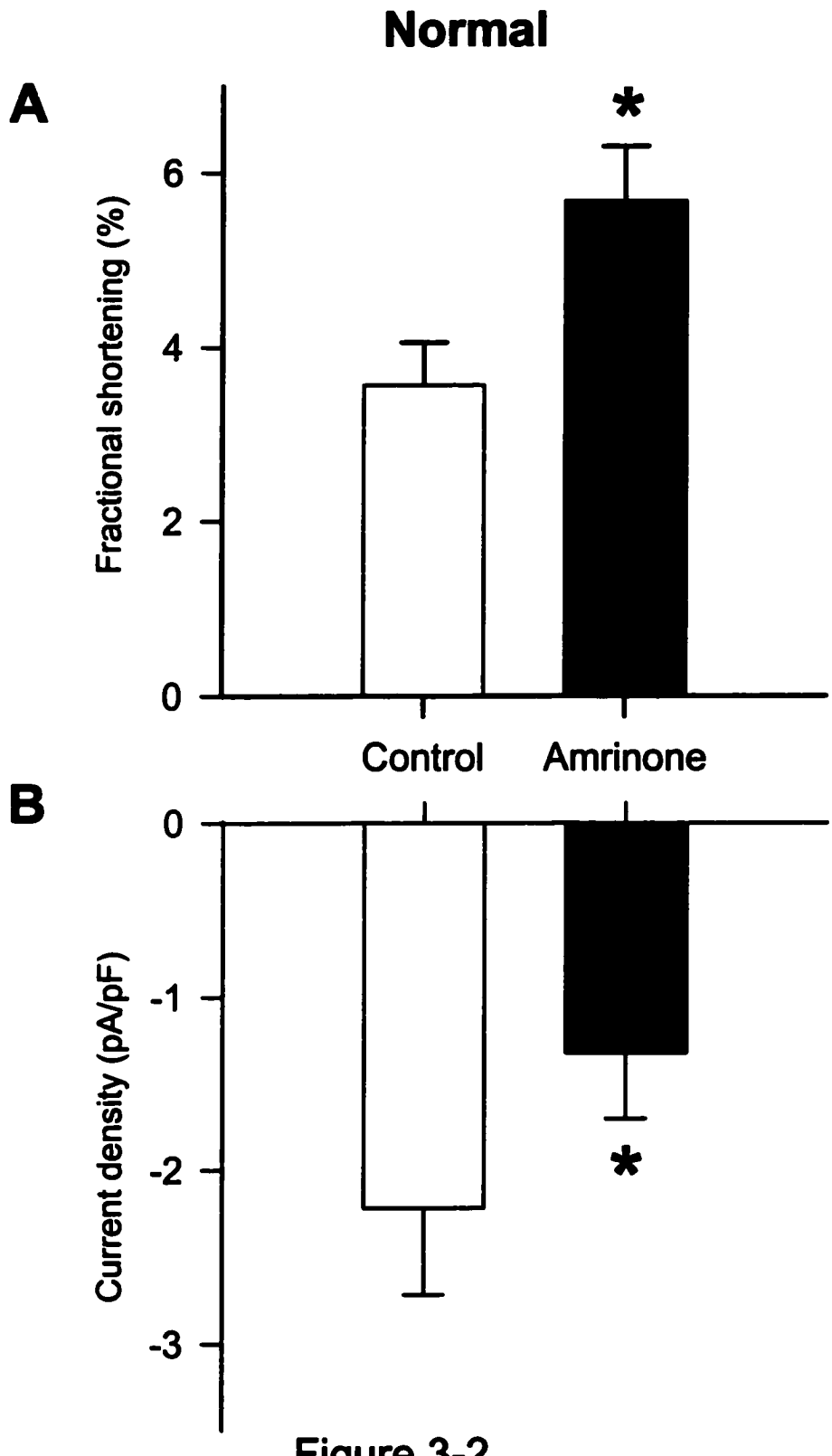
Normal
A
Fractional shortening (%)
6
4
2
0
*
Control
Amrinone
B
Current density (pA/pF)
0
-1
-2
-3
*

Figure 3-2

before and after exposure to amrinone are shown Figures 3-3A and B, respectively. Amrinone had little effect on the amplitude of contraction in the CM cell. The magnitude of inward current appeared to be slightly reduced in this example. Mean magnitude of contractions and inward current density are illustrated in Figure 3-4. In contrast to normal heart, amrinone had no effect on contractions in CM cells. However, inward current density also was reduced by 300 μM amrinone in CM cells ($p<0.05$). Therefore, amrinone did not increase cardiac contraction in ventricular myocytes from CM hamsters.

(2) Effects of amrinone on VSRM and CICR contractions in myocytes from normal and CM hearts

We have demonstrated that amrinone can selectively increase VSRM contractions in ventricular myocytes from guinea pigs. Therefore, the next series of studies were designed to determine whether amrinone has an effect on VSRM contractions in ventricular myocytes from normal and CM hamsters. Here we utilized the same voltage clamp protocol with sequential steps from –60 mV to –40 and 0 mV to separate the VSRM from CICR. Figure 3-5A shows representative recordings of contractions and currents from a normal myocyte elicited by voltage steps as shown at the top of the figure. VSRM contractions were increased by 300 μM amrinone, whereas CICR contractions were unaffected (Figure 3-2B). Amrinone also markedly reduced the magnitude of $I_{Ca\text{-}L}$. Mean data are shown in Figure 3-6. Figure 3-6A illustrates that VSRM contractions were significantly enhanced by 300 to 1000 μM amrinone in normal cells ($p<0.05$), whereas inward current density was not significantly different. In contrast,

Figure 3-3. Amrinone had little effect on cardiac contraction in CM myocytes. The voltage clamp protocol is shown at the top of the figure. **Panel A:** Representative traces show that a voltage step to +20 mV from a V_{PC} of –60 mV activated contractions (top) and inward currents (bottom) in a CM cell. **Panel B:** Representative traces show that amrinone had little effect on the amplitude of contraction (top), but inward currents (bottom) were slightly reduced in the CM cell.

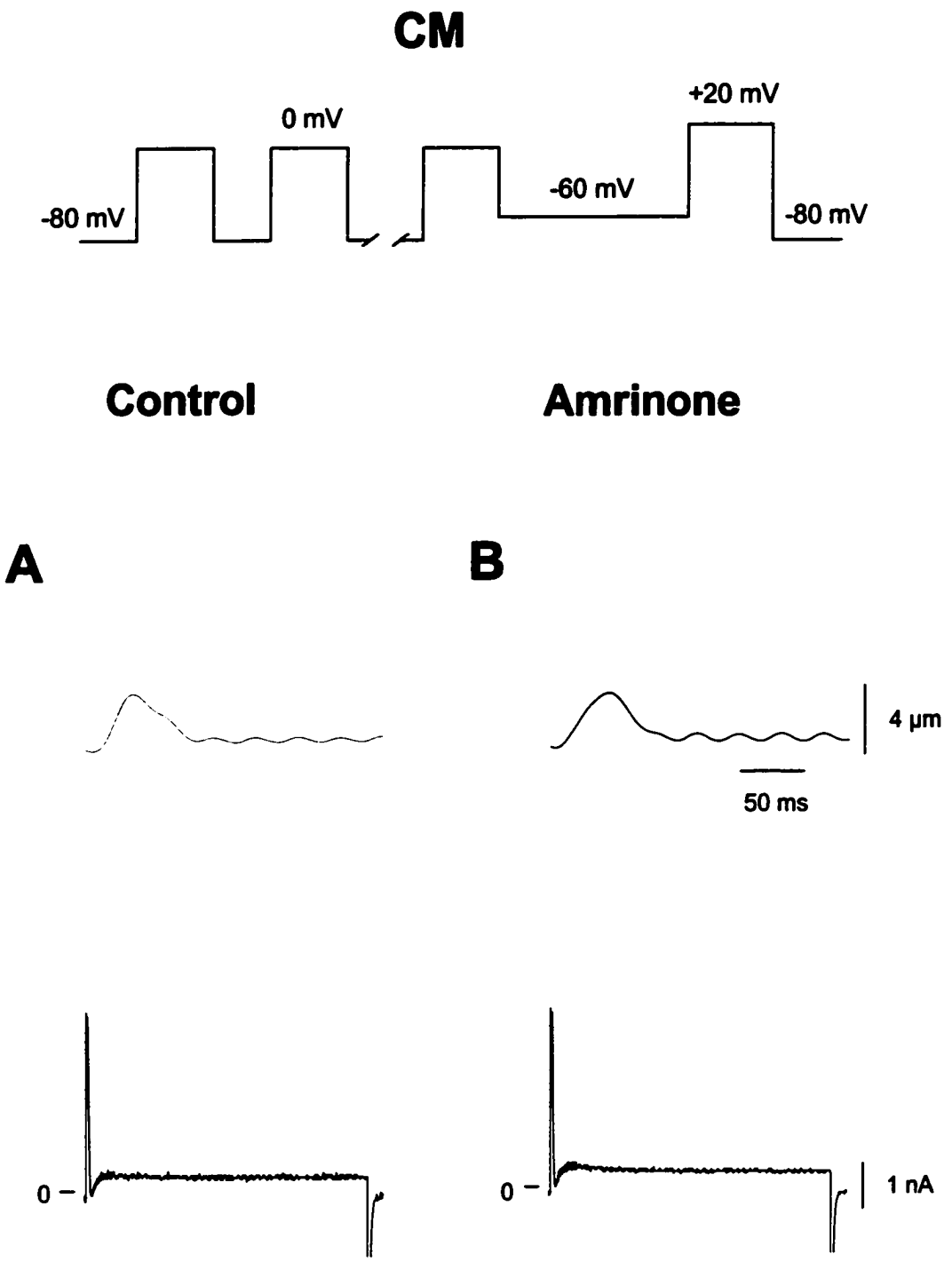
CM
0 mV
+20 mV
-80 mV
-60 mV
-80 mV
Control
Amrinone
A
B
4 µm
50 ms
0
0
1 nA

Figure 3-3

Figure 3-4. Mean data show that amrinone had no effect on fractional shortening elicited by a voltage step from –60 mV to +20 mV in CM cells. **Panel A:** The magnitude of contractions was similar before and after exposure to 300 μM amrinone. **Panel B:** Amrinone significantly decreased inward currents in CM cells. *Denotes significantly different from control ($p<0.05$), n= 6-11.

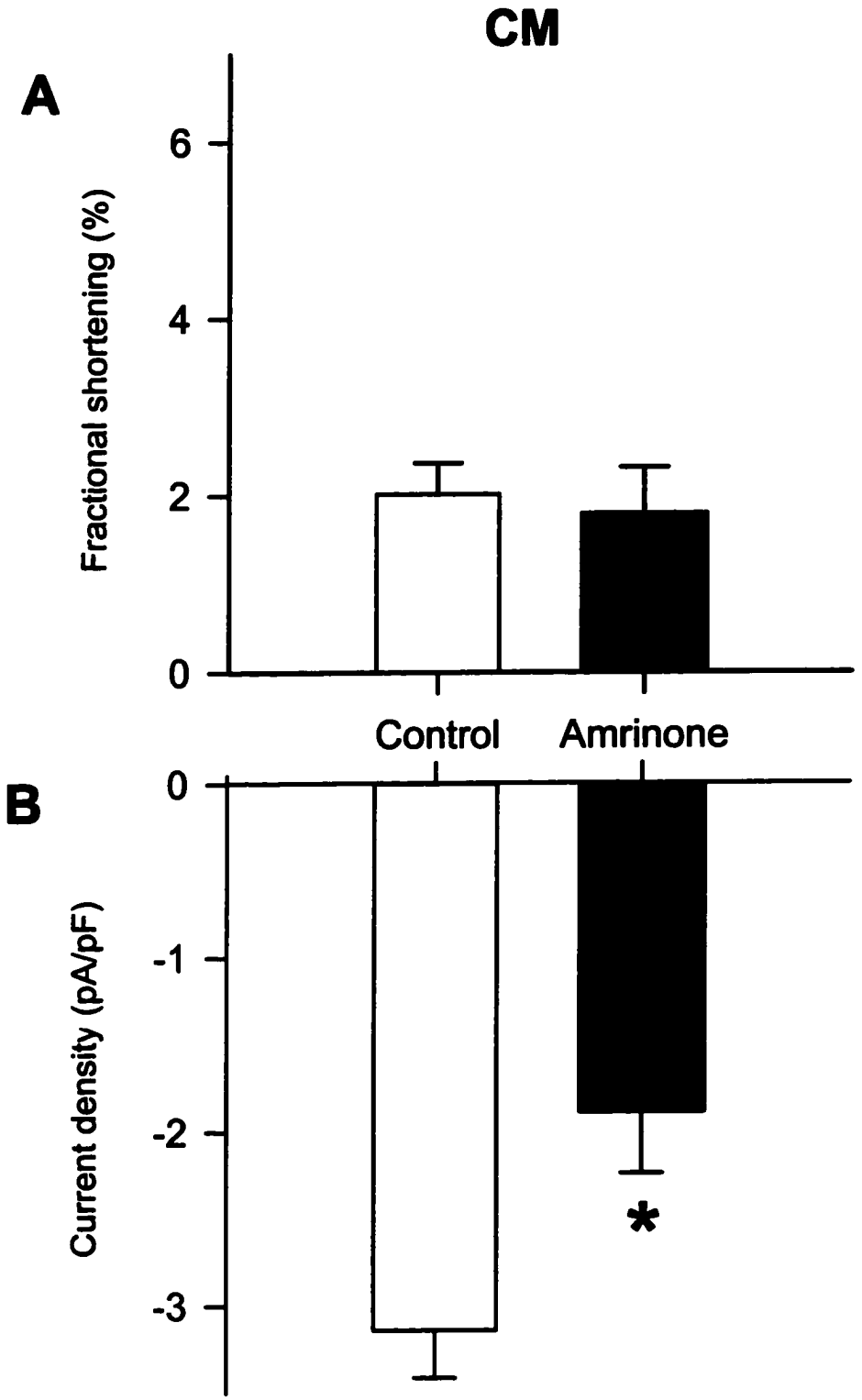
CM
A
Fractional shortening (%)
6
4
2
0
Control
Amrinone
B
Current density (pA/pF)
0
-1
-2
-3
*

Figure 3-4

Figure 3-5. The positive inotropic effect of amrinone was mediated by a selective increase in the magnitude of VSRM contractions in normal hamster myocytes. The voltage clamp protocol is shown at the top of the figure. **Panel A:** Sequential voltage steps from –60 to –40 and 0 mV activated VSRM and CICR contractions and inward currents in a normal myocyte. **Panel B:** Amrinone (300 μM) selectively increased VSRM contractions. In addition, amrinone had little effect on CICR contractions, although it decreased the magnitude of L-type Ca^{2+} current.

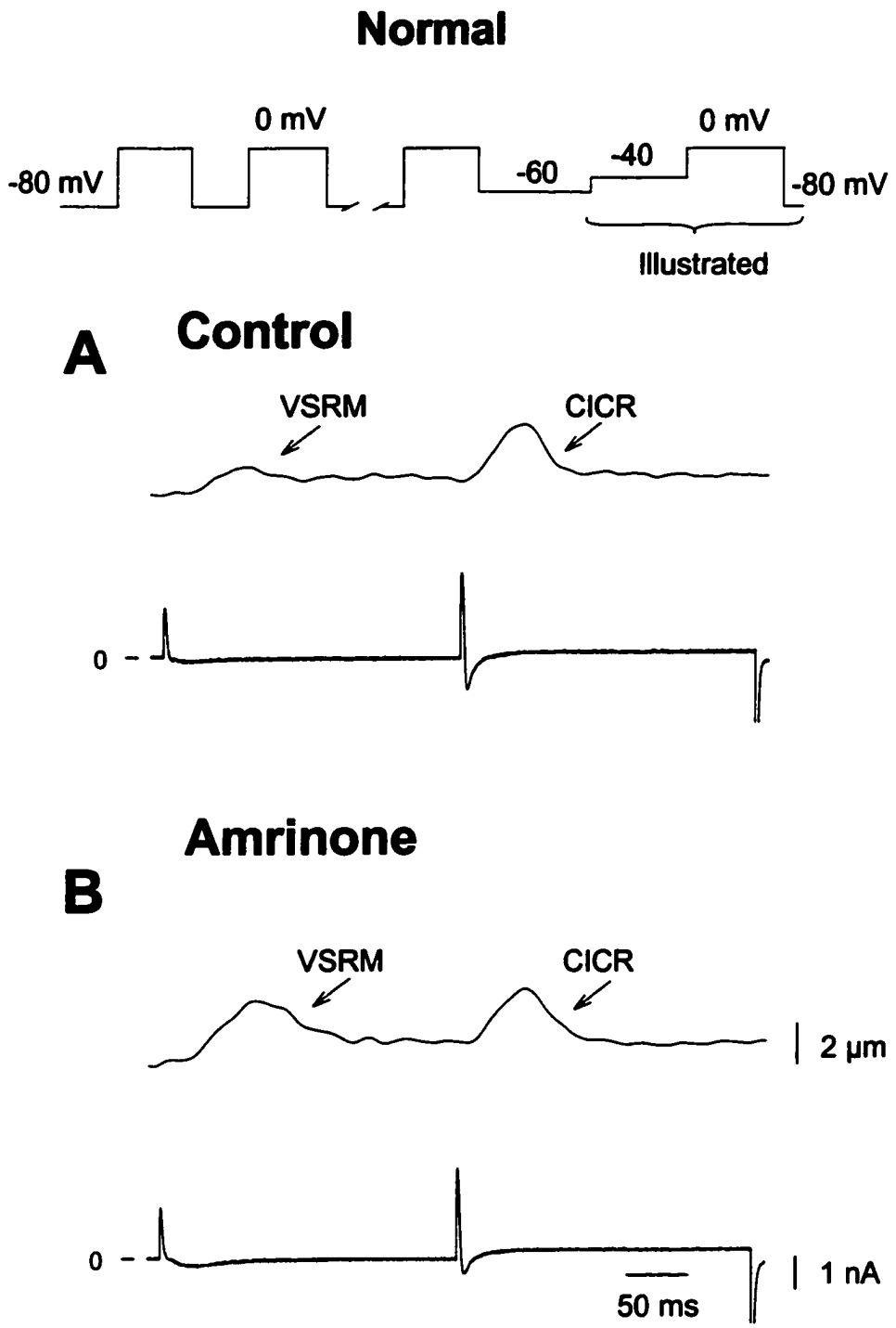
Normal
0 mV
0 mV
-80 mV
-60
-40
-80 mV
Illustrated
A
Control
VSRM
CICR
0
B
Amrinone
VSRM
CICR
2 µm
0
1 nA
50 ms

Figure 3-5

Figure 3-6. Mean data show that amrinone significantly increased the magnitude of VSRM contractions, but had little effect on contractions initiated by CICR in normal hamster myocytes. Panel A: VSRM contractions were significantly increased by amrinone. The magnitude of inward current activated by the step to –40 mV was slightly decreased by amrinone, although this effect was not significant. **Panel B:** Amrinone had no effect on the magnitude of CICR contractions, although it significantly decreased the magnitude of inward currents. *Denotes significantly different from control ($p<0.05$); n= 9.

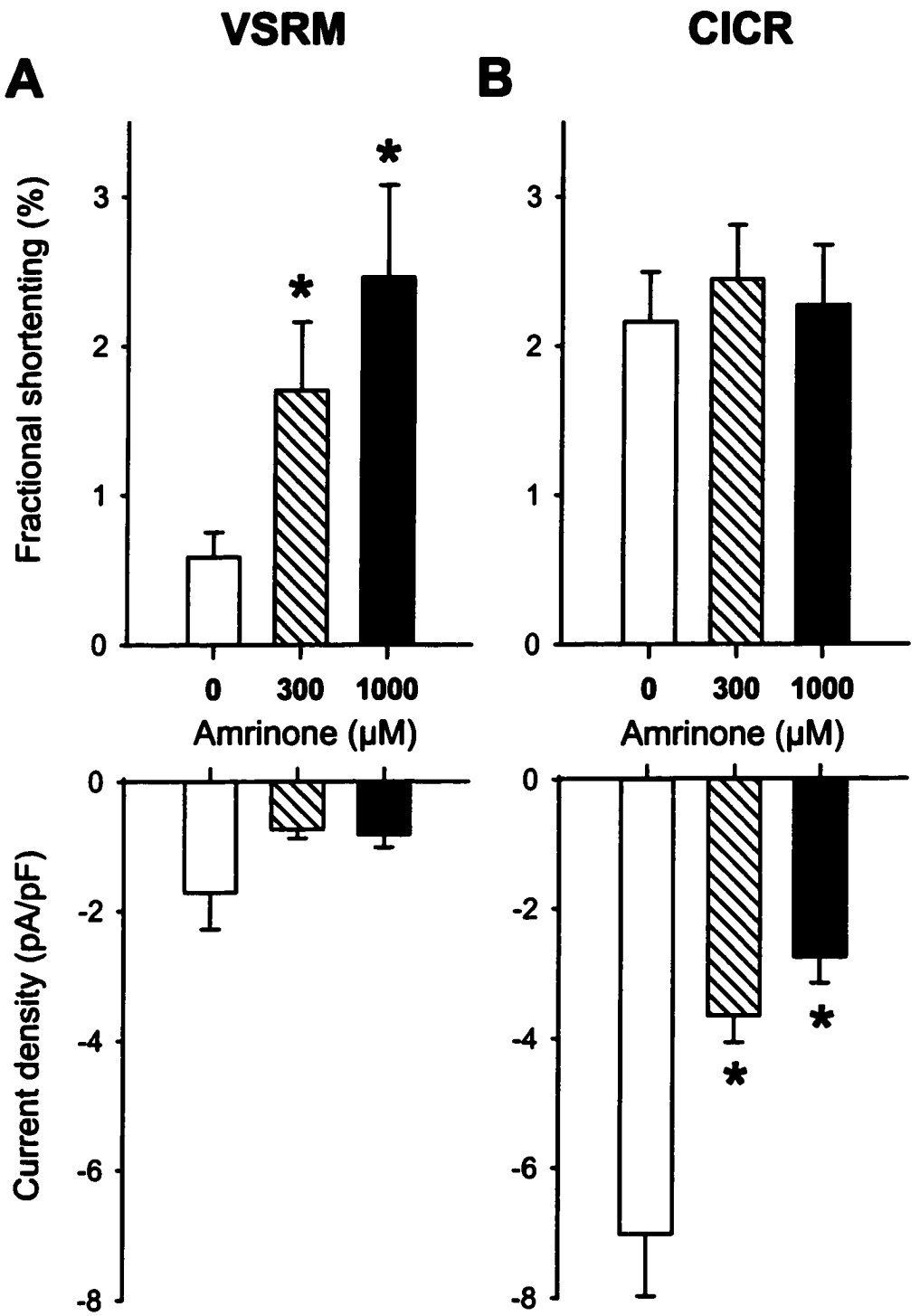
VSRM
CICR
A
B
Fractional shortening (%)
3
2
1
0
*
*
0
300
1000
Amrinone (μM)
Current density (pA/pF)
0
-2
-4
-6
-8
*
*

Figure 3-6

contractions initiated by CICR were not affected by amrinone, although $I_{Ca\text{-}L}$ density was decreased in the presence of amrinone ($p<0.05$).

Next, we compared the effects of amrinone in VSRM and CICR contractions in CM myocytes. Figure 3-7 shows representative recordings of contractions and membrane currents in a CM cell before and after exposure to 300 μM amrinone. Amrinone had little effect on both VSRM and CICR contractions in the CM cell. Mean data are shown in Figure 3-8. Amrinone, at concentrations up to 1000 μM, had no effect on contractions and currents elicited by the test step to –40 mV (Figure 3-8A). Amrinone also did not significantly affect the amplitude of CICR contractions in CM myocytes, although it significantly decreased $I_{Ca\text{-}L}$ ($p<0.05$).

To determine whether amrinone affected contraction-voltage and current-voltage relationships, contraction-voltage and current-voltage relationships in the absence and presence of amrinone were plotted. When the V_{PC} was –40 mV and contractions were activated by CICR alone, 100-1000 μM amrinone had no effect on contractions in normal myocytes (Figure 3-9A), although the magnitude of $I_{Ca\text{-}L}$ was significantly reduced (Figure 3-9B) ($p<0.05$). Figure 3-10A shows that, in CM myocytes, amrinone had no significant effect on contractions when they were triggered by depolarizing steps from a V_{PC} of –40 mV. However, the magnitude of $I_{Ca\text{-}L}$ was reduced in the presence of amrinone in CM cells ($p<0.05$).

Next, we determined the effects of amrinone had effect on contraction-voltage and current-voltage relationships determined from the V_{PC} of –60 mV to allow activation of the VSRM in normal cells (Figure 3-11). When the VSRM was available, the amplitudes of contractions were significantly increased in the presence of 300 and 1000 μM

Figure 3-7. Amrinone had virtually no effect on the magnitudes of VSRM and CICR contractions in CM myocytes. The voltage clamp protocol is shown at the top of the figure. **Panel A:** Sequential voltage steps from –60 to –40 and 0 mV were used to activate VSRM and CICR contractions. As described in earlier experiments, VSRM contractions were attenuated in CM myocytes compared to normal (see Figures 1-5 and 1-6). **Panel B:** Amrinone had no effect on the magnitude of either VSRM or CICR contractions.

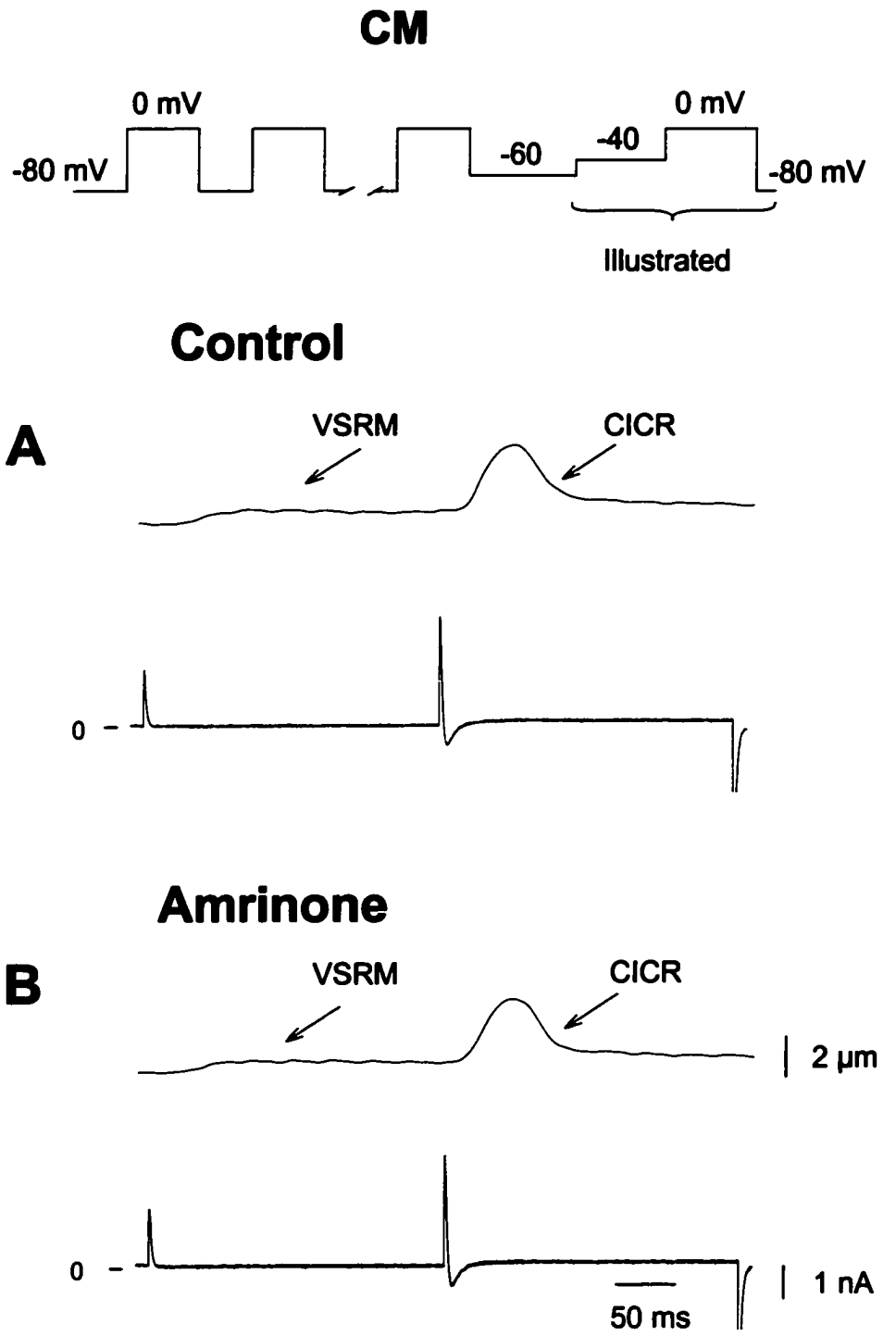
CM
0 mV
0 mV
-80 mV
-60
-40
-80 mV
Illustrated
Control
A
VSRM
CICR
0
Amrinone
B
VSRM
CICR
2 µm
0
1 nA
50 ms

Figure 3-7

Figure 3-8. Mean data show that amrinone had no effect on either VSRM or CICR contractions, but decreased inward current in CM myocytes. Panel A: Contractions and currents initiated by a voltage step to –40 mV were not affected by amrinone in CM cells. **Panel B:** Amrinone had little effect on the magnitude of CICR contractions, although it significantly decreased the magnitude of inward currents in CM cells. *Denotes significantly different from control ($p<0.05$); n= 6-10.

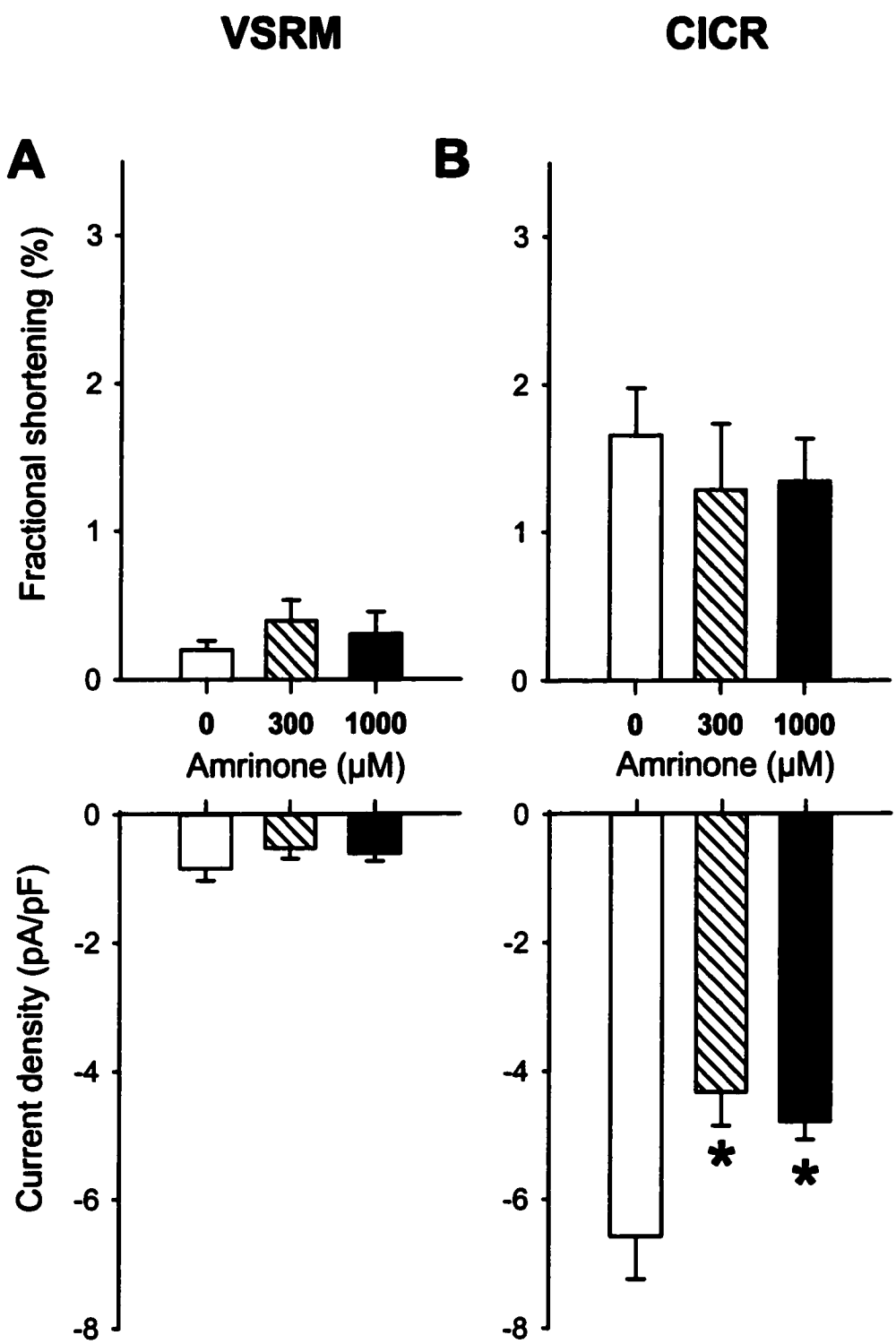
VSRM
CICR
A
B
Fractional shortening (%)
3
2
1
0
0
300
1000
Amrinone (μM)
Current density (pA/pF)
0
-2
-4
-6
-8
*
*

Figure 3-8

Figure 3-9. Although amrinone did not have effect on the magnitude of CICR contractions, it decreased the magnitude of L-type Ca^{2+} current in normal hamster myocytes. The voltage clamp protocol is shown at the top of the figure. **Panel A:** Contractions elicited by voltage steps from a V_{PC} of –40mV were not affected by amrinone. **Panel B:** The magnitude of L-type Ca^{2+} current was significantly decreased by increasing concentrations of amrinone in normal hamster myocytes (n= 9-11). *Denotes 300 μM amrinone significantly different from control, $p<0.05$. #Denotes 1000 μM amrinone significantly different from control, $p<0.05$.

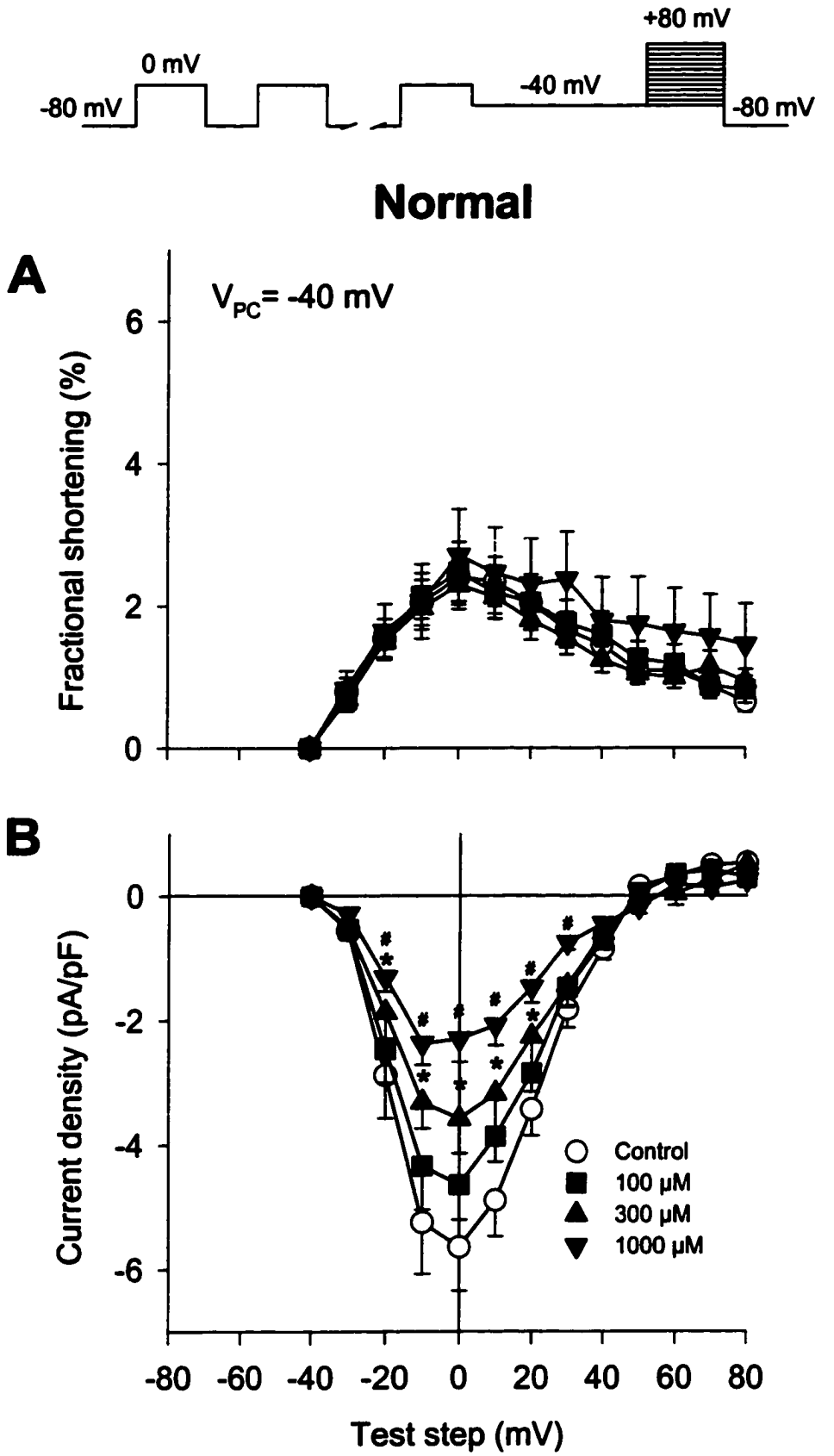
+80 mV
0 mV
-80 mV
-40 mV
-80 mV
Normal
A
V_{PC}= -40 mV
Fractional shortening (%)
6
4
2
0
B
Current density (pA/pF)
0
-2
-4
-6
Control
100 µM
300 µM
1000 µM
-80 -60 -40 -20 0 20 40 60 80
Test step (mV)

Figure 3-9

Figure 3-10. Amrinone had virtually no effect on the CICR contractions, but reduced L-type Ca^{2+} current in CM cells. The voltage clamp protocol is shown at the top of the figure. **Panel A:** Contractions triggered by CICR were not affected by amrinone in CM myocytes (n= 4-11). **Panel B:** The magnitude of L-type Ca^{2+} current was significantly decreased by increasing concentrations of amrinone in CM myocytes. *Denotes 300 μM amrinone significantly different from control, $p<0.05$. #Denotes 1000 μM amrinone significantly different from control, $p<0.05$.

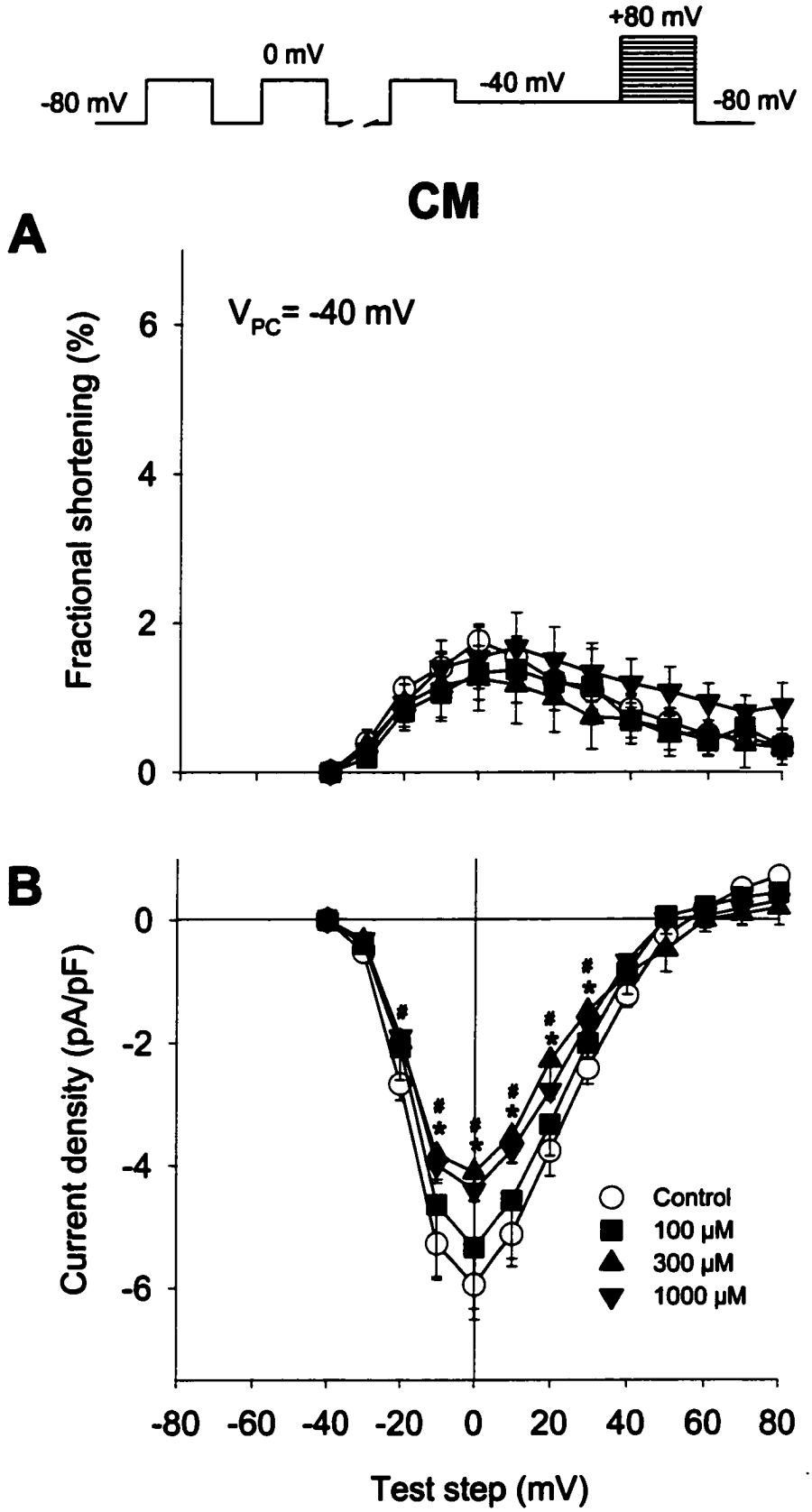
+80 mV
0 mV
-40 mV
-80 mV
-80 mV
CM
A
V_{PC}= -40 mV
Fractional shortening (%)
6
4
2
0
B
Current density (pA/pF)
0
-2
-4
-6
Control
100 µM
300 µM
1000 µM
-80 -60 -40 -20 0 20 40 60 80
Test step (mV)

Figure 3-10

Figure 3-11. Amrinone increased the magnitude of contractions when the VSRM was available in normal cells, although it decreased inward currents. The voltage clamp protocol was shown at the top of the figure. **Panel A:** Contractions elicited by voltage steps from a V_{PC} of –60 mV were significantly increased by 300 and 1000 μM amrinone. **Panel B:** The magnitude of inward currents was significantly decreased by amrinone in normal myocytes (n= 9-11).

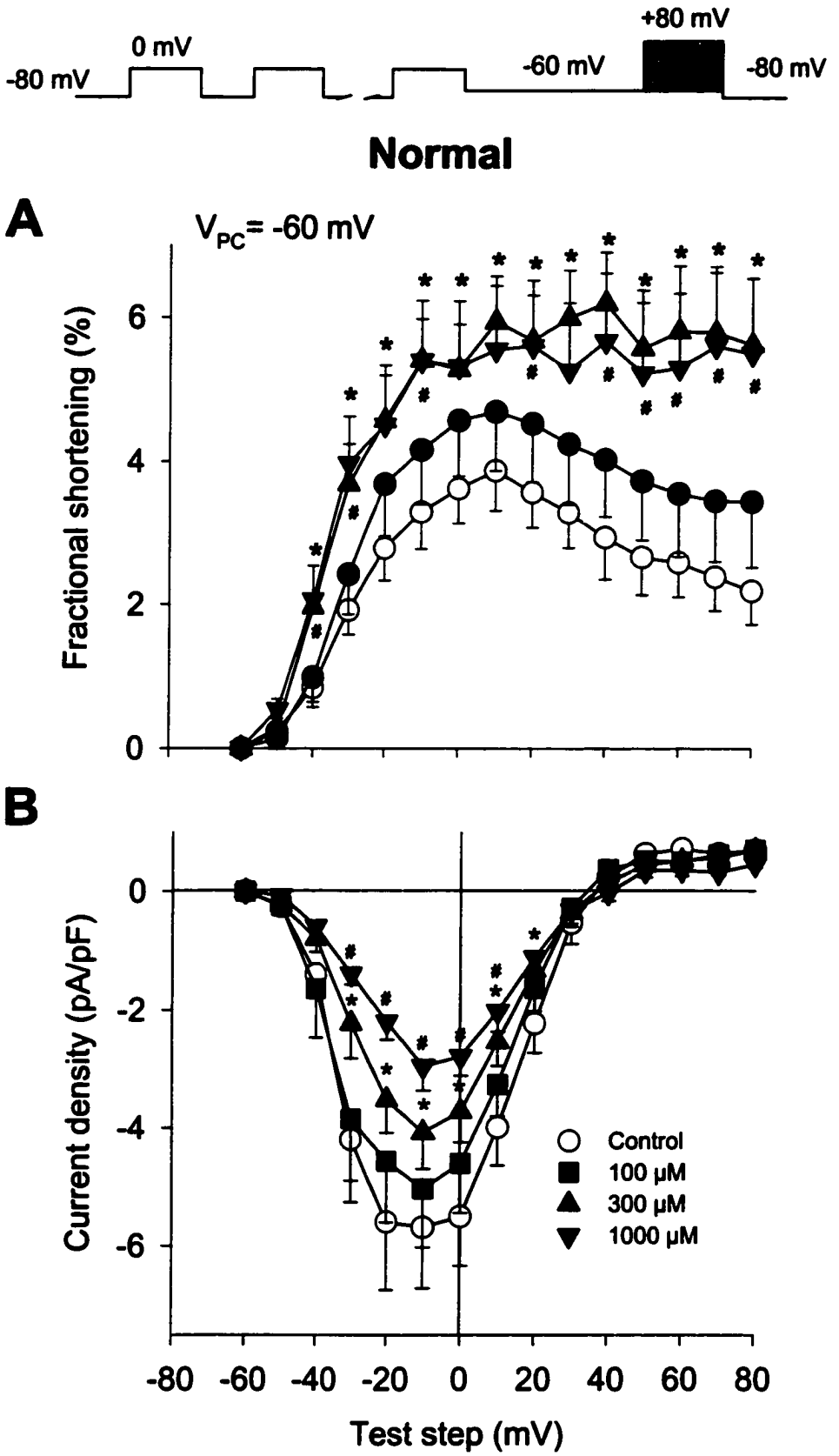
+80 mV
0 mV
-80 mV
-60 mV
-80 mV
Normal
A
V_{PC}= -60 mV
Fractional shortening (%)
6
4
2
0
B
Current density (pA/pF)
0
-2
-4
-6
Control
100 µM
300 µM
1000 µM
-80 -60 -40 -20 0 20 40 60 80
Test step (mV)

Figure 3-11

amrinone in normal cells (Figure 3-11A). Figure 3-11B shows that amrinone reduced the magnitude of inward current ($p<0.05$). However, in CM myocytes amrinone did not significantly affect the amplitude of contraction when cells were depolarized from a V_{PC} of –60 mV, although inward current density was reduced ($p<0.05$) (Figure 3-12). Thus, the positive inotropic effects of amrinone in normal hamster myocytes, which are manifest as potentiation of VSRM contractions, are absent in ventricular myocytes from CM hamsters.

(3) The role of fractional SR Ca^{2+} release by the VSRM in inotropic effects of amrinone in normal and CM myocytes

These experiments were designed to determine whether fractional SR Ca^{2+} release by the VSRM plays an important role in inotropic effects of amrinone in normal and CM hamster hearts. The effects of amrinone on caffeine-induced contractures and their associated inward currents were determined in both normal and CM hearts. Figure 3-13 shows representative traces of caffeine-induced contractures and inward currents before and after application of 300 μM amrinone in a normal hamster myocyte. Amrinone had little effect on the peak amplitude of the caffeine-induced contracture. The caffeine-induced current appeared similar in the absence and presence of amrinone in this example. Mean magnitudes of caffeine contractures and Na^{+}-Ca^{2+} exchange current are shown in Figure 3-14. Amrinone had no effect on the peak amplitude of caffeine-induced contractures in normal cells (Figure 3-14A). Figure 3-14B shows that the integral of the caffeine-induced Na^{+}-Ca^{2+} exchange current was slightly but significantly increased by amrinone in normal cells ($p<0.05$). This suggests that amrinone caused a small increase

Figure 3-12. Amrinone had no effect on contractions when the VSRM was available in CM cells, although it decreased inward currents. The voltage clamp protocol is shown at the top of the figure. **Panel A:** Contractions elicited by voltage steps from a V_{PC} of –60 mV were not affected by amrinone in CM cells. **Panel B:** The magnitude of inward currents was significantly decreased by amrinone in CM cells (n= 4-11). *Denotes 300 μM significantly different from control, $p<0.05$.

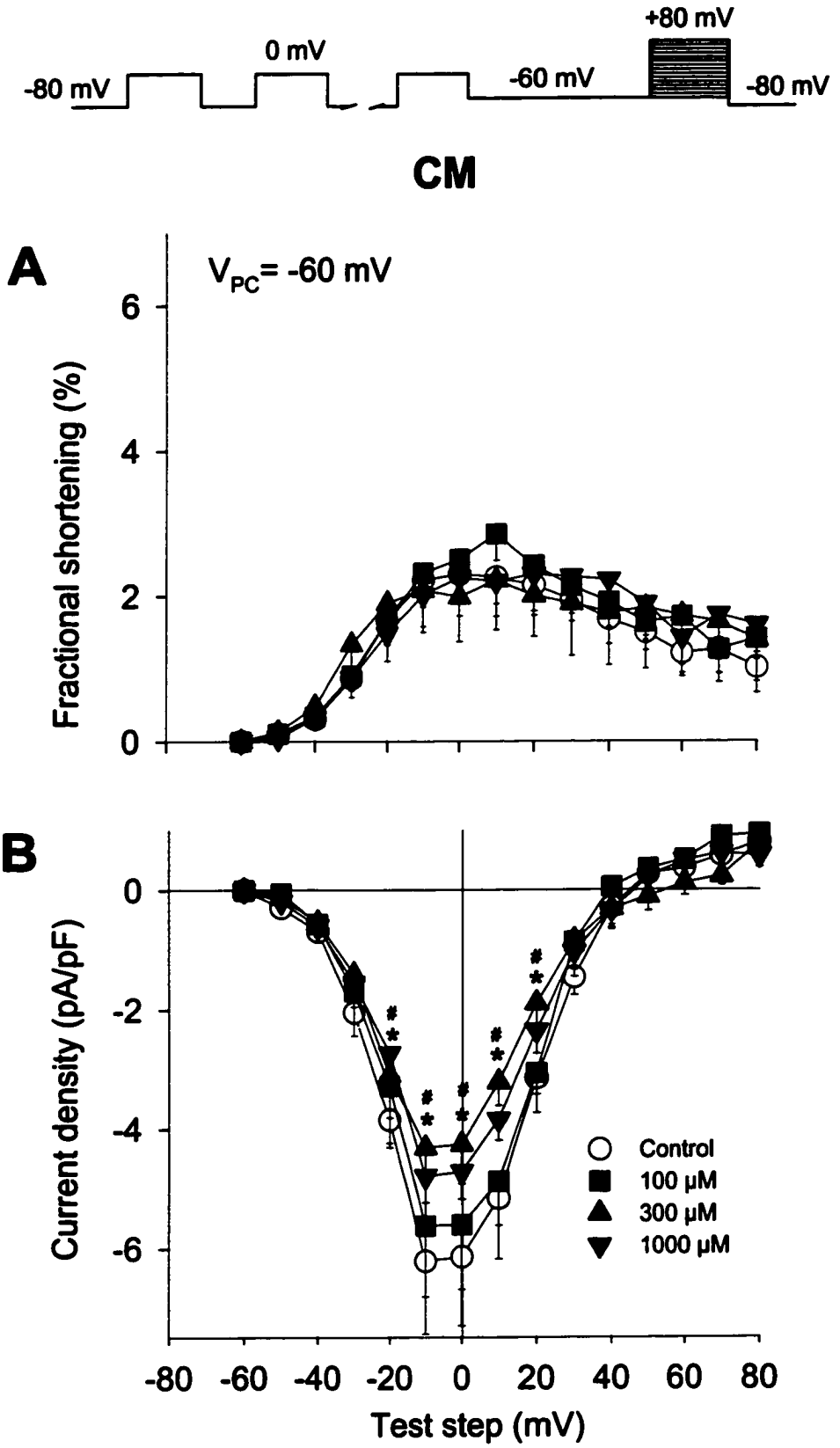
+80 mV
0 mV
-80 mV
-60 mV
-80 mV
CM
A
V_{PC}= -60 mV
Fractional shortening (%)
6
4
2
0
B
Current density (pA/pF)
0
-2
-4
-6
Control
100 µM
300 µM
1000 µM
-80 -60 -40 -20 0 20 40 60 80
Test step (mV)

Figure 3-12

Figure 3-13. Representative traces show that amrinone had little effect on the peak amplitude of caffeine-induced contracture and Na^+-Ca^{2+} exchange current. Caffeine (10 mM) was applied with a rapid switcher for 4s, 500 ms after the conditioning pulse train. **Panels A and B:** Representative traces of caffeine-induced contracture and Na^+-Ca^{2+} exchange current before exposure to 300 μM amrinone. **Panels C and D:** Representative traces show that 300 μM amrinone had little effect on the peak amplitude of caffeine-induced contracture and Na^+-Ca^{2+} exchange current.

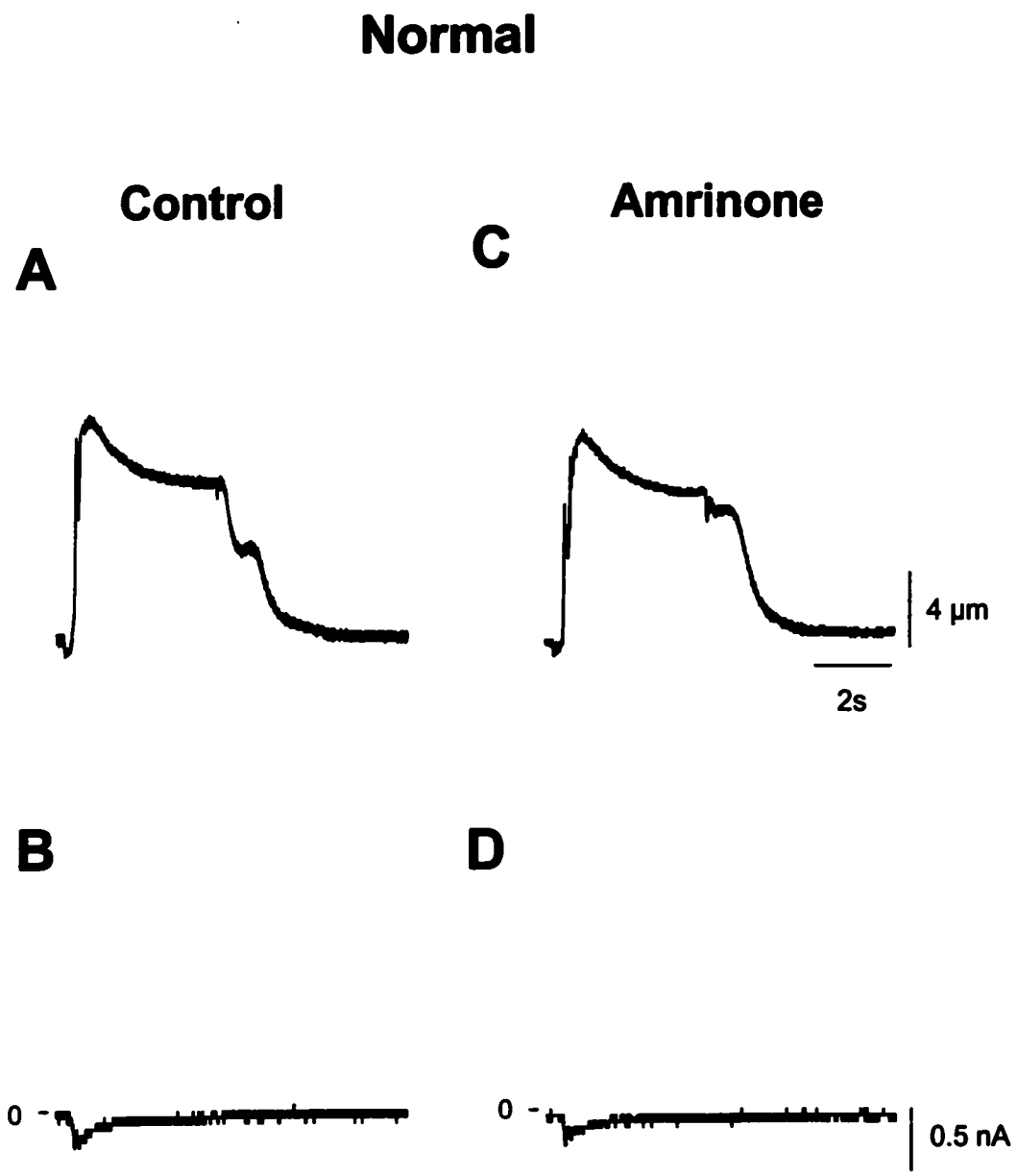

Figure 3-13

Figure 3-14. Mean data show that amrinone had no effect on the magnitude of caffeine-induced contractures, but caused a slight increase in the Na^+-Ca^{2+} exchange current in normal cells. The integral of caffeine-induced Na^+-Ca^{2+} exchange current was normalized to cell capacitance in each cell. **Panel A:** 300 μM amrinone had little effect on the magnitude of caffeine-induced contractures. **Panel B:** Amrinone caused a small but significant increase in the integral of the Na^+-Ca^{2+} exchange current in normal myocytes. *Denotes significantly different from control, $p<0.05$; $n= 5$.

Normal

A Caffeine-induced contractures

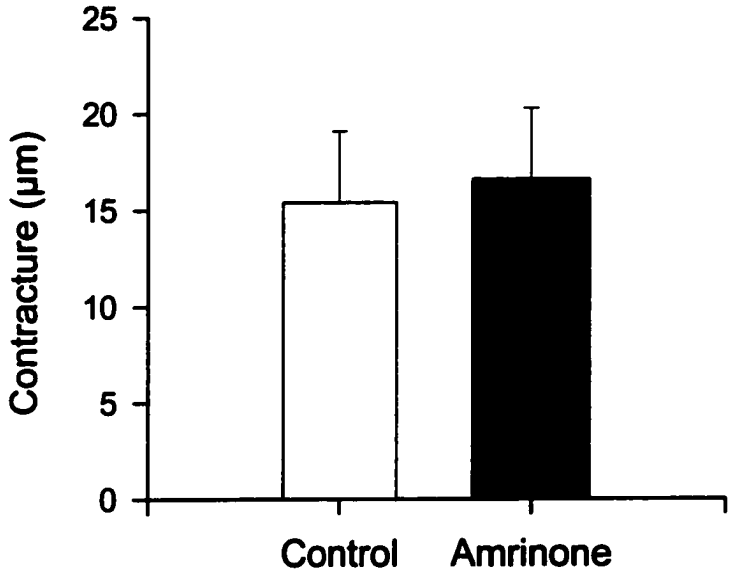

B Normalized $I_{Na^+-Ca^{2+}}$

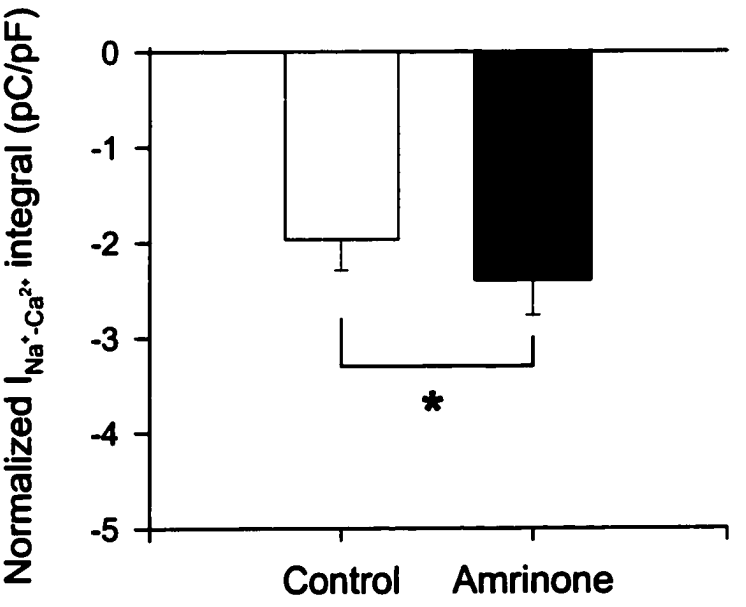

Figure 3-14

in SR Ca^{2+} content in normal myocytes. Next, we determined the effects of amrinone on caffeine-induced contractures and currents in CM cells. Figure 3-15A shows that amrinone had little effect on peak amplitude of caffeine-induced contractures. The caffeine-induced Na^{+}-Ca^{2+} exchange current appeared similar in the absence and presence of amrinone in this example (Figure 3-15B). Mean data (Figure 3-16) show that neither peak amplitudes of caffeine contractures nor integral of Na^{+}-Ca^{2+} exchange current was significantly reduced by amrinone. Thus, these results suggest that amrinone had little effect on SR Ca^{2+} stores in CM cells.

We have shown that, in guinea pigs ventricular myocytes, potentiation of the VSRM is associated with enhancement of fractional release of SR Ca^{2+} by the VSRM. Thus, we also examined the role of fractional release of SR Ca^{2+} by the VSRM in inotropic effects of amrinone in normal hamster cells. The voltage clamp protocol for Figure 3-17A is shown at the top of the figure. Sequential test steps from a V_{PC} of –60 mV to –40 and 0 mV activate the VSRM and CICR, respectively. Amrinone significantly increased the magnitude of VSRM contractions but not CICR contractions in normal cells (Figure 3-17A). The VSRM and CICR contractions were normalized to caffeine-induced contractures in each myocyte to estimate fractional SR Ca^{2+} release by each mechanism. Figure 3-17B shows that fractional release of SR Ca^{2+} by the VSRM was significantly increased by amrinone in normal cells ($p<0.05$). However, amrinone had no effect on SR Ca^{2+} release by CICR in myocytes from normal hamsters. These results suggest that enhancement of SR fractional Ca^{2+} release contributes to positive inotropy in normal hamster myocytes.

Figure 3-15. Representative traces show that amrinone had little effect on the peak amplitude of caffeine-induced contracture and Na^+-Ca^{2+} exchange current in a CM cell. Panels A and C: Representative traces show that 300 μM amrinone had little effect on the peak amplitude of caffeine-induced contracture. **Panels B and D**: Amrinone had little effect on Na^+-Ca^{2+} exchange current in a CM cell.

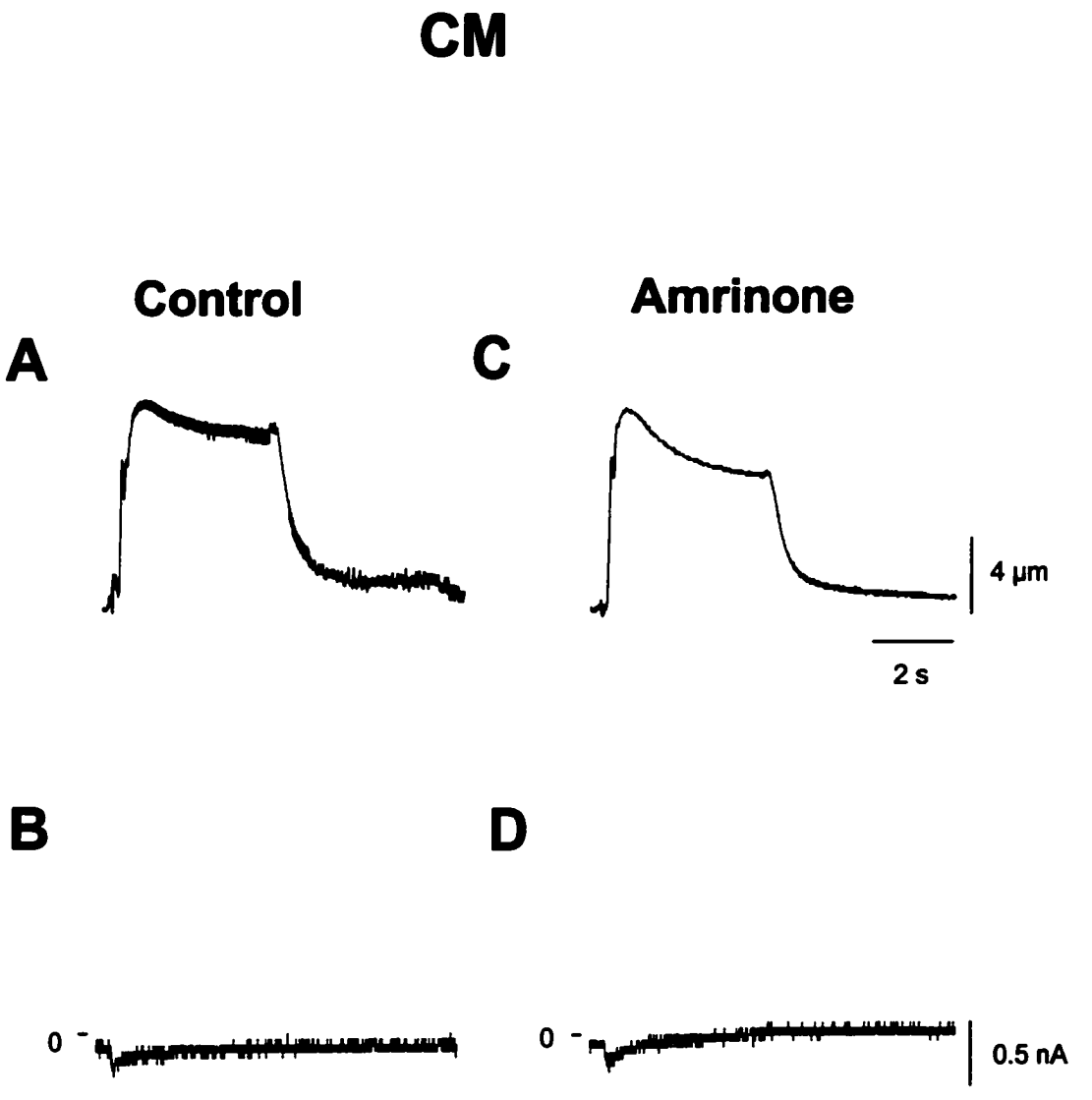

Figure 3-15

Figure 3-16. Mean data show that amrinone had little effect on either caffeine-induced contractures or Na^{+}-Ca^{2+} exchange current in CM cells. **Panel A:** 300 μM amrinone had no effect on the magnitude of caffeine-induced contractures in CM cells. **Panel B:** Amrinone had virtually no effect on the integral of Na^{+}-Ca^{2+} exchange current in CM cells (n= 14).

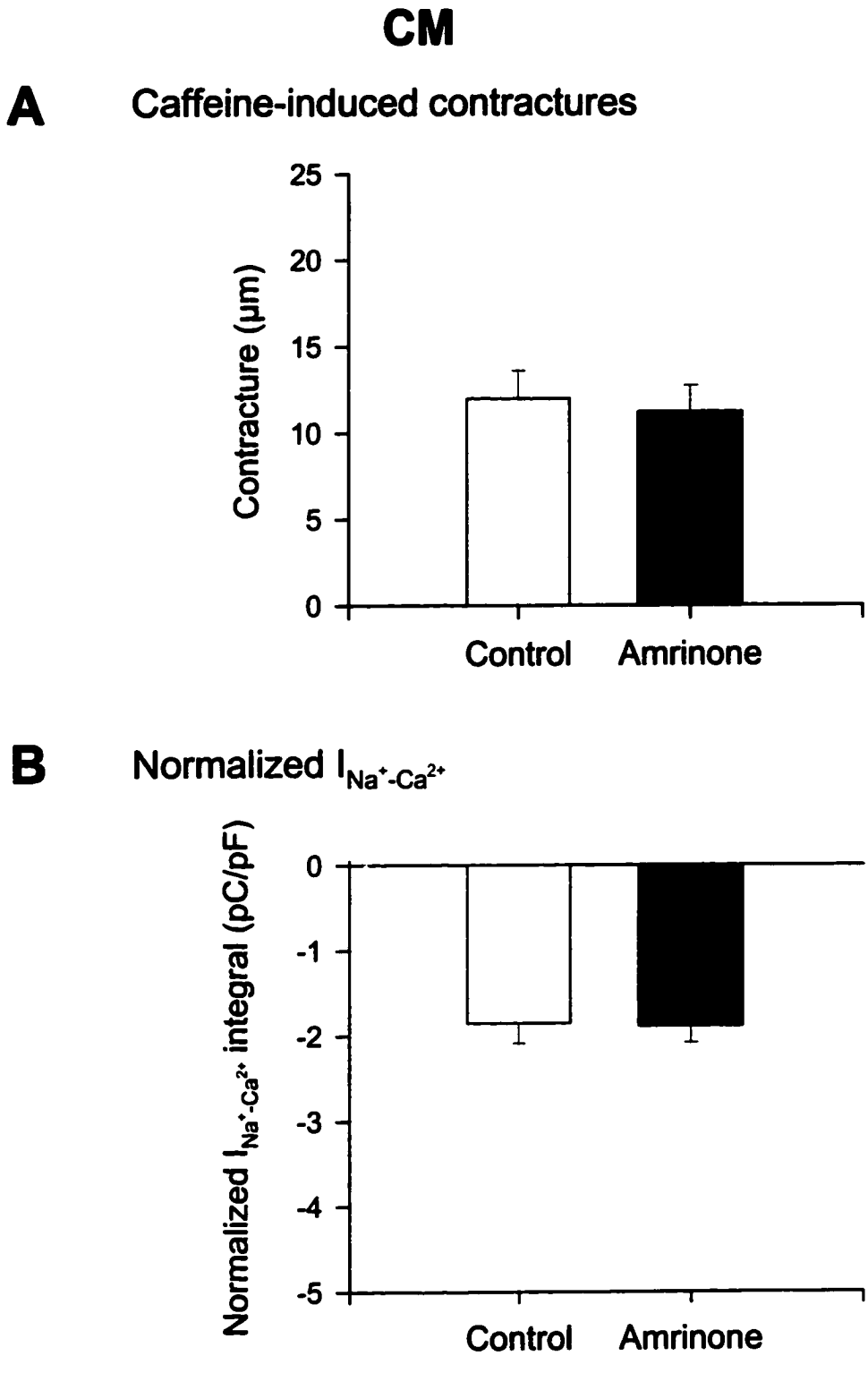
CM
A
Caffeine-induced contractures
Contracture (µm)
25
20
15
10
5
0
Control
Amrinone
B
Normalized $I_{Na^+-Ca^{2+}}$
Normalized $I_{Na^+-Ca^{2+}}$ integral (pC/pF)
0
-1
-2
-3
-4
-5
Control
Amrinone

Figure 3-16

Figure 3-17. Amrinone selectively increased fractional release of SR Ca^{2+} by the VSRM in normal cells. The voltage clamp protocol used in Panel A is shown at the top of the figure. Fractional release was estimated by normalizing VSRM and CICR contractions (Panel A) to the peak amplitude of caffeine-induced contractures (Figure 3-14A) in the same myocyte. **Panel A:** 300 μM amrinone significantly increased VSRM contractions, but had little effect on CICR contractions. **Panel B:** 300 μM amrinone significantly enhanced fractional release of SR Ca^{2+} by the VSRM, but did not affect fractional release of SR Ca^{2+} by the CICR. *Denotes significantly different from control ($p<0.05$), n= 5.

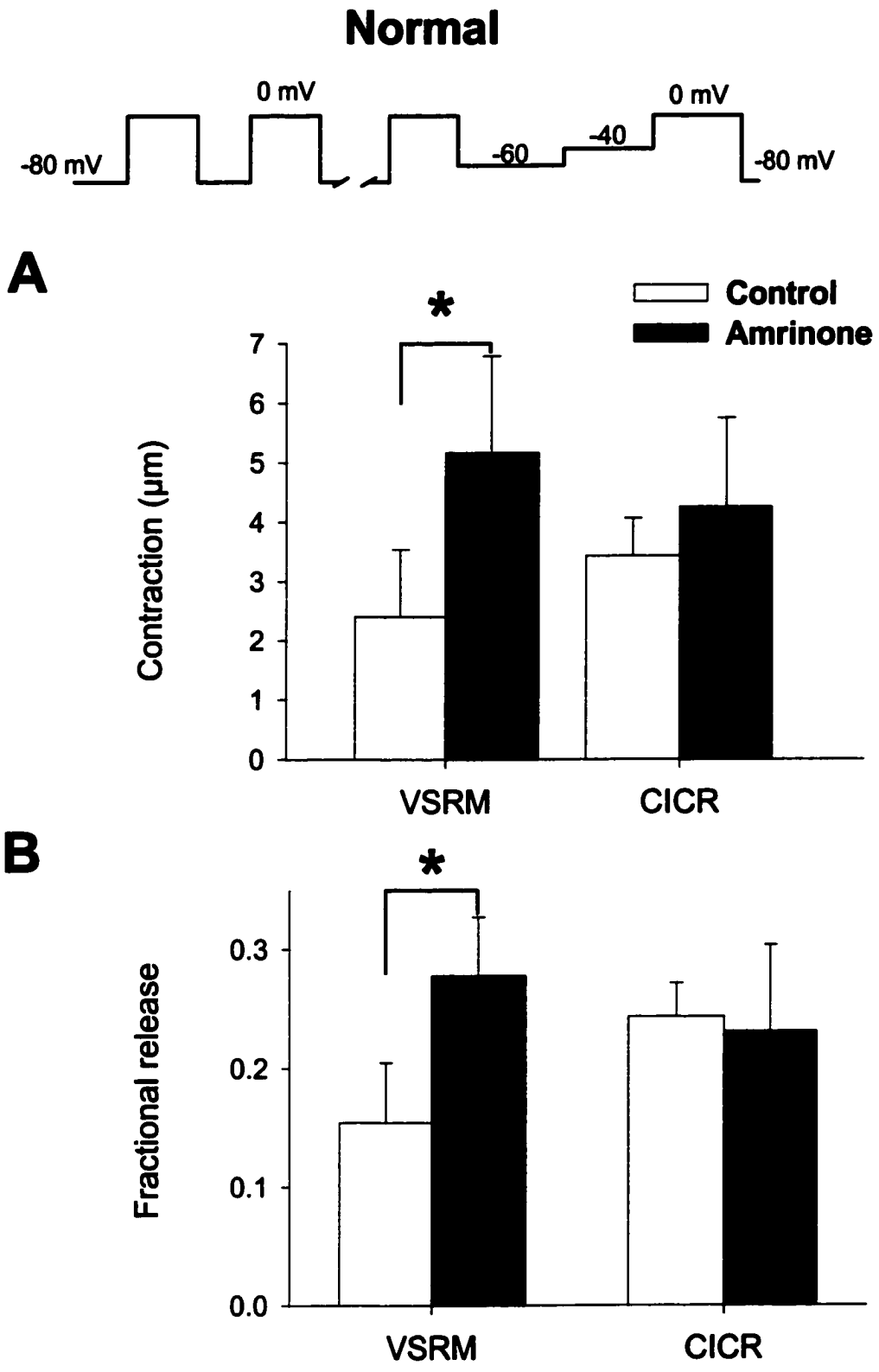
Normal
0 mV
0 mV
-80 mV
-60
-40
-80 mV
A
Control
Amrinone
*
Contraction (µm)
7
6
5
4
3
2
1
0
VSRM
CICR
B
*
Fractional release
0.3
0.2
0.1
0.0
VSRM
CICR

Figure 3-17

Next, we determined the role of fractional SR Ca^{2+} release in the inotropic effect of amrinone in CM myocytes. Amrinone had no effect on either VSRM or CICR contractions in CM cells (Figure 3-18A). Figure 3-18B shows that SR Ca^{2+} release by the VSRM was not significantly altered by amrinone. In addition, amrinone had no effect on fractional SR Ca^{2+} release by the VSRM in CM myocytes. These findings suggest that potentiation of fractional SR Ca^{2+} release by the VSRM in normal cells is absent in CM myocytes.

Taken together, these results show that amrinone cannot restore depressed contractions triggered by the VSRM in ventricular myocytes from CM hamster hearts. The absence of a positive inotropic effect of amrinone may be related to defective fractional SR Ca^{2+} release by the VSRM in CM myocytes.

Figure 3-18. Amrinone had no effect on fractional release of SR Ca^{2+} by the VSRM in CM myocytes. The voltage clamp protocol used in Panel A is shown at the top of the figure. Fractional release was estimated by normalizing VSRM and CICR contractions (Panel A) to the peak amplitude of caffeine-induced contractures (Figure 3-16A) in the same myocyte. **Panel A:** 300 μM amrinone had no effect on the magnitude of VSRM and CICR contractions in CM cells. **Panel B:** Fractional release of SR Ca^{2+} by the VSRM was not significantly enhanced by exposure to amrinone in CM cells (n= 14).

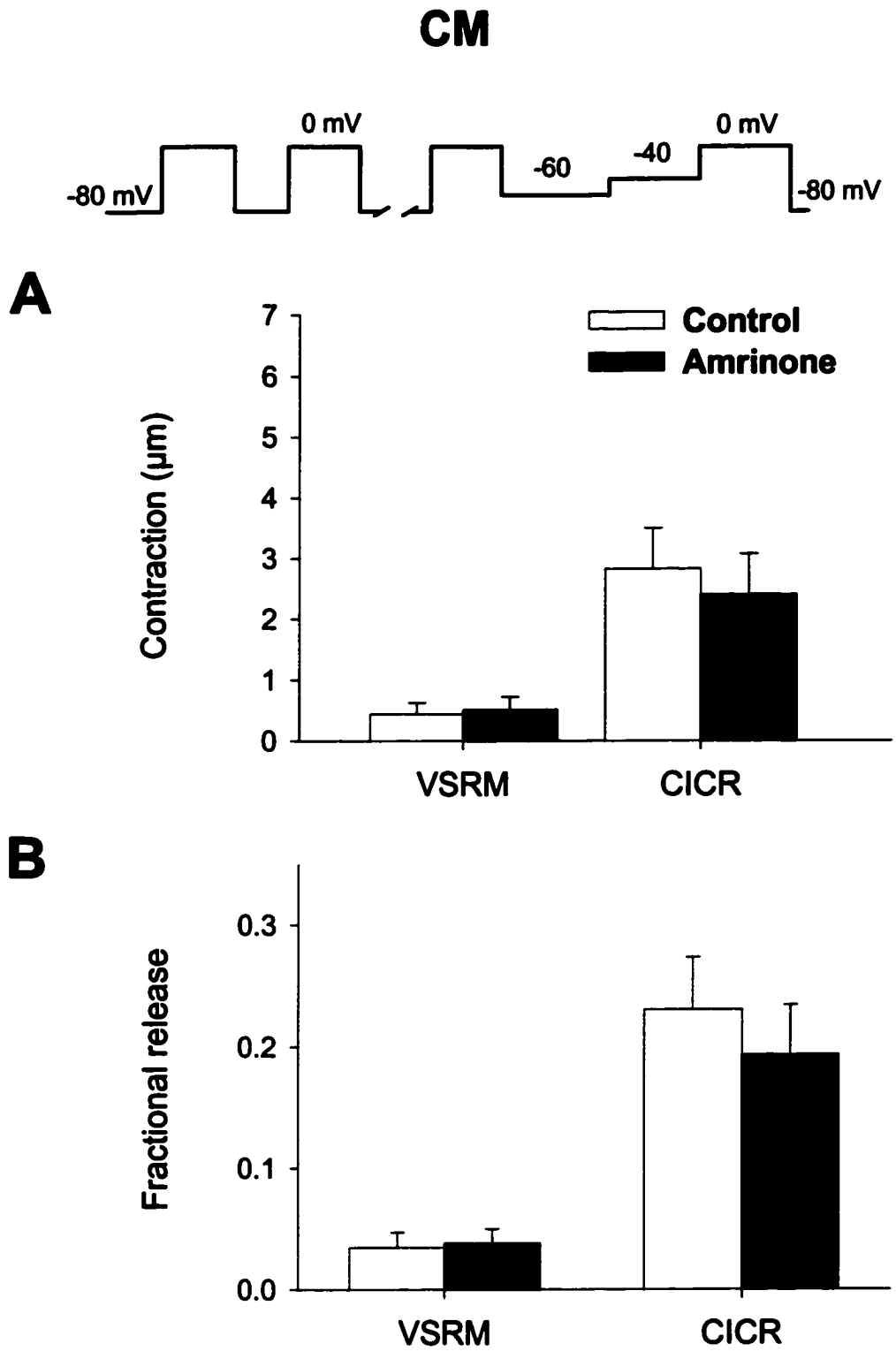
CM
0 mV
0 mV
-80 mV
-60
-40
-80 mV
A
Control
Amrinone
Contraction (µm)
7
6
5
4
3
2
1
0
VSRM
CICR
B
Fractional release
0.3
0.2
0.1
0.0
VSRM
CICR

Figure 3-18

DISCUSSION

The three main objectives of the current study are: 1) to determine whether CICR, the VSRM, or both mechanisms contribute to depressed contraction of ventricular myocytes from 90-100 day old CM hamsters; 2) to determine whether amrinone can increase contraction in ventricular cells from guinea pig hearts; and 3) to determine whether amrinone can restore depressed VSRM contractions in CM hamster myocytes.

Our results have shown that reduced cardiac contraction in 90-100 day old CM hamsters is attributable to a depression in the VSRM component of cardiac contraction. SR Ca^{2+} stores are similar in ventricular myocytes from normal and CM hamsters. However, defective SR Ca^{2+} release by the VSRM contributes to depressed cardiac contraction. The current study also has demonstrated that the PDE III inhibitor amrinone, selectively increases the magnitude of cardiac contractions triggered by the VSRM in guinea pig ventricular myocytes. Potentiation of VSRM contractions by amrinone is independent of stimulation of $I_{Ca\text{-}L}$. An increase in fractional release of SR Ca^{2+} stores by the VSRM may explain selective modulation of VSRM contractions by this PDE III inhibitor. However, our study also has shown that amrinone does not restore depressed VSRM contractions in ventricular myocytes from CM hamsters. Although amrinone does increase the fractional release of SR Ca^{2+} stores by the VSRM in normal myocytes, this action is absent in CM hamsters.

1. DEFECTIVE RELEASE OF SR CA^{2+} BY THE VSRM CONTRIBUTES TO REDUCED CARDIAC CONTRACTIONS IN MYOCYTES FROM CM HAMSTERS

The objectives of the study were 1) to determine whether decreased contraction in ventricular myocytes from 90-100 day old CM hamsters is accompanied by a defect in cardiac E-C coupling; and 2) to determine whether impaired contractile performance is attributable to depressed contractions initiated by CICR, the VSRM or both mechanisms. The current study has demonstrated that decreased cardiac contractions in 90-100 day old CM hamsters are attributable to selective depression of the VSRM. Furthermore, depressed contractile function is associated with defective fractional release of SR Ca^{2+} by the VSRM in CM myocytes.

Previous studies have shown depressed cardiac contractions at the single cell level in 8-month old CM hamsters (Sen et al., 1990c). However, a reduction in amplitude of cell shortening in ventricular myocytes from these CM hamster hearts cannot be attributed to changes in $I_{Ca\text{-}L}$, because no alteration in $I_{Ca\text{-}L}$ was found (Sen et al., 1990b). Similar observations have been made in another animal model of heart failure (Gomez et al., 1997). Gomez et al. have shown that although Ca^{2+} current remains unchanged, the ability of Ca^{2+} current to trigger Ca^{2+} transients measured as Ca^{2+} sparks is reduced in rats with heart failure resulting from hypertension (Gomez et al., 1997). These studies suggest that a defect in E-C coupling may contribute to poor contractile performance in animal models of heart failure, although $I_{Ca\text{-}L}$ itself may not contribute to impaired contractility.

However, since the VSRM component was not differentiated from CICR in these studies, it remains unclear whether a defect in the VSRM, CICR or both mechanisms contributes to depressed cardiac contractions in ventricular myocytes. Many studies have suggested that the VSRM is an important trigger for cardiac E-C coupling in ventricular myocytes (Ferrier and Howlett, 1995; Hobai et al., 1997; Howlett et al., 1998; Ferrier et

al, 1998; Mackiewicz et al., 2000; Zhu and Ferrier, 2000a). Nevertheless, the experimental conditions used in previous studies of cardiac E-C coupling may inhibit the VSRM. This might occur when a holding potential of –40 mV, room temperature, or patch-pipette solutions without addition of either exogenous cAMP or calmodulin is utilized. Therefore, as previous studies have utilized one or more of these conditions and have not examined the VSRM, it is important to examine contributions of the VSRM and CICR to contractile dysfunction in animal models of heart disease.

The golden CM Syrian hamster is a well-established animal model of cardiomyopathy and heart failure (Bajusz, 1968; Bajusz et al., 1969; Bajusz, 1969). CM hamsters with this genetic defect exhibit predictable and progressive cardiomyopathy with hypertrophy, dilatation and the terminal stages of heart failure (Jasmin and Proschek, 1982; Hunter et al., 1984). Previous studies at the muticellular level have observed a reduction in contraction in CM hearts from 80-85 day old hamsters, which were at the prehypertropic stage of disease (Bobet et al., 1991; Howlett et al., 1991). In the current study, we chose 90-100 day old CM hamsters because we wanted to determine whether depressed cardiac contraction is accompanied by a defect in E-C coupling at early stages of disease. This might predispose these animals to develop heart failure.

It has been shown that in BIO 14.6 strain of CM hamsters, there is a large genomic deletion in delta-sarcoglycan (SG) gene (Sakamoto et al, 1997), which leads to a deficiency in the dystrophin-associated glycoprotein on the sarcolemma in cardiac and skeletal muscles in CM hamsters (Roberds et al., 1993). Since this dystrophin-associated glycoprotein provides linkage between the subsarcolemmal cytoskeleton and the

extracellular matrix (Roberds et al., 1993), deficiency of the delta-SG may cause perturbation of dystrophin-glycoprotein complex and impair sarcolemmal integrity (Straub et al., 1998). Therefore, it is conceivable that impaired sarcolemmal integrity may contribute to disruption of functional coupling of sarcolemmal excitation to voltage-gated SR Ca^{2+} release.

Our results have shown that cell shortening evoked by action potentials is significantly decreased in CM myocytes. However, depressed cardiac contraction cannot be attributed to alterations in action potentials. Rossner observed that there were no significant changes in the configuration of action potentials between normal and CM hamsters at the prehypertrophic stage of disease (Rossner, 1985). In addition, in the current study, the profile and duration of action potentials remained the same in normal and CM ventricular myocytes. Since prolongation of the action potential is commonly observed in hypertrophy and heart failure (Nabauer and Kaab, 1998), the observation that action potential profile and duration are unchanged is consistent with the prehypertrophic stage of disease in the CM hamsters used in this study. Furthermore, no alterations in cell length or cell capacitance were observed in the present study. This suggests that cell size was not altered at this stage of disease. Therefore, depression of cell shortening cannot be attributed to cellular hypertrophy. Instead, these results suggest a defect in cardiac E-C coupling might contribute to contractile dysfunction in these animals.

This reduction in cell shortening in CM myocytes observed in voltage-clamp experiments might be due to depression of the VSRM, CICR or both components in CM heart. A decreased magnitude of $I_{Ca\text{-}L}$ could, in theory, lead to reduced contractions initiated by CICR. In the later stages of heart failure in CM hamsters, some studies

reported that $I_{Ca\text{-}L}$ did not change in diseased cells (Sen et al., 1990b; Sen and Smith, 1994). However, other studies showed that the magnitude of $I_{Ca\text{-}L}$ was decreased in myocytes from failing hearts (Hatem et al., 1994; Kruger et al., 1994). The latter indicates that reduced Ca^{2+} current may be responsible for depressed contractions triggered by CICR in heart (Hatem et al., 1994; Kruger et al., 1994). In CM hamsters at the prehypertrophic stage, Tawada-Iwata et al. reported that the magnitude of $I_{Ca\text{-}L}$ (Tawada-Iwata et al., 1993) was unchanged. Furthermore, our results showed that $I_{Ca\text{-}L}$ was similar in normal and CM ventricular myocytes, suggesting that the magnitude of $I_{Ca\text{-}L}$ itself does not contribute to depressed cardiac contraction at the prehypertrophic stage in CM hamsters. Moreover, neither the magnitude of contractions initiated by CICR nor the bell-shaped contraction-voltage relationships were different between normal and CM cells. These findings suggest that depressed contractions in CM heart cannot be attributed to changes in CICR, at least at the prehypertrophic stage of disease.

The absence of a change in CICR contractions in CM myocytes raises the possibility that the defect resides in the VSRM. In the current study, results showed that contractions triggered by the VSRM were significantly decreased in myocytes from CM hamsters compared to control. When the VSRM was available, cardiac contractions were depressed in CM myocytes whereas the magnitude of inward currents was identical between normal and CM myocytes. Depressed contractions triggered by the VSRM cannot be attributed to changes in the voltage dependence of activation and inactivation of the VSRM because normalized activation and inactivation curves are virtually identical between normal and CM hamsters (Howlett et al., 1999). Thus, a defect in the VSRM as a trigger for SR Ca^{2+} release appears to be responsible for the reduced

magnitude of cardiac contractions in CM hamsters. Our findings are supported and extended by other investigators (Van Wagoner et al., 1999; Sjaastad et al., 2000). In myocytes from rats with heart failure resulting from coronary ligation, contractions initiated by the VSRM are significantly depressed with little change in CICR contractions (Sjaastad et al., 2000). In human failing atrium, Ca^{2+} transients initiated by the VSRM are significantly reduced (Van Wagoner et al., 1999). Therefore, it is possible that the depressed VSRM component of contraction may be a therapeutic target in treatment of heart failure.

SR Ca^{2+} release can be affected by SR Ca^{2+} content (Eisner et al., 1998). Since Ca^{2+} in the SR is taken up into the SR via an SR Ca^{2+} pump, SR Ca^{2+} content can be affected by changes in activity of the SR Ca^{2+} pump. Although SR Ca^{2+} pump activity may be reduced in heart failure (reviewed by de Tombe, 1998), this has not been reported in all models of heart disease and failure. Whitmer et al. suggest that Ca^{2+} uptake by the SR is unchanged in hearts from hypertrophic CM hamsters at 3 and 9 months of age (Whitmer et al., 1988). However, in another strain of CM hamsters without hypertrophy at 9 months of age, Ca^{2+} uptake by the SR in hearts is significantly depressed (Whitmer et al., 1988). Furthermore, in 220 to 300 day old hypertrophic CM hamsters, SR Ca^{2+} content in ventricular cells, assessed by caffeine-induced Na^{+}-Ca^{2+} exchange current, is unchanged compared to normal (Hatem et al., 1994). In the present study, SR Ca^{2+} content, estimated by caffeine contractures and the integral of caffeine-induced Na^{+}-Ca^{2+} exchange current, also was similar in normal and CM hamsters. Thus, these results suggest that depressed cardiac contraction cannot be attributed to decreased SR Ca^{2+} content in the present study. It appears that the SR Ca^{2+} content is unaltered in this strain

of hypertrophic CM hamsters at many different ages when compared to normal. However, our results also showed that fractional release of SR Ca^{2+} by the VSRM was significantly reduced in CM hearts, whereas fractional release by CICR was similar in normal and CM ventricular myocytes. Taken together, these observations provide evidence that depressed cardiac contraction is associated with a defect in the VSRM as a trigger for the SR Ca^{2+} release.

There are several possibilities that may contribute to this defect in the VSRM in CM hamster myocytes. The cAMP-PKA pathway has been shown to play an important role in activation of the VSRM (Zhu et al., 1997; Hobai et al., 1997; Ferrier et al., 1998). However, in CM hearts, a number of studies provide evidence for defective β-adrenoceptor-adenylyl cyclase-cAMP-PKA pathway. The content of cAMP is reduced in CM hamster heart (Wikman-Coffelt et al., 1986). Furthermore, functional uncoupling of G_s to adenylyl cyclase was found in CM hamsters at 90 days of age (Ikegaya et al., 1992) or younger (Kessler et al., 1989). In addition, increased content and functional activity of G_i was observed in CM hearts (Sethi et al., 1994; Kaura et al., 1996). Moreover, decreased β_1-adrenoceptors have been reported in CM hearts (Kaura et al., 1996). Thus, a reduction in cAMP formation in CM hamster hearts may affect phosphorylation by the cAMP-PKA pathway and consequently contribute to the defect in the VSRM in CM hearts.

Another explanation for depression of the VSRM in CM hearts is associated with AKAPs. AKAPs provide a link between PKA and phosphorylation of proteins by binding to both of them (Rubin, 1994; Scott and McCartney, 1994). Moreover, since distinct AKAPs bind to specific intracellular targets, AKAPs can direct PKA to specific

subcellular locations, thereby mediating precise control of the cAMP-PKA pathway (Rubin, 1994; Scott and McCartney, 1994). Zakhary et al. have suggested that AKAP targeting of PKA is impaired in heart failure, which may contribute to the reduced cAMP-dependent phosphorylation of proteins (Zakhary et al., 2000). Thus, either reduced formation of cAMP or dysfunction of AKAPs may cause a disruption in regulation of the VSRM through a reduction in phosphorylation and lead to poor contractile performance in CM hamsters.

Our results argue against the suggestion that the VSRM can be explained by CICR (Piacentino et al., 2000). First, the difference in the amplitude of VSRM contractions occurs with the same magnitude of inward current. Second, one may argue that a defect in the SR other than the VSRM in CM cells, such as a reduction in SR Ca^{2+} content, causes depression of the VSRM. However, it cannot explain our observation that there is no difference in the magnitude of CICR contractions in normal and CM cells because VSRM and CICR contractions are measured in the same cells with no change in the SR Ca^{2+}.

In summary, our results have shown that a reduction in cardiac contraction in CM heart is attributable to selective depression of the VSRM component of contraction. $I_{Ca\text{-}L}$ and CICR are unchanged in ventricular myocytes from 90-100 day old CM hamsters. Furthermore, a reduction in cardiac contractions in CM heart cannot be attributed to decreased SR Ca^{2+} content in CM hamsters. Our observations suggest that a defective fractional release of SR Ca^{2+} by the VSRM contributes to poor contractile performance. The VSRM component of cardiac contraction is selectively depressed at early stages of

cardiomyopathy. This defect in the VSRM could contribute to development of heart failure in CM hamsters.

2. IN CONTRAST TO IBMX, AMRINONE SELECTIVELY INCREASES VSRM CONTRACTIONS WITHOUT STIMULATION OF CICR IN VENTRICULAR MYOCYTES FROM GUINEA PIGS

Studies have shown that the cAMP-PKA pathway is involved in modulation of the VSRM (Hobai et al., 1997; Ferrier et al., 1998). IBMX and amrinone can increase intracellular cAMP levels by prevention of the breakdown of cAMP. The specific objectives of this part of the present study are: 1) to determine whether amrinone can increase contraction in ventricular cells from guinea pig hearts; and 2) to determine whether the effects of amrinone are mediated by effects on contractions initiated by CICR, the VSRM or both mechanisms. Our results have shown that non-specific PDE inhibitor IBMX, increases the magnitudes of contractions and currents activated by test steps to both –40 and 0 mV. In contrast, the specific PDE III inhibitor amrinone can achieve positive inotropy through selective enhancement of VSRM contractions, which is associated with potentiation of fractional release of SR Ca^{2+} by the VSRM.

Intracellular cAMP levels are dependent on both synthesis and degradation of cAMP. PDEs can hydrolyze cAMP and reduce intracellular cAMP levels (Burns et al., 1996; Houslay and Millligan, 1997). Since PDEs are ubiquitous in myocytes, a non-specific PDE inhibitor such as IBMX (Shahid and Nicholson, 1990) would be expected to lead to a universal increase in intracellular cAMP levels. Therefore, all the target proteins of PKA may be phosphorylated, including L-type Ca^{2+} channels (McDonald et al, 1994).

Studies have shown that IBMX can increase the magnitude of $I_{Ca\text{-}L}$ in ventricular myocytes from guinea pigs and rats (Mubagwa et al., 1993; Verde et al., 1999). In the current study, IBMX stimulated currents activated by test steps to both –40 and 0 mV. Since IBMX caused a large inward current to appear with the step to –40 mV, it is difficult to determine whether IBMX increased only VSRM contractions with this test step. $I_{Ca\text{-}L}$ and CICR may have contributed to contractions activated at negative potentials in these experiments.

IBMX also increased the peak of current-voltage and contraction-voltage relationships. A large increase in inward current at negative potentials was observed in the presence of IBMX. Since IBMX may lead to a universal increase in intracellular cAMP level and consequently phosphorylation of many proteins including ion channels, it is not surprising that IBMX cause a substantial inward current at negative potentials. Similarly, stimulation of β-adrenoceptor with isoproterenol may lead to a global increase in cAMP and cause an increase in inward current at potentials negative to –40 mV (Piacentino et al., 2000). Since phosphorylation of many proteins occurs in the presence of IBMX or isoproterenol, neither of these agents allows the enhanced component of contractions to be distinguished between the VSRM and CICR.

The present study has demonstrated that, in contrast to IBMX, the specific PDE III inhibitor amrinone (Harrison et al., 1986; Weishaar et al, 1986) selectively potentiates VSRM contractions with very little effect on CICR or $I_{Ca\text{-}L}$. Amrinone increased the VSRM contractions in a concentration-dependent manner. In contrast, amrinone had no effect on contractions initiated by CICR. These results indicate that the VSRM is separately regulated from CICR. Our studies were conducted at 37 °C, because the

VSRM can be inhibited at lower temperature (Ferrier and Redondo, 1996). Sys et al. have shown that amrinone can increase contractility of cat papillary muscles at 37 °C, but not 29 °C (Sys et al., 1986). The marked temperature dependence of these inotropic actions of amrinone indicates that experimental temperature is a crucial issue for these actions of amrinone (Sys et al., 1986). Taken together, these studies suggest that the VSRM plays an important role in the positive inotropic effects of amrinone.

The findings of the present study suggest that modulation of the VSRM is associated with compartmentalization of cAMP. Compelling evidence has supported compartmentalization of cAMP in myocardium (Buxton and Brunton, 1983; Aass et al., 1988; Hohl and Li, 1991; Jurevicius and Fischmeister, 1996). Studies showed evidence that positive inotropy (Aass et al., 1988) and enhanced peak amplitude of Ca^{2+} transient (Hohl and Li, 1991) of β-adrenergic stimulation have good correlation with cAMP levels in the particulate fraction but not in the cytosolic fraction. Although many cellular events are controlled by the cAMP-PKA pathway, downstream targets of the cAMP-PKA pathway are tightly controlled at specific subcellular locations by several regulatory mechanisms (Gray et al., 1998b).

First, PDEs are critical determinants that modulate intracellular cAMP concentrations and biological effects of cAMP (Manganiello et al., 1995). Activities of PDE III are present in both cytosolic and SR-enriched fractions of mammalian myocardium (Kithas et al., 1988; Artman et al., 1989; Smith et al., 1993). However, the positive inotropic effect of PDE III inhibitors is associated with inhibition of membrane-bound PDE III (Weishaar et al., 1987). Kauffman et al. showed that the effect of the specific PDE III inhibitor LY195115 (indolidan) was mainly due to inhibition of PDE III

in the SR (Kauffman et al., 1986; Kauffman et al., 1989). Their observations have been confirmed and extended by other studies, which showed that PDE III in the SR was a major target of PDE III inhibitors (Kithas et al., 1988; Lugnier et al., 1993). In addition, cytosolic and SR PDE IIIs are distinct pools of PDE III with marked differences in sensitivity to inhibition by cGMP and specific PDE III inhibitors (Kithas et al., 1988). The particulate PDE III activity associated with the SR was 60-fold more sensitive to inhibition by milrinone, an amrinone analog, than was the cytosolic form. Furthermore, Lugnier et al. showed evidence that PDE III was primarily located in T-tubule/junctional SR structures (Lugnier et al., 1993). These studies suggest that localized increases in cAMP in subcellular compartments near T-tubule/junctional SR membranes are responsible for the positive inotropic responses to specific PDE III inhibitors (Weishaar et al., 1992).

Second, different types of PKAs (type 1 and type 2) contribute to compartmentalization of PKA. The regulatory subunits (RI and RII) of PKA have different subcellular localization and different binding affinity to cAMP (Corbin et al., 1975; Taylor et al., 1990). Type I PKA is largely found in the cytosol, whereas type II PKA is predominantly anchored to specific locations by binding to distinct AKAPs (Rubin, 1994; Scott and McCartney, 1994). Since distinct AKAPs bind to specific intracellular targets, AKAPs can direct PKA to specific subcellular locations, thereby mediating downstream events in the cAMP-PKA pathway (Rubin, 1994; Scott and McCartney, 1994). In the heart, AKAP15/18 targets the sarcolemma and is involved in modulation of $I_{Ca\text{-}L}$ activity (Gray et al., 1998a; Fraser et al., 1998). AKAP100/mAKAP is localized to the region of the T-tubule/junctional SR (McCartney et al., 1995; Yang et

al., 1998). A recent report showed that cardiac contractile function and substrate phosphorylation by PKA are regulated by targeting of PKA by AKAPs (Fink et al., 2001). Therefore, these mechanisms contribute to the precise control of intracellular signal transduction by the second messenger cAMP, by targeting its action to specific subcellular compartments (Figure A).

Studies of the effects of PDE III inhibitors on Ca^{2+} current have reported conflicting results (Kondo et al., 1983; Malecot et al., 1985; Matsui et al., 1995; Verde et al., 1999). Some studies showed that PDE III inhibitors increased the magnitude of Ca^{2+} current (Kondo et al., 1983; Malecot et al., 1985; Matsui et al., 1995). However, Verde et al. have shown that PDE III inhibitors have no effect on the magnitude of Ca^{2+} current (Verde et al., 1999). The present study has shown that amrinone has very little effect on the magnitude of $I_{Ca\text{-}L}$. This observation may be explained by findings that the inotropic effect of PDE III inhibitors are predominantly associated with inhibition of PDE III bound to the SR (Kauffman et al., 1986, Kauffman et al., 1989; Lugnier et al., 1993; Ashikaga et al., 1996).

A small increase in caffeine contractures and the integral of caffeine-induced Na^{+}-Ca^{2+} exchange current was observed in the presence of amrinone, which indicates that SR Ca^{2+} content is increased slightly by amrinone. Previous studies have shown that the PDE III inhibitor milrinone, an amrinone analogue, can enhance SR Ca^{2+}-ATPase activity and SR Ca^{2+} uptake in heart (Yano et al., 2000). One may speculate that increased SR Ca^{2+} stores would enhance both CICR and VSRM contractions. However, we found that amrinone had no effect on CICR contractions. Thus, the increase in VSRM contractions is not likely to be due to increased SR Ca^{2+} content. Increased VSRM contractions did

Figure B. Schematic model of cardiac EC coupling including the VSRM and CICR in cardiac myocytes. The VSRM and CICR are depicted as independent mechanisms for cardiac EC coupling. CICR is triggered by Ca^{2+} entry through an L-type Ca^{2+} channel. The VSRM is illustrated as a physical link between the SR Ca^{2+} release channel and a voltage sensor. The β-adrenoceptor (β-AR) is coupled to adenylyl cyclase (AC) through a stimulatory guanine nucleotide-binding protein (Gs). Putative phosphorylation sites for PKA on SR Ca^{2+} release channel, SR Ca^{2+} pump, L-type Ca^{2+} channel and myofilaments via putative A-kinase anchoring proteins (AKAP)s also are shown. PDE III is located in the vicinity of SR Ca^{2+} release channels because PDE III in the junctional SR is closely associated with the positive inotropic effect of specific PDE III inhibitors (Lugnier et al., 1993).

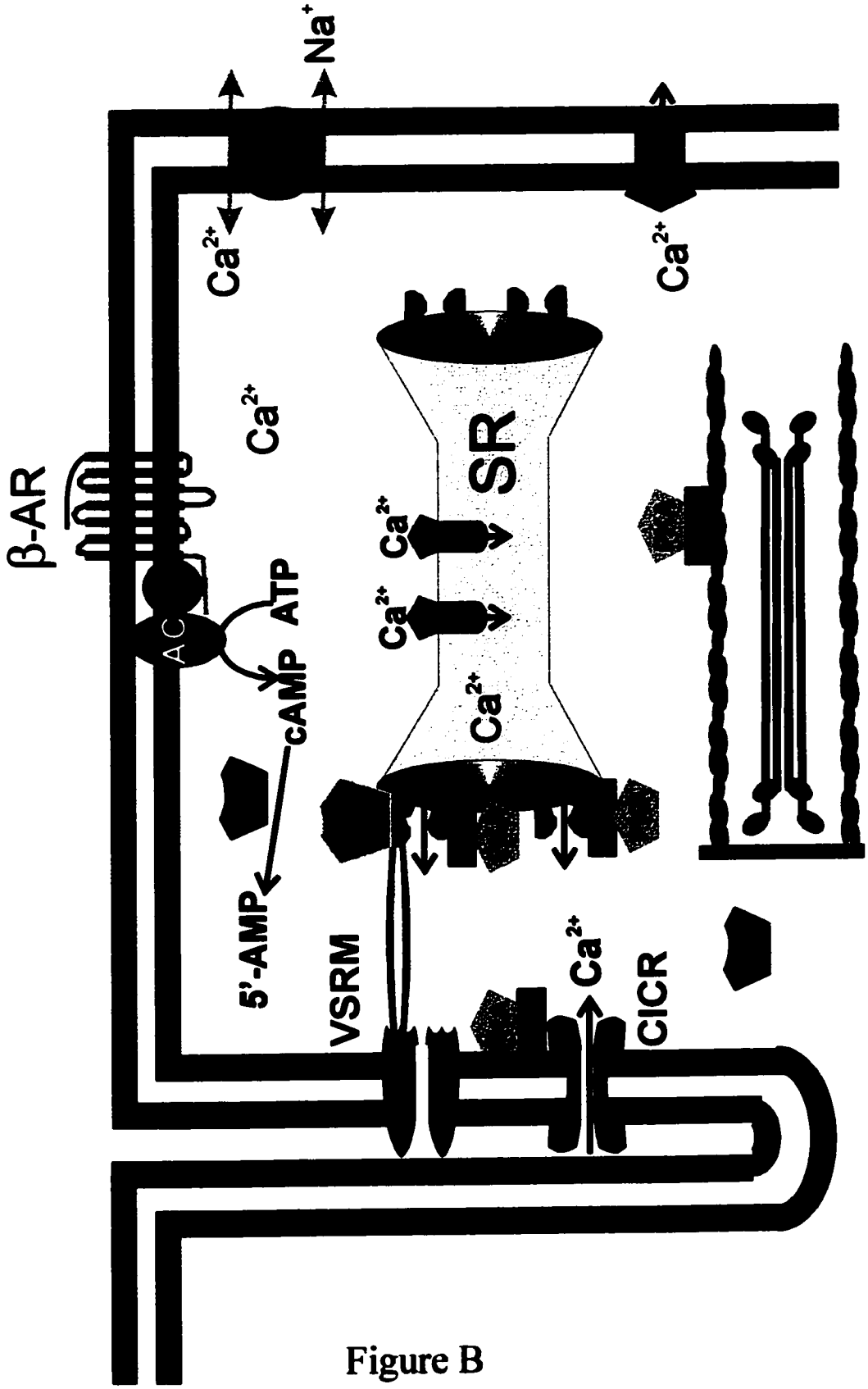

Figure B

appear to be related to an increase in fractional release of SR Ca^{2+} by the VSRM. In contrast, although SR Ca^{2+} content was slightly increased, fractional release of SR Ca^{2+} by CICR remained unchanged. These observations suggest that amrinone can modulate the VSRM independently of the SR Ca^{2+} releasable stores.

Unlike amrinone, IBMX stimulated both $I_{Ca\text{-}L}$ and CICR contractions. Interestingly, IBMX enhanced fractional release of SR Ca^{2+} by the VSRM, but not by CICR. Therefore, potentiation of CICR contractions by IBMX is attributable to increases in $I_{Ca\text{-}L}$ and SR Ca^{2+} stores, rather than an increase in fractional release by CICR. These results suggest that the VSRM and CICR are separately regulated by the cAMP-PKA pathway.

These results have shown that amrinone can selectively enhance VSRM contractions without stimulation $I_{Ca\text{-}L}$. This argues against the suggestion that the VSRM can be explained by CICR (Piacentino et al., 2000). Our results also are consistent with previous reports that inotropic effects of PDE III inhibitors are predominantly associated with inhibition of PDE III bound to the SR (Kauffman et al., 1986, Kauffman et al., 1989; Lugnier et al., 1993; Ashikaga et al., 1996).

In summary, this study has demonstrated that, in contrast to IBMX, amrinone selectively increases VSRM contractions without stimulation of $I_{Ca\text{-}L}$ or CICR. Furthermore, activation of the cAMP-PKA pathway leads to a greater fractional release of SR Ca^{2+} by the VSRM, but not by CICR. These findings suggest that the VSRM can be modulated independently of CICR and $I_{Ca\text{-}L}$, which supports previous observations that the VSRM is a mechanism for cardiac E-C coupling separate from CICR. Our results also indicate that PKA-mediated phosphorylation of the VSRM is under the control of PDE III. Modulation of the VSRM by amrinone without effect on CICR and $I_{Ca\text{-}L}$ may be

associated with compartmentalization of cAMP in the vicinity of phosphorylation sites for the VSRM. Therefore, the present study utilized pharmacological tools to provide evidence that the VSRM is a distinct cardiac E-C coupling mechanism, which is also a major site targeted by specific PDE III inhibitors.

3. REDUCED INOTROPIC RESPONSE TO AMRINONE IN CM HAMSTERS IS RELATED TO DEFECTIVE CA^{2+} RELEASE BY THE VSRM

The specific objectives of the third part of my studies are: 1) to determine whether amrinone can improve impaired contractile performance in CM hamster heart; and 2) to determine whether depressed VSRM contractions can be restored by amrinone. Our results have shown that amrinone cannot enhance contractility in CM hamster heart. Also, amrinone cannot restore depressed VSRM contractions in ventricular myocytes from CM hamsters. Furthermore, amrinone has no effect on SR Ca^{2+} release by the VSRM in CM cells, which may be related to the absence of positive inotropic effects in CM myocytes.

In normal guinea pig ventricular myocytes, we found that amrinone, a specific PDE III inhibitor, can increase cardiac contraction via selective potentiation of the VSRM without stimulation of CICR. Similarly, in normal hamster myocytes, amrinone enhances contractility by potentiation of the VSRM. Furthermore, in the current study, amrinone had little effect on the amplitude of CICR contractions in either normal or CM hamster myocytes. These results are consistent with our observations in guinea pig ventricular myocytes, indicating that stimulation of CICR is not required for potentiation of the VSRM by amrinone. As we have discussed in Section 2, the positive inotropic effect of

amrinone in normal cells is likely related to compartmentalization of cAMP in the myocardium. PDE III in the SR is a major target of PDE III inhibitors (Kithas et al., 1988; Lugnier et al., 1993). Taken together, our results demonstrate that the VSRM plays an important role in the positive inotropic effects of amrinone.

The present study has demonstrated that amrinone cannot restore depressed contractions via potentiation of the VSRM in ventricular myocytes from CM hamsters that are at the prehypertrophic stage of disease. The golden Syrian CM hamster is an animal model of cardiomyopathy and heart failure (Bajusz, 1969; Bajusz et al., 1969). However, heart failure is a clinical syndrome and has numerous etiologies including cardiomyopathy. A reduced or absent positive inotropic effect of PDE III inhibitors in human heart failure has been reported previously (Feldman et al., 1987; Bohm et al., 1988). For example, Feldman et al. observed that positive inotropic effects of milrinone are absent in ventricular muscle fibers from patients with end-stage heart failure (Feldman et al., 1987). Furthermore, another study demonstrated that positive inotropic effects of milrinone are reduced in isolated papillary muscle strips from patients with severe heart failure compared to those with moderate heart failure (Bohm et al., 1988). Thus, the positive inotropic effects of PDE III inhibitors may be reduced or absent in failing human heart. These earlier studies did not differentiate between VSRM contractions and CICR contractions. However, since our findings suggest that PDE III inhibitors can selectively enhance VSRM contractions and this action is absent in CM hamster heart, it is possible that an inability of PDE III inhibitors to potentiate the VSRM may also contribute to the markedly reduced or absent positive inotropic effects in these studies.

Since amrinone and milrinone are clinical medications for treatment of heart failure, the absence of positive inotropic effects in isolated myocytes and multicellular preparations could be partially associated with *in vitro* conditions *per se*. First, a large portion of the therapeutic effect *in vivo* may be due to the vasodilatory properties of amrinone and milrinone (Wilmshurst et al., 1984; Morgan et al., 1986; Ludmer et al., 1986). Various PDE III inhibitors may differ in their ratio of positive inotropy to vasodilatory action. At inotropically equipotent concentrations, the order of potency of vasodilation for various PDE III inhibitors is amrinone > milrinone > sulmazole > piroximone > enoximore (reviewed by Honerjager, 1991). A study by Sys et al. suggested that, at therapeutic concentrations, positive inotropic and vasodilatory effects might be equal for amrinone (Sys et al., 1987). This suggests that the therapeutic actions of amrinone *in vivo* may be partially due to its positive inotropic effects. Second, other studies on specific PDE III inhibitors have suggested that the lack of catecholamine *in vitro* plays a role in the absence of positive inotropy of PDE III inhibitors in heart failure (Ludmer et al., 1986; Feldman et al., 1987). Isolated ventricular muscle fibers from patients with end-stage heart failure show little positive inotropic response to milrinone (Feldman et al., 1987). However, Ludmer et al. showed evidence of positive inotropic effects of milrinone when it was infused via coronary arteries in patients with end-stage heart failure (Ludmer et al., 1986). This may be due to high levels of catecholamines in the plasma of patients with heart failure (Hasking et al., 1986; Davis et al., 1988). Catecholamines may stimulate synthesis of cAMP via G protein-coupled β-adrenoceptors, despite the existence of down regulation and uncoupling of β-

adrenoceptors in heart failure. Therefore, absent or markedly diminished efficacy of PDE III inhibitors in heart failure may be at least partially attributable to *in vitro* studies *per se*.

However, some studies have shown that positive inotropic effects of PDE III inhibitors are reduced *in vivo*. There is a markedly reduced positive inotropic effect of milrinone in conscious dogs with heart failure, compared to the inotropic effect before induction of heart failure by rapid ventricular pacing (Sato et al., 1999). The blunted response to PDE III inhibitors was explained by reduced formation of cAMP (Danielsen et al., 1989; Bethke et al., 1991; von der Leyen et al., 1991). Since PDE III inhibitors cannot lead to synthesis of cAMP *de novo*, a low basal level of cAMP may persist in the presence of PDE III inhibitors.

The β-adrenoceptor-adenylyl cyclase-cAMP pathway is an important pathway by which many positive inotropic agents enhance cardiac contractility. The alterations in this pathway in heart failure are associated with high plasma catecholamine levels (Hasking et al., 1986; Davis et al., 1988), increased G_i proteins (Feldman et al., 1988; Neumann et al., 1988; Bohm et al., 1990; Eschenhagen et al., 1992b; Kiuchi et al., 1993; Bohm et al., 1994), downregulation of β-adrenoceptors (Bristow et al., 1989; Steinfath et al., 1991; Kiuchi et al., 1993) and enhanced expression of β-adrenoceptor kinase which is related to receptor uncoupling (Ungerer et al., 1993; Ungerer et al., 1994). High levels of catecholamines resulting from increased sympathetic activity are thought to eventually lead to deterioration of cardiac function. It has been shown that chronic stimulation by catecholamine infusion can cause increased G_i expression (Eschenhagen et al., 1992a; Mende et al., 1992) and decreased density of β-adrenoceptors (Mende et al., 1992). Increased G_i protein levels contribute to diminution of β-adrenoceptor-cAMP-mediated

signaling in heart failure. Taken together, the studies suggest that defective cAMP-mediated signaling pathway may lead to a reduction in cAMP formation, thereby causing markedly diminished or absent responses to PDE III inhibitors. Since the cAMP-PKA pathway has been demonstrated to play an important role in modulation of the VSRM (Hobai et al., 1997; Ferrier et al., 1998), the reduced formation of cAMP may contribute to absence of potentiation of the VSRM in CM hamster ventricular myocytes.

In CM hamster hearts, a number of studies have provided evidence for defects in the β-adrenoceptor-adenylyl cyclase-cAMP-PKA pathway. Cardiac norepinephrine concentrations are markedly increased in CM hamsters compared with control hamsters at 90 days of age (Ikegaya et al., 1992). Moreover, functional uncoupling of G_s to adenylyl cyclase has been demonstrated in CM hamster heart at 90 days of age (Ikegaya et al., 1992) or younger (Kessler et al., 1989). Furthermore, increased G_i content (Sen et al., 1990a; Sethi et al., 1994; Kaura et al., 1996) and functional G_i activity (Sethi et al., 1994; Kaura et al., 1996) has been demonstrated in CM hamsters. Finally, decreased β_1-adrenoceptor density (Kaura et al., 1996) has been observed in CM hearts. Therefore, decreased phosphorylation by the cAMP-PKA pathway in CM hearts may be due to an increase in norepinephrine concentrations, a reduction in β_1-adrenoceptors, augmentation of G_i activity and functional uncoupling of G_s to adenylyl cyclase.

The results of previous studies of PDE III activity in heart failure are conflicting. Some studies showed that basal PDE III activity, kinetic properties and inhibition by PDE inhibitors are unchanged in failing hearts (Bethke et al., 1991; von der Leyen et al., 1991; Steinfath et al., 1992), whereas other studies suggest that membrane-associated PDE III mRNA expression (Silver et al., 1990; Smith et al., 1997) and activity (Smith et al., 1997)

are decreased in heart failure. Assuming PDE III activity is reduced, it may be a compensatory response to decreased cAMP formation. Thus, the efficacy of PDE III inhibitors may be diminished due to reduced membrane-associated PDE III activity (Smith et al., 1997).

As in guinea pig ventricular myocytes, amrinone caused a small increase in SR Ca^{2+} content in normal hamsters cells. In both of these species, amrinone had little effect on the amplitude of CICR contractions. Thus, a small increase in SR Ca^{2+} content *per se* does not appear to markedly increase VSRM contractions. In fact, we observed that amrinone increased fractional SR Ca^{2+} release independently of SR Ca^{2+} content in normal cells, whereas this action was absent in CM myocytes. As discussed above, these results may be attributable to a defect in cAMP-mediated signaling pathways affecting phosphorylation of proteins involved in regulation of the VSRM.

In contrast to the effect of amrinone on $I_{Ca\text{-}L}$ in guinea pig ventricular myocytes, we found that amrinone reduced the magnitude of $I_{Ca\text{-}L}$ in normal and CM hamster cells. The precise mechanism underlying this difference in effect on $I_{Ca\text{-}L}$ remains unclear. However, it may be related to differences in animal species. PDE III hydrolyzes both cAMP and cGMP with high affinity, although the Vmax for cGMP hydrolysis is only about one tenth of that for cAMP (Beavo 1995; Conti et al., 1995; Manganiello et al, 1995). The magnitude of $I_{Ca\text{-}L}$ can be affected by both cAMP and cGMP (Hartzell and Fischmeister, 1986; Thakkar et al., 1988; Levi et al., 1989; Mery et al., 1991; Sumii and Sperelakis, 1995). $I_{Ca\text{-}L}$ can be enhanced in magnitude by cAMP, but most studies have shown cGMP may reduce the magnitude of $I_{Ca\text{-}L}$ (Thakkar et al., 1988; Levi et al., 1989; Mery et al.,

1991; Ono and Trautwein, 1991; Sumii and Sperelakis, 1995). Thus, an increase in cGMP levels may lead to a reduction in the magnitude of $I_{Ca\text{-}L}$.

The increased cAMP levels and activation of PKA can enhance $I_{Ca\text{-}L}$ in heart muscle by phosphorylating Ser 1928 residue in the C-terminus of α_{1C} subunit (Gao et al., 1997) and increasing open probability of Ca^{2+} channels (Reuter, 1983; Tsien et al., 1986). On the other hand, accumulating evidence suggests that cGMP and cGMP-dependent protein kinase (PKG) are involved in reduction of $I_{Ca\text{-}L}$ by several mechanisms (Thakkar et al., 1988; Levi et al., 1989; Mery et al., 1991; Sumii and Sperelakis, 1995). PKG activation induced by cGMP prolongs closed time of single Ca^{2+} channels without an effect on open time or single channel conductance (Tohse and Sperelakis, 1991). A recent study showed evidence that cGMP inhibited $I_{Ca\text{-}L}$ by phosphorylation of Ser 533 residue in the α_{1C} subunit of the channel (Jiang et al., 2000). In addition to the cGMP /PKG pathway, cGMP may also modulate $I_{Ca\text{-}L}$ via two other pathways, depending on animal species. In frog ventricle, $I_{Ca\text{-}L}$ is inhibited by intracellular perfusion with cGMP, which decreased cAMP levels via cGMP-stimulated PDE (PDE II) (Hartzell and Fischmeister, 1986). In mammals, many studies have reported that cGMP inhibits cAMP-stimulated Ca^{2+} current (Thakkar et al., 1988; Levi et al., 1989; Mery et al., 1991; Sumii and Sperelakis, 1995). However, one study showed that cGMP further enhanced cAMP-stimulated $I_{Ca\text{-}L}$ in guinea pig cells, presumably due to activation of cGMP-inhibited PDE (PDE III) (Ono and Trautwein, 1991). Studies of the effects of cGMP on basal $I_{Ca\text{-}L}$ yield conflicting results. Some reports showed cGMP had no effect on basal $I_{Ca\text{-}L}$ (Hartzell and Fischmeister, 1986; Levi et al., 1989; Mery et al., 1991; Ono and Trautwein, 1991), but other studies demonstrated that cGMP (Thakkar et al., 1988; Wahler et al., 1990; Tohse

and Sperelakis, 1991) or PKG (Haddad et al., 1995; Sumii and Sperelakis, 1995) inhibited basal $I_{Ca\text{-}L}$. Thus, it is possible that cGMP may cause a decrease in the magnitude of basal $I_{Ca\text{-}L}$.

Effects of cGMP on $I_{Ca\text{-}L}$ between different animal species vary widely (Sperelakis, 1988). According to the effects of cGMP, as well as the effects of PDE II and PDE III inhibitors on $I_{Ca\text{-}L}$, the following relative order of potency of the three cGMP pathways regarding their regulation of Ca^{2+} current has been proposed: PDE II > PDE III >> PKG in frogs; PDE III > PKG >> PDE II in guinea pigs; PKG > PDE III >> PDE II in rats (Rivet-Bastide et al., 1997). Since rats and hamsters are classified under muridae and guinea pigs belong to carviomorpha (Carleton, 1984), it is possible that hamster myocytes are more similar to cells from rats than guinea pigs. If this is true, we speculate that increased cGMP levels predominantly activate PKG, thereby inhibiting $I_{Ca\text{-}L}$ in hamster ventricular myocytes.

In summary, our results demonstrate that depressed VSRM contractions in ventricular myocytes from CM hamster hearts cannot be restored by amrinone. Furthermore, amrinone has no effect on SR Ca^{2+} release by the VSRM in CM myocytes, which may contribute to the absence of positive inotropic effects in CM myocytes. It is possible that low formation of cAMP persists in the presence of amrinone in CM cells, which may lead to the absence of potentiation of the VSRM by this drug. The reduction in the magnitude of $I_{Ca\text{-}L}$ by amrinone in normal and CM hamster myocytes could be related to activation of PKG. However, despite a reduction in $I_{Ca\text{-}L}$ in normal hamster cells, VSRM contractions are enhanced by amrinone, which suggests that the VSRM may be regulated separately from CICR.

4. CONCLUSION

Our results demonstrate that the positive inotropic effects of an important class of drugs, the PDE III inhibitors, are mediated by effects on the VSRM. The specific PDE III inhibitor amrinone can selectively enhance VSRM contractions in normal hearts without stimulation of $I_{Ca\text{-}L}$. This effect is attributable to potentiation of fractional SR Ca^{2+} release by the VSRM, an effect that is independent of SR Ca^{2+} content. Our results also suggest that the VSRM plays an important role in heart disease. Moreover, depressed cardiac contractility in CM hamster heart is attributable to selective depression of the VSRM contraction in 90-100 day old CM hamsters. This appears to be due to a defective fractional release of SR Ca^{2+} by the VSRM, rather than to a reduction in SR content. Furthermore, defective fractional SR Ca^{2+} release by the VSRM in CM heart may play an important role in the absence of positive inotropic effects of amrinone in CM heart.

FUTURE WORK

1. We would like to measure calcium transients with fluorescent dye and determine effects of amrinone on SR Ca^{2+} release in normal and CM myocytes.

2. We would like to further examine and confirm whether reduced cAMP levels play an important role in the absence of potentiation of the VSRM by application of low concentrations of forskolin to stimulate synthesis of cAMP prior to subsequent exposure to amrinone in normal and CM myocytes.

3. We would like to further confirm selective potentiation of the VSRM by amrinone via rapid application of cadmium in the presence of amrinone in normal guinea pig ventricular myocytes.

4. With the aid of confocal microscopy, we will determine the relations between SR Ca^{2+} release, which is visualized as "calcium sparks", and Ca^{2+} release triggers (the VSRM and Ca^{2+} current) in both normal and CM myocytes.

REFERENCES

Aass H, Skomedal T, Osnes JB. Increase of cyclic AMP in subcellular fractions of rat heart muscle after β-adrenergic stimulation: prenalterol and isoprenaline caused different distribution of bound cyclic AMP. J Mol Cell Cardiol. 20:847-60, 1988.

Aggarwal R, Shorofsky SR, Goldman L, Balke CW. Tetrodotoxin-blockable Ca^{2+} currents in rat ventricular myocytes; a third type of cardiac cell sodium current. J Physiol. 505:353-69, 1997.

Alvarez R, Banerjee GL, Bruno JJ, Jones GL, Littschwager K, Strosberg AM, Venuti MC. A potent and selective inhibitor of cyclic AMP phosphodiesterase with potential cardiotonic and antithrombotic properties. Mol Pharmacol. 29:554-60, 1986.

Arreola J, Dirksen RT, Shieh RC, Williford DJ, Sheu SS. Ca^{2+} current and Ca^{2+} transients under action potential clamp in guinea pig ventricular myocytes. Am J Physiol. 261:C393-7, 1991.

Artman M, Robertson DW, Mahony L, Thompson WJ. Analysis of the binding sites for the cardiotonic phosphodiesterase inhibitor [3H]LY186126 in ventricular myocardium. Mol Pharmacol. 36:302-11, 1989.

Ashikaga T, Robertson DW, Sportsman RJ, Strada SJ, Thompson WJ. Comparison of indolidan analog binding sites of drug antibody and sarcoplasmic reticulum with inhibition of cyclic AMP phosphodiesterase. J Recept Signal Transduct Res. 16:315-37, 1996.

Awad SS, Welty JD. Comparisons of hemodynamics throughout the life span of the Bio 14.6 cardiomyopathic with the F1B normal hamster. Comp Biochem Physiol A. 97:487-91, 1990.

Baartscheer A, Schumacher CA, Opthof T, Fiolet JW. The origin of increased cytoplasmic Ca^{2+} upon reversal of the Na^{+}/Ca^{2+}-exchanger in isolated rat ventricular myocytes. J Mol Cell Cardiol. 28:1963-73, 1996.

Bajusz E. Hereditary cardiomyopathy: a new disease model. Am Heart J.77:686-96, 1969.

Bajusz E, Baker JR, Nixon CW, Homburger F. Spontaneous, herditary myocardial degeneration and congestive heart failure in a strain of Syrian hamsters. Ann N Y Acad Sci. 156:105-29, 1969.

Bajusz E. Dystrophic calcification of myocardium as conditioning factor in genesis of congestive heart failure. An experimental study. Am Heart J. 78:202-10, 1969.

Bajusz E, Lossmitzer K. A new disease model of chronic congestive heart failure: studies on its pathogenesis. Trans N Y Acad Sci. 30:939-48, 1968.

Barcenas-Ruiz L, Beuckelmann DJ, Wier WG. Sodium-calcium exchange in heart: membrane currents and changes in $[Ca^{2+}]i$. Science. 238:1720-2, 1987.

Barcenas-Ruiz L, Wier WG. Voltage dependence of intracellular $[Ca^{2+}]i$ transients in guinea pig ventricular myocytes. Circ Res. 611:148-54, 1987.

Bassani RA, Bassani JW, Bers DM. Mitochondrial and sarcolemmal Ca^{2+} transport reduce $[Ca^{2+}]i$ during caffeine contractures in rabbit cardiac myocytes. J Physiol. 453:591-608, 1992.

Bassani JW, Yuan W, Bers DM. Fractional SR Ca release is regulated by trigger Ca and SR Ca content in cardiac myocytes. Am J Physiol. 268:C1313-9, 1995.

Bazan E, Sole MJ, Schwartz A, Johnson CL. Dihydropyridine receptor binding sites in the cardiomyopathic hamster heart are unchanged from control. J Mol Cell Cardiol. 23:111-7, 1991.

Bean BP. Two kinds of calcium channels in canine atrial cells. Differences in kinetics, selectivity, and pharmacology. J Gen Physiol. 86:1-30, 1985.

Beavo JA. Cyclic nucleotide phosphodiesterases: functional implications of multiple isoforms. Physiol Rev. 75:725-48, 1995.

Beavo JA, Reifsnyder DH . Primary sequence of cyclic nucleotide phosphodiesterase isozymes and the design of selective inhibitors. Trends Pharmacol Sci. 11:150-5, 1990.

Bern, RM and Levy, MN. The cardiac pump. In: Cardiovascular Physiology. RM Bern and MN Levy, ed. Mosby-Year Book, Inc. Saint Louis. pp. 35-81, 1997

Bers DM. Mechanisms contributing to the cardiac inotropic effect of Na pump inhibition and reduction of extracellular Na. J Gen Physiol. 90:479-504, 1987.

Bers, DM. Excitation-contraction coupling and cardiac contraction. Kluwer Academic Publishers, Dordrecht, 1991.

Bers DM. Calcium fluxes involved in control of cardiac myocyte contraction. Circ Res. 87:275-81, 2000.

Bers DM, Bridge JH, Spitzer KW. Intracellular Ca^{2+} transients during rapid cooling contractures in guinea-pig ventricular myocytes. J Physiol. 417:537-53, 1989.

Bers DM, Christensen DM, Nguyen TX. Can Ca entry via Na-Ca exchange directly activate cardiac muscle contraction? J Mol Cell Cardiol. 20:405-14, 1988.

Bers DM, Perez-Reyes E. Ca channels in cardiac myocytes: structure and function in Ca influx and intracellular Ca release. Cardiovasc Res. 42:339-60, 1999.

Bethke T, Klimkiewicz A, Kohl C, von der Leyen H, Mehl H, Mende U, Meyer W, Neumann J, Schmitz W, Scholz H, et al. Effects of isomazole on force of contraction and phosphodiesterase isoenzymes I-IV in nonfailing and failing human hearts. J Cardiovasc Pharmacol. 18:386-97, 1991.

Beuckelmann DJ, Nabauer M, Kruger C, Erdmann E. Altered diastolic [Ca^{2+}]i handling in human ventricular myocytes from patients with terminal heart failure. Am Heart J. 129:684-9, 1995.

Beuckelmann DJ, Wier WG. Mechanism of release of Ca^{2+} from sarcoplasmic reticulum of guinea-pig cardiac cells. J Physiol. 405:233-55, 1988.

Beuckelmann DJ, Wier WG. Sodium-calcium exchange in guinea-pig cardiac cells: exchange current and changes in intracellular Ca^{2+}. J Physiol. 414:499-520, 1989.

Bobet J, Howlett SE, Gordon T. Possible mechanisms underlying differences in force production between normal and cardiomyopathic hamster atria. Am J Physiol. 261:H1603-8, 1991.

Bode DC, Kanter JR, Brunton LL. Resolution of soluble rat cardiac phosphodiesterases by high performance liquid chromatography. Second Messengers Phosphoproteins. 12:235-40; 1988-89.

Bohm M, Diet F, Kemkes B, and Erdmann E. Enhancement of the effectiveness of milrinone to increase force of contraction by stimulation of cardiac beta-adrenoceptors in the failing human heart. *Klin Wochenschr* 66:957-962, 1988.

Bohm M, Eschenhagen T, Gierschik P, Larisch K, Lensche H, Mende U, Schmitz W, Schnabel P, Scholz H, Steinfath M, et al. Radioimmunochemical quantification of Gi alpha in right and left ventricles from patients with ischaemic and dilated cardiomyopathy and predominant left ventricular failure. J Mol Cell Cardiol. 26:133-49, 1994.

Bohm M, Gierschik P, Jakobs KH, Pieske B, Schnabel P, Ungerer M, Erdmann E. Increase of Gi alpha in human hearts with dilated but not ischemic cardiomyopathy. Circulation. 82:1249-65, 1990.

Bolger GB, Erdogan S, Jones RE, Loughney K, Scotland G, Hoffmann R, Wilkinson I, Farrell C, Houslay MD. Characterization of five different proteins produced by

alternatively spliced mRNAs from the human cAMP-specific phosphodiesterase PDE4D gene. Biochem J. 328 :539-48, 1997.

Bristow MR, Hershberger RE, Port JD, Minobe W, Rasmussen R. Beta 1- and beta 2-adrenergic receptor-mediated adenylate cyclase stimulation in nonfailing and failing human ventricular myocardium. Mol Pharmacol. 35:295-303, 1989.

Brooksby P, Levi AJ, Jones JV. The electrophysiological characteristics of hypertrophied ventricular myocytes from the spontaneously hypertensive rat. J Hypertens. 11:611-22. 1993.

Brown LA, Harding SE. The effect of pertussis toxin on beta-adrenoceptor responses in isolated cardiac myocytes from noradrenaline-treated guinea-pigs and patients with cardiac failure. Br J Pharmacol. 106:115-22, 1992.

Burk SE, Lytton J, MacLennan DH, Shull GE. cDNA cloning, functional expression, and mRNA tissue distribution of a third organellar Ca^{2+} pump. J Biol Chem. 264:18561-8, 1989.

Burns F, Zhao AZ, Beavo JA. Cyclic nucleotide phosphodiesterases: gene complexity, regulation by phosphorylation, and physiological implications. Adv Pharmacol. 36:29-48, 1996

Buxton IL, Brunton LL. Compartments of cyclic AMP and protein kinase in mammalian cardiomyocytes. J Biol Chem. 258:10233-9, 1983.

Callewaert G, Cleemann L, Morad M. Caffeine-induced Ca^{2+} release activates Ca^{2+} extrusion via Na^{+}-Ca^{2+} exchanger in cardiac myocytes. Am J Physiol. 257:C147-52, 1989.

Cannell MB, Berlin JR, Lederer WJ. Effect of membrane potential changes on the calcium transient in single rat cardiac muscle cells. Science. 238:1419-23, 1987

Cannell MB, Cheng H, Lederer WJ. Spatial non-uniformities in $[Ca^{2+}]i$ during excitation-contraction coupling in cardiac myocytes. Biophys J. 67:1942-56, 1994.

Cannell MB, Cheng H, Lederer WJ The control of calcium release in heart muscle. Science. 268:1045-9, 1995.

Cannell MB, Soeller C Mechanisms underlying calcium sparks in cardiac muscle. J Gen Physiol. 113:373-6, 1999.

Capasso JM, Olivetti G, Anversa P. Mechanical and electrical properties of cardiomyopathic hearts of Syrian hamsters. Am J Physiol. 257:H1836-42, 1989.

Carl SL, Felix K, Caswell AH, Brandt NR, Ball WJ Jr, Vaghy PL, Meissner G, Ferguson DG. Immunolocalization of sarcolemmal dihydropyridine receptor and sarcoplasmic reticular triadin and ryanodine receptor in rabbit ventricle and atrium. J Cell Biol. 129:672-682, 1995.

Carleton, M. Introduction to rodents. In: Orders and Families of Recent Mammals of the World. S Anderson and J K Jones Jr., ed. John Wiley and Sons, New York. pp 255-265, 1984

Cerbai E, Barbieri M, Li Q, Mugelli A. Ionic basis of action potential prolongation of hypertrophied cardiac myocytes isolated from hypertensive rats of different ages. Cardiovasc Res. 28:1180-7, 1994.

Chalovich JM. Actin mediated regulation of muscle contraction. Pharmacol Ther. 55:95-148, 1992.

Charbonneau H, Beier N, Walsh KA, Beavo JA. Identification of a conserved domain among cyclic nucleotide phosphodiesterases from diverse species. Proc Natl Acad Sci U S A. 83:9308-12, 1986.

Cheng H, Lederer WJ, Cannell MB Calcium sparks: elementary events underlying excitation-contraction coupling in heart muscle. Science. 262:740-4, 1993.

Cleemann L, Morad M. Role of Ca^{2+} channel in cardiac excitation-contraction coupling in the rat: evidence from Ca^{2+} transients and contraction. J Physiol. 432:283-312, 1991.

Collier ML, Thomas AP, Berlin JR Relationship between L-type Ca^{2+} current and unitary sarcoplasmic reticulum Ca^{2+} release events in rat ventricular myocytes. J Physiol. 516 :117-28, 1999.

Conti M, Nemoz G, Sette C, Vicini E. Recent progress in understanding the hormonal regulation of phosphodiesterases. Endocr Rev. 16:370-89, 1995.

Conti M, Swinnen JV, Tsikalas KE, Jin SL. Structure and regulation of the rat high-affinity cyclic AMP phosphodiesterases. A family of closely related enzymes. Adv Second Messenger Phosphoprotein Res. 25:87-99, 1992.

Corbin JD, Keely SL, Park CR. The distribution and dissociation of cyclic adenosine 3':5'-monophosphate-dependent protein kinases in adipose, cardiac, and other tissues. J Biol Chem. 250:218-25, 1975.

Coronado R, Morrissette J, Sukhareva M, Vaughan DM Structure and function of ryanodine receptors. Am J Physiol. 266:C1485-504, 1994.

Danielsen W, v der Leyen H, Meyer W, Neumann J, Schmitz W, Scholz H, Starbatty J, Stein B, Doring V, Kalmar P. Basal and isoprenaline-stimulated cAMP content in failing versus nonfailing human cardiac preparations. J Cardiovasc Pharmacol. 14:171-3, 1989.

Davis D, Baily R, Zelis R. Abnormalities in systemic norepinephrine kinetics in human congestive heart failure. Am J Physiol. 254:E760-6, 1988.

Degerman E, Belfrage P, Manganiello VC. Structure, localization, and regulation of cGMP-inhibited phosphodiesterase (PDE3). J Biol Chem. 272:6823-6, 1997.

Degerman E, Belfrage P, Newman AH, Rice KC, Manganiello VC. Purification of the putative hormone-sensitive cyclic AMP phosphodiesterase from rat adipose tissue using a derivative of cilostamide as a novel affinity ligand. J Biol Chem. 262:5797-807, 1987.

de Tombe PP. Altered contractile function in heart failure. Cardiovasc Res. 37:367-80, 1998.

duBell WH, Houser SR. Voltage and beat dependence of Ca^{2+} transient in feline ventricular myocytes. Am J Physiol. 257:H746-59, 1989.

Eisner DA, Trafford AW, Diaz ME, Overend CL, O'Neill SC. The control of Ca release from the cardiac sarcoplasmic reticulum: regulation versus autoregulation. Cardiovasc Res. 38:589-604, 1998.

Eschenhagen T, Mende U, Diederich M, Nose M, Schmitz W, Scholz H, Schulte am Esch J, Warnholtz A, Schafer H. (1992 a) Long term beta-adrenoceptor-mediated up-regulation of Gi alpha and G(o) alpha mRNA levels and pertussis toxin-sensitive guanine nucleotide-binding proteins in rat heart. Mol Pharmacol. 42:773-83, 1992.

Eschenhagen T, Mende U, Nose M, Schmitz W, Scholz H, Haverich A, Hirt S, Doring V, Kalmar P, Hoppner W, et al. (1992b) Increased messenger RNA level of the inhibitory G protein alpha subunit Gi alpha-2 in human end-stage heart failure. Circ Res. 70:688-96, 1992.

Fabiato, A. Rapid ionic modifications during the aequorin-detected calcium transient in a skinned canine cardiac Purkinje cell. J Gen Physiol. 85:189-246, 1985a.

Fabiato, A. Simulated calcium current can both cause calcium loading in and trigger calcium release from the sarcoplasmic reticulum of a skinned canine cardiac Purkinje cell. J Gen Physiol. 85:291-320, 1985b.

Fabiato, A. Time and calcium dependence of activation and inactivation of calcium-induced release of calcium from the sarcoplasmic reticulum of a skinned canine cardiac Purkinje cell. J Gen Physiol. 85:247-89, 1985c.

Fawcett L, Baxendale R, Stacey P, McGrouther C, Harrow I, Soderling S, Hetman J, Beavo JA, Phillips SC. Molecular cloning and characterization of a distinct human phosphodiesterase gene family: PDE11A. Proc Natl Acad Sci U S A. 97:3702-7, 2000.

Feldman MD, Copelas L, Gwathmey JK, Phillips P, Warren SE, Schoen FJ, Grossman W, and Morgan JP. Deficient production of cyclic AMP: pharmacologic evidence of an important cause of contractile dysfunction in patients with end-stage heart failure. *Circulation* 75:331-339, 1987.

Feldman AM, Cates AE, Veazey WB, Hershberger RE, Bristow MR, Baughman KL, Baumgartner WA, Van Dop C. Increase of the 40,000-mol wt pertussis toxin substrate (G protein) in the failing human heart. J Clin Invest. 82:189-97, 1988.

Ferrier GR, Howlett SE. Contractions in guinea-pig ventricular myocytes triggered by a calcium-release mechanism separate from Na^+ and L-currents. J Physiol. 484:107-22, 1995.

Ferrier GR and Howlett SE. Cardiac excitement-contraction coupling: the role of membrane potential in regulation of contraction. Am J Physiol Heart Circ Physiol. 280:H1928-44, 2001.

Ferrier GR. Low temperature inhibits cardiac contractions inhitbited by the voltage-sensitve release mechanism. J Mol Cell Cardiol, 28:A180, 1996.

Ferrier GR, Redondo, IM, Isac, M & Howlett, SE. The cardiac voltage sensitive release mechanism is located in a separate compartment from L-type Ca^{2+} current. Biophysical Journal 74, A54. 1998.

Ferrier GR, Redondo IM, Mason CA, Mapplebeck C, Howlett SE. Regulation of contraction and relaxation by membrane potential in cardiac ventricular myocytes. Am J Physiol Heart Circ Physiol. 278:H1618-26, 2000a.

Ferrier, GR, Redondo, IM, Zhu, JQ and Howlett, SE. A critical role for phosphodiesterase in regulation of the cardiac voltage-sensitive release mechanism (VSRM) by cAMP analogs in whole cell voltage clamp investigations. Biophys J 78:371A, 2000b

Finkel MS, Marks ES, Patterson RE, Speir EH, Steadman KA, Keiser HR. Correlation of changes in cardiac calcium channels with hemodynamics in Syrian hamster cardiomyopathy and heart failure. Life Sci. 41:153-9, 1987.

Fink MA, Zakhary DR, Mackey JA, Desnoyer RW, Apperson-Hansen C, Damron DS, Bond M. AKAP-mediated targeting of protein kinase a regulates contractility in cardiac myocytes. Circ Res. 88:291-7, 2001.

Fischmeister R, Hartzell HC. Regulation of calcium current by low-Km cyclic AMP phosphodiesterases in cardiac cells. Mol Pharmacol. 38:426-33, 1990.

Fischmeister R, Hartzell HC. Cyclic AMP phosphodiesterases and Ca^{2+} current regulation in cardiac cells. Life Sci. 48:2365-76, 1991.

Fisher DA, Smith JF, Pillar JS, St Denis SH, Cheng JB. Isolation and characterization of PDE8A, a novel human cAMP-specific phosphodiesterase. Biochem Biophys Res Commun. 246:570-7, 1998.

Fleischer S and Inui M, 1989 Biochemistry and biophysics of excitation-contraction coupling. Annu Rev Biophys Biophys Chem. 18:333-64, 1989.

Frank JS and Garfinkel A. Immunolocalization and structural configuration of membrane and cytoskeletal proteins involved in excitation-contraction coupling of cardiac muscle. In: The Myocardium, GA Langer, ed. Acdemic Press, San Diego, pp. 1-32, 1997.

Fraser ID, Tavalin SJ, Lester LB, Langeberg LK, Westphal AM, Dean RA, Marrion NV, Scott JD. A novel lipid-anchored A-kinase Anchoring Protein facilitates cAMP-responsive membrane events. EMBO J. 17:2261-72, 1998.

Gao T, Yatani A, Dell'Acqua ML, Sako H, Green SA, Dascal N, Scott JD, Hosey MM. cAMP-dependent regulation of cardiac L-type Ca^{2+} channels requires membrane targeting of PKA and phosphorylation of channel subunits. Neuron. 19:185-96, 1997.

Gomez AM, Valdivia HH, Cheng H, Lederer MR, Santana LF, Cannell MB, McCune SA, Altschuld RA, Lederer WJ. Defective excitation-contraction coupling in experimental cardiac hypertrophy and heart failure. Science. 276:800-6, 1997.

Grant PG, Colman RW. Purification and characterization of a human platelet cyclic nucleotide phosphodiesterase. Biochemistry. 23:1801-7, 1984.

Gray PC, Johnson BD, Westenbroek RE, Hays LG, Yates JR, Scheuer T, Catterall WA, Murphy BJ. (1998a) Primary structure and function of an A kinase anchoring protein associated with calcium channels. Neuron. 20:1017-26, 1998.

Gray PC, Scott JD, Catterall WA. (1998b) Regulation of ion channels by cAMP-dependent protein kinase and A-kinase anchoring proteins. Curr Opin Neurobiol. 8:330-4, 1998.

Haddad GE, Sperelakis N, Bkaily G. Regulation of the calcium slow channel by cyclic GMP dependent protein kinase in chick heart cells. Mol Cell Biochem. 148:89-94, 1995.

Hagiwara N, Irisawa H, Kameyama M. Contribution of two types of calcium currents to the pacemaker potentials of rabbit sino-atrial node cells. J Physiol. 395:233-53, 1988.

Hajdu S, Leonard EJ. Action of ryanodine on mammalian cardiac muscle. Effects of contractitlity, and reversal of digitalis-induced ventricular arrthymias. Circ. Res. 9:1291-1283,1961.

Hammond HK. Mechanisms for myocardial beta-adrenergic receptor desensitization in heart failure. Circulation. 87:652-4, 1993.

Harrison SA, Reifsnyder DH, Gallis B, Cadd GG, Beavo JA. Isolation and characterization of bovine cardiac muscle cGMP-inhibited phosphodiesterase: a receptor for new cardiotonic drugs. Mol Pharmacol. 29:506-14, 1986.

Hartzell HC. Regulation of cardiac ion channels by catecholamines, acetylcholine and second messenger systems. Prog Biophys Mol Biol. 52:165-247, 1988.

Hartzell HC, Fischmeister R. Opposite effects of cyclic GMP and cyclic AMP on Ca^{2+} current in single heart cells. Nature. 323:273-5, 1986.

Hasenfuss G, Mulieri LA, Leavitt BJ, Allen PD, Haeberle JR, Alpert NR. Alteration of contractile function and excitation-contraction coupling in dilated cardiomyopathy. Circ Res. 70:1225-32, 1992.

Hasking GJ, Esler MD, Jennings GL, Burton D, Johns JA, Korner PI. Norepinephrine spillover to plasma in patients with congestive heart failure: evidence of increased overall and cardiorenal sympathetic nervous activity. Circulation. 73:615-21, 1986.

Hatem SN, Sham JS, Morad M. Enhanced Na^{+}-Ca^{2+} exchange activity in cardiomyopathic Syrian hamster. Circ Res. 74:253-61, 1994.

Heinemann SH, Terlau H, Stuhmer W, Imoto K, Numa S. Calcium channel characteristics conferred on the sodium channel by single mutations. Nature. 356:441-3, 1992.

Hidaka H, Endo T. Selective inhibitors of three forms of cyclic nucleotide phosphodiesterase--basic and potential clinical applications. Adv Cyclic Nucleotide Protein Phosphorylation Res. 16:245-59, 1984.

Hille, B . Ionic Channels of Excitable Membrane. Sinauer Assoc. Inc., Sunderland, ed. 5, pp 403-414, 1992.

Hirano Y, Fozzard HA, January CT. Characteristics of L- and T-type Ca^{2+} currents in canine cardiac Purkinje cells. Am J Physiol. 256:H1478-92, 1989.

Hobai IA, Howarth FC, Pabbathi VK, Dalton GR, Hancox JC, Zhu JQ, Howlett SE, Ferrier GR, Levi AJ. "Voltage-activated Ca release" in rabbit, rat and guinea-pig cardiac myocytes, and modulation by internal cAMP. Pflugers Arch. 435:164-73, 1997.

Hohl CM, Li QA. Compartmentation of cAMP in adult canine ventricular myocytes. Relation to single-cell free Ca^{2+} transients. Circ Res. 69:1369-79, 1991.

Honerjager P. Pharmacology of bipyridine phosphodiesterase III inhibitors. Am Heart J. 121:1939-44, 1991.

Hoppe UC, Johns DC, Marban E, O'Rourke B. Manipulation of cellular excitability by cell fusion: effects of rapid introduction of transient outward K current on the guinea pig action potential. Circ Res 84:964-72, 1999

Houslay MD, Milligan G. Tailoring cAMP-signalling responses through isoform multiplicity. Trends Biochem Sci. 22:217-24, 1997.

Howlett SE, Bobet J, Gordon T. Force-interval relation in normal and cardiomyopathic hamster atria. Am J Physiol. 261:H1597-602, 1991.

Howlett SE, Ferrier GR. The 1996 Merck Frosst Award. The voltage-sensitive release mechanism: a new trigger for cardiac contraction. Can J Physiol Pharmacol. 75:1044-57, 1997.

Howlett SE, Rafuse VF, Gordon T. [3H]-nitrendipine binding sites in normal and cardiomyopathic hamsters: absence of a selective increase in putative calcium channels in cardiomyopathic hearts. Cardiovasc Res. 22:840-6, 1988.

Howlett SE, Xiong W, Mapplebeck CL, Ferrier GR. Role of voltage-sensitive release mechanism in depression of cardiac contraction in myopathic hamsters. Am J Physiol. 277:H1690-700, 1999.

Howlett SE, Zhu JQ, Ferrier GR. Contribution of a voltage-sensitive calcium release mechanism to contraction in cardiac ventricular myocytes.Am J Physiol. 274:H155-70, 1998.

Hunter EG, Hughes V, White J. Cardiomyopathic hamsters, CHF 146 and CHF 147: a preliminary study. Can J Physiol Pharmacol. 62:1423-8, 1984.

Ikeda Y, Martone M, Gu Y, Hoshijima M, Thor A, Oh SS, Peterson KL, Ross J. Altered membrane proteins and permeability correlate with cardiac dysfunction in cardiomyopathic hamsters. Am J Physiol Heart Circ Physiol. 278:H1362-70, 2000.

Ikegaya T, Kobayashi A, Hong RB, Masuda H, Kaneko M, Noboru Y. Stimulatory guanine nucleotide-binding protein and adenylate cyclase activities in Bio 14.6

cardiomyopathic hamsters at the hypertrophic stage. Mol Cell Biochem. 110:83-90, 1992.

Ishikawa Y, Homcy CJ. The adenylyl cyclases as integrators of transmembrane signal transduction. Circ Res. 80:297-304, 1997.

Jasmin G, Proschek L. Hereditary polymyopathy and cardiomyopathy in the Syrian hamster. I. Progression of heart and skeletal muscle lesions in the UM-X7.1 line. Muscle Nerve. 5:20-5, 1982.

Jenden DJ, Fairhurst AS. The pharmacology of ryanodine. Pharmacol Rev. 21:1-25, 1969.

Jiang LH, Gawler DJ, Hodson N, Milligan CJ, Pearson HA, Porter V, Wray D. Regulation of cloned cardiac L-type calcium channels by cGMP-dependent protein kinase. J Biol Chem. 275:6135-43, 2000.

Jurevicius J, Fischmeister R. cAMP compartmentation is responsible for a local activation of cardiac Ca^{2+} channels by beta-adrenergic agonists. Proc Natl Acad Sci U S A. 93:295-9, 1996.

Kadambi VJ, Ponniah S, Harrer JM, Hoit BD, Dorn GW 2nd, Walsh RA, Kranias EG. Cardiac-specific overexpression of phospholamban alters calcium kinetics and resultant cardiomyocyte mechanics in transgenic mice. J Clin Invest. 97:533-9, 1996.

Kajimoto K, Hagiwara N, Kasanuki H, Hosoda S. Contribution of phosphodiesterase isozymes to the regulation of the L-type calcium current in human cardiac myocytes. Br J Pharmacol. 121:1549-56, 1997.

Kalmar P, Hoppner W, et al. Increased messenger RNA level of the inhibitory G protein alpha subunit Gi alpha-2 in human end-stage heart failure. Circ Res. 70:688-96, 1992.

Kasuya J, Goko H, Fujita-Yamaguchi Y. Multiple transcripts for the human cardiac form of the cGMP-inhibited cAMP phosphodiesterase. J Biol Chem. 270:14305-12, 1995.

Katoh H, Schlotthauer K, Bers DM Transmission of information from cardiac dihydropyridine receptor to ryanodine receptor: evidence from BayK 8644 effects on resting Ca^{2+} sparks. Circ Res. 87:106-11, 2000.

Kauffman RF, Crowe VG, Utterback BG, Robertson DW. LY195115: a potent, selective inhibitor of cyclic nucleotide phosphodiesterase located in the sarcoplasmic reticulum. Mol Pharmacol. 30:609-16, 1986.

Kauffman RF, Utterback BG, Robertson DW. Characterization and pharmacological relevance of high affinity binding sites for [3H]LY186126, a cardiotonic

phosphodiesterase inhibitor, in canine cardiac membranes. Circ Res. 65:154-63, 1989.

Kaura D, Takeda N, Sethi R, Wang X, Nagano M, Dhalla NS. Beta-adrenoceptor mediated signal transduction in congestive heart failure in cardiomyopathic (UM-X7.1) hamsters. Mol Cell Biochem. 157:191-6, 1996.

Kawano S, DeHaan RL. Low-threshold current is major calcium current in chick ventricle cells. Am J Physiol. 256:H1505-8, 1989.

Kessler PD, Cates AE, Van Dop C, Feldman AM. Decreased bioactivity of the guanine nucleotide-binding protein that stimulates adenylate cyclase in hearts from cardiomyopathic Syrian hamsters. J Clin Invest. 84:244-52, 1989.

Kimura J, Miyamae S, Noma A. Identification of sodium-calcium exchange current in single ventricular cells of guinea-pig. J Physiol 384:199-222, 1987.

Kirchberger MA, Tada M, Katz AM. Adenosine 3':5'-monophosphate-dependent protein kinase-catalyzed phosphorylation reaction and its relationship to calcium transport in cardiac sarcoplasmic reticulum. J Biol Chem. 249:6166-73, 1974.

Kithas PA, Artman M, Thompson WJ, Strada SJ. Subcellular distribution of high-affinity type IV cyclic AMP phosphodiesterase activity in rabbit ventricular myocardium: relations to the effects of cardiotonic drugs. Circ Res. 62:782-9, 1988.

Kiuchi K, Shannon RP, Komamura K, Cohen DJ, Bianchi C, Homcy CJ, Vatner SF, Vatner DE. Myocardial beta-adrenergic receptor function during the development of pacing-induced heart failure. J Clin Invest. 91:907-14, 1993.

Kondo N, Shibata S, Kodama I, Yamada K. Electrical and mechanical effects of amrinone on isolated guinea pig ventricular muscle. J Cardiovasc Pharmacol. 5:903-12, 1983.

Koss KL, Kranias EG. Phospholamban: a prominent regulator of myocardial contractility. Circ Res. 79:1059-63, 1996.

Kranias EG. Regulation of Ca^{2+} transport by cyclic 3',5'-AMP-dependent and calcium-calmodulin-dependent phosphorylation of cardiac sarcoplasmic reticulum. Biochim Biophys Acta. 844:193-9, 1985.

Kruger C, Erdmann E, Nabauer M, Beuckelmann DJ. Intracellular calcium handling in isolated ventricular myocytes from cardiomyopathic hamsters (strain BIO 14.6) with congestive heart failure. Cell Calcium. 16:500-8, 1994.

Lachnit WG, Phillips M, Gayman KJ, Pessah IN. Ryanodine and dihydropyridine binding patterns and ryanodine receptor mRNA levels in myopathic hamster heart. Am J Physiol. 267:H1205-13, 1994.

Langer, GA. Excitation-contraction coupling of calcium compartmentation. In: The Myocardium, GA Langer, ed. Acdemic Press, San Diego, pp. 181-233, 1997.

Leblanc N, Hume JR. Sodium current-induced release of calcium from cardiac sarcoplasmic reticulum. Science. 248:372-6; 1990.

Lederer WJ, Niggli E, Hadley RW. Sodium-calcium exchange in excitable cells: fuzzy space. Science. 248:283, 1990.

Lemaire S, Piot C, Leclercq F, Leuranguer V, Nargeot J, Richard S. Heart rate as a determinant of L-type Ca^{2+} channel activity: mechanisms and implication in force-frequency relation. Basic Res Cardiol. 93 Suppl 1:51-9, 1998.

Lemaire S, Piot C, Seguin J, Nargeot J, Richard S. Tetrodotoxin-sensitive Ca^{2+} and Ba^{2+} currents in human atrial cells. Receptors Channels. 3:71-81, 1995.

Le Peuch CJ, Haiech J, Demaille JG. Concerted regulation of cardiac sarcoplasmic reticulum calcium transport by cyclic adenosine monophosphate dependent and calcium--calmodulin-dependent phosphorylations. Biochemistry. 18:5150-7, 1979.

Leroy MJ, Degerman E, Taira M, Murata T, Wang LH, Movsesian MA, Meacci E, Manganiello VC. Characterization of two recombinant PDE3 (cGMP-inhibited cyclic nucleotide phosphodiesterase) isoforms, RcGIP1 and HcGIP2, expressed in NIH 3006 murine fibroblasts and Sf9 insect cells. Biochemistry. 35:10194-202, 1996.

Levesque PC, Leblanc N, Hume JR. Release of calcium from guinea pig cardiac sarcoplasmic reticulum induced by sodium-calcium exchange. Cardiovasc Res. 28:370-8, 1994.

Levi AJ, Hancox JC, Howarth FC, Croker J, Vinnicombe J. A method for making rapid changes of superfusate whilst maintaining temperature at 37 degrees C. Pflugers Arch. 432:930-7, 1996.

Levi AJ, Li J, Litwin SE, Spitzer KW. Effect of internal sodium and cellular calcium load on voltage-dependence of the Indo-1 transient in guinea-pig ventricular myocytes. Cardiovasc Res. 32:534-50, 1996.

Levi AJ, Spitzer KW, Kohmoto O, Bridge JH. Depolarization-induced Ca entry via Na-Ca exchange triggers SR release in guinea pig cardiac myocytes. Am J Physiol. 266:H1422-33, 1994.

Levi RC, Alloatti G, Fischmeister R. Cyclic GMP regulates the Ca-channel current in guinea pig ventricular myocytes. Pflugers Arch. 413:685-7, 1989.

Li GR, Ferrier GR, Howlett SE. Calcium currents in ventricular myocytes of prehypertrophic cardiomyopathic hamsters. Am J Physiol. 268:H999-1005, 1995.

Limas CJ, Olivari MT, Goldenberg IF, Levine TB, Benditt DG, Simon A. Calcium uptake by cardiac sarcoplasmic reticulum in human dilated cardiomyopathy. Cardiovasc Res. 21:601-5, 1987.

Lipp P, Niggli E. Sodium current-induced calcium signals in isolated guinea-pig ventricular myocytes. J Physiol. 474:439-46, 1994.

Lipp P, Niggli. Submicroscopic calcium signals as fundamental events of excitation--contraction coupling in guinea-pig cardiac myocytes. J Physiol. 492:31-8, 1996.

Lipp P, Niggli. Fundamental calcium release events revealed by two-photon excitation photolysis of caged calcium in Guinea-pig cardiac myocytes. J Physiol. 508 :801-9, 1998.

Litwin SE, Li J, Bridge JH. Na-Ca exchange and the trigger for sarcoplasmic reticulum Ca release: studies in adult rabbit ventricular myocytes. Biophys J. 75:359-71, 1998.

London B, Krueger JW. Contraction in voltage-clamped, internally perfused single heart cells. J Gen Physiol. 88:475-505, 1986.

Lopez-Lopez JR, Shacklock PS, Balke CW, Wier WG Local calcium transients triggered by single L-type calcium channel currents in cardiac cells. Science. 268:1042-5, 1995.

Ludmer PL, Wright RF, Arnold JM, Ganz P, Braunwald E, Colucci WS. Separation of the direct myocardial and vasodilator actions of milrinone administered by an intracoronary infusion technique. Circulation. 73:130-7, 1986.

Lugnier C, Muller B, Le Bec A, Beaudry C, Rousseau E. Characterization of indolidan- and rolipram-sensitive cyclic nucleotide phosphodiesterases in canine and human cardiac microsomal fractions. J Pharmacol Exp Ther. 265:1142-51, 1993.

Mackiewicz U, Emanuel K, Lewartowski B. Dihydropyridine receptors functioning as voltage sensors in cardiac myocytes. J Physiol Pharmacol. 51:777-98, 2000.

Malecot CO, Arlock P, Katzung BG. Amrinone effects on electromechanical coupling and depolarization-induced automaticity in ventricular muscle of guinea pigs and ferrets. J Pharmacol Exp Ther. 232:10-9, 1985.

Manganiello VC, Murata T, Taira M, Belfrage P, Degerman E. Diversity in cyclic nucleotide phosphodiesterase isoenzyme families. Arch Biochem Biophys. 322:1-13, 1995.

Manganiello VC, Taira M, Degerman E, Belfrage P. Type III cGMP-inhibited cyclic nucleotide phosphodiesterases (PDE3 gene family). Cell Signal. 7:445-55, 1995.

McCartney S, Little BM, Langeberg LK, Scott JD. Cloning and characterization of A-kinase anchor protein 100 (AKAP100). A protein that targets A-kinase to the sarcoplasmic reticulum. J Biol Chem. 270:9327-33, 1995.

Marx SO, Reiken S, Hisamatsu Y, Jayaraman T, Burkhoff D, Rosemblit N and Marks AR. PKA phosphorylation dissociates FKBP12.6 from the calcium release channel (ryanodine receptor): defective regulation in failing hearts. Cell 101:365-76, 2000

Marx SO, Ondrias K, Marks AR. Coupled gating between individual skeletal muscle Ca^{2+} release channels. Science. 281:818-21, 1998.

Mason, JW. Classification of cardiomyopathy. In: Hurst's the Heart: Arteries and Veins. RC Schlant and RW Alexander, ed. McGraw-Hill. New York. pp. 1585-1590, 1994

Matsui K, Kiyosue T, Wang JC, Dohi K, Arita M. Effects of pimobendan on the L-type Ca^{2+} current and developed tension in guinea-pig ventricular myocytes and papillary muscle: comparison with IBMX, milrinone, and cilostazol. Cardiovasc Drugs Ther. 13:105-13, 1999.

Matsui H, MacLennan DH, Alpert NR, Periasamy M. Sarcoplasmic reticulum gene expression in pressure overload-induced cardiac hypertrophy in rabbit. Am J Physiol. 268:C252-8, 1995.

Mayoux E, Callens F, Swynghedauw B, Charlemagne D. Adaptational process of the cardiac Ca^{2+} channels to pressure overload: biochemical and physiological properties of the dihydropyridine receptors in normal and hypertrophied rat hearts. J Cardiovasc Pharmacol. 12:390-6, 1988.

McCormack JG, Browne HM, Dawes NJ. Studies on mitochondrial Ca^{2+}-transport and matrix Ca^{2+} using fura-2-loaded rat heart mitochondria. Biochim Biophys Acta. 973:420-7, 1989.

McDonald TF, Pelzer S, Trautwein W, Pelzer DJ. Regulation and modulation of calcium channels in cardiac, skeletal, and smooth muscle cells. Physiol Rev. 74:365-507, 1994.

Meacci E, Taira M, Moos M, Smith CJ, Movsesian MA, Degerman E, Belfrage P, Manganiello V. Molecular cloning and expression of human myocardial cGMP-inhibited cAMP phosphodiesterase. Proc Natl Acad Sci U S A. 89:3721-5, 1992.

Meissner G. Ryanodine receptor/Ca^{2+} release channels and their regulation by endogenous effectors. Annu Rev Physiol. 56:485-508, 1994.

Mende U, Eschenhagen T, Geertz B, Schmitz W, Scholz H, Schulte am Esch J, Sempell R, Steinfath M. Isoprenaline-induced increase in the 40/41 kDa pertussis toxin substrates and functional consequences on contractile response in rat heart. Naunyn Schmiedebergs Arch Pharmacol. 345:44-50, 1992.

Mery PF, Lohmann SM, Walter U, Fischmeister R. Ca^{2+} current is regulated by cyclic GMP-dependent protein kinase in mammalian cardiac myocytes. Proc Natl Acad Sci U S A. 88:1197-201, 1991.

Mery PF, Pavoine C, Pecker F, Fischmeister R. Erythro-9-(2-hydroxy-3-nonyl)adenine inhibits cyclic GMP-stimulated phosphodiesterase in isolated cardiac myocytes. Mol Pharmacol. 48:121-30, 1995.

Meyer RB Jr, Miller JP. Analogs of cyclic AMP and cyclic GMP: general methods of synthesis and the relationship of structure to enzymic activity.Life Sci. 14:1019-40, 1974.

Mikami A, Imoto K, Tanabe T, Niidome T, Mori Y, Takeshima H, Narumiya S, Numa S. Primary structure and functional expression of the cardiac dihydropyridine-sensitive calcium channel. Nature. 340:230-3, 1989.

Mitra R, Morad M. Two types of calcium channels in guinea pig ventricular myocytes. Proc Natl Acad Sci U S A. 83:5340-4, 1986.

Moreno-Sanchez R, Hansford RG. Dependence of cardiac mitochondrial pyruvate dehydrogenase activity on intramitochondrial free Ca^{2+} concentration. Biochem J. 256:403-12, 1988.

Morgan JP, Gwathmey JK, DeFeo TT, Morgan KG. The effects of amrinone and related drugs on intracellular calcium in isolated mammalian cardiac and vascular smooth muscle. Circulation. 73:III65-77, 1986.

Movsesian MA, Smith CJ, Krall J, Bristow MR, Manganiello VC. Sarcoplasmic reticulum-associated cyclic adenosine 5'-monophosphate phosphodiesterase activity in normal and failing human hearts. J Clin Invest. 88:15-9, 1991.

Mubagwa K, Shirayama T, Moreau M, Pappano AJ. Effects of PDE inhibitors and carbachol on the L-type Ca current in guinea pig ventricular myocytes. Am J Physiol. 265:H1353-63, 1993.

Nabauer M, Callewaert G, Cleemann L, Morad M. Regulation of calcium release is gated by calcium current, not gating charge, in cardiac myocytes. Science. 244:800-3, 1989.

Nabauer M, Morad M. Ca^{2+}-induced Ca^{2+} release as examined by photolysis of caged Ca^{2+} in single ventricular myocytes. Am J Physiol. 258:C189-93, 1990.

Nabauer M, Kaab S. Potassium channel down-regulation in heart failure. Cardiovasc Res. 37:324-34, 1998.

Nargeot J, Lory P, Richard S. Molecular basis of the diversity of calcium channels in cardiovascular tissues. Eur Heart J. 18 Suppl A:A15-26, 1997.

Negretti N, Varro A, Eisner DA. Estimate of net calcium fluxes and sarcoplasmic reticulum calcium content during systole in rat ventricular myocytes. J Physiol. 486:581-91, 1995.

Neumann J, Schmitz W, Scholz H, von Meyerinck L, Doring V, Kalmar P. Increase in myocardial Gi-proteins in heart failure. Lancet. 2:936-7, 1988.

Nilius B. Possible functional significance of a novel type of cardiac Ca channel. Biomed Biochim Acta.45:K37-45, 1986.

Nilius B, Hess P, Lansman JB, Tsien RW. A novel type of cardiac calcium channel in ventricular cells. Nature. 316:443-6, 1985.

Nuss HB, Houser SR. Sodium-calcium exchange-mediated contractions in feline ventricular myocytes. Am J Physiol. 263:H1161-9, 1992.

O'Neill SC, Donoso P, Eisner DA. The role of $[Ca^{2+}]i$ and $[Ca^{2+}]$ sensitization in the caffeine contracture of rat myocytes: measurement of $[Ca^{2+}]i$ and [caffeine]i. J Physiol. 425:55-70, 1990.

Ono K, Trautwein W. Potentiation by cyclic GMP of beta-adrenergic effect on Ca^{2+} current in guinea-pig ventricular cells. J Physiol. 443:387-404, 1991.

Opie LH. The Heart. Grune & Stratton, Inc. Orlando, Florida, 1984.

Palmer D, Maurice DH. Dual expression and differential regulation of phosphodiesterase 3A and phosphodiesterase 3B in human vascular smooth muscle: implications for phosphodiesterase 3 inhibition in human cardiovascular tissues. Mol Pharmacol. 58:247-52, 2000.

Perez-Garcia MT, Chiamvimonvat N, Ranjan R, Balser JR, Tomaselli GF, Marban E. Mechanisms of sodium/calcium selectivity in sodium channels probed by cysteine mutagenesis and sulfhydryl modification. Biophys J. 72:989-96, 1997.

Philipson KD. Myocardial ion transporters. In: The Myocardium. GA Langer. ed. Acdemic Press, San Diego, pp. 143-179, 1997

Piacentino V 3rd, Dipla K, Gaughan JP, Houser SR. Voltage-dependent Ca^{2+} release from the SR of feline ventricular myocytes is explained by Ca^{2+}-induced Ca^{2+} release. J Physiol. 523:533-548, 2000.

Pieske B, Kretschmann B, Meyer M, Holubarsch C, Weirich J, Posival H, Minami K, Just H, Hasenfuss G. Alterations in intracellular calcium handling associated with the inverse force-frequency relation in human dilated cardiomyopathy. Circulation. 92:1169-78, 1995.

Pyne NJ, Cooper ME, Houslay MD. The insulin- and glucagon-stimulated 'dense-vesicle' high-affinity cyclic AMP phosphodiesterase from rat liver. Purification, characterization and inhibitor sensitivity. Biochem J. 242:33-42, 1987.

Rapundalo ST. Cardiac protein phosphorylation: functional and pathophysiological correlates. Cardiovasc Res. 38:559-88, 1998.

Rascon A, Lindgren S, Stavenow L, Belfrage P, Andersson KE, Manganiello VC, Degerman E. Purification and properties of the cGMP-inhibited cAMP phosphodiesterase from bovine aortic smooth muscle. Biochim Biophys Acta. 1134:149-56, 1992.

Reeves ML, Leigh BK, England PJ. The identification of a new cyclic nucleotide phosphodiesterase activity in human and guinea-pig cardiac ventricle. Implications for the mechanism of action of selective phosphodiesterase inhibitors. Biochem J. 241:535-41, 1987.

Reuter H. Calcium channel modulation by neurotransmitters, enzymes and drugs. Nature. 301:569-74, 1983.

Richard S, Leclercq F, Lemaire S, Piot C, Nargeot J. Ca^{2+} currents in compensated hypertrophy and heart failure. Cardiovasc Res. 37:300-11, 1998.

Rivet-Bastide M, Vandecasteele G, Hatem S, Verde I, Benardeau A, Mercadier JJ, Fischmeister R. cGMP-stimulated cyclic nucleotide phosphodiesterase regulates the basal calcium current in human atrial myocytes. J Clin Invest. 99:2710-8, 1997.

Roberds SL, Ervasti JM, Anderson RD, Ohlendieck K, Kahl SD, Zoloto D, Campbell KP. Disruption of the dystrophin-glycoprotein complex in the cardiomyopathic hamster. J Biol Chem. 268:11496-9, 1993.

Roos, KP. Mechanics and force production. In: The myocardium. GA Langer. ed. Acdemic Press, San Diego, pp235-323, 1997

Rossner KL. Isoprenaline-evinced disturbances in action potentials from hearts of young cardiomyopathic hamsters. Cardiovasc Res. 19:584-8, 1985.

Rossner KL. Calcium current in congestive heart failure of hamster cardiomyopathy. Am J Physiol. 260:H1179-86, 1991.

Rothschuh, KE. Histroy of Physiology. Translated and edited by G.B. Risse. Robert E. Krieger Publishing Co. Huntington, New York, 1973.

Rouleau JL, Juneau C, Stephens H, Shenasa H, Parmley WW, Brutsaert DL. Mechanical properties of papillary muscle in cardiac failure: importance of pathogenesis and of ventricle of origin. J Mol Cell Cardiol. 21:817-28, 1989.

Rubin CS. A kinase anchor proteins and the intracellular targeting of signals carried by cyclic AMP. Biochim Biophys Acta. 1224:467-79, 1994.

Sakamoto A, Abe M, Masaki T. Delineation of genomic deletion in cardiomyopathic hamster. FEBS Lett. 447:124-8, 1999.

Sakamoto A, Ono K, Abe M, Jasmin G, Eki T, Murakami Y, Masaki T, Toyo-oka T, Hanaoka F. Both hypertrophic and dilated cardiomyopathies are caused by mutation of the same gene, delta-sarcoglycan, in hamster: an animal model of disrupted dystrophin-associated glycoprotein complex. Proc Natl Acad Sci U S A. 94:13873-8, 1997.

Santana LF, Cheng H, Gomez AM, Cannell MB, Lederer WJ Relation between the sarcolemmal Ca^{2+} current and Ca^{2+} sparks and local control theories for cardiac excitation-contraction coupling. Circ Res. 78:166-71, 1996.

Santana LF, Gomez AM, Lederer WJ. Ca^{2+} flux through promiscuous cardiac Na^{+} channels: slip-mode conductance. Science. 279:1027-33, 1998.

Sato N, Asai K, Okumura S, Takagi G, Shannon RP, Fujita-Yamaguchi Y, Ishikawa Y, Vatner SF, Vatner DE. Mechanisms of desensitization to a PDE inhibitor (milrinone) in conscious dogs with heart failure. Am J Physiol. 276:H1699-705, 1999.

Scamps F, Mayoux E, Charlemagne D, Vassort G. Calcium current in single cells isolated from normal and hypertrophied rat heart. Effects of beta-adrenergic stimulation. Circ Res. 67:199-208, 1990.

Schuttler K, Wang SY, Pfeifer T, Meyer R. Late contraction in guinea-pig ventricular myocytes activated by the Na^{+}-Ca^{2+} exchange during the action potential. Ann N Y Acad Sci. 639:475-7, 1991.

Scott JD, McCartney S. Localization of A-kinase through anchoring proteins. Mol Endocrinol. 8:5-11, 1994.

Sen L, Liang BT, Colucci WS, Smith TW. Enhanced alpha 1-adrenergic responsiveness in cardiomyopathic hamster cardiac myocytes. Relation to the expression of pertussis

toxin-sensitive G protein and alpha 1-adrenergic receptors. Circ Res. 67:1182-92, 1990a.

Sen LY, O'Neill M, Marsh JD, Smith TW. Inotropic and calcium kinetic effects of calcium channel agonist and antagonist in isolated cardiac myocytes from cardiomyopathic hamsters. Circ Res. 67:599-608, 1990b.

Sen LY, O'Neill M, Marsh JD, Smith TW. Myocyte structure, function, and calcium kinetics in the cardiomyopathic hamster heart. Am J Physiol. 259:H1533-43, 1990c.

Sen L, Smith TW. T-type Ca^{2+} channels are abnormal in genetically determined cardiomyopathic hamster hearts. Circ Res. 75:149-55, 1994.

Sethi R, Bector N, Takeda N, Nagano M, Jasmin G, Dhalla NS.Alterations in G-proteins in congestive heart failure in cardiomyopathic (UM-X7.1) hamsters. Mol Cell Biochem. 140:163-70, 1994.

Shahid M, Nicholson CD. Comparison of cyclic nucleotide phosphodiesterase isoenzymes in rat and rabbit ventricular myocardium: positive inotropic and phosphodiesterase inhibitory effects of Org 30029, milrinone and rolipram. Naunyn Schmiedebergs Arch Pharmacol. 342:698-705, 1990.

Shakur Y, Pryde JG, Houslay MD. Engineered deletion of the unique N-terminal domain of the cyclic AMP-specific phosphodiesterase RD1 prevents plasma membrane association and the attainment of enhanced thermostability without altering its sensitivity to inhibition by rolipram. Biochem J. 292 :677-86, 1993.

Sham JS, Cleemann L, Morad M. Gating of the cardiac Ca^{2+} release channel: the role of Na^{+} current and Na^{+}-Ca^{2+} exchange. Science. 255:850-3, 1992.

Silver PJ, Allen P, Etzler JH, Hamel LT, Bentley RG, Pagani ED. Cellular distribution and pharmacological sensitivity of low Km cyclic nucleotide phosphodiesterase isozymes in human cardiac muscle from normal and cardiomyopathic subjects. Second Messengers Phosphoproteins. 13:13-25, 1990.

Simmerman HK, Collins JH, Theibert JL, Wegener AD, Jones LR. Sequence analysis of phospholamban. Identification of phosphorylation sites and two major structural domains. J Biol Chem. 261:13333-41, 1986.

Simmerman HK, Jones LR. Phospholamban: protein structure, mechanism of action, and role in cardiac function. Physiol Rev. 78:921-47, 1998.

Sipido KR, Carmeliet E, Van de Werf F. T-type Ca^{2+} current as a trigger for Ca^{2+} release from the sarcoplasmic reticulum in guinea-pig ventricular myocytes. J Physiol. 508 :439-51, 1998.

Sipido KR, Maes M, Van de Werf F. Low efficiency of Ca^{2+} entry through the Na^{+}-Ca^{2+} exchanger as trigger for Ca^{2+} release from the sarcoplasmic reticulum. A comparison between L-type Ca^{2+} current and reverse-mode Na^{+}-Ca^{2+} exchange. Circ Res. 81:1034-44, 1997.

Sjaastad, I., Birkeland, J.A., Ferrier, G.R., Howlett, S.E., Wasserstrom, J.A. & Sejersted, O.M, Rats with congestive heart failure exhibit a defect in excitation-contraction coupling caused by suppression of the voltage sensitive release mechanism. *Circulation*, 102:II-297, 2000.

Smith CJ, He J, Ricketts SG, Ding JZ, Moggio RA, Hintze TH. Downregulation of right ventricular phosphodiesterase PDE-3A mRNA and protein before the development of canine heart failure. Cell Biochem Biophys. 29:67-88, 1998.

Smith CJ, Huang R, Sun D, Ricketts S, Hoegler C, Ding JZ, Moggio RA, Hintze TH. Development of decompensated dilated cardiomyopathy is associated with decreased gene expression and activity of the milrinone-sensitive cAMP phosphodiesterase PDE3A. Circulation. 96:3116-23, 1997.

Smith CJ, Krall J, Manganiello VC, Movsesian MA. Cytosolic and sarcoplasmic reticulum-associated low Km, cGMP-inhibited cAMP phosphodiesterase in mammalian myocardium. Biochem Biophys Res Commun. 190:516-21, 1993.

Soderling SH, Bayuga SJ, Beavo JA. Identification and characterization of a novel family of cyclic nucleotide phosphodiesterases. J Biol Chem. 273:15553-8, 1998.

Soderling SH, Bayuga SJ, Beavo JA. Isolation and characterization of a dual-substrate phosphodiesterase gene family: PDE10A. Proc Natl Acad Sci U S A. 96:7071-6, 1999.

Sperelakis N. Regulation of calcium slow channels of cardiac muscle by cyclic nucleotides and phosphorylation. J Mol Cell Cardiol. 20 Suppl 2:75-105, 1988.

Steinfath M, Danielsen W, von der Leyen H, Mende U, Meyer W, Neumann J, Nose M, Reich T, Schmitz W, Scholz H, et al. Reduced alpha 1- and beta 2-adrenoceptor-mediated positive inotropic effects in human end-stage heart failure. Br J Pharmacol. 105:463-9, 1992.

Steinfath M, Geertz B, Schmitz W, Scholz H, Haverich A, Breil I, Hanrath P, Reupcke C, Sigmund M, Lo HB. Distinct down-regulation of cardiac beta 1- and beta 2-adrenoceptors in different human heart diseases. Naunyn Schmiedebergs Arch Pharmacol. 343:217-20, 1991.

Strand MA, Louis CF and Mickelson JR. Phosphorylation of the porcine skeletal and cardiac muscle sarcoplasmic reticulum ryanodine receptor. *Biochim Biophys Acta* 1175:319-26, 1993.

Straub V, Duclos F, Venzke DP, Lee JC, Cutshall S, Leveille CJ, Campbell KP. Molecular pathogenesis of muscle degeneration in the delta-sarcoglycan-deficient hamster. Am J Pathol. 153:1623-30, 1998.

Strobeck JE, Factor SM, Bhan A, Sole M, Liew CC, Fein F, Sonnenblick EH. Hereditary and acquired cardiomyopathies in experimental animals: mechanical, biochemical, and structural features. Ann N Y Acad Sci. 317:59-88, 1979.

Sumii K, Sperelakis N. cGMP-dependent protein kinase regulation of the L-type Ca^{2+} current in rat ventricular myocytes. Circ Res. 77:803-12, 1995.

Sutko JL, Airey JA Ryanodine receptor Ca^{2+} release channels: does diversity in form equal diversity in function? Physiol Rev. 76:1027-71, 1996.

Sys SU, Goenen MJ, Chalant CH, Brutsaert DL. Inotropic effects of amrinone and milrinone on contraction and relaxation of isolated cardiac muscle. Circulation. 73:III25-35, 1986.

Tada M, Kirchberger MA, Repke DI, Katz AM. The stimulation of calcium transport in cardiac sarcoplasmic reticulum by adenosine 3':5'-monophosphate-dependent protein kinase. J Biol Chem. 249:6174-80, 1974.

Taira M, Hockman SC, Calvo JC, Taira M, Belfrage P, Manganiello VC. Molecular cloning of the rat adipocyte hormone-sensitive cyclic GMP-inhibited cyclic nucleotide phosphodiesterase. J Biol Chem. 268:18573-9, 1993.

Takasago T, Imagawa T and Shigekawa M. Phosphorylation of the cardiac ryanodine receptor by cAMP-dependent protein kinase. *J Biochem (Tokyo)* 106:872-7, 1989.

Talosi L, Edes I, Kranias EG. Intracellular mechanisms mediating reversal of beta-adrenergic stimulation in intact beating hearts. Am J Physiol. 264:H791-7, 1993.

Tawada-Iwata Y, Imagawa T, Yoshida A, Takahashi M, Nakamura H, Shigekawa M. Increased mechanical extraction of T-tubule/junctional SR from cardiomyopathic hamster heart. Am J Physiol. 264:H1447-53, 1993.

Taylor SS, Buechler JA, Yonemoto W. cAMP-dependent protein kinase: framework for a diverse family of regulatory enzymes. Annu Rev Biochem.59:971-1005, 1990.

Terrar DA, White E. Mechanisms and significance of calcium entry at positive membrane potentials in guinea-pig ventricular muscle cells. Q J Exp Physiol. 74:121-39, 1989.

Thakkar J, Tang SB, Sperelakis N, Wahler GM. Inhibition of cardiac slow action potentials by 8-bromo-cyclic GMP occurs independent of changes in cyclic AMP levels. Can J Physiol Pharmacol. 66(8):1092-5, 1988.

Thompson WJ, Terasaki WL, Epstein PM, Strada SJ. Assay of cyclic nucleotide phosphodiesterase and resolution of multiple molecular forms of the enzyme. Adv Cyclic Nucleotide Res.10:69-92, 1979.

Tobacman LS. Thin filament-mediated regulation of cardiac contraction. Annu Rev Physiol. 58:447-81, 1996.

Tohse N, Sperelakis N. cGMP inhibits the activity of single calcium channels in embryonic chick heart cells. Circ Res. 69:325-31, 1991.

Tomaselli GF, Marban E. Electrophysiological remodeling in hypertrophy and heart failure. Cardiovasc Res. 42:270-83, 1999.

Torphy TJ, Page C. Phosphodiesterases: the journey towards therapeutics. Trends Pharmacol Sci. 21:157-9, 2000.

Tseng GN, Boyden PA. Multiple types of Ca^{2+} currents in single canine Purkinje cells. Circ Res. 65:1735-50, 1989.

Tsien RW, Bean BP, Hess P, Lansman JB, Nilius B, Nowycky MC. Mechanisms of calcium channel modulation by beta-adrenergic agents and dihydropyridine calcium agonists. J Mol Cell Cardiol. 18:691-710, 1986.

Tytgat J, Vereecke J, Carmeliet E. A combined study of sodium current and T-type calcium current in isolated cardiac cells. Pflugers Arch. 417:142-8, 1990.

Ueyama T, Ohkusa T, Hisamatsu Y, Nakamura Y, Yamamoto T, Yano M, Matsuzaki M. (1998a) Alterations in cardiac SR Ca^{2+}-release channels during development of heart failure in cardiomyopathic hamsters. Am J Physiol. 274:H1-7, 1998.

Ueyama T, Ohkusa T, Yano M, Matsuzaki M. (1998b) Growth hormone preserves cardiac sarcoplasmic reticulum Ca^{2+} release channels (ryanodine receptors) and enhances cardiac function in cardiomyopathic hamsters. Cardiovasc Res. 40:64-73, 1998.

Ungerer M, Bohm M, Elce JS, Erdmann E, Lohse MJ. Altered expression of beta-adrenergic receptor kinase and beta 1-adrenergic receptors in the failing human heart. Circulation. 87:454-63, 1993.

Ungerer M, Parruti G, Bohm M, Puzicha M, DeBlasi A, Erdmann E, Lohse MJ. Expression of beta-arrestins and beta-adrenergic receptor kinases in the failing human heart. Circ Res. 74:206-13, 1994.

Valdeolmillos M, O'Neill SC, Smith GL, Eisner DA Calcium-induced calcium release activates contraction in intact cardiac cells. Pflugers Arch. 413:676-8, 1989.

Van Wagoner, D.R., Kirian, M., Arakako, B., and Lamorgese, M. Voltage sensitive calcium release in human atrial myocytes. Biophys. J. 76 A459, 1999.

Vassort G, Alvarez J. Cardiac T-type calcium current: pharmacology and roles in cardiac tissues. J Cardiovasc Electrophysiol. 5:376-93, 1994.

Veksler VI, Ventura-Clapier R, Lechene P, Vassort G. Functional state of myofibrils, mitochondria and bound creatine kinase in skinned ventricular fibers of cardiomyopathic hamsters. J Mol Cell Cardiol. 20:329-42, 1988.

Verde I, Vandecasteele G, Lezoualc'h F, Fischmeister R. Characterization of the cyclic nucleotide phosphodiesterase subtypes involved in the regulation of the L-type Ca^{2+} current in rat ventricular myocytes. Br J Pharmacol. 127:65-74, 1999.

Vites AM, Wasserstrom JA. Fast sodium influx provides an initial step to trigger contractions in cat ventricle. Am J Physiol. 271:H674-86, 1996.

von der Leyen H, Mende U, Meyer W, Neumann J, Nose M, Schmitz W, Scholz H, Starbatty J, Stein B, Wenzlaff H, et al. Mechanism underlying the reduced positive inotropic effects of the phosphodiesterase III inhibitors pimobendan, adibendan and saterinone in failing as compared to nonfailing human cardiac muscle preparations. Naunyn Schmiedebergs Arch Pharmacol. 344:90-100, 1991.

Wahler GM, Rusch NJ, Sperelakis N. 8-Bromo-cyclic GMP inhibits the calcium channel current in embryonic chick ventricular myocytes. Can J Physiol Pharmacol. 68:531-4, 1990.

Wasserstrom JA, Vites AM. The role of Na^{+}-Ca^{2+} exchange in activation of excitation-contraction coupling in rat ventricular myocytes. J Physiol. 493:529-42, 1996.

Wegener AD, Simmerman HK, Lindemann JP, Jones LR. Phospholamban phosphorylation in intact ventricles. Phosphorylation of serine 16 and threonine 17 in response to beta-adrenergic stimulation. J Biol Chem. 264:11468-74, 1989.

Weishaar RE, Burrows SD, Kobylarz DC, Quade MM, Evans DB. Multiple molecular forms of cyclic nucleotide phosphodiesterase in cardiac and smooth muscle and in platelets. Isolation, characterization, and effects of various reference phosphodiesterase inhibitors and cardiotonic agents. Biochem Pharmacol. 35:787-800, 1986.

Weishaar RE, Cain MH, Bristol JA. A new generation of phosphodiesterase inhibitors: multiple molecular forms of phosphodiesterase and the potential for drug selectivity. J Med Chem. 28:537-45, 1985.

Weishaar RE, Kobylarz-Singer DC, Kaplan HR. Subclasses of cyclic AMP phosphodiesterase in cardiac muscle. J Mol Cell Cardiol. 19:1025-36, 1987.

Weishaar RE, Kobylarz-Singer D, Keiser JA, Wright CD, Cornicelli J, Panek R. Cyclic nucleotide phosphodiesterases in the circulatory system. Biochemical, pharmacological, and functional characteristics. Adv Second Messenger Phosphoprotein Res. 25:249-69, 1992.

Weishaar RE, Kobylarz-Singer DC, Steffen RP, Kaplan HR. Subclasses of cyclic AMP-specific phosphodiesterase in left ventricular muscle and their involvement in regulating myocardial contractility. Circ Res. 61:539-47, 1987.

Whitmer JT, Kumar P, Solaro RJ. Calcium transport properties of cardiac sarcoplasmic reticulum from cardiomyopathic Syrian hamsters (BIO 53.58 and 14.6): evidence for a quantitative defect in dilated myopathic hearts not evident in hypertrophic hearts. Circ Res. 62:81-5, 1988.

Wikman-Coffelt J, Sievers R, Parmley WW, Jasmin G. Verapamil preserves adenine nucleotide pool in cardiomyopathic Syrian hamster. Am J Physiol. 250:H22-8, 1986.

Wilmshurst PT, Walker JM, Fry CH, Mounsey JP, Twort CH, Williams BT, Davies MJ, Webb-Peploe MM. Inotropic and vasodilator effects of amrinone on isolated human tissue. Cardiovasc Res. 18:302-9, 1984.

Witcher DR, Kovacs RJ, Schulman H, Cefali DC, Jones LR. Unique phosphorylation site on the cardiac ryanodine receptor regulates calcium channel activity. J Biol Chem. 266:11144-52, 1991.

Xu L, Tripathy A, Pasek DA, Meissner G Potential for pharmacology of ryanodine receptor/calcium release channels. Ann N Y Acad Sci. 853:130-48, 1998.

Yang J, Drazba JA, Ferguson DG, Bond M. A-kinase anchoring protein 100 (AKAP100) is localized in multiple subcellular compartments in the adult rat heart. J Cell Biol. 142:511-22, 1998.

Yano M, Kohno M, Ohkusa T, Mochizuki M, Yamada J, Kohno M, Hisaoka T, Ono K, Tanigawa T, Kobayashi S, Matsuzaki M. Effect of milrinone on left ventricular relaxation and Ca^{2+} uptake function of cardiac sarcoplasmic reticulum. Am J Physiol Heart Circ Physiol. 279:H1898-905, 2000.

Yoshida A, Takahashi M, Imagawa T, Shigekawa M, Takisawa H, Nakamura. Phosphorylation of ryanodine receptors in rat myocytes during beta-adrenergic stimulation. J Biochem (Tokyo). 111:186-90, 1992.

You Y, Pelzer DJ, Pelzer S. Modulation of calcium current density by intracellular calcium in isolated guinea pig ventricular cardiomyocytes. Biochem Biophys Res Commun. 204:732-40, 1994.

Zakhary DR, Moravec CS, Bond M. Regulation of PKA binding to AKAPs in the heart: alterations in human heart failure. Circulation. 101:1459-64, 2000.

Zhou Z, January CT. Both T- and L-type Ca^{2+} channels can contribute to excitation-contraction coupling in cardiac Purkinje cells. Biophys J. 74:1830-9, 1998.

Zhou Z, Lipsius SL. T-type calcium current in latent pacemaker cells isolated from cat right atrium. J Mol Cell Cardiol. 26:1211-9, 1994.

Zhu J, Ferrier GR. Regulation of a voltage-sensitive release mechanism by Ca^{2+}-calmodulin-dependent kinase in cardiac myocytes. Am J Physiol Heart Circ Physiol. 279:H2104-15, 2000.

Zhu JQ, Howlett SE and Ferrier GR. A role of cAMP in activation of the voltage-sensitive release mechanism for cardiac contraction. Biophys J 73:A161, 1997.

Zot AS, Potter JD. Structural aspects of troponin-tropomyosin regulation of skeletal muscle contraction. Annu Rev Biophys Biophys Chem.16:535-59, 1987.